Molecular analysis of plant innate immunity triggered by secreted effectors from bacterial and fungal pathogens of apple

A thesis presented in partial fulfilment of the requirements for the degree of

Doctor of Philosophy (PhD)
in Plant Science

Institute of Agriculture and Environment
Massey University, New Zealand.

Maxim Prokchorchik

December 2017

Abstract

In comparison to animals, plants do not have a dedicated immune system with mobile immune cells to protect themselves. Instead they rely on the innate immunity of each cell. Plant immunity branches into two classical layers: PTI (PAMP-triggered immunity) and ETI (Effector-triggered immunity). PTI detects the conserved molecular patterns (PAMPs) associated with pathogens and often can be overcome by pathogens translocating effector molecules into plant cells to inhibit the PTI. ETI, in turn, relies on intracellular receptors that can specifically recognize effectors or their activity and activate a rapid and robust response.

The research presented in this thesis is focused on two pathogens of apple plants: the bacterial pathogen *Erwinia amylovora* (the causal agent of fire blight) and fungal pathogen *Venturia inaequalis* (the causal agent of apple scab disease). As both bacterial and fungal pathogens deliver effector molecules in order to promote their virulence, ETI engineering is a promising universal strategy to control these pathogens.

In Chapter 3, the main aim was to elucidate the requirements and precise mechanism of how an important effector of *E. amylovora*, AvrRpt2, is recognized by the MR5 disease resistance (R) protein, derived from a hybrid apple *Malus* x *robusta* 5. I identified that a fragment of the guardee apple protein RIN4 was required and sufficient and required for MR5 activation. I further identified crucial amino acid residues responsible for this activation. Interestingly, cognate residues in RIN4 guardee homolog from *Arabidopsis thaliana* are responsible for suppression of the autoactivity of R protein RPS2. These findings led to the proposal of a novel hypothesis for evolutionary guardee adaption to the pool of R proteins present in plants.

In Chapter 4, the main focus was to apply newly acquired whole-genome sequencing data of *V. inaequalis* for identifying the previously mapped AvrRvi8 effector, as well as several novel effectors predicted *in silico*. The sequences of these effectors were validated by amplification and resequencing of candidate genes from *V. inaequalis* cDNA. Further functional analysis of the selected gene candidates was performed. In addition, a library of constructs for generating *V. inaequalis* knock-out strains was prepared for future work.

The findings from this thesis expected to be useful for breeders of apple to battle two economically important pathogens devastating the industry.

Deployment of the MR5 system in apples should facilitate fire blight resistance in pipfruit and offers the opportunity for further engineering of MR5 to detect other pathogens.

Furthermore, the effector library developed for *V. inaequalis* offers a novel tool for studying both virulence and avirulence mechanisms present in the apple-scab pathosystem. It is envisaged that further effector research will elucidate authentic targets critical for resistance development in apple.

Acknowledgments

I would like to thank my supervisor, Prof. Kee Hoon Sohn, for his support, scientific guidance and overall help while undertaking my PhD. His excellent knowledge of the field and creativity always served as a beacon, helping me navigate a sea of data and failed experiments. His support and enthusiasm encouraged me to never give up or stop the journey of my PhD. I also want to thank Dr. Cecile Segonzac for the invaluable guidance in the lab, as well as in the world of Western Blotting and CoIPs.

I am very grateful to Dr. Janet Reid, Dr. Vincent Bus and Dr. David Chagne for their guidance, insightful discussions and support. I want to thank Dr. Rosie Bradshaw and Dr. Joanna Bowen for the enormous help with thesis preparation and scientific advice. I enjoyed my time doing research and having fun weekends with the "PhD awesome foursome" of KSL lab, including Jay, Sera and Toby. I also want to thank members of KSL in Korea, including Jeongmin, Hayoung and Haseong for their help to get used to a completely different country.

I am thankful to my parents for their endless support and understanding during my ups and downs. Even from far away they made me feel that they are very close. Finally, I would like to thank my partner Sera, who coped with me through the long course of this PhD, listening to my endless ideas during the good times and my limitless moaning during the bad.

Table of contents

List of figures

List of tables

Abbreviations

aa	Amino acids
ABA	Abscisic acid
At	Arabidopsis thaliana
ABC	ATP-binding cassette
Avr	Avirulence
bp	Base pair
BAK1	BRASSINOSTEROID INSENSITIVE 1-associated receptor kinase 1
BIC	Biotrophic interfacial complex
BIK1	BOTRYITIS INDUCED KINASE 1 (a cytoplasmic kinase)
BR	Brassinosteroid
CC	Coiled-coil (a domain in NB-LRRs)
cDNA	Complementary deoxyribonucleic acid
CEBiP	CHITIN OLIGOSACCHARIDE ELICITOR BINDING PROTEIN
CIN1	Cellophane induced protein 1
CIN3	Cellophane induced protein 3
CK	Cytokinin
CNL	Coiled-coil nucleotide-binding leucine-rich-repeat receptor
CSP	Cold-shock protein
CWDE	Cell wall-degrading enzymes
DNA	Deoxyribonucleic acid
dpi	Days post inoculation
DTT	dithiothreitol
EDS1	Enhanced disease susceptibility 1
EDTA	ethylenediamine tetraacetic acid
EFR	EF-Tu receptor (a sensor PRR/RLK)
EF-Tu	Elongation factor thermo unstable
EIX	ETHYLENE-INDUCING XYLANASES
elf18	EF Tu-derived epitope from Escherichia coli
Ea	*Erwinia amylovora*
ET	Ethylene
ETI	Effector-triggered immunity
EV	Empty vector

FLS2	Flagellin-sensitive 2 (a sensor PRR/RLK)
flg22	Flagellin-derived epitope from Pseudomonas aeruginosa g gram
FOB	Free on board
GA	Gibberellic acid
h	hours
His	Histidine
Hpa	*Hyaloperonospora arabidopsidis*
hpi	Hours post infiltration
HR	Hypersensitive response
HSP90	Heat shock protein 90
IFP	Integrated fruit production
IP	Invasion pattern
IPR	Invasion pattern receptor
IPTR	Invasion pattern triggered response
JA	Jasmonic acid
kb	kilobase
kDa	kilodaltons
LPS	Lipopolysaccharide
LRD	leucine-rich domain
LRR	Leucine rich repeat
Leu	Leucine
M	molar
MAPK	Mitogen-activated protein kinase
Md	*Malus domestica*
mg	milligram
min	minutes
mL	millilitre
mM	millimolar
Mr5	*Malus* x *robusta* 5
NBS	Nucleotide binding site (domain of NB-LRR)
NLR	Nod-like receptors
NLS	Nuclear localization signal
NDR1	Nonrace-specific disease resistance 1
NOI	NO_3-induce domain

OD	Optical density of bacterial suspension with 600nm wavelength light
PAD4	Phytoalexin deficient 4
PAMP	Pathogen-associated molecular pattern
PDA	Potato dextrose agar
PCD	Programmed cell death
PCR	Polymerase chain reaction
PG	polygalacturonase
PGN	Peptidoglycan
PR	Pathogenesis-related
PRR	Pattern recognition receptor
PTI	PAMP-triggered immunity
Pf	*Pseudomonas fluorescens*
Pp	*Pyrus pyrifolia*
Ps	*Pseudomonas syringae*
Pto	*Pseudomonas syringae pv. tomato*
Pu	*Pyrus ussuriensis*
qPCR	Quantitative polymerase chain reaction
RIN4	RPM1-interacting 4
RLCK	Receptor-like cytoplasmic kinase (intracellular)
RLK	Receptor-like kinase (a class of PRR)
RLP	Receptor-like protein (a class of PRR)
RNA	Ribonucleic acid
ROS	Reactive oxygen species
RPP	Resistance to *Peronospora parasitica* (NLRs for *Hyaloperonospora arabidopsidis*)
RPM1	RESISTANCE TO PSEUDOMONAS SYRINGAE PV. MACULICOLA 1
RPS2	RESISTANCE TO PSEUDOMONAS SYRINGAE 2
RPS4	RESISTANCE TO PSEUDOMONAS SYRINGAE 4
RPS5	RESISTANCE TO PSEUDOMONAS SYRINGAE 5
RRS1	RESISTANCE TO RALSTONIA SOLANACEARUM 1
s	seconds
SA	Salicylic acid
SAG101	Senescence associated gene 101
SAR	Systemic acquired resistance

SDS	Sodium dodecyl sulphate
SGT1	Suppressor of G2 allele of skp1 (required for most NLRs)
SID2	Salicylic acid induction deficient 2
SOBIR1	Suppressor of bir1-1 (a helper RLK)
TAE	tris acetate EDTA
TAL	Transcriptional activator-like (effector)
TCE	Tray equivalent (18 kg sale weight)
TEMED	N,N,N',N'-tetramethyl-ethylenediamine
TEV	Tobacco etch virus
TIR	Toll-interleukin-1 receptor (a domain in NB-LRRs)
TNL	Toll-interleukin-1 receptor nucleotide-binding leucine-rich-repeat receptor
Tris	tris(hydroxymethyl)aminomethane
Trp	Tryptophan
T1SS	Type I secretion system
T3SS	Type-three secretion system
T3E	Type-three secreted effector (bacterial)
Vi	*Venturia inaequalis*
ViCE	*Venturia inaequalis* candidate effector
µL	microlitre
µM	micromolar

Chapter 1. General introduction

1.1 Apple industry in New Zealand

Apples are the 2nd largest fresh fruit export of New Zealand. Overall it is one of the most important crops in New Zealand, as the climate is favorable for industrial growth of apples. New Zealand apples exported in 2015 were valued at $561 million. They were exported to 65 countries, nine of which imported an average of $45 million each, with 43% ($241m) going to Asian countries. Overall the apple fruit industry seems to show a steady but stable growth (Table 1.1), which is ensured by intensive research and apple breeding programs resulting in new varieties such as Rockit®, Smitten® and Koru® (http://www.freshfacts.co.nz, 2015 issue).

While the New Zealand climate is very favorable for apple growing, it is equally favorable for apple disease development. The most important apple diseases are 'apple scab' (caused by *Venturia inaequalis*), 'powdery mildew' (*Podosphaera leucotricha*), and the bacterial 'fire blight' disease (*Erwinia amylovora*).

Year Crop volumes ('000 tonnes)	2010	2011	2012	2013	2014	2015
National export production	260	300	285	320	311	331
Growing method: IFP	94%	94%	96%	95%	94%	94%
Certified organic	6%	6%	4%	5%	6%	6%
General statistics						
Export FOB $/TCE	$22.93	$21.79	$23.04	$27.69	$29.64	$32.83
Area planted (ha)	8,630	8,470	8,324	8,372	8,429	8,566
Export orchards (no.)	985	976	953	953	921	919
Export Packhouses (no.)	62	70	65	61	56	56
No. of exporters	95	90	88	84	76	79

Table 1.1: New Zealand apple fresh fruit industry overview and dynamics. IFP: Integrated Fruit Production sustainability; TCE: tray equivalents 18 kg sale weight. Source: Pipfruit New Zealand, Fresh facts, issue 2015 (http://www.freshfacts.co.nz).

The major problem with the management of apple pests and diseases is that the industry currently relies heavily on chemical-based control methods. It is of note that apple is the most heavily sprayed fruit crop in New Zealand with an average of 33 kg/ha of pesticides applied each year. (Holland & Rahman, 1999).

This situation is concerning since routine application of chemicals applies evolutionary pressure on pests and pathogens to quickly evolve resistance. This drives farmers to apply even more pesticides or lose crop yield. Consequently, the market value of apple suffers, as contemporary customers prefer a "clean" product with less use of pesticides and other chemicals.

An appropriate alternative to chemical means of control would be developing apple cultivars with natural resistance to disease-inducing pathogens. Large apple-breeding programs are being deployed in New Zealand and worldwide, but methods of conventional selective breeding are slow and not precise enough to adequately respond to rapidly evolving pathogens. To ensure the successful development of resistant apple cultivars, we need to research the mechanisms of how pathogens and apple plants interact with each other; this would provide clues to develop a robust and long-lasting resistance.

1.2 *Venturia inaequalis* is the causal agent of apple scab disease

Apple scab or black spot is a disease caused by *Venturia inaequalis* which infects domesticated apple cultivars as well as some other members of *Rosaceae*, such as *Malus* (Crabapple), *Cotoneaster integerrima*, *Crataegus oxycantha* (Hawthorn*), Loquat, Pyracantha* (Firethorn), *Sarcocephalus esculantus*, *Sorbus* (Mountain Ash), and *Viburnum* sp*.* It is one of the most devastating diseases of apple and it is reported to be found in nearly every region where apples are cultivated industrially (MacHardy, 1996; Sutton et al., 2016).

Scab symptoms in apple plants include formation of circular olive colored velvety, necrotic or chlorotic lesions, single or scattered on the leaf surface, or spots on infected sepals and pedicels. Symptoms visible on fruits include dark sharply bordered brown and corky lesions on young fruits and small black spots termed as "pin-point scab" on mature fruits. In addition, fruit shape deformation, size reduction, early fruit fall and enhanced susceptibility of trees to cold is observed (Figure 1.1) (MacHardy et al., 2001).

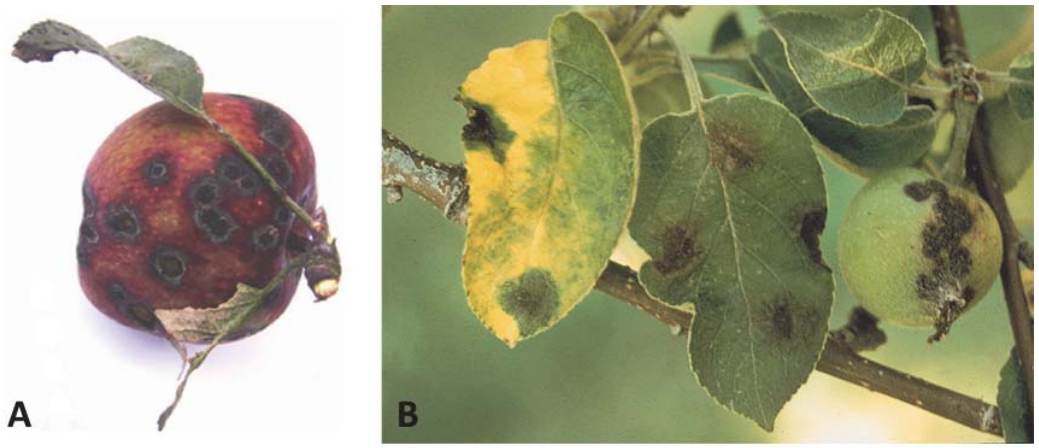

Figure 1.1: Apple scab disease on apple fruits (A) and apple leaves (B) caused by *Venturia inaequalis*. Reproduced from: **A** – J. Gopaljee et al., 2009 and **B** photo by A.L. Jones.

V. inaequalis is an obligate biotrophic heterothallic fungus with a genome consisting of 7 haploid chromosomes (Day et al., 1956). The number of chromosomes was defined independently by two research groups using cytological methods (Day et al., 1956; Julien, 1958). Further linkage group analysis was carried out and the best linkage group map suggested the presence of 11 linkage groups, which is more than expected for 7 chromosomes (Xu et al., 2009). This discrepancy may be due to very small physical chromosome size making them difficult to observe by microscopy, or due to low marker resolution in the linkage group analysis. Current research on the *V. inaequalis* genome involves next-generation sequencing which, coupled with previously acquired data, will allow precise genome characterization of this pathogen. *V. inaequalis* has sexual and asexual phases and during both can infect apple.

The pathogenic stage of the *V. inaequalis* life cycle starts with ascospore (sexual spore) germination on the plant leaves during the warm season. The fungus colonizes the host tissues and finally forms subcuticular mycelia and consequently conidiophores and conidia (asexual spores). Conidia are smooth, 0-1 septate, pale to mid-olivaceous brown in color, and are the source of secondary infections. They are often spread by wind or splashing rain drops, which leads to a high chance of spreading the disease even if only one tree was initially infected in the orchard (MacHardy, 1996).

Additionally, several cycles of conidia formation and secondary infection occur during a single warm season, increasing the infection rate. At the beginning of the cold season, the mycelium penetrates deeper into the leaf tissue and switches to sexual reproduction. This happens during leaf fall and results in two mating types of mycelium being formed in the leaf tissue on the ground. Those mycelia undergo sexual reproduction (mating), followed by pseudothecium formation (Gadoury & MacHardy, 1985). Pseudothecia generate bitunicate, cylindrical, double walled, and loculus asci, which produce ascospores. Each ascospore consists of two unequal sized cells with a thin outer wall and a thick elastic inner wall, enabling the pathogen to survive through the winter season (MacHardy, 1996).

The fungi usually persist through winter on fallen leaves, yet some reports showed that persistence on twigs and fruits is also possible, but in this case ascospores are not produced and conidia serve as the primary inoculum for a new infection. Ascospore maturation is synchronized with apple bud breaking time, which ensures successful infection due to the fact that host tissues are the most susceptible during this time (Vaillancourt and Hartman, 2000).

Once ascospores become mature, they are released from the asci and get disseminated by wind and rain. In addition, the presence of light is important for optimal discharge of the ascospores (MacHardy et al., 2001; Stensvand et al., 2009). Ascospores need to adhere, germinate, and form infection structures to penetrate the host cell wall in order to successfully establish the disease. *V. inaequalis* conidia and ascospores attach to the wet and hydrophobic surface of apple where they germinate, forming germ tubes.

Germ tubes generally proliferate from the apical end of conidia or any of the two cells in the ascospore, then the pathogen enters the host through the cuticle, not through stomata (MacHardy, 1996). When the ascospore/conidia generated germ tube gets into direct contact with cuticle, it differentiates into an appressorium and produces adhesive mucilaginous substances assumed to facilitate attachment to the host surface (Smereka et al., 1987).

In agreement with this theory, germinating conidia and mycelia were reported to produce extracellular cutinases (Koller & Parker, 1989; Koller et al., 1991). The theory is further supported by the observation that treatment of a specific cutinase inhibitor is able to prevent subcuticular growth and penetration

of the cuticle by the pathogen (Koller et al., 1991). In addition, esterase-like activity during germination of conidia has been reported; this is hypothesized to lead to cutin softening and making the penetration of the cuticle easier for the pathogen (Nicholson et al., 1972). After cuticle penetration, the infection hyphae proliferate into primary hyphae, which grow further and form subcuticular stroma generating conidiophores with conidia. The conidia and conidiophores break through the host cell wall and point outside the epidermis through lesions, which are characteristic scab symptoms (Figure 1.2).

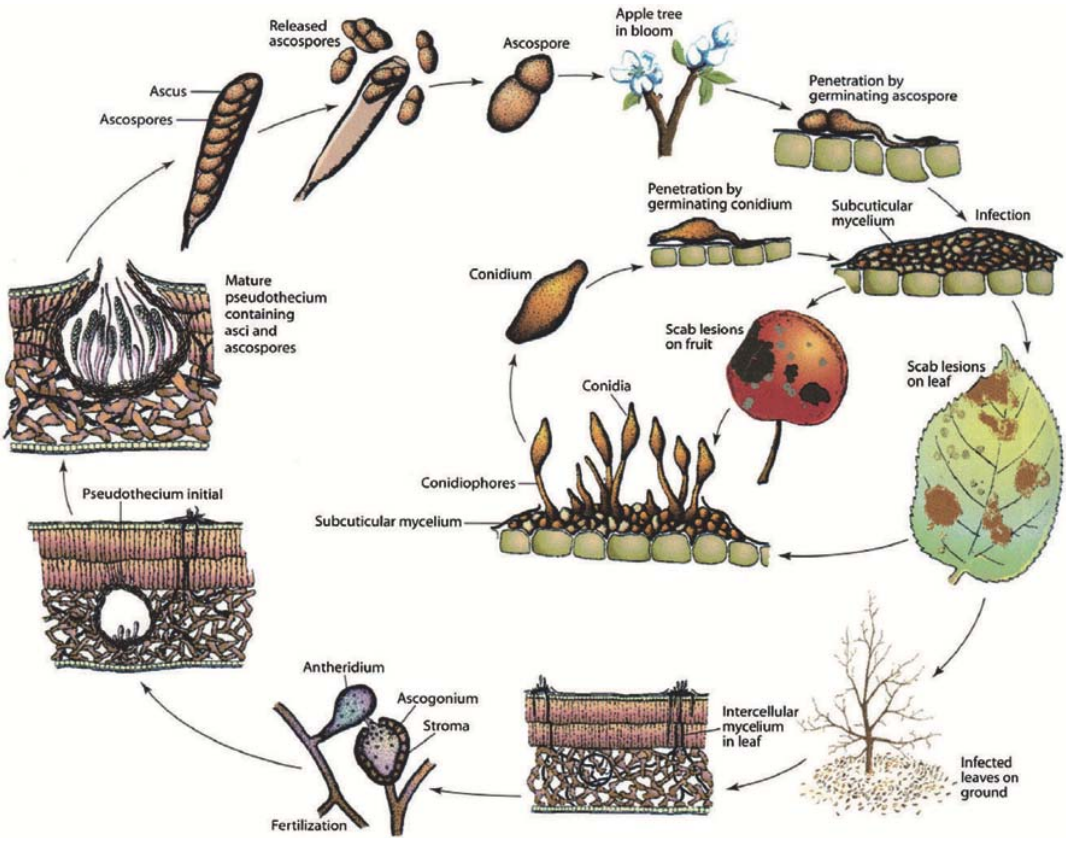

Figure 1.2: *Venturia inaequalis* life cycle. The host plants can be infected by ascospore (sexual spore) germinating on the plant leaves during the warm season. Fungi then colonize the host tissues and finally develop subcuticular mycelia. The mycelia forms conidiophores and conidia (asexual spores), which can re-infect new apple plants or they proceed to the sexual phase during the cold season. Reproduced from Agrios, *Plant Pathology*, p. 506. Copyright Elsevier 2005.

Interestingly *V. inaequalis* conidia can adhere and germinate on non-host plants such as *Pyrus communis*, however further disease development does not occur (Chevalier et al., 2004). In laboratory conditions, conidia can be germinated on cellophane membranes placed over PDA (Potato Dextrose Agar) plates; these conidia form appressoria and subcuticular hyphae-like structures, mimicking growth during infection *in planta* (Kucheryava et al., 2008). The fact that *V. inaequalis* can be cultivated on cellophane membranes allowed it to become a model organism for studying interactions between the fungus and its plant host. Using the cellophane membrane method, *Cin1* and *Cin3* genes were found to be induced during *V. inaequalis* growth on cellophane as well as *in planta* (Kucheryava et al., 2008).

One of the most interesting features of this pathogen is the fact that it can form subcuticular stroma without significant damage to host tissues. It is assumed that this pathogen utilizes cell wall-degrading enzymes (CWDEs) for breaching the plant cell wall for uptake of nutrients without haustorium formation. However, the fact that damage to host plant tissue becomes obvious only at the conidiation stage of pathogenesis suggests a minor role of these enzymes for nutrient uptake. *V. inaequalis* culture supernatant shows cellulolytic, cutinolytic, pectinolytic, and *β*-D-glucosidase activities. In addition, endo-polygalacturonase- (PG) and exo-PG-like activities were reported during *in vitro* growth (Kollar, 1998; Valsangiacomo & Gessler, 1992).

Based on these data it is theorized that CWDEs of *Venturia* might be tightly attached to its cell wall and they are released in a precisely regulated manner to degrade the host cell wall to allow nutrient uptake. This is in contrast to other pathogens where CWDE regulation is less rigid, triggering plant defense responses (Jha et al., 2005, 2007; Ryan & Farmer, 1991). Tightly regulated release of CWDEs might be a strategy of *Venturia* to prevent recognition by the host defense system that, if successfully activated, would prevent growth of the pathogen. Melanin, which is generally present as melanoprotein, produced by *V. inaequalis* seems to play a role in CWDE tethering, allowing their slow release (Jacobson, 2000). It also assists the pathogen to uptake nutrients, possibly via altering membrane permeability (MacHardy, 1996).

In addition to the fact that *Venturia inaequalis* is a very important pathogen for industrial apple growing, it also has the traits of a good model organism to

study biotrophic fungus pathogenesis. These traits include the ease of isolation for ascospores produced by a single meiotic event (Day et al., 1956), allowing segregation analysis, centromere mapping and study of fungal meiosis in general. Furthermore, *V. inaequalis* can be cultured *in vitro* facilitating controlled propagation for genetic studies. Finally, the *V. inaequalis*-apple pathosystem is a product of the long course of coevolution, during which *V. inaequalis* evolved traits to avoid recognition by the host plant cell. Furthermore, through a similar co-evolutionary process, apple has evolved mechanisms to prevent severity of the disease and thus many interesting mechanisms of fungal-host interactions are yet to be discovered from this system (Jha et al., 2009).

1.3 *Erwinia amylovora* is the causal agent of apple fire blight disease

Fire blight disease is caused by a Gram-negative bacterium *Erwinia amylovora* that is able to infect most *Rosaceae* plants. It is a devastating necrogenic disease believed to be the most significant for the *Rosaceae* family, including important ornamental species. It was first reported in New York in the late 1700s in apple, pear, and quince, which were introduced into North America during European settlement. Pioneering research of fire blight by T.J. Burrill, J.C. Arthur, and M.B. Waite proposed that it could be caused by bacterial pathogens transmitted by insects (Griffith et al., 2003). In the 1920s, the bacterial pathogen *Erwinia amylovora* was identified as the fire blight causal agent.

Infected plant parts show water-soaked symptoms, turning dark green then wilting and finally turning a brownish to black color. In all cases, sticky, amber-like ooze drops can be observed on blighted plant parts. These are full of viable bacteria coated with a polysaccharide matrix (Figure 1.3).

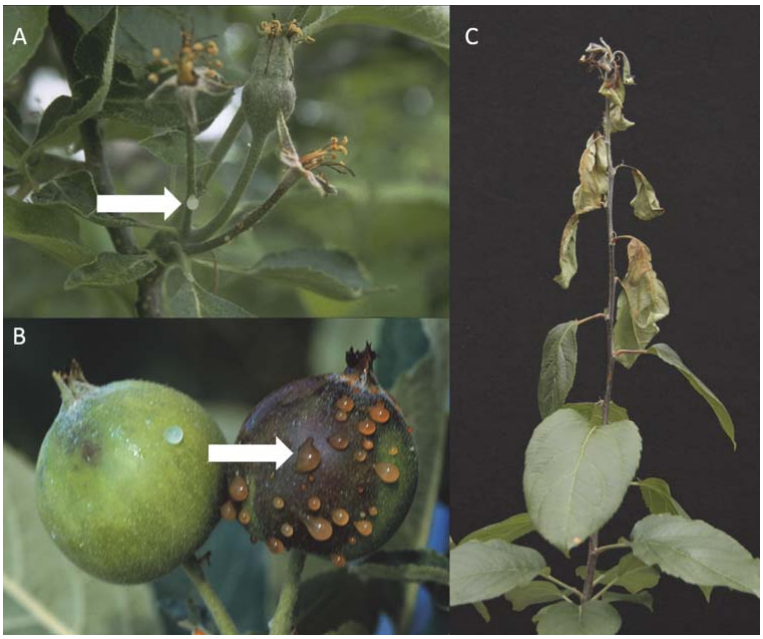

Figure 1.3: Fire blight symptoms in apple caused by *Erwinia amylovora* on (A) blossoms, (B) fruits and (C) shoots. The arrow points to bacterial ooze, a common symptom of fire blight infections. Photo reproduced from J. Norelli.

There are several well distinguished phases of the disease, including blossom blight, shoot blight, and rootstock blight (Norelli et al., 2003; Vanneste, 2000). *E. amylovora* overwinters in cankers, from which the bacterium emerges in a form of ooze in response to warmer spring weather. The ooze contains bacterial cells embedded in a polysaccharide matrix. This prevents the bacteria from drying out and helps to resist other abiotic stresses. In addition, this rich ooze is very attractive to insects which play a significant role in spreading the bacterial cells to new host plants.

The stigma surface of young blossoming flowers is the major site of pathogen multiplication, as it generates exudates supporting pathogen growth to densities as large as 10^5–10^6 cells per flower (Thomson, 1986). *E. amylovora* multiplication rates on stigmas is heavily dependent on the environmental temperature with that between 21°C to 27°C being the most favorable. Moisture from rain and heavy dew allows bacteria to migrate downward along the outer surface of stigmata where the pathogen infects the plant tissues through the floral nectaries, leading to the development of blossom blight symptoms. Further

dissemination among different flowers occurs mainly via pollinating insects, such as bees, and also via wind and rain (Pusey & Curry, 2004).

After entering the host organism, *E. amylovora* cells migrate through host tissues and can emerge into the environment again as ooze, which acts as a source of secondary infection through flowers and shoots. Shoot infection mostly occurs on actively growing young shoots, presumably through microscopic wounds caused by numerous biotic and abiotic factors (Vanneste, 2000). Hail damage is one of the major causes of fire blight epidemics as it wounds the young shoots and is also associated with rain that spreads the ooze. In addition, rootstock crowns can also be infected by *E. amylovora* cells migrating downward through plant tissues from scions, or via direct infection of rootstock suckers or wounds (Momol et al., 1998; Norelli et al., 2003) (Figure 1.4).

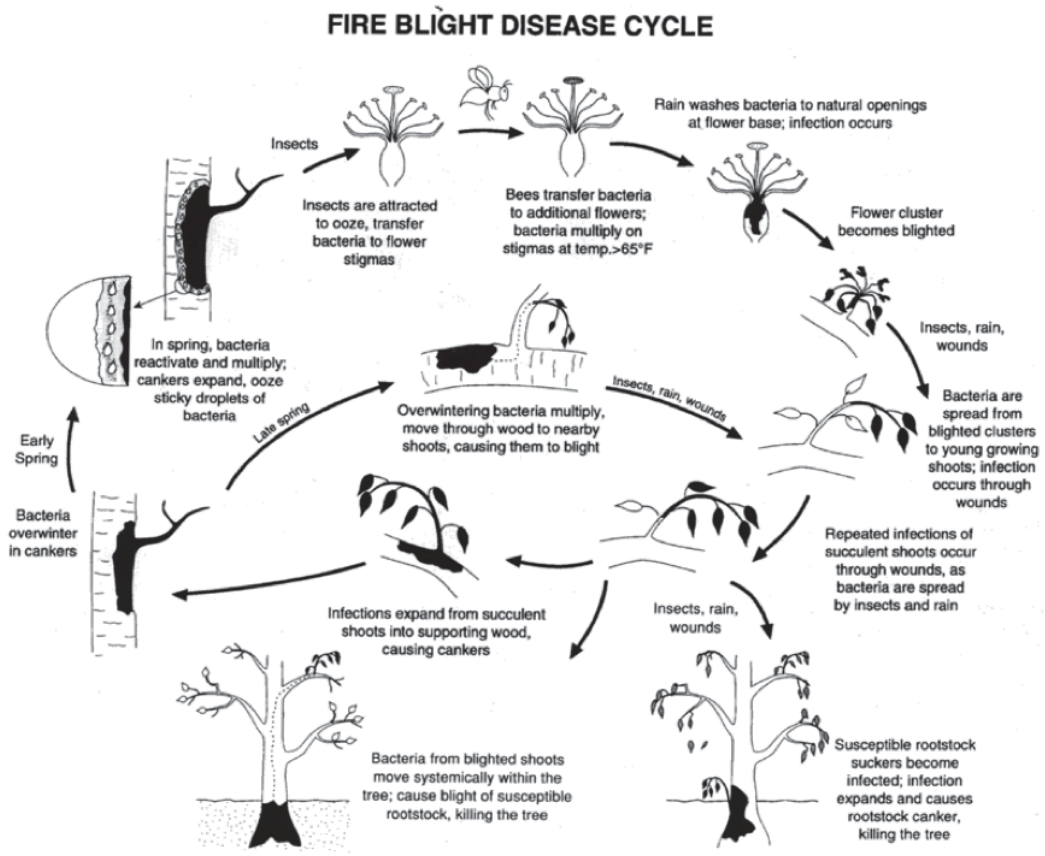

Figure 1.4: Fire blight disease cycle. In early spring *E. amylovora* cells multiply and form sticky ooze which attracts insects spreading the pathogen to new hosts. Primary infection of new host plants occurs through blooming flowers, secondary infection can occur through wounds in plant branches. Pathogen cells move systemically through the plant and finally results in rootstock infection resulting in death of the whole tree. Reproduced from Wilcox, F. Wayne, Ornamentals Fact Sheet, 1994.

At the present time, a complex of different methods is employed to control fire blight. That includes more classical approaches like cultural control, including pruning and removal of infected tissues. While this helps to reduce the amount of inoculum, this method is laborious, time-consuming, and does not have high efficiency (Duffy et al., 2005).

Antibiotic application is the most widespread and efficient practice to control fire blight to date (McManus et al., 2002). It is especially efficient when applied to *E. amylovora* populations on floral surfaces to prevent secondary infections from the primary infected plants. The risk of antibiotic use is that after

a certain time *E. amylovora* has a good chance of developing antibiotic resistance. In addition, this resistance can be transferred to clinically important human pathogens. This is the reason why antibiotic control of fire blight is banned in the European Union and some other Western European countries.

In agreement with these concerns, in countries where antibiotic control of fire blight is currently widely used, including the United States, Canada, Israel, Lebanon, and New Zealand, there have been reports of *E. amylovora* strains resistant to streptomycin (McManus et al., 2002; Rezzonico et al., 2009). This fact raises the importance of appropriate and efficient biocontrol development and employment to solve the fire blight problem in the near future.

One means of biocontrol is application of naturally antagonistic organisms for fire blight control. This approach is already used widely in complex with traditional methods. Several commercial products are available based on *Pseudomonas fluorescens* (Blight Ban®), *Bacillus subtilis* (BioPro®, Serenade®), and *Aureobasidium pullulans* (Blossom Protect®) (Broggini et al., 2005; Johnson & Stockwell, 1998). In addition, new products are at various stages of development in Europe, North America, and New Zealand, (Blossom Bless®) based on *Pantoea agglomerans* (formerly *Erwinia herbicola, Enterobacter agglomerans*) (Pusey et al., 2011). *P. agglomerans* is a very common bacterial species isolated from fire blight–susceptible plants and it reduces fire-blight development by antibiosis and outcompeting *E. amylovora* (Johnson & Stockwell, 1998; Wang et al., 2012).

Further research to gain a deep understanding of the molecular interactions between *E. amylovora* and its known natural antagonistic microbes would lead to the creation of next-generation fire-blight control products. The complex of fire blight control measures mentioned here has better efficacy on the moderately susceptible or resistant apple cultivars. Contemporary apple cultivars vary in susceptibility to fire blight infection (Table 1.2).

Table 1.2: Relative susceptibility of common apple and pear cultivars to fire blight		
Highly Susceptible	**Moderately Susceptible**	**Moderately Resistant**
Apple		
Beacon Cortland Fuji Gala Granny Smith Idared Jonathan Lodi Monroe Mutsu (Crispin) Paulared Rome Beauty Wayne Wealthy Yellow Transparent Ginger gold	Dutchess Empire Golden Delicious Haralson Jonagold Jonamac Jerseymac Liberty McIntosh Minjon Northern Spy Novamac Spartan Honeycrisp Braeburn Winsap/Staymen strains	Jonafree Melrose Northwestern Greening Nova Easygro Prima Priscilla Quinte Red Delicious Red Free Sir Prize Pristine Liberty Goldrush Enterprize Sundance Williams Pride
Pear		
Aurora Bartlett Bosc Clapp's Favorite Red Bartlett Reimer Red Starkrimson	Maxine Seckel Beurre D'Anjou	Kieffer Magness Moonglow Harrow Delight Honeysweet Blake's Pride

Research also showed that there are several varieties of wild *Malus* species which are resistant to fire blight. They can serve as sources of resistance for breeding programs (Durel et al., 2009; Gardiner et al., 2012; Harshman et al., 2017). Traditional breeding would be the slowest method for those resistant traits to be transferred into commercial varieties. In addition, the resulting cultivars could have unpredictable phenotypes in terms of fruit quality and other industrially important traits.

Molecular marker-assisted breeding would be a powerful tool for resistance transfer but is still time-consuming. The quickest and most precise method would be apple plant transformation with well-characterized genes, conferring resistance to pathogens. For that, intensive research of the apple – *E. amylovora* pathosystem should be carried out to identify precise molecular mechanisms of resistance. Then, candidate genes can be transformed into already well-established apple cultivars to confer fire blight resistance.

1.4 Plant immunity general overview

Plants are immobile organisms; they are severely limited in their ability to avoid the variety of pathogens present in the environment. Plants develop and reproduce under constant pressure of pathogenic microbes, such as bacteria, viruses, fungi and oomycetes. Nevertheless, the majority of plants are resistant to the majority of the pathogens they encounter.

As the simplest means of protection, plants defend themselves from a variety of pathogens by physical barriers, including a rigid plant cell wall, leaf cuticle and the production of secondary metabolites with antimicrobial effects (Hematy et al., 2009; Martin, 1964; Paiva et al., 2010). Another weak point for microbial invasion is opened stomata, hence plants have evolved a mechanism of stomata closure following pathogen perception (Sawinski et al., 2013). Despite this, some successful pathogens can overcome these barriers and eventually get through the cell wall. As plants do not have specialized immune cells freely migrating throughout their body, each cell of the plant is capable of detecting the pathogen itself, or the modifications of plant host targets mediated by the pathogen. This consequently results in an innate immunity response restricting pathogen growth and multiplication.

Contemporary understanding of plant immunity states it as a multi-layered system, and it can be divided into two branches: PAMP (pathogen-associated molecular pattern)- triggered immunity (PTI), and effector-triggered immunity (ETI) (Figure 1.5). Effectors are molecules translocated by a pathogen into the host plant cell or extracellular matrix in order to suppress innate immunity, consequently promoting the pathogen's ability to colonize the plant host. Effectors usually suppress PTI as it is the first layer of immunity. Plants, in turn, evolved

resistance (R) proteins which can recognize effectors resulting in ETI; this was first reported in flax as gene-for-gene interactions (Flor, 1942, 1955).

Under evolutionary pressure, pathogens constantly develop/acquire new effectors to suppress plant immunity. Meanwhile plants, in response, develop new R proteins in order to recognize these new effectors and activate ETI. This situation is commonly referred to as a co-evolutionary arms race (Jones & Dangl, 2006).

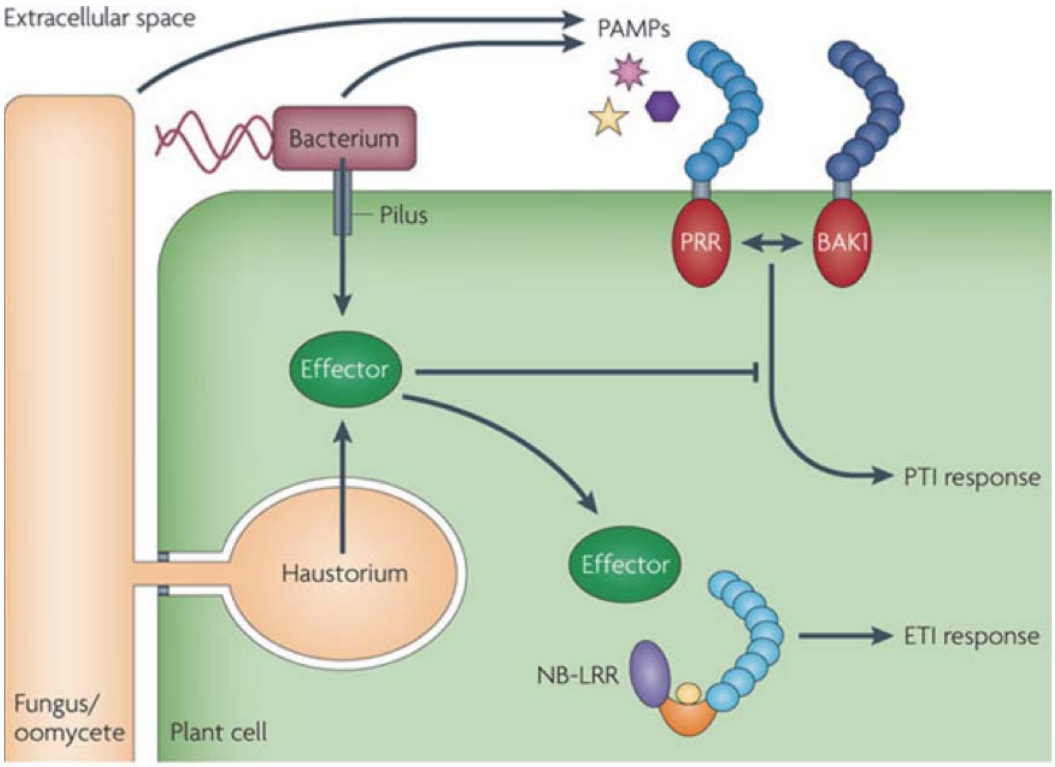

Figure 1.5: Schematic representation of plant immunity. Bacterial and fungus/oomycete pathogens' PAMPs (Pathogen Associated Molecular Patterns) can be recognized by PRRs (Pattern Recognition Receptor) resulting in activation of PTI (Pathogen Triggered Immunity). Pathogens secrete effectors into the host plant to suppress PTI, these effectors can be recognized by intercellular receptors activating ETI (Effector Triggered Immunity). Reproduced from P. Dodds and J. Rathjen, Nature Review Genetics, 2010.

As more data have been acquired about plant immunity, it has become clear that we cannot always clearly divide PTI and ETI, or PAMPs and effectors (Thomma et al., 2011). Taking that into account, a new alternative model of plant immunity was proposed where plant IP receptors (IPRs) recognize so-called invasion patterns (IPs), leading to an IP-triggered response(s) (IPTR) (Cook et al., 2015).

1.5 PAMP-triggered immunity

If a pathogen is able to penetrate the physical barriers of the host, including the waxy cuticle and cell wall, it faces the first line of innate immunity – PTI. PTI is activated in plants in response to molecules that are typically conserved among a broad range of pathogens, therefore called pathogen associated molecular patterns (PAMPs). PAMPs are generally highly conserved, usually surface exposed or secreted molecules from the pathogen into the plant host extracellular matrix, where they are recognized by plant host pattern-recognition receptors (PRRs) located in the plant cell membrane (Figure 1.6). These PRRs specifically bind their corresponding PAMPs and activate a signaling cascade in the plant cell, associated with defense (Chisholm et al., 2006; Zipfel & Robatzek, 2010).

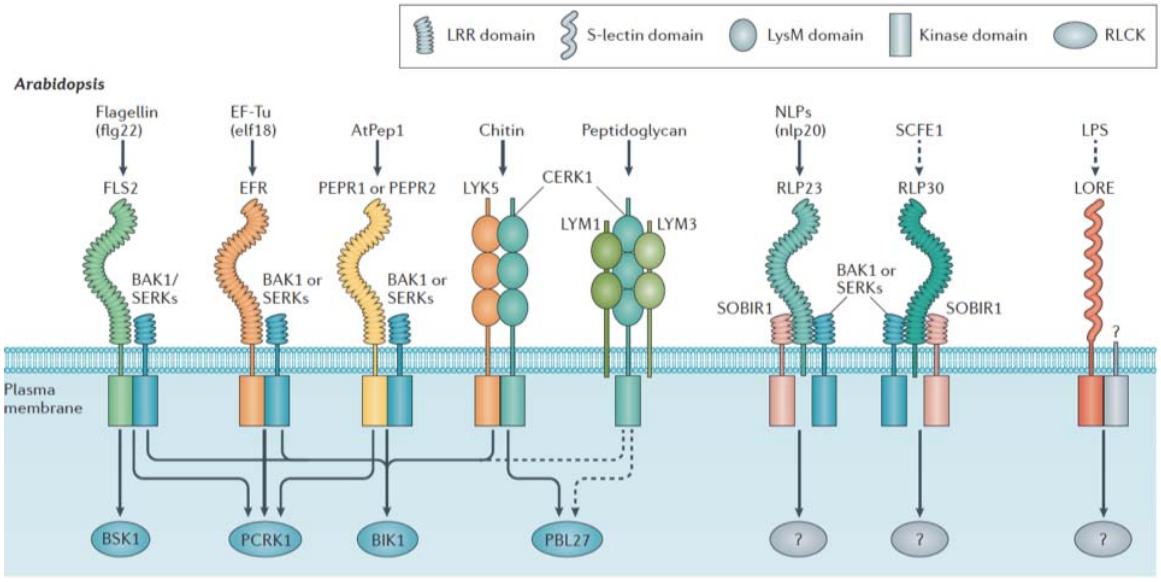

Figure 1.6: Pattern recognition receptors (PRRs) recognize multiple PAMPs from bacteria (flagellin, EF-Tu, peptidoglycan, LPS), fungi (chitin, SCFE1), necrosis-inducing peptides (NLPs), or damage-associated molecules (AtPep1). PRRs signal downstream with different RLCKs: in Arabidopsis, BAK1 (BRI1-ASSOCIATED KINASE 1)/SERK3 (SOMATIC EMBRYOGENESIS RECEPTOR KINASE 3), related SERKs and CERK1 (CHITIN ELICITOR RECEPTOR KINASE 1) are recruited upon flagellin, EF-Tu and AtPep1 perception. LRR–RLP–SOBIR1 (SUPPRESSOR OF BIR1,1) complexes recruit BAK1 and SERKs for NLPs and SCFE1 perception. No RLCKs interacting with the LPS-detecting LORE S-lectin-receptor kinase have yet been identified. Reproduced from Couto & Zipfel, 2016.

Bacterial PAMPs reported to date include flagellin, which forms motility structure flagellum (Felix et al., 1999); elongation factor-Tu (EF-Tu) (Kunze et al., 2004); peptidoglycan (PGN) – structural element of bacterial cell walls (Gust, 2015); lipopolysaccharide (LPS) embedded in cell walls of Gram-negative bacteria (Newman et al., 2007); and cytoplasmic cold-shock protein (CSP) (Felix & Boller, 2003).

A good example of fungus-derived PAMPs is chitin, which is recognized by CHITIN OLIGOSACCHARIDE ELICITOR BINDING PROTEIN (CEBiP) carrying a LysM-domain in rice and Arabidopsis (Kaku et al., 2006). Another fungal PAMP is ETHYLENE-INDUCING XYLANASES (EIX) recognized in tomato by receptor-like protein PRRs LeEIX1 and LeEIX2 (Ron & Avni, 2004).

1.5.1 PAMP recognizing receptors

The best-studied example of a PAMP is flagellin. It is a structural element of bacterial flagella, so it is present in most bacterial species, hence most known plants can recognize it (Felix et al., 1999). It was shown that a specific epitope at the N-terminus of the flagellin peptide comprising 22 amino acids in length (flg22) can be recognized via direct binding by the plant leucine-rich repeat receptor-like kinase (LRR-RLK) PRR, FLAGELLIN SENSING 2 (FLS2) (Chinchilla et al., 2006). Another well-studied PAMP, EF-Tu was shown to be recognized by a *Brassicaceae* specific LRR-RLK, ELONGATION FACTOR-TU RECEPTOR (EFR) (Kunze et al., 2004; Zipfel et al., 2006). Furthermore, PGN was shown to be recognized in Arabidopsis by a paired LysM-domain carrying receptor, consisting of LYM1 and LYM3 in complex with LysM-domain carrying RLK, CERK1/LYK1 (Willmann et al., 2011). In a recent study, the PRRs recognizing LPS (a bulb-type lectin S-domain-1 receptor-like kinase, LORE) was found in Arabidopsis (Ranf et al., 2015). Another PRR, recognizing cold-shock proteins (the RLK-type COLD SHOCK PROTEIN RECEPTOR, CORE) was identified in *N. benthamiana* (Wang et al., 2016). Interestingly, EF-Tu and cold-shock protein are intracellular and it is not clearly known how are they sensed *in planta*, even though there is a theory stating that bacterial cell wall rupture during infection allows the release of some PAMPs, leading to their recognition (Granado et al., 1995).

Significantly less is known about fungal PAMPs, including ethylene-inducing xylanases (EIX) and chitin. EIX are recognized in tomato by receptor-like protein

PRRs LeEIX1 and LeEIX2 (Ron & Avni, 2004) and chitin is recognized by LysM-domain carrying chitin oligosaccharide elicitor binding protein (CEBiP) in Arabidopsis and rice (Kaku et al., 2006).

Mutant plants with non-functional PRRs are more susceptible to infection and cannot recognize the corresponding PAMPs. This was shown in Arabidopsis where plants with *fls2*, *efr*, *lore* or *lym1/lym3* knock out mutations show increased susceptibility to pathogen infection (Ranf et al., 2015; Willmann et al., 2011; Zipfel, 2014; Zipfel et al., 2006; Zipfel et al., 2004).

1.5.2 Signaling during PTI

Perception of bacterial flagellin by FLS2 was the first PAMP recognition characterized in plants (Gomez-Gomez & Boller, 2000). It was found that the minimal domain of flagellin comprising 22 amino acid residues (flg22) is sufficient to initiate defense signaling (Chinchilla et al., 2006). It was shown that upon flg22 treatment, FLS2 associates with BAK1 (BRI1-ASSOCIATED KINASE 1) mediating FLS2 endocytosis in Arabidopsis (Chinchilla et al., 2007). Interestingly, BAK1-silenced plants lack a broad range of PAMP signaling responses and this indicates a shared signaling mechanism downstream with different PRRs (Heese et al., 2007; Liebrand et al., 2014; Zipfel, 2008). These include EFR, PEPR1/PEPR2 that recognize damage-signaling peptide Pep1 produced by the host plant (Postel et al., 2010; Yamaguchi et al., 2010; Yamaguchi et al., 2006), RLP23 recognizing necrosis and ethylene-inducing peptide 1-like proteins (NLPs) from a variety of pathogens (Albert et al., 2015), RLP30 recognizing *Sclerotinia sclerotiorum* PAMP SsE1 (Zhang et al., 2013), and CORE recognizing cold-shock protein from bacteria (Wang et al., 2016). Interestingly BAK1 is not required for recognition of chitin (via CERK1) or LPS (via LORE), suggesting the presence of several downstream signaling regulators involved in PTI.

In addition to BAK1, another downstream signaling component was found in tomato. Tomato RLPs Cf-4 (considered an ETI component recognizing the effector Avr4 from fungal pathogen *Cladosporium fulvum*) and Ve1 (recognizing Ave1 from fungal pathogen *Verticillium dahliae*) were shown to require a homolog of Arabidopsis RLK protein SUPPRESSOR OF BIR1,1/EVERSHED (SOBIR1/EVR) (Liebrand et al., 2013). Further research showed that SOBIR1 is required for immunity triggered by many RLPs, including already mentioned RLP30 and

RLP23, also dependent on BAK1 (Albert et al., 2015; Zhang et al., 2013). Taken together these data indicate that SOBIR1 is a regulatory RLK specifically involved in RLP complexes. Initially, the *SOBIR1* gene was identified as a suppressor of autoimmunity triggered by the absence of the RLK *BIR1* (BAK1-INTERACTING RECEPTOR1) (Gao et al., 2009).

Based on these findings, the current model proposes that BIR1 and its homologs act as suppressors for BAK1 and SOBIR1 signaling, triggered by their associations with each other (Dominguez-Ferreras et al., 2015; Liu et al., 2016). FLS2, EFR and CERK1 also interact with receptor like cytoplasmic kinase BOTRYTIS-INDUCED KINASE1 (BIK1) which was reported to be phosphorylated by BAK1 and is involved in PTI signaling (Lu et al., 2010). This phosphorylation event is followed by rapid calcium influx and calcium-dependent kinase activation (Boudsocq et al., 2010), mitogen-activated protein kinase (MAPK) cascade activation (Pitzschke et al., 2009) and reactive oxygen species accumulation (ROS burst) through NADPH oxidases like RBOHD (Smith & Heese, 2014).

PTI results in a variety of chemical and biological responses; this includes ion fluxes, rapid ROS production, cell wall reinforcement (including callose deposition), MAPK cascade activation and rapid defense gene expression (Bigeard et al., 2015; Zhang & Klessig, 2001; Zipfel, 2008). Research was conducted to elucidate how signaling occurs from an activated PRR to MAPK cascade and consequently to transcription factors for plant defense genes. The current understanding is that after PRR activation, the direct transphosphorylation of receptor like cytoplasmic kinases (RLCKs), like BIK1 and other PBS1-like (PBLs) RLCKs, results in phosphorylation of MAPKKKs/MEKKs (like MEKK1 or MAPKKK5), which is followed by phosphorylation of MAPKKs (like MKK4/MKK5 or MKK1/MKK2), then phosphorylation and activation of MAPKs (MPK3/MPK6 or MPK4/MPK11); this finally results in activation of transcription factors (Bigeard et al., 2015; Couto & Zipfel, 2016; Yamada et al., 2016).

1.6 Effectors of plant pathogens

In order to overcome plant innate immunity, many oomycete, fungal and bacterial plant pathogens deliver effectors into plant cells. Many pathogens initially invade the plant organism through open stomata and wounds in the plant epidermis. In addition, oomycete and fungal pathogens often develop specialized

structures called appressoria to penetrate the waxy cuticle of plants to get to the apoplast (Stergiopoulos & de Wit, 2009).

When primary physical barriers of plant defense are overcome, plant pathogenic bacteria mostly utilize a type III secretion system (T3SS) to translocate effectors into the plant host cell, prevent immunity responses and promote virulence (Feng & Zhou, 2012). The T3SS is an ancient structure and appears to be related to the flagellar system of bacteria, nevertheless there are more secretion systems playing a role in pathogenicity and may also be of interest.

In contrast to bacteria, fungal and oomycete effectors and their delivery systems are far less studied to date. It is known that fungal and oomycete effectors are largely translocated through haustoria (e.g. *Melamspora lini* and *Phytophtora infestans*) or directly through many filamentous hyphae within the plant tissue (e.g. *Cladosporium fulvum*) (Dou & Zhou, 2012; Stergiopoulos & de Wit, 2009). While these structures have been known for a long time, the precise molecular mechanisms underlying fungal and oomycete effector delivery remain unclear.

1.6.1 Effector delivery from bacterial pathogens

As plant pathogenic bacteria do not have any specialized structures for plant tissue entry, they usually utilize open stomata or wounds on a leaf surface; in addition bacteria can utilize feeding structures of their insect vectors (Jin et al., 2003; Katagiri et al., 2002). Members of the *Pseudomonas* family developed an interesting way to cause wounds in plants via expression of ice nucleating proteins, which allow ice crystal formation and plant tissue rupture (Hirano & Upper, 2000). The moment bacterial pathogens get into the plant apoplast, their gene expression profile changes dramatically, allowing them to assemble effector delivery structures and perform effector translocation into plant cells to cause disease (Tang et al., 2006). Type III and IV are the most studied effector delivery systems in bacteria to date, however other systems may play an important role and more research in this area is required.

The type I secretion system (T1SS), was studied in *Escherichia coli* and allows haemolysin secretion (Koronakis et al., 1991). This basic system comprising three components is responsible for protein transport across the cell membrane of the majority of Gram-negative mammalian pathogens. This system involves an ATP-binding cassette (ABC) transporter or a proton-antiporter, an adaptor protein

connecting the inner membrane and outer membrane, and an outer membrane pore protein. Type 1 secretion is a simple one step process and it is involved in the transport of cytotoxins, lipases, bacteriocins and haem-acquisition proteins in mammalian pathogens (Fronzes et al., 2009; Omori & Idei, 2003). *Xanthomonas oryzae pv. oryzae* avirulent AvrXa21/RaxX is the only effector known to date in plant pathogenic bacteria to be translocated through the T1SS (Lee et al., 2006; Pruitt et al., 2015).

The type III secretion system is the most important and consequently the best studied pathogenic bacterial effector delivery system to date. It forms a complex injectisome that is able to pierce the host cell membrane and deliver effectors in one step from the bacterial cytoplasm to the host cell of either mammals or plants (Cornelis & Van Gijsegem, 2000; Galan & Wolf-Watz, 2006; Hueck, 1998). The T3SS is a major pathogenicity determinant in plant-bacterial interactions; consequently, loss of the T3SS often results in complete loss of pathogenicity (He et al., 2004).

There is a strong evolutionary link between the bacterial flagella assembly system and the T3SS. Injectisome complex formation comprises ordered secretion and assembly, a system highly similar to flagellum assembly (Kubori et al., 2000; Van Gijsegem et al., 1995) (Figure 1.7); this suggests that the T3SS originated from flagella assembly systems.

The T3SS of plant pathogenic bacteria is encoded by *hrp* (hypersensitive response and pathogenicity) and *hrc* (hr and conserved) gene clusters (Buell et al., 2003; Diepold & Wagner, 2014). *hrp/hrc* gene clusters of model plant pathogen *Pseudomonas syringae* pv. tomato DC3000 are well studied and contain at least 27 open reading frames (ORFs) including around 3-5 genes coding for transcriptional regulators, around 15 coding for structural components, and a set of putative secreted effectors (Buttner, 2012; Galan & Wolf-Watz, 2006; Jin et al., 2003).

While regulation and structure of the T3SS shows relative conservation, the set of translocated effectors varies significantly among bacterial species. The central part of the T3SS is the needle complex, first identified in *Salmonella typhimurium* (Kubori et al., 1998). This complex is assembled by *hrp/hrc* gene products expressed under control of a cis-acting hrp-box promoter. This promoter element activates gene expression under the conditions typical for plant interior such as low osmotic strength, low pH and low nutrition availability (Jin et al., 2003;

Tang et al., 2006). HrpL, HrpR and HrpS are known regulators of the T3SS in *P.* syringae (Innes et al., 1993; Xiao et al., 1994), where HrpL is an alternative sigma factor of RNA polymerase regulated by HrpR and HrpS. The HrpL sigma factor RNA polymerase recognizes the hrp-box (with consensus: GGAACC–n15-17-C/ACACNCA), which can be found upstream of injectisome-related and effector-related genes (Ferreira et al., 2006; He et al., 2004).

As mentioned before, genes coding for injectisome structural proteins and its regulators are well conserved among bacterial species, while genes coding for effector-related proteins seem to be significantly diversified. This fact allows speculation that the effector set present in a bacterial pathogen defines its host specificity (Alfano & Collmer, 2004).

Most, if not all, T3SS translocated proteins carry a non-cleavable secretion signal at the N-terminus required for T3SS-mediated delivery, but no clear peptide conservation has been found yet (Samudrala et al., 2009). In addition, some effectors are too big to be translocated through the T3SS in a folded state, so they require their own specific chaperone proteins often encoded in the same operon with the effector itself. In addition to transport, these chaperones can be important for correct effector protein folding after translocation, as well as for targeting to the T3SS (Lohou et al., 2013).

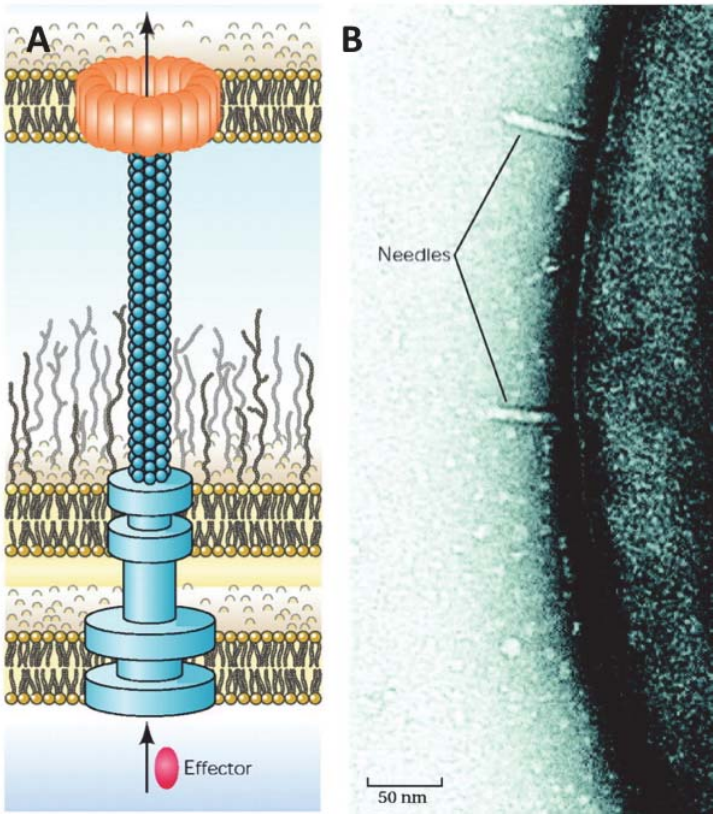

Figure 1.7: Bacterial pathogens deliver effectors through type 3 secretion system (T3SS). T3SS pilus is used upon the contact with the host cell for translocation of effectors into the host cell cytosol **(A)**. Electron micrograph **(B)** of the surface of *Yersinia enterocolitica* with protruding needles. Image courtesy of L. Journet (Biozentrum der Universität Basel). Reproduced from P. Troisfontaines and G.R. Cornelis, Physiology, 2005.

The type IV secretion system (T4SS) was characterized in the crown gall pathogen *Agrobacterium tumefaciens*. The T4SS is assumed to be evolutionailry related to bacterial twitching motility and ancient bacterial conjugation processes. Similar to the T3SS, the T4SS seems to originate from these systems via specialization (Christie et al., 2005; Mattick, 2002). A notable feature of the T4SS is the ability to translocate both proteins and DNA; this is utilized by *A. tumefaciens* to deliver its T-DNA into the plant host. The translocated T-DNA integrates into the plant genome and causes crown gall development when expressed *in planta*. Most T4SSs identified in other bacterial species are closely related to *A. tumefaciens* virB/virD4 system employing around 12 proteins to deliver a wide variety of substrate proteins for many functions (Fronzes et al., 2009). In *Agrobacterium*,

these T4SS components are often encoded by a Ti (tumor-inducing) plasmid (Vergunst et al., 2000).

There are more secretion systems known in bacteria, but none of them except the mentioned ones, were shown to play a role in plant-bacterial interactions.

1.6.2 Effector delivery from oomycete and fungal pathogens

After getting into the host plant apoplast, oomycete and fungal pathogens secrete effectors to promote their virulence. These pathogens can form cellular invaginations called haustoria or invasive hyphae, which are used for effector delivery and as feeding structures for nutrient intake (e.g. *Hyaloperonospora*, *Albugo*, *Phytophthora*, *Colletotrichum*, *Melampsora*, *Blumeria*, and *Magnaporthe*), or the pathogen simply secretes effectors into the plant apoplast by the many filamentous hyphae (eg. *Cladosporium*, *Botrytis*, *Sclerotinia*, *Leptosphaeria*, and *Fusarium*) (Dou & Zhou, 2012; Petre & Kamoun, 2014; Selin et al., 2016; Stergiopoulos & de Wit, 2009) (Figure 1.8).

Based on the studies of *Hyaloperonospora arabidopsidis* and *Phytophthora* spp., effectors of oomycete pathogens often carry one of three known amino acid motifs at their N-terminus, which are predicted to participate in secretion into the plant cell: an RxLR (often followed by a downstream dEER) motif, LxLFLAK (or crinkler/CRN) motif, or CHxC motif. These motifs are located downstream of the signal peptide, which is employed for peptide transport from the pathogen (Jiang et al., 2008; Rehmany et al., 2005; Selin et al., 2016). The RxLR-dEER motif is the best-studied example of translocation signal peptide (Jiang et al., 2008; Tyler et al., 2006). Further study of its RxLR part revealed the fact that these motifs are involved in binding the plant-derived phospholipid PI3P abundant at the haustoria/plant interface, this binding allows transport of the effector into the plant cell via lipid raft-mediated endocytosis (Kale et al., 2010). Recent study implies importance of the RxLR motif for effector processing. The RxLR motif of effector protein AVR3a from *P. infestans* is cleaved off before or during effector secretion so its traditional role in uptake by the plant is questioned. Supporting this, the cleavage site where RxLR is processed is conserved among *P. infestans* effectors (Wawra et al., 2017). In addition, the domain downstream of the RxLR appears to be N-acetylated, and this only occurs inside the host plant cell (Starheim

et al., 2012; Wawra et al., 2017). Interestingly, another RxLR effector Avh241 from *Phytophthora sojae* has a myristoylation motif just following its RxLR motif and myristoylation is known to mainly occur at protein N-termini (Yu et al., 2012).

Due to these contradicting experiments, there is no clear consensus on how RxLR-dEER effectors are delivered into the plant cell (Petre & Kamoun, 2014; Yaeno & Shirasu, 2013). Recent bioinformatics analysis of *Phytophthora* RxLR effectors identified a secondary C-terminal three-α-helix fold called WY motif, suggested to bind PI3P as well (Jiang et al., 2013; Win et al., 2012; Yaeno & Shirasu, 2013).

Fungal pathogens initially penetrate the plant epidermal layer through stomata, wounds or using hyphopodia and appressoria. When the hyphae gets to the apoplast, the pathogen develops intracellular invasive hyphae or extracellular hyphae that generate feeding structures (haustoria) into host cells (Lo Presti & Kahmann, 2017). The haustoria is not penetrating the cell membrane but surrounded by it.

In case of *Ustilago maydis* and maize pathosystem interface matrix between invasive hyphae and the host plasma membrane is continuous with plant apoplast (Bauer et al., 1997). In contrast, in case of *Magnaporthe oryzae* and rice pathosystem this interface matrix is separated from plant apoplast by a neckband (structure formed at the hyphae invasion site) (Heath, 1976). Further effector delivery mechanisms were studies in different fungal pathogen species. For example, powdery mildew and smut fungi induce the formation of exosomes/vesicles in the interface matrix between haustoria and host plant membrane and multivesicular bodies in the fungal and plant cells which seem to be responsible for fungal effector transport (Qianli et al., 2006; Ridout et al., 2006; Rutter & Innes, 2017).

In the *M. oryzae* and rice pathosystem cytoplasmic effectors are proposed to be translocated by unconventional, golgi-independent, secretory pathway. They accumulate in so called biotrophic interfacial complexes (BICs) prior entering the plant cell (Giraldo et al., 2013; Khang et al., 2010). BICs are membrane-rich plant structures which firstly form at the tip of biotrophic hyphae and then move to the side of differentiated invasive hyphae (Khang et al., 2010). Recently the role of Rbf1 effector was shown as contribution to invasive hyphae and BICs formation

(Nishimura et al., 2016). Unfortunately, precise molecular mechanisms of fungal effector delivery are yet to be discovered.

Several studies identified RxLR-like motifs, but with no analogous dEER motif downstream in some fungal secreted peptides in aforementioned BICs. This is to further support convergent evolution of RxLR-like motifs in oomycete and fungal pathogens and the importance of PI3P binding for the effector uptake into the pant cell (Kale et al., 2010; Rafiqi et al., 2010; Tyler et al., 2013).

MiSSP7 effector from *Laccaria bicolor* uptake was shown to be dependent on degenerate RXLR-like motif, similarly to oomycete effector translocation (Plett et al.). Similar RXLR-like motifs were also identified in wheat rust effector Ps87, *Fusarium oxysporum* f.sp. *lycopersici* effector Avr2, *Leptosphaerica maculans* effector AvrLm6 and flax rust effector AvrL567. Their role is speculated to be similar to one in oomycete effector uptake via PI3P-mediated endocytosis by a plant host cell (Gu et al., 2011; Kale et al., 2010).

Interestingly, recent studies point out that uptake of the *F. oxysporum* f.sp. *lycopersici* Avr2 effector is dependent on an unknown factor provided by this pathogen and, interestingly, by *Agrobacterium tumefaciens* (Di et al., 2016). In contrast, flax rust effector AvrM uptake by a plant cell was reported to be mediated by hydrophobic patch rather than by a degenerate RXLR-like motif of the effector (Rafiqi et al., 2010; Ve et al., 2013).

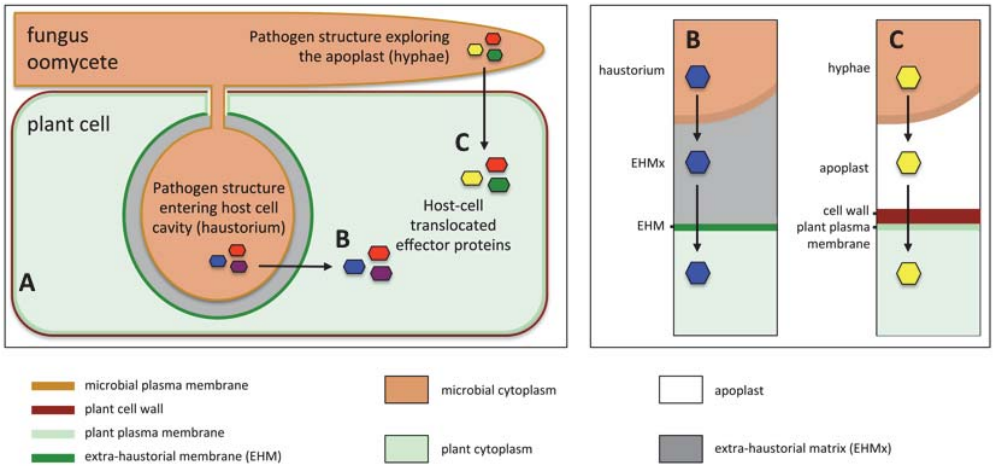

Figure 1.8: Fungal and oomycete structures for effector secretion. (A) Oomycete and fungal plant pathogens differentiate infection structures such as invasive hyphae and haustoria that penetrate the host cell and invaginate the plasma membrane. Haustoria **(B)** and hyphae **(C)** secrete effectors that are translocated into the host cell cytoplasm by unknown mechanisms. Reproduced from B. Petre, S. Kamoun, 2014.

1.7 Effectors and their recognition

Pathogen-delivered effectors were initially discovered in the context of their recognition by the plant immune system triggering an avirulence response, usually resulting in a localized and tightly controlled cell death of infected plant tissue – a process also known as the hypersensitive response (HR). Based on that, effectors were characterized as avirulence proteins, encoded by *avr* genes (Bent et al., 1993; Dong et al., 1991; Staskawicz et al., 1984).

The first plant pathogenic bacterial effector to be cloned was *P. syringae* AvrA, which induced an avirulence response in soybean plants having the *RPG2 R* gene (Staskawicz et al., 1984). Since then, constant improvement of bacterial and plant genome manipulation techniques and accumulating genome sequencing data, along with sophisticated bioinformatics tool development, allowed researchers to identify and characterize a number of avirulence effectors from a variety of plant-microbe pathosystems (Rouxel & Balesdent, 2010).

One of the most well-studied is the pathosystem of *P. syringae* with Arabidopsis. Availability of genome sequence information, well-developed and robust methods for avirulence screening, and easy propagation of the pathogen as well as the host plant allowed for quick discovery of many effectors in this system (Katagiri et al., 2002).

One of the early effectors identified in this system is AvrRpt2, coding for a cysteine protease, which triggers an immune response in Arabidopsis carrying the corresponding *R* gene *RPS2* (Mindrinos et al., 1994). Another example is AvrPto that triggers an immune response dependent on a specific allele of the *Pto R* gene in tomato (Ronald et al., 1992). In addition to AvrRpt2, *P. syringae* pv. *maculicola* and its avirulence effector AvrRpm1 was discovered to trigger recognition in Arabidopsis plants carrying the *RPM1 R* gene (Dangl et al., 1992). Moreover, another avirulent effector of *P. syringae* pv. glycinea race 4, AvrB, was found to be recognized by RPM1 in Arabidopsis and RPG1 in soybean (Innes et al., 1993). Interestingly, most bacterial effectors do not share significant homology with each other and possess a wide variety of biological activities.

In contrast to bacterial pathogens, there is significantly less known about fungal and oomycete effectors. Most of the well-characterized fungal effectors are identified and cloned from corn powdery mildew pathogen *Blumeria graminis*, barley and rye scald pathogen *Rhynchosporium secalis*, tomato leaf mold causing

Cladosporium fulvum, Fusarium wilt pathogen *Fusarium oxysporum*, rice blast pathogen *Magnaporthe oryzae* and *Brassicaceae* blackleg disease causal agent *Leptosphaeria maculans* (Stergiopoulos & de Wit, 2009).

For example, lengthy and laborious mapping of *avr* loci in segregating populations of *C. fulvum* combined with RNA sequencing data analysis led to discovery of several effectors. Of them, Avr2 is an inhibitor of the plant protease Rcr3 and is recognized by the Cf-2 resistance gene (Dixon et al., 1996), Avr4 can bind chitin to protect fungal cell walls from plant chitinases and is recognized by Cf-4 (Thomas et al., 1997), Avr4E is recognized independently by a Cf-4E homolog (Takken et al., 1999; Westerink et al., 2004), Avr5 has an unknown virulence function but recognition is facilitated by Cf-5 (Dixon et al., 1998; Mesarich et al., 2014), and Avr9 functions as a carboxypeptidase inhibitor and can be recognized by Cf-9 (Jones et al., 1994). Research on these effectors allowed identification of their corresponding *R* genes conferring resistance in wild tomato varieties, which had already been transferred into commercially cultivated tomato lines, generating *C. fulvum* resistant lines (Boukema, 1981).

Another example of a well-studied fungal plant pathogen is the causal agent of rice blast - *Magnaporthe oryzae.* Avirulent effectors, along with corresponding *R* genes, were discovered including the metalloprotease effector AVR-Pita with the rice R protein Pi-ta, AvrPia recognized by rice Pia, AvrPiz-t recognized by Piz-t, and Ace1 recognized by the R protein Pi33 (Rouxel & Balesdent, 2010). Discovery and analysis of fungal avirulence proteins is far more complicated in comparison to bacterial ones. This is due to limited genome sequence availability, the complex structure of fungal genomes, difficulties during fungal cultivation and genetic manipulation, as well as difficult plant host genetic manipulation and host genome complexity.

Similar difficulties slow down novel effector identification in oomycete plant pathogens. The most research in this field is done in potato and tomato late-blight pathogen *Phytophthora infestans*, soybean stem and root rot causal agent *Phytophthora sojae* and cruciferous downy mildew pathogen *Hyaloperonospora arabidopsidis* (Kamoun, 2006).

Most of the effectors mentioned in this chapter were identified via classical mapping approaches. Nowadays, the constantly growing volume of genomic and transcriptomic data available to researchers allow adoption of bioinformatics

methods to mine for effector candidates in a variety of fungal and oomycete pathogens. Typical pipelines to predict novel effectors involve picking the genes which code for proteins: (i) carrying secretion signals; (ii) that are rather small (usually maximum 300-400 aa in length); (iii) that are cysteine-rich (since it helps the effectors' stability in harsh extracellular conditions); (iv) carrying known effector motifs or a nuclear localization signal; (v) exhibiting similarity to haustorial proteins; and/or (vi) carrying no predicted PFAM domains, except ones associated with pathogenicity. If transcriptome data is available candidates are further filtered for: (i) upregulated expression upon pathogen proliferation in the host plant; (ii) genes with long intergenic regions; and (iii) genes containing internal repeats (Nemri et al., 2014; Saunders et al., 2012; Selin et al., 2016). To avoid complicated fungal transformation, the shortlisted effector candidates can be tested via bacterial delivery into plant host cells to validate their physiological role during pathogenesis or recognition by plant immunity components (Fabro et al., 2011; Sohn et al., 2007). The combination of bioinformatics-based effector prediction and rapid synthetic *in planta* testing will likely accelerate the discovery of novel fungal and oomycete effectors.

1.7.1 Effectors suppressing PTI

As described before, PTI can restrict pathogen growth inside the plant. Successful pathogens evolved effectors targeting PTI signaling regulators and can, therefore, prevent PTI-induced growth restriction. Other effectors were shown to target PRRs and associated proteins. In addition, some effectors target MAPK signaling cascades, essential components of PTI responses.

AvrPto from *P. syringae* was shown to interact with the kinase domains of FLS2 and EFR in order to prevent their autophosphorylation. A point mutation in AvrPto (Y89D) abolishes its interaction with FLS2 and EFR and consequently prevents PTI suppression in Arabidopsis (Xiang et al., 2008). Furthermore, AvrPto interaction with FLS2 appears to suppress BIK1 phosphorylation (Xiang et al., 2011). In addition, AvrPto also binds the RLK BAK1 preventing the formation of FLS2-BAK1 complex (Shan et al., 2008; Zhou et al., 2014). In agreement with this, AvrPto with a point mutation (S46P), which abolishes interaction with BAK1, also cannot suppress PTI (He et al., 2006).

AvrPtoB is another effector able to suppress PTI. AvrPtoB is sequence-unrelated to AvrPto and is suggested to be activated in the plant cell via serine residue phosphorylation in position 258. It is likely that AvrPtoB mimics an unknown substrate of conserved plant kinases (Xiao et al., 2007). Mutation S258A results in a non-functional AvrPtoB variant, indicating that this phosphorylation event is required for effector function (Xiao et al., 2007). AvrPtoB carries a C-terminal E3 ubiquitin-ligase domain, which leads to proteasomal degradation of its plant targets (Abramovitch et al., 2006; Gimenez-Ibanez et al., 2009; Gohre et al., 2008; Janjusevic et al., 2006). AvrPtoB was shown to target CERK1, BAK1 and FLS2, where it leads to FLS2 and CERK1 degradation via the 26S proteasome, and BAK1 kinase activity inhibition (Cheng et al., 2011; Gimenez-Ibanez et al., 2009; Gohre et al., 2008).

The HopAO1 effector from *P. syringae* is a tyrosine phosphatase and interacts with the kinase domain of EFR (Macho et al., 2014). This interaction results in reduced tyrosine phosphorylation of EFR following binding of EF-Tu (Macho et al., 2014). It was shown that Y836 in cytoplasmic EFR is required for downstream signaling but not required for EFR kinase activity. It is still to be revealed if HopAO1 interferes with Y836 phosphorylation. Interestingly, even catalytically inactive HopAO1 mediated a 20% reduction in EFR phosphorylation. In addition, HopAO1 interacts with the kinase and cytoplasmic domains of FLS2 and interferes with FLS2-mediated defense (Macho et al., 2014). Precise mechanisms of this FLS2 interference are yet to be discovered.

AvrAC (or also known as XopAC) from *X. campestris* pv. *campestris* and AvrPphB from *P. syringae* pv. *phaseolicola* both target BIK1. AvrPphB is a well-studied cysteine protease effector, which is translocated by the T3S system in an inactive state and then self-cleaves to release the active form (Puri et al., 1997; Shao et al., 2002). This active form is myristoylated inside the plant cell to target the plasma membrane where it binds and cleaves BIK1, resulting in PTI suppression (Dowen et al., 2009; Zhang et al., 2010). Additional targets of AvrPphB include receptor like cytoplasmic kinase (RLCK) PBS1 and PBS1-like (PBL) RLCKs. They all carry the Gly-Asp-Lys cleavage site processed by AvrPphB (Shao et al., 2003; Zhang et al., 2010). Finally, AvrPphB was recently shown to process RIPK (RPM1-induced protein kinase), which plays an important role in phosphorylation of RIN4 (an important immunity regulator) (Russell et al., 2015). Interestingly,

AvrPphB-mediated cleavage of PBS1 triggers immunity in plants carrying the *R* gene RPS5; further mechanism of this recognition will be described in subchapter 1.9.2 (Shao et al., 2003).

AvrAC carries an N-terminal LRR domain and C-terminal Fic (filamentation-induced by c-AMP) domain. This composition allows AvrAC to act as a uridylyl transferase and transfer uridine 5′-monophosphate (UMP) to its plant target BIK1 (Feng & Zhou, 2012). This UMP transfer event inhibits BIK1 activity and therefore suppresses the normal PTI immune response. In addition to BIK1, AvrAC also targets RIPK, PBL2 and other RLCKs of family VII, which play important roles in plant immunity (Feng & Zhou, 2012; Guy et al., 2013; Wang et al., 2015). PBL2, when uridylylated, gains the ability to interact with a preformed complex of pseudokinase RKS1 and the R protein ZAR1 and this event results in an immunity response in Arabidopsis (Wang et al., 2015).

Finally, three fungal effectors were shown to interfere with the PTI immune response. Mg3LysM from *Mycosphaerella graminicola* (Marshall et al., 2011), ECP6 from *Cladosporium fulvum* (de Jonge et al., 2010; Sanchez-Vallet et al., 2015) and Slp1 from *Magnaporthe oryzae* (Mentlak et al., 2012) are LysM containing proteins and they bind chitin to inhibit fungus recognition by plant chitin receptors. The importance of these effectors in fungal pathogenicity was shown by knock-out fungal strains lacking them that caused decreased disease symptoms on host plants (de Jonge et al., 2010; Lee et al., 2014; Mentlak et al., 2012).

1.7.2 Effectors manipulating plant phytohormones

Phytohormones are chemical regulators of plant physiology and play a very important role in plant development, reproduction, and biotic and abiotic stress responses. Rather than acting alone, hormones act in a fine-tuned balanced system to ensure plants exhibit adequate stress responses (Gimenez-Ibanez & Solano, 2013; Robert-Seilaniantz et al., 2011). Research in model plant Arabidopsis revealed that jasmonic acid (JA), ethylene (ET) and salicylic acid (SA) are key players in plant defense against pathogens. SA is often involved in response to biotrophic and hemibiotrophic pathogens, while JA and ET, acting usually antagonistically to SA, promote resistance against necrotrophic pathogens (Glazebrook, 2005).

As these major phytohormones make up a balanced system, perturbation of this system is an attractive goal for pathogens. In addition, recent research showed an important role of other phytohormones, including brassinosteroids, abscisic acid, auxin, cytokinins, and gibberellins in plant-pathogen interactions (Gimenez-Ibanez & Solano, 2013; Kazan & Lyons, 2014). As an effective strategy plant pathogens can produce phytohormone mimics to perturb the plant hormone balance.

The most studied example is the phytotoxin coronatine, synthesized by several *P. syringae* pathovars. Coronatine mimics the action of bioactive JA-isoleucine (JA-Ile) (Katsir et al., 2008). In addition to phytohormone mimics, plant pathogens can deliver effectors that target the hormone signaling pathways in the host plant cell.

For example, both HopX1 and HopZ1a from *P. syringae* target JAZ (jasmonate ZIM-domain) proteins important for correct JA signaling. JAZ proteins act as transcriptional repressors by interacting with specific transcription factors. The HopX1 effector from *P. syringae* pv. *tabaci* strain 11528 is a cysteine protease able to directly or indirectly degrade at least 8 out of 12 JAZ protein family members. This degradation event leads to JA-response activation and SA-response suppression, which is favorable for biotrophic *P. syringae* (Gimenez-Ibanez et al., 2014). JAZ proteins are also targeted by *P. syringae* effector HopZ1a. Research showed that these effectors interact with JAZ proteins from Arabidopsis and soybean plants (Jiang et al., 2013). HopZ1a is predicted to degrade JAZ proteins via the 26S proteasome pathway (Jiang et al., 2013).

One of the early discovered bacterial effectors, AvrRpt2, is a cysteine protease from *P. syringae* shown to interfere with auxin signaling (Chen et al., 2007). Studies reported that AvrRpt2 induces the degradation of the Aux/IAA (auxin/indole acetic acid) transcriptional repressor protein AXR2 and this promotes the effect of auxin (Cui et al., 2013). Interestingly, AXR2 degradation was shown to be a proteasome-dependent process, rather than mediated by direct cleavage by AvrRpt2 protease (Cui et al., 2013).

The XopD effector from *Xanthamonas* was shown to manipulate ET levels (Kim et al., 2013). This effector is nuclear localized and contains a C-terminal cysteine protease domain and ERF-associated amphiphilic repression (EAR) motifs, which were previously shown to participate in plant transcriptional

regulator activity (Kazan, 2006). The XopD cysteine protease domain shares structural similarity with yeast ubiquitin-like protease ULP1 and was reported to cleave off the SUMO protein modifier from SUMOylated proteins in tomato (Chosed et al., 2007; Hotson et al., 2003). One of the known targets is *Sl*ERF4, which is involved in ET biosynthesis regulation. In agreement with XopD-mediated destabilization of *Sl*ERF4, a reduced level of ET is observed in the plant tissues in the presence of XopD (Kim et al., 2013).

An example of a fungal effector targeting plant hormone signaling is Cmu1 from *Ustilago maydis*. This protein is a chorismate mutase that can inhibit SA biosynthesis through redirecting chorismate away from the SA biosynthetic pathway (Djamei et al., 2011). In addition, protein interactome studies of *H. arabidopsidis* and *Golovinomyces orontii* (a powdery mildew-causing fungus) allowed the identification of secreted proteins binding plant JAZ repressors, implying that the JA pathway can also be manipulated by fungal and oomycete pathogens (Mukhtar et al., 2011; Wessling et al., 2014).

1.7.3 Effectors targeting gene expression machinery

Upon pathogen invasion, plant gene expression is dramatically changed, which allows for a quick and robust response against the invading pathogen. It is a useful strategy from the side of the pathogen to interfere with the defense gene expression machinery at transcriptional or posttranscriptional levels.

A good example of effectors directly imported into the plant host cell nucleus and binding DNA are transcription activator-like (TAL) effectors from *Xanthomonas* spp. Characteristic traits of the TAL effector family include a C-terminal acidic activation domain and a nuclear localization signal (NLS) (Boch & Bonas, 2010). The NLS ensures the transport of effectors into the plant cell nucleus, while DNA binding is mediated by the central part of the TAL effectors.

This central region consists of 1.5 to 33.5 repeats with an average of approximately 17 repeats (Boch & Bonas, 2010). These repeats are nearly identical in peptide sequence and usually 33 to 35 amino acids long. The DNA sequence specific binding of TAL effectors is dependent on the polymorphic amino acids at positions 12 and 13 of each repeat, exposed on a short loop in between nearly identical alpha helices (Deng et al., 2012; Mak et al., 2012). Different sets of amino

acids in position 12 and 13 in the repeats specify binding to different nucleotides in DNA (Boch et al., 2009; Moscou & Bogdanove, 2009).

Even though the discovery of a TAL protein specific interaction with DNA sequences opens the door for new exciting biotechnological tools, the precise mechanisms of how TAL effectors alter plant gene expression is still poorly understood. Interaction studies show that TAL effectors interact with both RNA polymerase II (Domingues et al., 2012) and with negative regulators of RNA polymerase II and III (de Souza et al., 2012; Soprano et al., 2013). That would mean that TAL effectors bind the promoters of their plant target genes, altering the expression of them, consequently reducing the plant defense response.

Interestingly there are known examples of *R* genes having TAL effector recognized sequences in their promoters (Boch et al., 2014). An example of this is a group of executor *R* genes whose expression is activated via TAL effectors binding their promoter regions (Zhang et al., 2015). There are several genes, including Bs3 from pepper and Xa10, Xa23 and Xa27 from rice activated by this mechanism. Engineered executor like *R* genes with specific recognition sequences in their promoters can become a powerful tool for artificially developing defense into plant crop species (Boch et al., 2014).

Another example of an effector manipulating plant gene expression machinery is PopP2 from *Ralstonia solanacearum*. This effector localizes to the plant nucleus and acetylates lysine residues of WRKY transcription factors (Deslandes et al., 2003; Le Roux et al., 2015; Sarris et al., 2015). WRKY transcription regulators carry an N-terminal WRKY motif and zinc finger structure allowing them to bind a conserved DNA sequence, called the W box (TTGACC/T), in the promoters of target genes (Bakshi & Oelmuller, 2014; Llorca et al., 2014; Rushton et al., 2010). WRKY acetylation by PopP2 results in WRKY transcription factor dissociation from DNA and consequently inhibits target gene expression (Le Roux et al., 2015; Sarris et al., 2015). Interestingly, PopP2 is recognized by the R protein RRS1-R, which carries a C-terminal WRKY-domain mimicking effector targets (Le Roux et al., 2015; Sarris et al., 2015). Further details of this recognition will be discussed in subchapter 1.9.3.

1.7.4 Effectors interfering with the plant cell cytoskeleton

The plant cell cytoskeleton mainly consists of actin filaments and microtubules, and plays a role in many processes such as plant cell growth and division, organelle movement, vesicle trafficking, endocytosis, opening and closing stomata, and plant immune responses (Day et al., 2011; Henty-Ridilla et al., 2013). Infiltration of latrunculin B, which is a chemical able to inhibit actin polymerization, promotes susceptibility of Arabidopsis to bacterial infections and results in an increased growth of *P. syringae* pv. *tomato* DC3000 as well as its T3S-deficient mutant (Henty-Ridilla et al., 2013). Similarly, treatment of Arabidopsis with oryzalin, which disrupts microtubules, enhances the growth of *P. syringae* pv. tomato DC3000 but not of the T3S-deficient strain (Lee et al., 2012). Based on these observations it was speculated that some effectors may target microtubules in order to promote pathogen growth (Lee et al., 2012).

The HopW1 effector protein from *P. syringae* pv. *maculicola* was found to form a complex with actin after transient expression in *Nicotiana benthamiana* plants (Kang et al., 2014). Further experiments showed that HopW1 delivery by *P. syringae* pv. *tomato* DC3000 or its expression in *N. benthamiana* leaves or Arabidopsis protoplasts leads to the disruption of actin cytoskeleton of the host plant cell. This activity was also observed *in vitro* and, in agreement with this, HopW1 was shown to inhibit protein trafficking in ER and vacuole (Kang et al., 2014). The precise molecular mechanism of how HopW1 destabilizes actin is still to be elucidated.

Another two effectors that target the plant cytoskeleton are members of the YopJ family of effectors, HopZ1a from *P. syringae* and AvrBsT from *Xanthomonas* spp. HopZ1a was shown to disrupt microtubules 16 hours after delivery by *P. syringae* pv. *tomato* DC3000. Interestingly, however, no effect of HopZ1a on the actin cytoskeleton was observed (Lee et al., 2012). In agreement with this, transient expression of HopZ1a in *N. benthamiana* leaves interfered with secretion of the secGFP reporter protein to the apoplast, a process reliant on microtubules (Boutte et al., 2007; Lee et al., 2012).

AvrBsT is another effector from the YopJ family, speculated to indirectly interfere with microtubule formation. AvrBsT binds and acetylates the putative tubulin-binding protein ACIP1 (Acetylated interacting protein 1), which is also involved in plant immunity (Cheong et al., 2014). Experiments show that growth

of virulent and avirulent *P. syringae* pv. *tomato* DC3000 strains was increased in *ACIP1*-silenced Arabidopsis Pi-0 plants (Cheong et al., 2014). ACIP1 colocalizes with microtubules and, in the presence of AvrBsT, ACIP1 forms aggregates, suggesting that this effector alters the localization of ACIP1 (Cheong et al., 2014).

It is still not known if AvrBsT acetylates ACIP1 to interfere with the plant immune response and microtubule formation. Further details of these processes are subject for future research.

1.8 Effector triggered immunity in plants and R proteins

To cope with an enormous variety of effectors secreted by plant pathogens, plants had to evolve, so-called effector triggered immunity (ETI), the second layer of plant innate immunity. The ETI system recognizes specific effectors or modifications in a plant cell, mediated by these effectors. The basis of ETI is a suite of resistance genes (*R* genes) in each plant species. The classical gene for gene model postulates that each *R* gene usually confers resistance to one effector (DeYoung & Innes, 2006; Flor, 1971). *R* genes are divided into classes based on their structure and mechanism of function. There are four big groups of ETI-related *R* genes: Nucleotide-binding Leucine- rich repeat (NB-LRRs) which is by far the largest group, serine/threonine kinases that have been found to act in conjunction with NB-LRRs, receptor-like proteins (RLPs), and receptor-like kinases (RLKs). They encode R proteins that facilitate the effector recognition.

As ETI is the second line of defense, the recognition events mostly happen inside the plant host cell. Effector recognition by an R protein can be through direct interaction of an R protein and effector, or through the surveillance of plant effector targets, detecting the effector-mediated modifications of them. After recognition and activation of an R protein the signaling cascade occurs, which often culminates in a localized hypersensitive response (HR), providing the appropriate resistance against a variety of pathogens. This long-term resistance is termed as systemic acquired resistance (SAR) (Jones & Dangl, 2006; Ross, 1961). The HR is understood as a quick and very localized cell death at the infection site, which prevents further spread of pathogen cells in the plant organism (Burdon & Thrall, 2003; Dong et al., 1991; Johansson et al., 2015).

1.8.1 NB-LRRs

Nucleotide-binding leucine-rich repeat (NB-LRR) proteins comprise the largest group of plant R proteins with more than 150 members identified to date in Arabidopsis (Meyers et al., 2003). These R proteins usually consist of a variable N-terminal domain, central domain containing nucleotide binding site (NB) and two ARC subdomains (these resemble Apoptotic protease activating factor-1, R protein and *Caenorhabiditis elegans* death-4 protein domains), and a C-terminal leucine rich repeat (LRR) domain (Van Ooijen et al., 2008).

Interestingly, the aforementioned NB-LRR proteins show a certain similarity to animal NLR proteins (nucleotide-binding oligomerization domain (NOD)- and LRR-containing proteins), which play a similar role in animal immunity and cell death control.

Plant NB-LRRs possess a variable N terminal domain, which is usually either a coiled coil domain (CC) or toll/interleukin-1 receptor (TIR) domain. This domain defines the requirement for different downstream signaling components (Aarts et al., 1998). Most TIR-NB-LRRs (TNLs) require Enhanced Disease Susceptibility 1 (EDS1) and most of CC-NB-LRRs (CNL) require Non-race specific Disease Resistance 1 (NDR1) for immune response activation. In addition, the CC domain was shown to be important for interaction with accessory proteins (Lukasik & Takken, 2009). In contrast, the TIR domain is suggested to be required not only for accessory protein binding, but also for defining effector recognition specificity, and initiation of the HR (Lukasik & Takken, 2009; Swiderski et al., 2009).

The central NB-ARC domain is responsible for nucleotide binding and exchange/hydrolysis, which is required for conformational changes associated with “on” and “off” states. Furthermore, this domain is speculated to be important for additional downstream signaling functions (Collier & Moffett, 2009; Lukasik & Takken, 2009). This is supported by a report, which demonstrates that the NB domain alone of the CNL Rx is sufficient to trigger HR (Rairdan et al., 2008).

The most conserved part of NB-ARC domain is the NTPase P-loop region consisting of Walker A and Walker B domains. The P-loop has the consensus sequence GxxxxGKS/T (where x indicates any residue), in which lysine (K) binds the b- and g-phosphates while S/T binds an Mg2+ ion. This domain is necessary for the protein functions; this is supported by many loss-of-function mutations

generated to date. For example, mutation of the conserved lysine in the P-loop in most cases abolishes ATP binding (Tameling et al., 2002).

Mutations in the Walker B consensus hhhhDD/E, (where h is mostly a hydrophobic residue), also lead to loss of function phenotypes confirming the importance of the conserved aspartate (D), which is required for the indirect coordination of the Mg2+ ion via a water molecule (Hanson & Whiteheart, 2005; Leipe et al., 2004). Another hhhhToR signature (o designates an alcoholic residue) (known as the RNBS-B motif), detects the presence of the g–phosphate and relays this information to the other parts of protein (Ogura & Wilkinson, 2001).

At the end of NB-ARC domain there is a highly conserved MHD-motif (hxhHD) (Leipe et al., 2004). The histidine (H) in this motif directly interacts with the b-phosphate in APAF-1, and it seem to be involved in nucleotide-dependent conformational changes (Riedl et al., 2005). Interestingly, mutagenesis of either the histidine or aspartate in most plant NLRs leads to autoactivation and consequently a constitutive HR (Figure 1.9).

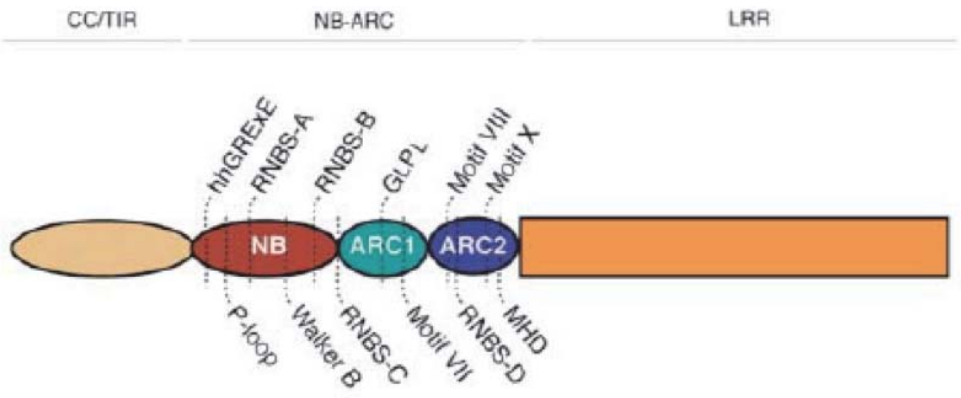

Figure 1.9: Schematic representation of important domains in NOD-Like Receptors (NLRs). P-loop motif and MHD-motif are of particular importance for NLR functioning. Reproduced from van Ooijen G et al., Annual Reviews of Phytopathology, 2007.

The LRR domain is located at the C-terminal fraction of plant NB-LRRs and is composed of a set of tandem leucine rich repeats. The structure of the LRR was studied in several non-plant LRRs crystallized to date. These repeats were shown to form barrel-like structures with a parallel β-sheet lining the inner concave

surface and α-helical structures comprising much of the rest of the domain (Kobe & Deisenhofer, 1994).

The LRR domain of plant NB-LRR proteins has been suggested as specific recognition of pathogen effector molecules. This is supported by data from animal LRR research, suggesting its involvement in protein-protein interactions (Kobe & Deisenhofer, 1994). In addition, the β-sheet portion of the LRR domain, suggested to act as a ligand-binding interface, seems to be under significant diversifying selection in many plant NB-LRR proteins (Michelmore & Meyers, 1998). The best-known evidence of effector-LRR interactions arises from the flax *L* locus research. Many structural and sequence polymorphisms in *L* alleles are confined to the LRR coding region confirming the involvement of the LRR domain in direct effector binding (Ellis et al., 1999). Furthermore, changing of the L6 or L10 alleles' native LRR domain for the one from L2 results in L2-like effector specificity (Ellis et al., 1999).

Another example is the LRR domain of rice R protein Pi-ta binding its corresponding effector Avr-Pita (Bryan et al., 2000; Jia et al., 2000). Additional function of LRR is suggested to be regulation of R protein signaling. Several studies in plants and animals are supporting this idea. For example, deletion of the LRR domain in RPS2, RPS5 and RPP1 results in an autoactive R protein variant causing constitutive activation of defense responses (Michael Weaver et al., 2006; Tao et al., 2000). Similarly, truncation of the LRR domain of the potato R protein Rx results in stronger HR, even though it is observed in an overexpression system (Bendahmane et al., 2002). In contrast to RPS5 and Rx, truncation of the LRR domain in tomato NB-LRR protein I-2 does not result in constitutive activity (Tameling et al., 2006).

In addition, many variants and loci encoding LRR truncations in the genome do not demonstrate constitutive activity (Anderson et al., 1997; Ayliffe et al., 1999; Dinesh-Kumar & Baker, 2000; Lawrence et al., 1995; Parker et al., 1997; Tameling et al., 2006). Furthermore, mutation in the RPS5 LRR domain resulted in loss of function phenotype rather than constitutive defense response activation (Warren et al., 1998). Taken together this suggests that the LRR domain indeed has a regulatory function, but the precise mechanism of this regulation is different in a variety of R proteins.

The modular structure of NLRs allows them to maintain the stable "off" state with the ability to quickly switch to "on" state and facilitate immune signaling. The central NB-ARC domain seems to facilitate this switch activity, while N- and C-terminal domains play a role in self-regulation and signal transduction. The crystal structures of CED-4 and Apaf-1 proteins from animals indicate that ATP or ADP is bound in a pocket that is mostly formed by the NB-ARC domain (Riedl et al., 2005; Yan et al., 2005). ADP seems to be bound in the inactive form of NLR. In this 'off' state, ADP coordinates many intramolecular interactions among the NB-ARC subdomains, stabilizing this structure (Riedl et al., 2005). Exchange of ADP for ATP triggers a series of conformational changes resulting in activation. Interestingly, most of the mutations in the NB-ARC domain that lead to autoimmunity map to the amino acid residues which form the ADP binding pocket (DeYoung & Innes, 2006) (Figure 1.10).

Although a lot of research was carried out on R protein function, still little is known about the mechanism of signaling activation via NLRs. It is speculated that complex interactions between NLR domains facilitates its activity.

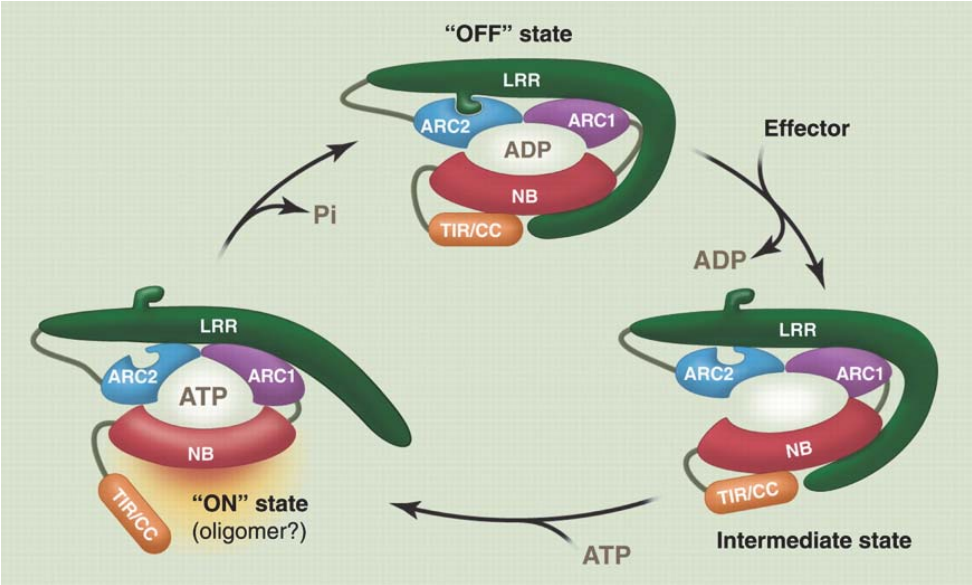

Figure 1.10: Current understanding of NLR activation. In 'OFF' state the nucleotide binding (NB) domain of NLRs is binding ADP. Upon effector perception via Leucine Reach Repeat (LRR) domain the NB domain exchanges ADP for ATP, triggering a series of conformational changes resulting in 'ON' state, which is often associated with NLR oligomerization via their Coiled Coil (CC) or Toll-Interleukin Receptor like (TIR) N-terminal domain. Reproduced from W. Tameling and F. Takken, Science, 2009.

1.8.2 Cytoplasmic serine/threonine kinases

Cytoplasmic serine/threonine kinases and pseudokinases play a significant role in ETI signaling. A small group of them have been discovered and characterized, including Pto and Fen in tomato; ZED1, PBS1, CRCK3 and PBL2 in Arabidopsis; and a novel *Rpg5* gene in barley (Bendahmane et al., 2002; Brueggeman et al., 2008; Lewis et al., 2013; Swiderski & Innes, 2001; Wang et al., 2015; Zhang et al., 2017). These kinases do not play a central role in the ETI response but they are required for correct functioning of some NLRs (Spoel & Dong, 2012).

Pto and Fen were found in wild tomato species providing resistance to *P. syringae* pv. tomato strains carrying AvrPto and AvrPtoB (Kim et al., 2002; Ronald et al., 1992). Further research identified the Pto locus carrying multiple serine/threonine kinase homologs (including Fen) that resulted in resistance in the presence of the NLR, called Prf, from the same genetic locus (Chang et al., 2002; Martin et al., 1993). Later studies provided the evidence that Pto/Prf and Fen/Prf form a multimeric transphosphorylated (P+1) molecular complex, which traps the kinase inhibitor effectors like AvrPto/AvrPtoB (Ntoukakis et al., 2013).

Another AVRPPHB SUSCEPTIBLE1 (PBS1) cytoplasmic serine/threonine kinase was identified in Arabidopsis during studies of loss of resistance against *P. syringae* pv. phaseolicola race 3 avirulent effector AvrPphB (Shao et al., 2003; Swiderski & Innes, 2001). PBS1 mimics important PTI-related kinases such as BIK1, targeted by AvrPphB, and is believed to act as a decoy activating the CNL RPS5 upon processing by AvrPphB (Zhang et al., 2010).

1.8.3 Downstream signaling during ETI

NB-LRRs are the most important and central part of ETI related proteins, yet they require a lot of other components to transduce and relay the signals for successful ETI. The major gap in contemporary understanding of ETI lies between R protein mediated effector recognition events and defense gene activation resulting in HR (Qi & Innes, 2013). However, several key regulators of ETI responses downstream of NLRs have been identified (Aarts et al., 1998). The vast majority of NLRs require members of the chaperone complex (SGT1-HSP90 complex) which is necessary for correct folding of NLRs and cellular trafficking (Shirasu, 2009).

Another NLR-downstream signaling component is ENHANCED DISEASE SUSCEPTIBILITY 1 (EDS1) that is required for signaling from the majority of known TIR N-terminal containing NLRs. EDS1 was discovered as a signaling component required for RPP1-mediated recognition of *H. arabidopsidis* effector ATR1 (Parker et al., 1996). It was shown that that the TIR domain is involved in signaling through EDS1, but it is still unknown if direct interaction is required for that (Buscaill & Rivas, 2014). Another homolog of EDS1, PHYTOALEXIN DEFICIENT 4 (PAD4), was reported to be involved in phytoalexin production and induction of PATHOGENESIS RELATED (PR) gene expression (known ETI related genes) (Feys et al., 2001; Jirage et al., 1999). EDS1 interacts with PAD4 or SENESCENCE ASSOCIATED GENE 101 (SAG101) gene products to form a complex involved in the SA signaling pathway and TNL-related plant defense signaling (Feys et al., 2005; Rietz et al., 2011).

Similar to how EDS1 is required for TNL-mediated signaling, another membrane-bound protein NON-RACE-SPECIFIC DISEASE RESISTANCE 1 (NDR1) is required for signaling via most CC-NB-LRRs, which are also generally targeted to the membrane (Aarts et al., 1998; Day et al., 2006). The molecular mechanisms underlying the signal transduction through EDS1 and NDR1 are still to be studied in detail. It seems that after these components signaling occurs through MAPK cascades, possibly overlapping with MAPK cascades involved in PTI (Dodds & Rathjen, 2010).

1.9 Direct and indirect recognition of effectors

1.9.1 Direct effector recognition

Plant NLR proteins can recognize their corresponding effectors directly or indirectly. Direct interaction was reported for a very limited pool of NLRs (Spoel & Dong, 2012). A good example of direct recognition is the Avr-Pita effector from the rice blast pathogen *Magnaporthe oryzae*. This effector is recognized by R protein Pi-ta. Pi-ta is an NB-LRR protein with a novel leucine-rich domain (LRD) located at the C-terminus, and this domain directly binds the metalloprotease Avr-Pita to facilitate recognition (Jia et al., 2000).

Another example of direct recognition is the AvrL5/6/7 effectors from flax rust pathogen *M. lini*, which are recognized by their corresponding R proteins L5,

L6 and L7. As mentioned before, recognition is mediated by highly polymorphic LRR domains of the R protein (Dodds et al., 2006).

Similar to AvrL effectors, ATR1 (ARABIDOPSIS THALIANA RECOGNIZED1) from oomycete pathogen *H. arabidopsidis (Hpa)* can be recognized by the TNL R protein RPP1 (RECOGNITION OF PERONOSPORA PARASITICA1) via direct interaction through the LRR domain (Botella et al., 1998). Direct binding of ATR1 to RPP1 was reported and several alleles of both effector and NLR were studied in depth. For example, the Niederzenz (NdA) allele of RPP1 was shown to recognize the *Hpa* Emoy2 allele of ATR1, while the Wassilewskija (WsB) allele of RPP1 can recognize *Hpa* Emoy2, Maks9, and Emco5 ATR1 alleles (Rehmany et al., 2005).

No natural alleles of RPP1 could recognize *Hpa* Cala2 ATR1, but gain of function mutations were identified to provide this recognition in an artificially generated RPP1 allele (Steinbrenner et al., 2015).

1.9.2 Indirect effector recognition and guard-guardee/decoy hypothesis

Lack of evidence of a direct interaction of effector with their corresponding R proteins, as well as the fact that some effectors can interfere with recognition of other effectors facilitated by different R proteins, led to the proposal of the indirect effector recognition model (DeYoung & Innes, 2006).

In this model, not the effector itself but the modifications mediated by the effector activity on its plant target activates the R protein. This model seems to be more evolutionary advanced because in the case of direct recognition the pathogen effectors can generate novel alleles losing the interaction with the cognate R protein but still conserving biochemical activity, thus evading the resistance. In contrast, in the case of indirect recognition the effector's biochemical activity itself triggers the immunity. This means that the effector allele should be altered to change the biochemical activity, which is, in most cases, important for pathogen virulence. The guarded protein can be an important component of the plant immunity response and thus guarded by an R protein, or it can be a so-called "decoy" which is not important for the plant but it mimics the true effector target and is guarded by an R protein.

A typical example of guarded protein is RPM1 INTERACTIN PROTEIN 4 (RIN4) which is guarded by two R proteins RPS2 and RPM1 in Arabidopsis. RIN4 is an important regulator of plant immunity and was shown to act as a PTI

regulator (Afzal et al., 2011; Afzal et al., 2013; Liu et al., 2009a; Liu et al., 2009b). At least three unrelated effectors target RIN4 – AvrRpt2, AvrRpm1 and AvrB (Axtell & Staskawicz, 2003; Chung et al., 2011; Liu et al., 2011; Mackey et al., 2003; Mackey et al., 2002).

AvrRpt2 is a cysteine protease which is delivered into the plant cell in inactive form. When inside the plant cell this effector is activated by plant host factor ROC1, which allows AvrRpt2 to cleave itself in order to release the active form, which then cleaves its plant cell targets, including RIN4, leading to RPS2 R protein activation (Coaker et al., 2006; Day et al., 2005; Mackey et al., 2003). In contrast, AvrRpm1 and AvrB stimulate the major kinase complex, including RIPK in Arabidopsis and consequently induces phosphorylation of RIN4 in three amino acid positions, leading to RPM1 activation (Chung et al., 2011; Liu et al., 2011).

Either phosphorylation or cleavage of RIN4 results in its dissociation from the corresponding R protein leading to ETI activation (Figure 1.11). Interestingly, if RIN4 is cleaved by AvrRpt2, it can no longer be effectively phosphorylated via AvrRpm1, hence failing to activate RPM1 (Mackey et al., 2002). This observation initially led researchers to speculate on the common target of these effectors.

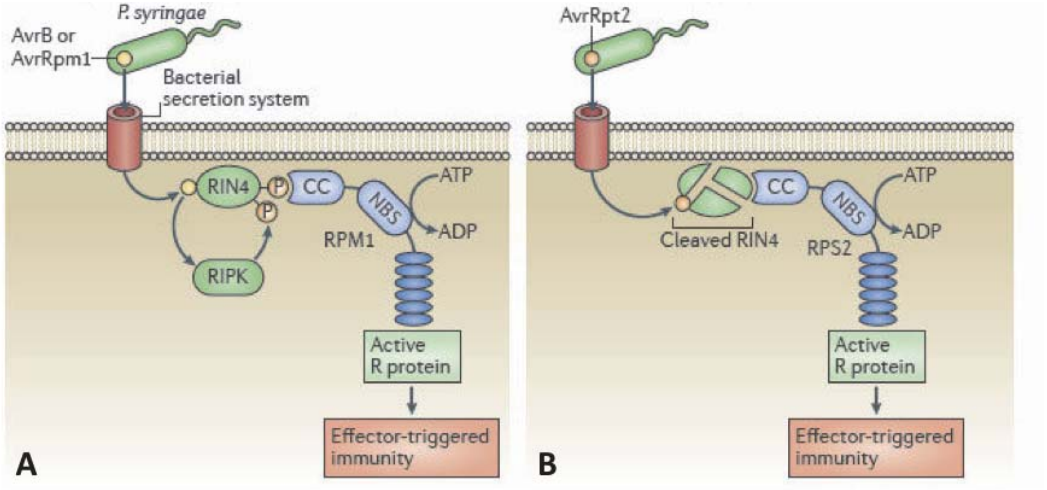

Figure 1.11: Recognition of AvrB and AvrRpm1 or AvrRpt2 effectors by RPM1 and RPS2 NLRs respectively. AvrB and AvrRpm1 stimulate plant kinase complex to phosphorylate RIN4 leading to activation of RPM1 **(A).** AvrRpt2 is a cysteine protease cleaving RIN4 in two sites to release RPS2 negative regulation and consequently activate RPS2 mediated immune response **(B).** Reproduced from S.H. Spoel and X. Dong, Nature Reviews Immunology, 2012.

An example of a guarded decoy protein is PBS1. It was not shown to be important for immune signaling, but without it the CNL RPS5 cannot facilitate AvrPphB recognition (Ade et al., 2007; Shao et al., 2003; Swiderski & Innes, 2001). AvrPphB is another cysteine protease undergoing self-cleavage in the plant cell releasing its active form, which then targets PBS1 to cleave it into two parts (Shao et al., 2003). PBS1 directly interacts with RPS5 forming the complex for AvrPphB recognition.

RPS5 'senses' the PBS1 cleavage and, thus, activates ETI (Ade et al., 2007). Interestingly, both parts of PBS1 resulting from AvrPphB-mediated cleavage are required for RPS5 activation. Furthermore, insertion of additional alanine residues in the cleavage site of PBS1 leads to RPS5 activation in the absence of AvrPphB-mediated cleavage of PBS1 (DeYoung et al., 2012). In addition, a recent study showed that native AvrPphB-processed site of PBS1 can be swapped for AvrRpt2, or Tobacco Etch Virus (TEV) protease-processed site resulting in change of effector recognition specificity (Kim et al., 2016) (Figure 1.12).

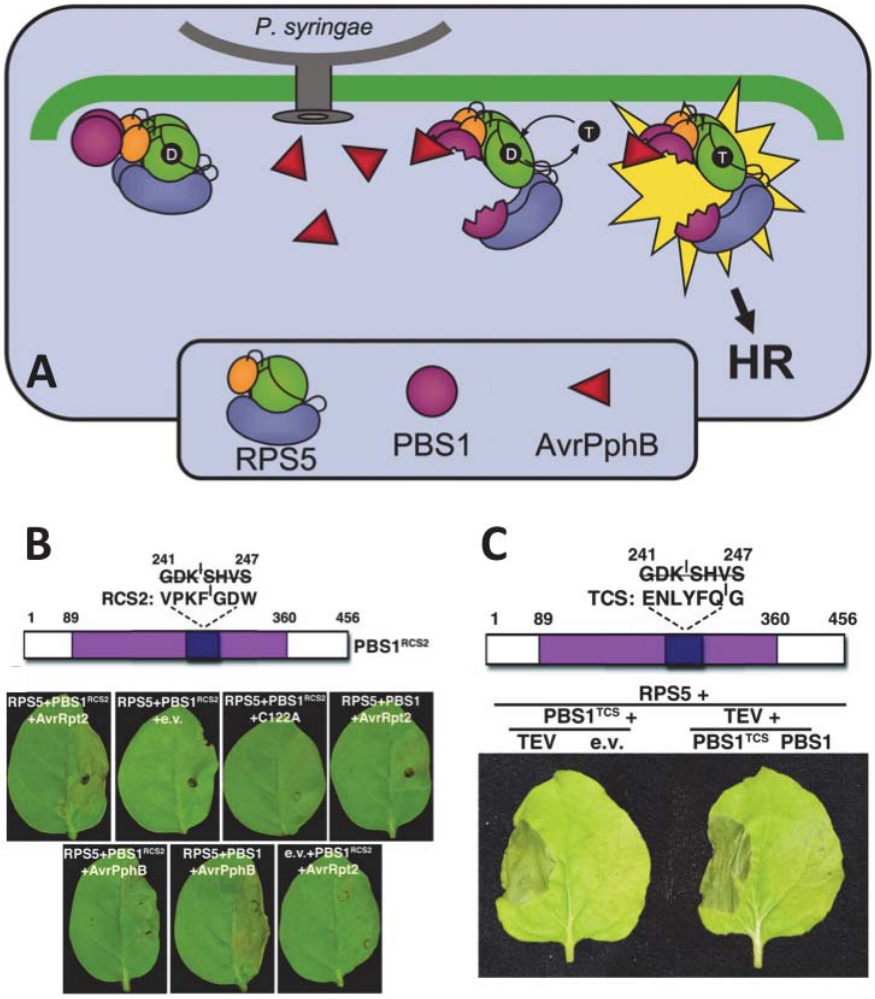

Figure 1.12: Recognition of AvrPphB effector by RPS5. RPS5 is guarding PBS1 protein which is a target of cysteine protease AvrPphB effector. AvrPphB cleaves PBS1 in two parts, both of which are required for RPS5 activation **(A)**. Native cleavage site can be replaced with the one from RIN4 (processed by AvrRpt2) **(B)** or from plant virus polyprotein (processed by viral protease protein) **(C)**, switching the RPS5 recognition from AvrPphB to AvrRpt2 or viral protease from TEV (Tobacco Etch Virus). Reproduced from J. Ade et al., PNAS, 2007 and S.H. Kim et al., Science, 2016.

This can be a promising strategy to create a new generation of engineered resistance in crops. Finally, PBS1 does not have an important function in plant physiology, so it is referred to as a decoy to trap AvrPphB for RPS5 recognition.

1.9.3 Integrated decoy as a strategy to trap effectors

A variation of direct recognition, yet showing certain similarity to the guard/decoy model, is the integrated decoy model. Some R proteins seem to incorporate the certain domains of effector targets from plants to employ them as traps or sensors to facilitate the recognition (Ellis, 2016; Sarris et al., 2016). An example of the integrated decoy model is recognition of the PopP2 effector from *Ralstonia solanacearum* by RPS4/RRS1-R paired TNLs from Arabidopsis.

PopP2 is an acetyltransferase which targets multiple WRKY transcription factors, important for plant defense signaling (Le Roux et al., 2015; Sarris et al., 2015). When PopP2 acetylates WRKY transcription factors it also acetylates the WRKY domain incorporated into the RRS1-R C-terminus. This acetylation event leads to RPS4/RRS1-R complex activation and ETI activation (Le Roux et al., 2015). It is suggested that in the RPS4/RRS1-R complex, RRS1-R acts as a sensor for PopP2, while RPS4 is an executor protein to trigger plant defense (Williams et al., 2014). This is further supported by the fact that the RRS1 variant with mutations in the P-loop still supports RPS4 activation in the presence of PopP2 (Williams et al., 2014) (Figure 1.13).

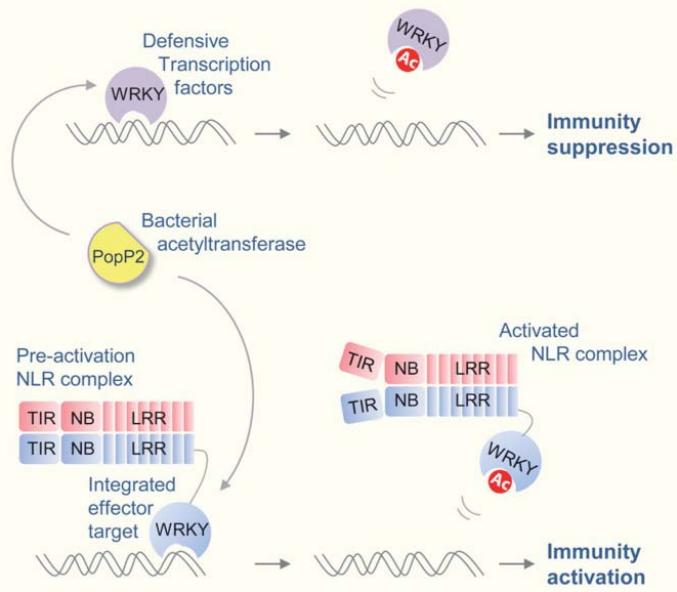

Figure 1.13: Recognition of PopP2 effector from *Ralstonia solanacearum* by RPS4-RRS1 complex. PopP2 is an acetyltransferase targeting WRKY transcription factors. PopP2 also targets the WRKY like C-terminal domain of RRS1 and this activates the RPS4-RRS1 complex. WRKY domain of RRS1 can be referred as a bait to trap the effector. Reproduced from P. Sarris et al., Cell, 2015.

1.10 Aims of this study

As apple is an important export fruit in New Zealand and is significantly affected by both bacterial and fungal pathogens, the focus of the current research was on effectors and their recognition in the host plant. Both fungal and bacterial effectors are recognized in a similar way by host plants, which allows universal strategies to be utilized for engineering resistance.

Erwinia amylovora has been studied for several decades. At the moment, fire blight disease of apple and pear plants caused by this pathogen can be controlled only by a combination of chemical, horticultural and biological means (Duffy et al., 2005; McManus et al., 2002). This situation calls for development of fire blight resistant apple and pear cultivars, which would reduce the use of chemicals and simplify horticultural methods of fire blight control.

Recently the novel and promising fire blight resistance gene, MR5 from *Malus* x *robusta* 5 hybrid apple, was discovered (Fahrentrapp et al., 2013). This gene grants significant resistance against *E. amylovora* strains carrying the AvrRpt2 effector (Broggini et al., 2014; Vogt et al., 2013). But several strains of this pathogen carrying the AvrRpt2^{C156S} variant avoid this defense (Vogt et al., 2013).

The aim of the research in Chapter 3 was to validate and identify the molecular mechanism of AvrRpt2 recognition by MR5 R protein. To achieve this aim the following objectives were addressed:

1. **Validate MR5 as a receptor able to recognize AvrRpt2.**
   To express MR5 in *N. benthamiana* to test for microscopic cell death response to AvrRpt2 from *P. syringae* and *E. amylovora*.
2. **Based on the well-characterized RPS2/RIN4 system from *Arabidopsis thaliana* define the requirement of apple RIN4 homologs for MR5 functioning.**
   To express MR5 and apple RIN4 homologs in *N. benthamiana* to recapitulate the natural system from *Malus* x *robusta* 5 and to determine if there is a recognition of AvrRpt2.

3. **Determine the reason why AvrRpt2^{C156S} is able to avoid MR5-mediated resistance.**

   To express AvrRpt2^{C156S} in *N. benthamina*, with MR5/MdRIN4 and RPS2/AtRIN4 systems to determine if there is there is a recognition.

Venturia inaequalis is another important pathogen of apple plants, causing apple scab disease. This pathogen is particularly devastating in New Zealand due to its favorable climate for disease development and spread (MacHardy, 1996; Manktelow et al., 1996). No effector genes from *V. inaequalis* were yet cloned and characterized (Deng et al., 2017). In addition, only two resistance loci (*Rvi6* and *Rvi15*) from apple have been characterized (Belfanti et al., 2004; Joshi et al., 2011; Schouten et al., 2014; Vinatzer et al., 2001).

The first aim of the research in Chapter 4 was to identify and analyze the function of *AvrRvi8* effector gene candidates from *V. inaequalis*. To achieve this aim the following objectives were addressed:

1. **Cloning and sequence validation of *AvrRvi8* gene candidates predicted bioinformatically by J. Bowen research group, PFR, NZ.**

   To use *V. inaequalis* cDNA to amplify the candidate genes, carry out sequencing and analysis for intron and STOP-codon mis-annotations.
2. **Functional validation of the cloned *AvrRvi8* gene candidates in model plants and resistant/susceptible apple lines.**

   To sub-clone the top candidate of *AvrRvi8* genes into bacterial delivery vector or binary expression vector, in order to carry out delivery via T3SS into the plant cells or express it via agroinfiltration or particle bombardment methods.

The second aim of the research in Chapter 4 was to identify and analyze the function of the bioinformatically predicted novel effector candidates from *V. inaequalis* 120. To achieve this aim the following objectives were addressed:

1. **Cloning and sequence validation of the novel effector candidates bioinformatically predicted by J. Bowen research group, PFR, NZ.**

   To use *V. inaequalis* 120 cDNA to amplify the candidate genes, carry out sequencing and analysis for intron and STOP-codon mis-annotations.

2. **Functional validation of the cloned candidate effectors in model plants and apple.**

   To sub-clone the set of top candidates into binary expression vector, to validate their expression *in planta*. Further sub-cloning into bacterial delivery vector and delivery via T3SS into the host plants is planned.

Chapter 2. Materials and Methods

2.1 Materials

2.1.1 Bacterial strains used in this study:

***Escherichia coli* DH5α:** *fhuA2 lacΔU169 phoA glnV44 Φ80' lacZΔM15 gyrA96 recA1 relA1 endA1 thi-1 hsdR17* was used for all the cloning in this study (Taylor et al., 1993).

***E. coli* HB101:** *hsd20(r_B, m_B^-) recA13, rpsL20, leu, proA2,* carrying pRK2013 plasmid was used as a helper strain in triparental mating (Boyer & Roulland-Dussoix, 1969).

***Pseudomonas fluorescens* Pf0-1** carrying stably integrated pLN18 type III secretion system of *P. syringae pv. syringae* 61 with HopA1 deleted (Thomas et al., 2009). It was used for infiltration of isolated type III secreted effectors from *Pseudomanas syringae* JL1065 and *Erwinia amylovora* expressed using broad-host range vector pBBR1 MCS-5.

***Agrobacterium tumefaciens* AGL1:** [AGL0 (C58 pTiBo542) recA::bla, T-region deleted Mop(+) Cb^R] (Lazo et al., 1991) was used for transient protein expression in *Nicotiana benthamiana*. This strain was also used to generate stable transgenic lines of *Arabidopsis thaliana* by floral dip method.

The GV3101::pMP90 strain [C58C1, Rif^R ; pMP90 is Ti plasmid pTiC58 with T-DNA deleted, Gm^R] (Koncz and Schell, 1986) was used for expressing KSG700 construct.

Erwinia amylovora (Fb12-027) was used as a gene source for molecular cloning of AvrRpt2, as well as for apple plant infiltrations. Source: Plant and Food, Palmerston North.

2.1.2 Plasmids and constructs used in this study:

Figures representing the maps of standard vectors used in this study can be found in appendices, Figures 6.8 – 6.14.

Standard constructs and vectors for Golden Gate cloning used in this study are listed in Table 2.1 on page 72.

Constructs generated for *Venturia inaequalis* 120 *AvrRvi8* orthologs cloning are listed in Table 2.2 on page 75.

List of constructs generated for *Venturia inaequalis* 120 *AvrRvi8* transient protein expression and T3SS delivery to plant cells listed in Table 2.3 on page 76.

Constructs used for bacterial effector cloning are listed in Table 2.4 on page 77.

Constructs used for bacterial effector T3SS delivery and transient expression are listed in Table 2.5 on page 78.

Constructs used for plant genes cloning are listed in Table 2.6 on page 80.

Constructs used for plant protein transient expression and stable transformation are listed in Table 2.7 on page 83.

Constructs used for *V. inaequalis* predicted candidate effectors (ViCE) cloning are listed in Table 2.8 on page 94.

Constructs used for *V. inaequalis* predicted candidate effectors (ViCE) transient expression without signal peptide are listed in Table 2.9 on page 95.

Constructs used for *V. inaequalis* predicted candidate effectors (ViCE) transient expression fused wit PR1α signal peptide are listed in Table 2.10 on page 97.

Table 2.1 Standard constructs and vectors for Golden Gate cloning.

KSC #	Vector name	A/b resistance	Description	Source/reference
743	pICSL50005	Spec	Carrying C-term YFP tag	Sylvestre Marillonnet
740	pICSL50002	Spec	Carrying C-term YFP-c split tag, to generate constructs to use in BiFC assay	Sylvestre Marillonnet
741	pICSL50003	Spec	Carrying C-term YFP-n split tag, to generate constructs to use in BiFC assay	Sylvestre Marillonnet
714	pICSL50008	Spec	Carrying C-term GFP tag	Sylvestre Marillonnet
715	pICSL50009	Spec	Carrying C-term 6xHA tag	Sylvestre Marillonnet
716	pICSL50010	Spec	Carrying C-term 4xMyc tag	Sylvestre Marillonnet
717	pICSL50013	Spec	Carrying C-term T7 tag	Sylvestre Marillonnet
718	pICH41421	Spec	Carrying Nos terminator	Sylvestre Marillonnet
726	pICH41373	Spec	Carrying 35S CaMV promoter with CCAT 3' overhang	Sylvestre Marillonnet
728	pICH51266	Spec	Carrying 35S CaMV promoter with AATG 3' overhang	Sylvestre Marillonnet
1179	pICH41021::RPS2_pro	Amp	Carrying *A. thaliana* RPS2 native promoter with AATG 3' overhang	This study
1840	pICH41021::RIN4_pro	Amp	Carrying *A. thaliana* RIN4 native promoter with AATG 3' overhang	This study
733	pICSL30004	Spec	Carrying N-term YFP tag	Sylvestre Marillonnet
734	pICSL30005	Spec	Carrying N-term 3xFLAG tag	Sylvestre Marillonnet
735	pICSL30006	Spec	Carrying N-term GFP tag	Sylvestre Marillonnet
737	pICSL30008	Spec	Carrying N-term 6xHA tag	Sylvestre Marillonnet
738	pICSL30009	Spec	Carrying N-term 4xMyc tag	Sylvestre Marillonnet
730	pICSL30001	Spec	Carrying N-term YFP-n split tag, to generate constructs to use in BiFC assay	Sylvestre Marillonnet

KSC #	Vector name	A/b resistance	Description	Source/reference
731	pICSL30002	Spec	Carrying N-term YFP-c split tag, to generate constructs to use in BiFC assay	Sylvestre Marillonnet
746	pICH41021	Amp	Modified pUC19b shuttle vector with mutagenized *Bsa*I-sites, used for gene cloning and Golden Gate assembly	Sylvestre Marillonnet
747	pICH86966	Km	Binary vector for transient protein expression and stable plant transformation (a/b resistance in plants – Km), needs promoter, N-term tag and NosT modules for assembly	Sylvestre Marillonnet
724	pICH86988	Km	Binary vector for transient protein expression and stable plant transformation (a/b resistance in plants – Km), contains 35S CaMV promoter and NosT terminator	Sylvestre Marillonnet
751	EpiGreenB5::Spec::GG	Km Spec	Binary vector used in this study for stable transformation of plants. This vector is Golden Gate compatible and contains Spec resistance cassette replaced when assembled with gene of interest. It carries BASTA resistance for transgenic plant selection and requires pSOUP for replication in *Agrobacterium*	(Hellens et al., 2000) Modified by Melissa Guo
81	pSOUP	Tet	Modified RK2 plasmid. Required as helper plasmid for efficient plant transformation with pGreen and derivitives. Carries the pSA replicase gene intended to act in trans upon the pSA replication origin in pGreen.	(Hellens et al., 2000)
1216	pICH41021::PR1α SP	Amp	Carrying PR1α signal peptide from *N. benthamiana*	This study
1444	pICH47742	Amp	Construct to assemble level 2 Golden Gate vector carrying 2x35S CaMV promoter, hCas9, NosT	Sylvestre Marillonnet
1135	pICH47742::Cas9 linker	Amp	Construct to assemble level 2 Golden Gate vector carrying disrupted hCas9 cassette, acts as a linker for assembly	Sylvestre Marillonnet
1136	pICH47732::NosP::Bar::NosT	Amp	Construct to assemble level 2 Golden Gate vector carrying Bar gene under NosP promoter (BASTA resistance in plants)	Sylvestre Marillonnet

KSC #	Vector name	A/b resistance	Description	Source/reference
1137	pICH47732::NosP::nptII::NosT	Amp	Construct to assemble level 2 Golden Gate vector carrying nptII gene under NosP promoter (Km resistance in plants)	Sylvestre Marillonnet
1138	pICH41766 (end linker)	Spec	Construct to assemble level 2 Golden Gate vector carrying end linker	Sylvestre Marillonnet
1139	pICH41780 (end linker)	Spec	Construct to assemble level 2 Golden Gate vector carrying end linker	Sylvestre Marillonnet
1134	pAGM4723	Km	Level 2 binary vector to assemble two gene on one backbone	Sylvestre Marillonnet
994	pBBR1MCS-5B::AvrRps4pro	Gm	Golden gate cloning compatible broad host-range vector with AvrRps4 promoter driven expression, used for *P. fluorescens* Pf0-1 delivery of effectors	Kee Hoon Sohn
1265	pBBR1MCS-5B:: AvrRps4pro+136_N-term aa	Gm	Golden gate cloning compatible broad host-range vector with AvrRps4 promoter and first N-term 136 aa of AvrRps4, used for *P. fluorescens* Pf0-1 delivery of effectors	Kee Hoon Sohn
1266	pBBR1MCS-5B:: AvrRpm1pro+89 N-term aa	Gm	Golden gate cloning compatible broad host-range vector with AvrRpm1 promoter and first N-term 89 aa of AvrRpm1, used for *P. fluorescens* Pf0-1 delivery of effectors	This study

Table 2.2. Constructs generated for *Venturia inaequalis* 120 *AvrRvi8* candidates cloning.

KSC #	Vector	Insert	Source/reference
1156	pICH41021::avrRvi8-1/2 (1)	*V. inaequalis* 120 *AvrRvi8-7* candidate ortholog – 1/2, version 1	This study
1157	pICH41021::avrRvi8-1/2 (2)	*V. inaequalis* 120 *AvrRvi8-7* candidate ortholog – 1/2, version 2	This study
1158	pICH41021::avrRvi8-1/2 (3)	*V. inaequalis* 120 *AvrRvi8-7* candidate ortholog – 1/2, version 3	This study
1159	pICH41021::avrRvi8-1/2 (4)	*V. inaequalis* 120 *AvrRvi8-7* candidate ortholog – 1/2, version 4	This study
1160	pICH41021::avrRvi8-1/2 (5)	*V. inaequalis* 120 *AvrRvi8-7* candidate ortholog – 1/2, version 5	This study
1161	pICH41021::avrRvi8-1/2 (6)	*V. inaequalis* 120 *AvrRvi8-7* candidate ortholog – 1/2, version 6	This study
1162	pICH41021::avrRvi8-3	*V. inaequalis* 120 *AvrRvi8-7* candidate ortholog – 3	This study
1163	pICH41021::avrRvi8-4	*V. inaequalis* 120 *AvrRvi8-7* candidate ortholog – 4	This study
1172	pICH41021::avrRvi8-5	*V. inaequalis* 120 *AvrRvi8-7* candidate ortholog – 5	This study
1164	pICH41021::avrRvi8-6	*V. inaequalis* 120 *AvrRvi8-7* candidate ortholog – 6	This study
1173	pICH41021::avrRvi8-7	*V. inaequalis* 120 *AvrRvi8-7* candidate	This study
1181	pICH41021::AvrRvi8-7_noSP	*V. inaequalis* 120 *AvrRvi8-7* candidate without signal peptide	This study
1165	pICH41021::avrRvi8-8	*V. inaequalis* 120 *AvrRvi8-7* candidate ortholog – 8	This study
1180	pICH41021::AvrRvi8-9	*V. inaequalis* 120 *AvrRvi8-7* candidate ortholog – 9	This study
1593	pICH41021::AvrRvi8-10	*V. inaequalis* 120 *AvrRvi8* candidate 10	This study
1596	pICH41021::AvrRvi8-11	*V. inaequalis* 120 *AvrRvi8* candidate 11	This study
1597	pICH41021::AvrRvi8-12	*V. inaequalis* 120 *AvrRvi8* candidate 12	This study

- *Venturia inaequalis AvrRvi8* orthologs 1 and 2 were cloned using the same pair of primers and 6 colonies were sequenced in order to get both variants cloned, but sequencing showed the presence of 6 different variants with small differences.

Table 2.3. Constructs used for *Venturia inaequalis* 120 AvrRvi8 transient protein expression and T3SS delivery to plant cells.

KSC #	Host strain	Vector	Epitope tag	Description	Source/reference
1182	*A. tumefaciens* AGL1	pICH86988::AvrRvi8-7::HA	C-term 6xHA	for *V. inaequalis* 120 AvrRvi8-7 transient expression	This study
1183	*A. tumefaciens* AGL1	pICH86988::AvrRvi8-7_noSP::HA	C-term 6xHA	for *V. inaequalis* 120 AvrRvi8-7 transient expression without signal peptide	This study
1271	*P. fluorescens* Pf0-1 (T3S)	pBBR1MCS-5::AvrRps4(N-term) ::AvrRvi_8-7::HA	C-term 6xHA	for *V. inaequalis* 120 AvrRvi8-7 effector delivery via T3SS of *P. fluorescens,* driven by AvrRps4 promoter, contains AvrRps4 N-term 136 amino acid residues	This study
1272	*P. fluorescens* Pf0-1 (T3S)	pBBR1MCS-5::AvrRps4(N-term) ::AvrRvi_8-7_noSP::HA	C-term 6xHA	for *V. inaequalis* 120 AvrRvi8-7 effector without signal peptide delivery via T3SS of *P. fluorescens,* driven by AvrRps4 promoter, contains AvrRps4 N-term 136 amino acid residues	This study
1278	*P. fluorescens* Pf0-1 (T3S)	pBBR1MCS-5::AvrRpm1(N-term)::AvrRvi_8-7::HA	C-term 6xHA	for *V. inaequalis* 120 AvrRvi8-7 effector delivery via T3SS of *P. fluorescens,* driven by AvrRpm1 promoter, contains AvrRpm1 N-term 89 amino acid residues	This study
1279	*P. fluorescens* Pf0-1 (T3S)	pBBR1MCS-5::AvrRpm1(N-term)::AvrRvi_8-7_noSP::HA	C-term 6xHA	for *V. inaequalis* 120 AvrRvi8-7 effector without signal peptide delivery via T3SS of *P. fluorescens,* driven by AvrRpm1 promoter, contains AvrRpm1 N-term 89 amino acid residues	This study

Table 2.4. Constructs used for bacterial effector cloning.

KSC #	Host strain	Vector	Description	Source/reference
1151	*E. coli* DH5α	pICH41021::PsAvrRpt2	carrying *P. syringae* JL 1065 AvrRpt2	This study
1155	*E. coli* DH5α	pICH41021::EaAvrRpt2	carrying *E. amylovora* Fb12-027 AvrRpt2 with CTG start codon mutagenised to ATG	This study
1171	*E. coli* DH5α	pICH41021::EaAvrRpt2^{C156S}	carrying *E. amylovora* Fb12-027 AvrRpt2 with CTG start codon mutagenised to ATG and C156S aminoacid transition	This study
1184	*E. coli* DH5α	pICH41021::PsAvrRpt2^{C122A}	carrying *P. syringae* JL 1065 AvrRpt2 with C122A mutation	This study
1185	*E. coli* DH5α	pICH41021::EaAvrRpt2^{C88A}	carrying *E. amylovora* Fb12-027 AvrRpt2 with CTG start codon mutagenised to ATG and C88A mutation	This study
1186	*E. coli* DH5α	pICH41021::EaAvrRpt2 C88A+C156S	carrying *E. amylovora* Fb12-027 AvrRpt2 with CTG start codon mutagenised to ATG and C88A, C156S mutations	This study

Table 2.5. Constructs used for bacterial effector T3SS delivery and transient expression:

KSC #	Host strain	Vector	Epitope tag	Description	Source/reference
1176	*A. tumefaciens* AGL1	pICH96988::PsAvrRpt2::HA	C-term 6xHA	for *P. syringae* JL 1065 AvrRpt2 transient expression	This study
1177	*A. tumefaciens* AGL1	pICH96988::EaAvrRpt2::HA	C-term 6xHA	for *E. amylovora* Fb12-027 AvrRpt2 transient expression	This study
1178	*A. tumefaciens* AGL1	pICH96988:: EaAvrRpt2^{C156S}::HA	C-term 6xHA	for *E. amylovora* Fb12-027 AvrRpt2 C156S transient expression	This study
1212	*A. tumefaciens* AGL1	pICH96988:: PsAvrRpt2^{C122A}::HA	C-term 6xHA	for *P. syringae* JL 1065 AvrRpt2 C122A transient expression	This study
1213	*A. tumefaciens* AGL1	pICH96988:: EaAvrRpt2^{C88A}::HA	C-term 6xHA	for *E. amylovora* Fb12-027 AvrRpt2 C88A transient expression	This study
1214	*A. tumefaciens* AGL1	pICH96988:: EaAvrRpt2$^{C88A+C156S}$::HA	C-term 6xHA	for *E. amylovora* Fb12-027 AvrRpt2 C88A, C156S transient expression	This study
1282	*A. tumefaciens* AGL1	pK7FWG2::AvrRpm1	C-term GFP	Binary vector with 35S CaMV promoter, AvrRpm1 gene and C-term GFP	This study
496	*A. tumefaciens* AGL1	pBin19::AvrB::HA	C-term 6xHA	Binary vector with 35S CaMV promoter, AvrB gene and C-term HA tag	This study
1206	*P. fluorescens* Pf0-1 (T3S)	pBBR1MCS-5::PsAvrRpt2::HA	C-term 6xHA	for *P. syringae* JL 1065 AvrRpt2 T3SS delivery	This study
1207	*P. fluorescens* Pf0-1 (T3S)	pBBR1MCS-5:: PsAvrRpt2^{C122A}::HA	C-term 6xHA	for *P. syringae* JL 1065 AvrRpt2 C122A T3SS delivery	This study
1208	*P. fluorescens* Pf0-1 (T3S)	pBBR1MCS-5::EaAvrRpt2::HA	C-term 6xHA	for *E. amylovora* Fb12-027 AvrRpt2 T3SS delivery	This study
1209	*P. fluorescens* Pf0-1 (T3S)	pBBR1MCS-5:: EaAvrRpt2^{C156S}::HA	C-term 6xHA	for *E. amylovora* Fb12-027 AvrRpt2 T3SS delivery C156S	This study

KSC #	Host strain	Vector	Epitope tag	Description	Source/reference
1210	*P. fluorescens* Pf0-1 (T3S)	pBBR1MCS-5:: EaAvrRpt2^{C88A}::HA	C-term 6xHA	for *E. amylovora* Fb12-027 AvrRpt2 C88A T3SS delivery	This study
1211	*P. fluorescens* Pf0-1 (T3S)	pBBR1MCS-5:: EaAvrRpt2$^{C88A+C156S}$::HA	C-term 6xHA	for *E. amylovora* Fb12-027 AvrRpt2 C88A, C156S T3SS delivery	This study

Table 2.6. Constructs used for plant genes cloning.

KSC #	Host strain	Vector	Insert	Source/reference
1150	*E. coli* DH5α	pICH41021::AtRIN4	RIN4 from *Arabidopsis thaliana* Col-0, for C-terminal tagging	This study
657	*E. coli* DH5α	pICH41021::AtRIN4_CLV1	cleavage product 1 fused with N-term GFP tag of RIN4 from *A. thaliana* Col-0	This study
652	*E. coli* DH5α	pICH41021::AtRIN4_CLV2	cleavage product 2 of RIN4 from *A. thaliana* Col-0	This study
653	*E. coli* DH5α	pICH41021::AtRIN4_CLV3	cleavage product 3 of RIN4 from *A. thaliana* Col-0	This study
1838	*E. coli* DH5α	pICH41021:: AtRIN4_CLV3_pt1_D153E	N-term part of AtRIN4 cleavage product 3with D153E mutation	This study
1610	*E. coli* DH5α	pICH41021::AtRIN4_CLV3_pt1 _N158D	N-term part of AtRIN4 cleavage product 3with N158D mutation	This study
1564	*E. coli* DH5α	pICH41021::AtRIN4_CLV3_pt1 _S160A	N-term part of AtRIN4 cleavage product 3with S160A mutation	This study
1614	*E. coli* DH5α	pICH41021::AtRIN4_CLV3_pt1 _Y165F	N-term part of AtRIN4 cleavage product 3with Y165F mutation	This study
1637	*E. coli* DH5α	pICH41021::At-RIN4_CLV3_pt1 N158D+ Y165F	N-term part of AtRIN4 cleavage product 3with N158D and Y165F mutation	This study
1598	*E. coli* DH5α	pICH41021::RPS2pt1	RPS2 module 1 from *A. thaliana* Col-0	This study
277	*E. coli* DH5α	pICH41021::RPS2_CC-domain(1-153aa)	first 153 aa of RPS2	This study
1599	*E. coli* DH5α	pICH41021::RPS2pt2	RPS2 module 2 from *A. thaliana* Col-0	This study
1600	*E. coli* DH5α	pICH41021::RPS2pt3	RPS2 module 3 from *A. thaliana* Col-0	This study
1167	*E. coli* DH5α	pICH41021::MR5pt1	MR5 module 1 from *Malus* x *robusta* 5 (amplified from *Malus* x *robusta* 5 gDNA, source – PFR)	This study
1168	*E. coli* DH5α	pICH41021::MR5pt2	MR5 module 2 from *Malus* x *robusta* 5	This study

KSC #	Host strain	Vector	Insert	Source/reference
465	*E. coli* DH5α	pICH41021::MR5pt2(1-582 aa)	first 582 aa of MR5 when assembled with MR5 module 1	This study
466	*E. coli* DH5α	pICH41021::MR5pt2(1-711 aa)	first 711 aa of MR5 when assembled with MR5 module 1	This study
467	*E. coli* DH5α	pICH41021::MR5pt2(1-873 aa)	first 873 aa of MR5 when assembled with MR5 module 1	This study
1169	*E. coli* DH5α	pICH41021::MR5pt3	FB_MR5 module 3 from *Malus* x *robusta* 5 (amplified from *Malus x robusta* 5 gDNA, source – PFR)	This study
1170	*E. coli* DH5α	pICH41021::MR5pt4	FB_MR5 module 4 from *Malus* x *robusta* 5	This study
1215	*E. coli* DH5α	pICH41021::AtRIN4	RIN4 for N-term epitope tag assembly from *A. thaliana* Col-0	This study
287	*E. coli* DH5α	pICH41021::AtRIN4_ppp	*A. thaliana* RIN4 with phosphorylation mimic mutations in all three sites	This study
294	*E. coli* DH5α	pICH41021::MdRIN4_ppp	*Malus domestica* RIN4 with phosphorylation mimic mutations in all three sites	This study
1236	*E. coli* DH5α	pUC57::MR5pt1	FB_MR5 module 1 synthesised by Genescript	This study
162	*E. coli* DH5α	pICH41021::MR5_CC-domain (1-122aa)	first 122 aa of MR5	This study
163	*E. coli* DH5α	pICH41021::MR5_CC-domain (1-136aa)	first 136 aa of MR5	This study
164	*E. coli* DH5α	pICH41021::MR5_CC-domain (1-161aa)	first 161 aa of MR5	This study
464	*E. coli* DH5α	pICH41021::MR5pt1(1-455 aa)	first 455 aa of MR5	This study
469	*E. coli* DH5α	pICH41021::MR5pt1(169-1388 aa)	169-1388 aa of MR5 when assembled with MR5 modules 2, 3 and 4	This study
1237	*E. coli* DH5α	pUC57::MR5pt3	FB_MR5 module 3 synthesised by Genescript	This study

KSC #	Host strain	Vector	Insert	Source/reference
468	*E. coli* DH5α	pICH41021::MR5pt3(1-1151 aa)	first 1151 aa of MR5 when assembled with MR5 modules 1 and 2	This study
1238	*E. coli* DH5α	pUC57::MdRIN4-1	*M. domestica* RIN4-1 homolog cDNA synthesised by Genescript	This study
658	*E. coli* DH5α	pICH41021::MdRIN4-1_CLV1	cleavage product 1 fused with N-term GFP tag of RIN4 from *M. domestica*	This study
654	*E. coli* DH5α	pICH41021::MdRIN4-1_CLV2	cleavage product 2 of RIN4 from *M. domestica*	This study
655	*E. coli* DH5α	pICH41021::MdRIN4-1_CLV3	cleavage product 2 of RIN4 from *M. domestica*	This study
1838	*E. coli* DH5α	pICH41021::MdRIN4_CLV3_pt1_E181D	N-term part of MdRIN4 cleavage product 3 with E181D mutation	This study
1611	*E. coli* DH5α	pICH41021::MdRIN4_CLV3_pt1_D186N	N-term part of MdRIN4 cleavage product 3 with D186N mutation	This study
1612	*E. coli* DH5α	pICH41021::MdRIN4_CLV3_pt1_A188S	N-term part of MdRIN4 cleavage product 3 with A188S mutation	This study
1613	*E. coli* DH5α	pICH41021::MdRIN4_CLV3_pt1_F193Y	N-term part of MdRIN4 cleavage product 3 with F193Y mutation	This study
1638	*E. coli* DH5α	pICH41021::MdRIN4_CLV3_pt1_D186N+F193Y	N-term part of MdRIN4 cleavage product 3 with D186N and F193Y mutation	This study
798	*E. coli* DH5α	pICH41021::MdRIN4_CLV3_AAA	MdRIN4_CLV3 with CCC201-203 mutagenized to AAA	This study
681	*E. coli* DH5α	pICH41021::MdRIN4_RSC1	MdRIN4 gene with F10A mutation in RSC1, which blocks the cleavage in this site	This study
682	*E. coli* DH5α	pICH41021::MdRIN4_RSC2	MdRIN4 gene with F179A mutation in RSC1, which blocks the cleavage in this site	This study
683	*E. coli* DH5α	pICH41021::MdRIN4_RSC1+2	MdRIN4 gene with F10A and F179A mutations blocking cleavage in both sites	This study

KSC #	Host strain	Vector	Insert	Source/reference
1239	*E. coli* DH5α	pUC57::MdRIN4-2	*M. domestica* RIN4-2 homolog cDNA synthesised by Genescript	This study

Table 2.7. Constructs used for plant protein transient expression and stable transformation.

KSC #	Host strain	Vector	Epitope tag	Description	Source/reference
988	*A. tumefaciens* AGL1	pICH86988::MR5::Myc	C-term 4xMyc	for MR5 transient expression	This study
838	*A. tumefaciens* AGL1	pICH86988::MR5::Flag	C-term 3xFlag	for MR5 transient expression	This study
166	*A. tumefaciens* AGL1	pICH86988::MR5_CC-domain (1-122aa)::Flag	C-term 3xFlag	for transient expression of 1-122 aa fragment of MR5	This study
167	*A. tumefaciens* AGL1	pICH86988::MR5_CC-domain (1-136aa)::Flag	C-term 3xFlag	for transient expression of 1-136 aa fragment of MR5	This study
168	*A. tumefaciens* AGL1	pICH86988::MR5_CC-domain (1-161aa)::Flag	C-term 3xFlag	for transient expression of 1-161 aa fragment of MR5	This study
470	*A. tumefaciens* AGL1	pICH86988:MR5(1-455 aa)::Myc	C-term 4xMyc	for transient expression of 1-455 aa fragment of MR5	This study
471	*A. tumefaciens* AGL1	pICH86988:MR5(1-582 aa)::Myc	C-term 4xMyc	for transient expression of 1-582 aa fragment of MR5	This study
472	*A. tumefaciens* AGL1	pICH86988::MR5(1-711 aa)::Myc	C-term 4xMyc	for transient expression of 1-711 aa fragment of MR5	This study
473	*A. tumefaciens* AGL1	pICH86988::MR5(1-873 aa)::Myc	C-term 4xMyc	for transient expression of 1-873 aa fragment of MR5	This study
474	*A. tumefaciens* AGL1	pICH86988::MR5(1-1151 aa)::Myc	C-term 4xMyc	for transient expression of 1-1151 aa fragment of MR5	This study
475	*A. tumefaciens* AGL1	pICH86988::MR5(169-1388 aa)::Myc	C-term 4xMyc	for transient expression of 169-1388 aa fragment of MR5	This study

KSC #	Host strain	Vector	Epitope tag	Description	Source/reference
989	*A. tumefaciens* AGL1	pICH86966::35Spro:: Flag::MdRIN4-1	N-term 3xFlag	for *M. domestica* RIN4-1 homolog transient expression	This study
840	*A. tumefaciens* AGL1	pICH86966::35Spro:: Myc::MdRIN4-1	N-term 4xMyc	for *M. domestica* RIN4-1 homolog transient expression	This study
696	*A. tumefaciens* AGL1	pICH86966::35Spro:: Myc::MdRIN4-1^{F10A}	N-term 4xMyc	for *M. domestica* RIN4-1 with mutation F10A in RCS1 transient expression	This study
697	*A. tumefaciens* AGL1	pICH86966::35Spro:: Myc::MdRIN4-1^{F179A}	N-term 4xMyc	for *M. domestica* RIN4-1 with mutation F179A in RCS2 transient expression	This study
801	*A. tumefaciens* AGL1	pICH86966::35Spro:: Myc::MdRIN4-1$^{F10A+F179A}$	N-term 4xMyc	for *M. domestica* RIN4-1 with mutation F10A and F179A in RCS1 and 2 transient expression	This study
673	*A. tumefaciens* AGL1	pICH86988::GFP::MdRIN4_CLV1	N-term GFP	for *M. domestica* RIN4-1 homolog cleavage product 1 transient expression	This study
676	*A. tumefaciens* AGL1	pICH86988::GFP::AtRIN4_CLV1	N-term GFP	for *A. thaliana* RIN4 cleavage product 1 transient expression	This study
563	*A. tumefaciens* AGL1	pICH86988::MdRIN4_CLV2	No tag	for *M. domestica* RIN4-1 homolog cleavage product 2 transient expression	This study
565	*A. tumefaciens* AGL1	pICH86988::AtRIN4_CLV2	No tag	for *A. thaliana* RIN4 cleavage product 2 transient expression	This study
564	*A. tumefaciens* AGL1	pICH86988::MdRIN4-1_CLV3	No tag	for *M. domestica* RIN4-1 homolog cleavage product 3 transient expression	This study
808	*A. tumefaciens* AGL1	pICH86988::MdRIN4_CLV3_AAA	No tag	for *M. domestica* RIN4-1 homolog cleavage product 3 transient expression with mutated membrane anchoring sequence	This study
685	*A. tumefaciens* AGL1	pICH86988::MdRIN4-2_CLV3	No tag	for *M. domestica* RIN4-2 homolog cleavage product 3 transient expression	This study

KSC #	Host strain	Vector	Epitope tag	Description	Source/reference
684	*A. tumefaciens* AGL1	pICH86966::35Spro:: Flag::Md_RIN4-1_CLV3	N-term 3xFlag	for *M. domestica* RIN4-1 homolog cleavage product 3 transient expression	This study
792	*A. tumefaciens* AGL1	pICH86988::35Spro:: HA::MdRIN4_CLV3	N-term 6xHA	for *M. domestica* RIN4-1 homolog cleavage product 3 transient expression	This study
793	*A. tumefaciens* AGL1	pICH86988::35Spro:: Myc::MdRIN4_CLV3	N-term 4xMyc	for *M. domestica* RIN4-1 homolog cleavage product 3 transient expression	This study
566	*A. tumefaciens* AGL1	pICH86988::AtRIN4_CLV3	No tag	for *A. thaliana* RIN4 cleavage product 3 transient expression	This study
841	*A. tumefaciens* AGL1	pICH86966::35Spro:: Myc::AtRIN4_CLV3	N-term 4xMyc	for *A. thaliana* RIN4 cleavage product 3 transient expression	This study
1508	*A. tumefaciens* AGL1	pICH86988:: At-MdRIN4_CLV3_Chimera	No tag	for At-MdRIN4_CLV3 chimeric protein expression	This study
1509	*A. tumefaciens* AGL1	pICH86966::35Spro:: Myc::At-MdRIN4_CLV3_Chimera	N-term 4xMyc	for At-MdRIN4_CLV3 chimeric protein expression	This study
1855	*A. tumefaciens* AGL1	pCIH86988:: At-MdRIN4_CLV3^{D153E}	No tag	for At-MdRIN4_CLV3 chimeric protein expression with D153E mutation	This study
1569	*A. tumefaciens* AGL1	pCIH86988:: At-MdRIN4_CLV3^{N158D}	No tag	for At-MdRIN4_CLV3 chimeric protein expression with N158D mutation	This study
1628	*A. tumefaciens* AGL1	pCIH86988:: At-MdRIN4_CLV3^{S160A}	No tag	for At-MdRIN4_CLV3 chimeric protein expression with S160A mutation	This study
1629	*A. tumefaciens* AGL1	pCIH86988:: At-MdRIN4_CLV3^{Y165F}	No tag	for At-MdRIN4_CLV3 chimeric protein expression with Y165F mutation	This study
1649	*A. tumefaciens* AGL1	pCIH86988:: At-MdRIN4_CLV3$^{N158D+Y165F}$	No tag	for At-MdRIN4_CLV3 chimeric protein expression with N158D and Y165F mutations	This study

KSC #	Host strain	Vector	Epitope tag	Description	Source/reference
1535	*A. tumefaciens* AGL1	pICH86988::Md-AtRIN4_CLV3_Chimera	No tag	for Md-AtRIN4_CLV3 chimeric protein expression	This study
1537	*A. tumefaciens* AGL1	pICH86966::35Spro::Myc ::Md-AtRIN4_CLV3_Chimera	N-term 4xMyc	for Md-AtRIN4_CLV3 chimeric protein expression	This study
1856	*A. tumefaciens* AGL1	pICH86988:: Md-AtRIN4_CLV3^{E181D}	No tag	for Md-AtRIN4_CLV3 chimeric protein expression with E181D mutation	This study
1570	*A. tumefaciens* AGL1	pCIH86988:: Md-AtRIN4_CLV3^{D186N}	No tag	for Md-AtRIN4_CLV3 chimeric protein expression with D186N mutation	This study
1571	*A. tumefaciens* AGL1	pICH86988:: Md-AtRIN4_CLV3^{A188S}	No tag	for Md-AtRIN4_CLV3 chimeric protein expression with A188S mutation	This study
1572	*A. tumefaciens* AGL1	pICH86988:: Md-AtRIN4_CLV3^{F193Y}	No tag	for Md-AtRIN4_CLV3 chimeric protein expression with F193Y mutation	This study
1650	*A. tumefaciens* AGL1	pICH86988:: Md-AtRIN4_CLV3$^{D186N+ F193Y}$	No tag	for Md-AtRIN4_CLV3 chimeric protein expression with D186N and F193Y mutation	This study
990	*A. tumefaciens* AGL1	pICH86966::35Spro:: Flag::MdRIN4-2	N-term 3xFlag	for *M. domestica* RIN4-2 homolog transient expression	This study
825	*A. tumefaciens* AGL1	pICH96988::AtRIN4::Flag	C-term 3xFlag	for *A. thaliana* RIN4 transient expression	This study
844	*A. tumefaciens* AGL1	pICH86966::35Spro:: Myc::AtRIN4_CLV1-2:: MdRIN4_CLV3	N-term 4xMyc	for chimeric protein expression carrying CLV1-2 from *A. thaliana* and CLV3 from *M. domestica*	This study
845	*A. tumefaciens* AGL1	pICH86966::35Spro:: Myc::MdRIN4_CLV1-2:: AtRIN4_CLV3	N-term 4xMyc	for chimeric protein expression carrying CLV1-2 from *M. domestica* and CLV3 from *A. thaliana*	This study
1661	*A. tumefaciens* AGL1	pICH86988::Myc::AtRIN4^{N158D}	N-term 4xMyc	for AtRIN4 with N158D mutation transient expression	This study

KSC #	Host strain	Vector	Epitope tag	Description	Source/reference
1662	*A. tumefaciens* AGL1	pICH86988::Myc::AtRIN4^{Y165F}	N-term 4xMyc	for AtRIN4 with Y165F mutation transient expression	This study
1663	*A. tumefaciens* AGL1	pICH86988:: Myc::AtRIN4$^{N158D+Y165F}$	N-term 4xMyc	for AtRIN4 with N158D and Y165F mutations transient expression	This study
1743	*A. tumefaciens* AGL1	pICH86988:: Myc::AtRIN4_TEV_RCS	N-term 4xMyc	for AtRIN4 variant with native RCS2 replaced for TEV RCS transient expression	This study
1744	*A. tumefaciens* AGL1	pICH86988:: Myc::AtRIN4^{N158D}_TEV_RCS	N-term 4xMyc	for AtRIN4 variant with native RCS2 replaced for TEV RCS and N158D mutation transient expression	This study
1745	*A. tumefaciens* AGL1	pICH86988:: Myc::AtRIN4^{Y165F}_TEV_RCS	N-term 4xMyc	for AtRIN4 variant with native RCS2 replaced for TEV RCS and Y165F mutation transient expression	This study
1746	*A. tumefaciens* AGL1	pICH86988:: Myc::AtRIN4$^{N158D+Y165F}$_TEV_RCS	N-term 4xMyc	for AtRIN4 variant with native RCS2 replaced for TEV RCS and N158D + Y165F mutations transient expression	This study
1703	*A. tumefaciens* AGL1	pICH86988:: Myc::AtRIN4_CLV3^{N158D}	N-term 4xMyc	for AtRIN4_CLV3 with N158D mutation transient expression	This study
1704	*A. tumefaciens* AGL1	pICH86988:: Myc::AtRIN4_CLV3^{Y165F}	N-term 4xMyc	for AtRIN4_CLV3 with Y165F mutation transient expression	This study
1705	*A. tumefaciens* AGL1	pICH86988:: Myc::AtRIN4_CLV3$^{N158D+Y165F}$	N-term 4xMyc	for AtRIN4_CLV3 with N158D and Y165F mutations transient expression	This study
1664	*A. tumefaciens* AGL1	pICH86988::Myc::MdRIN4^{D186N}	N-term 4xMyc	for MdRIN4 with D186N mutation transient expression	This study
1665	*A. tumefaciens* AGL1	pICH86988::Myc::MdRIN4^{F193Y}	N-term 4xMyc	for MdRIN4 with F193Y mutation transient expression	This study

KSC #	Host strain	Vector	Epitope tag	Description	Source/reference
1666	*A. tumefaciens* AGL1	pICH86988:: Myc::MdRIN4$^{D186N+F193Y}$	N-term 4xMyc	for MdRIN4 with D186N and F193Y mutations transient expression	This study
1747	*A. tumefaciens* AGL1	pICH86988:: Myc::MdRIN4_TEV_RCS	N-term 4xMyc	for MdRIN4 variant with native RCS2 replaced for TEV RCS transient expression	This study
1748	*A. tumefaciens* AGL1	pICH86988:: Myc::MdRIN4^{D186N}_TEV_RCS	N-term 4xMyc	for MdRIN4 variant with native RCS2 replaced for TEV RCS and D186N mutation transient expression	This study
1749	*A. tumefaciens* AGL1	pICH86988:: Myc::MdRIN4^{F193Y}_TEV_RCS	N-term 4xMyc	for MdRIN4 variant with native RCS2 replaced for TEV RCS and F193Y mutation transient expression	This study
1750	*A. tumefaciens* AGL1	pICH86988:: Myc::MdRIN4$^{D186N+F193Y}$ TEV_RCS	N-term 4xMyc	for MdRIN4 variant with native RCS2 replaced for TEV RCS and D186N+ F193Y mutations transient expression	This study
1706	*A. tumefaciens* AGL1	pICH86988:: Myc::MdRIN4_CLV3^{D186N}	N-term 4xMyc	for MdRIN4_CLV3 with D186N mutation transient expression	This study
1707	*A. tumefaciens* AGL1	pICH86988:: Myc::MdRIN4_CLV3^{F193Y}	N-term 4xMyc	for MdRIN4_CLV3 with F193Y mutation transient expression	This study
1708	*A. tumefaciens* AGL1	pICH86988:: Myc::MdRIN4_CLV3$^{D186N+F193Y}$	N-term 4xMyc	for MdRIN4_CLV3 with D186N and F193Y mutations transient expression	This study
826	*A. tumefaciens* AGL1	pICH96988::RPS2::Myc	C-term 4xMyc	for *A. thaliana* RPS2 transient expression	This study
297	*A. tumefaciens* AGL1	pICH86988::RPS2_CC-domain (1-153aa)::Myc	C-term 4xMyc	for *A. thaliana* RPS2 CC domain only expression, first 153 aa	This study
826	*A. tumefaciens* AGL1	pICH96988::RPS2::Flag	C-term 3xFlag	for *A. thaliana* RPS2 transient expression	This study

KSC #	Host strain	Vector	Epitope tag	Description	Source/reference
948	*A. tumefaciens* AGL1	pICH89966::35Spro::Flag::AtRIN4	N-term 3xFlag	for *A. thaliana* RIN4 transient expression	This study
829	*A. tumefaciens* AGL1	pICH89966::35Spro::Myc::AtRIN4	N-term 4xMyc	for *A. thaliana* RIN4 transient expression	This study
1871	*A. tumefaciens* AGL1	pAGM4723::BAR::rin4pro::Myc::AtRIN4 + rps2pro::RPS2::Flag	N-term 4xMyc and C-term 3xFlag	level 2 Golden Gate construct which carries RPS2 gene under control of native rps2 promoter and with C-term FLAG tag and AtRIN4 under native rin4 promoter with N-term Myc tag. For plant stable and transient transformation	This study
1872	*A. tumefaciens* AGL1	pAGM4723::BAR::rin4pro::Myc::AtRIN4$^{N158D+Y165F}$ + rps2pro::RPS2::Flag	N-term 4xMyc and C-term 3xFlag	level 2 Golden Gate construct which carries RPS2 gene under control of native rps2 promoter and with C-term FLAG tag and AtRIN4 with N158D+Y165F mutation under native rin4 promoter with N-term Myc tag. For plant stable and transient transformation	This study
1873	*A. tumefaciens* AGL1	pAGM4723::BAR::rin4pro::Myc::MdRIN4 + rps2pro::RPS2::Flag	N-term 4xMyc and C-term 3xFlag	level 2 Golden Gate construct which carries RPS2 gene under control of native rps2 promoter and with C-term FLAG tag and MdRIN4 under native rin4 promoter with N-term Myc tag. For plant stable and transient transformation	This study

KSC #	Host strain	Vector	Epitope tag	Description	Source/reference
1874	*A. tumefaciens* AGL1	pAGM4723::BAR:: rin4pro::Myc:: MdRIN4$^{D186N+F193Y}$ + rps2pro::RPS2::Flag	N-term 4xMyc and C-term 3xFlag	level 2 Golden Gate construct which carries RPS2 gene under control of native rps2 promoter and with C-term FLAG tag and MdRIN4 with D186F+F193Y mutation under native rin4 promoter with N-term Myc tag. For plant stable and transient transformation	This study
1979	*A. tumefaciens* AGL1	pAGM4723::BAR::rin4_pro:: Myc::GFP + rps2_pro::RPS2::Flag	N-term 4xMyc and C-term 3xFlag	level 2 Golden Gate construct which carries RPS2 gene under control of native rps2 promoter and with C-term FLAG tag and GFP under native rin4 promoter with N-term Myc tag. For plant stable and transient transformation	This study
1870	*A. tumefaciens* AGL1	pAGM4723::BAR::35Spro::Myc ::AtRIN4 + 35Spro::RPS2::Flag	N-term 4xMyc and C-term 3xFlag	level 2 Golden Gate construct which carries RPS2 gene under control of 35S CaMV promoter and with C-term FLAG tag and AtRIN4 under 35S CaMV promoter with N-term Myc tag. For plant stable and transient transformation	This study
2378	*A. tumefaciens* AGL1	pAGM4723::BAR:: 35Spro::Myc::AtRIN4$^{N158D+Y165F}$ + 35Spro::RPS2::Flag	N-term 4xMyc and C-term 3xFlag	level 2 Golden Gate construct which carries RPS2 gene under control of 35S CaMV promoter and with C-term FLAG tag and AtRIN4 with N158D+Y165F mutations and under 35S CaMV promoter with N-term Myc tag. For plant stable and transient transformation	This study

KSC #	Host strain	Vector	Epitope tag	Description	Source/reference
2379	*A. tumefaciens* AGL1	pAGM4723::BAR::35Spro::Myc ::MdRIN4 + 35Spro::RPS2::Flag	N-term 4xMyc and C-term 3xFlag	level 2 Golden Gate construct which carries RPS2 gene under control of 35S CaMV promoter and with C-term FLAG tag and MdRIN4 under 35S CaMV promoter with N-term Myc tag. For plant stable and transient transformation	This study
2380	*A. tumefaciens* AGL1	pAGM4723::BAR:: 35Spro::Myc:: MdRIN4$^{D186N+F193Y}$ + 35Spro::RPS2::Flag	N-term 4xMyc and C-term 3xFlag	level 2 Golden Gate construct which carries RPS2 gene under control of 35S CaMV promoter and with C-term FLAG tag and AtRIN4 with D186N+F193Y mutations and under 35S CaMV promoter with N-term Myc tag. For plant stable and transient transformation	This study
2351	*A. tumefaciens* AGL1	pAGM4723::BAR::rin4pro::My c::GFP + 35S::RPS2::Flag	N-term 4xMyc and C-term 3xFlag	level 2 Golden Gate construct which carries RPS2 gene under control of 35S CaMV promoter and with C-term FLAG tag and GFP under native rin4 promoter with N-term Myc tag. For plant stable and transient transformation	This study
2374	*A. tumefaciens* AGL1	EpiGreenB5-GG::35Spro::Myc::AtRIN4	N-term 4xMyc	used for stable plant transformation. Carries AtRIN4 gene under 35S CaMV promoter and with N-term Myc tag. Needs to be co-transformed with pSOUP	This study
2375	*A. tumefaciens* AGL1	EpiGreenB5-GG::35Spro:: Myc::AtRIN4$^{N158D+Y165F}$	N-term 4xMyc	used for stable plant transformation. Carries MdRIN4 gene with N158D and Y165F mutations, under 35S CaMV promoter and with N-term Myc tag. Needs to be co-transformed with pSOUP	This study

KSC #	Host strain	Vector	Epitope tag	Description	Source/reference
1115	*A. tumefaciens* AGL1	EpiGreenB5-GG::35Spro::Flag::MdRIN4	N-term 3xFlag	used for stable plant transformation. Carries MdRIN4 gene under 35S CaMV promoter and with N-term FLAG tag. Needs to be co-transformed with pSOUP	This study
2376	*A. tumefaciens* AGL1	EpiGreenB5-GG::35Spro::Myc::MdRIN4	N-term 4xMyc	used for stable plant transformation. Carries MdRIN4 gene under 35S CaMV promoter and with N-term Myc tag. Needs to be co-transformed with pSOUP	This study
2377	*A. tumefaciens* AGL1	EpiGreenB5-GG::35Spro::Myc::MdRIN4$^{D186N+F193Y}$	N-term 4xMyc	used for stable plant transformation. Carries MdRIN4 gene with D186N and F193Y mutations, under 35S CaMV promoter and with N-term Myc tag. Needs to be co-transformed with pSOUP	This study
1116	*A. tumefaciens* AGL1	EpiGreenB5-GG::35Spro::Myc::MdRIN4_CLV3	N-term 4xMyc	used for stable plant transformation. Carries MdRIN4_CLV3 coding sequence under 35S CaMV promoter and with N-term Myc tag. Needs to be co-transformed with pSOUP	This study
2355	*A. tumefaciens* AGL1	EpiGreenB5-GG::35Spro::Myc::MdRIN4_CLV3$^{D186N+F193Y}$	N-term 4xMyc	used for stable plant transformation. Carries MdRIN4_CLV3 coding sequence with D186N and F193Y mutations, under 35S CaMV promoter and with N-term Myc tag. Needs to be co-transformed with pSOUP	This study
554	*A. tumefaciens* AGL1	EpiGreenB5-GG::rps2pro::MR5::Myc	C-term 4xMyc	used for stable plant transformation. Carries MR5 gene under RPS2 native promoter and with C-term Myc tag. Needs to be co-transformed with pSOUP nt transformation.	This study

Table 2.8. Constructs used for *Venturia inaequalis* predicted candidate effectors (ViCE) cloning.

KSC #	Host strain	Vector	Insert	Source/reference
1187	*E. coli* DH5α	pICH41021::ViCE1_noSP	*V. inaequalis* 120 ViCE 1 without signal peptide	This study
1188	*E. coli* DH5α	pICH41021::ViCE2_noSP	*V. inaequalis* 120 ViCE 2 without signal peptide	This study
1189	*E. coli* DH5α	pICH41021::ViCE5_noSP	*V. inaequalis* 120 ViCE 5 without signal peptide	This study
1190	*E. coli* DH5α	pICH41021::ViCE6_noSP	*V. inaequalis* 120 ViCE 6 without signal peptide	This study
1191	*E. coli* DH5α	pICH41021::ViCE8_noSP	*V. inaequalis* 120 ViCE 8 without signal peptide	This study
1192	*E. coli* DH5α	pICH41021::ViCE9_noSP	*V. inaequalis* 120 ViCE 9 without signal peptide	This study
1193	*E. coli* DH5α	pICH41021::ViCE10_noSP	*V. inaequalis* 120 ViCE 10 without signal peptide	This study
1194	*E. coli* DH5α	pICH41021::ViCE11_noSP	*V. inaequalis* 120 ViCE 11 without signal peptide	This study
1195	*E. coli* DH5α	pICH41021::ViCE12_noSP	*V. inaequalis* 120 ViCE 12 without signal peptide	This study
1196	*E. coli* DH5α	pICH41021::ViCE13_noSP	*V. inaequalis* 120 ViCE 13 without signal peptide	This study
1197	*E. coli* DH5α	pICH41021::ViCE14_noSP	*V. inaequalis* 120 ViCE 14 without signal peptide	This study
1198	*E. coli* DH5α	pICH41021::ViCE15_noSP	*V. inaequalis* 120 ViCE 15 without signal peptide	This study
1199	*E. coli* DH5α	pICH41021::ViCE16_noSP	*V. inaequalis* 120 ViCE 16 without signal peptide	This study
1200	*E. coli* DH5α	pICH41021::ViCE17_noSP	*V. inaequalis* 120 ViCE 17 without signal peptide	This study
1201	*E. coli* DH5α	pICH41021::ViCE18_noSP	*V. inaequalis* 120 ViCE 18 without signal peptide	This study
1202	*E. coli* DH5α	pICH41021::ViCE19_noSP	*V. inaequalis* 120 ViCE 19 without signal peptide	This study
1203	*E. coli* DH5α	pICH41021::ViCE20_noSP	*V. inaequalis* 120 ViCE 20 without signal peptide	This study
1204	*E. coli* DH5α	pICH41021::ViCE21_noSP	*V. inaequalis* 120 ViCE 21 without signal peptide	This study
1205	*E. coli* DH5α	pICH41021::ViCE22_noSP	*V. inaequalis* 120 ViCE 22 without signal peptide	This study

Table 2.9. Constructs used for *Venturia inaequalis* predicted candidate effectors (ViCE) transient expression without signal peptide.

KSC #	Host strain	Vector	Epitope tag	Description	Source/reference
1217	*A. tumefaciens* AGL1	pICH89988::ViCE1_noSP::HA	C-term 6xHA	for *V. inaequalis* 120 ViCE 1 transient expression without signal peptide	This study
1218	*A. tumefaciens* AGL1	pICH89988::ViCE2_noSP::HA	C-term 6xHA	for *V. inaequalis* 120 ViCE 2 transient expression without signal peptide	This study
1219	*A. tumefaciens* AGL1	pICH89988::ViCE6_noSP::HA	C-term 6xHA	for *V. inaequalis* 120 ViCE 6 transient expression without signal peptide	This study
1220	*A. tumefaciens* AGL1	pICH89988::ViCE9_noSP::HA	C-term 6xHA	for *V. inaequalis* 120 ViCE 9 transient expression without signal peptide	This study
1221	*A. tumefaciens* AGL1	pICH89988::ViCE10_noSP::HA	C-term 6xHA	for *V. inaequalis* 120 ViCE 10 transient expression without signal peptide	This study
1222	*A. tumefaciens* AGL1	pICH89988::ViCE11_noSP::HA	C-term 6xHA	for *V. inaequalis* 120 ViCE 11 transient expression without signal peptide	This study
1223	*A. tumefaciens* AGL1	pICH89988::ViCE12_noSP::HA	C-term 6xHA	for *V. inaequalis* 120 ViCE 12 transient expression without signal peptide	This study
1224	*A. tumefaciens* AGL1	pICH86988::ViCE13_noSP::HA	C-term 6xHA	for *V. inaequalis* 120 ViCE 13 transient expression without signal peptide	This study
1225	*A. tumefaciens* AGL1	pICH89988::ViCE14_noSP::HA	C-term 6xHA	for *V. inaequalis* 120 ViCE 14 transient expression without signal peptide	This study
1226	*A. tumefaciens* AGL1	pICH89988::ViCE15_noSP::HA	C-term 6xHA	for *V. inaequalis* 120 ViCE 15 transient expression without signal peptide	This study
1227	*A. tumefaciens* AGL1	pICH89988::ViCE16_noSP::HA	C-term 6xHA	for *V. inaequalis* 120 ViCE 16 transient expression without signal peptide	This study

KSC #	Host strain	Vector	Epitope tag	Description	Source/reference
1228	*A. tumefaciens* AGL1	pICH89988::ViCE17_noSP::HA	C-term 6xHA	for *V. inaequalis* 120 ViCE 17 transient expression without signal peptide	This study
1229	*A. tumefaciens* AGL1	pICH89988::ViCE18_noSP::HA	C-term 6xHA	for *V. inaequalis* 120 ViCE 18 transient expression without signal peptide	This study
1230	*A. tumefaciens* AGL1	pICH86988::ViCE19_noSP::HA	C-term 6xHA	for *V. inaequalis* 120 ViCE 19 transient expression without signal peptide	This study
1231	*A. tumefaciens* AGL1	pICH89988::ViCE20_noSP::HA	C-term 6xHA	for *V. inaequalis* 120 ViCE 20 transient expression without signal peptide	This study
1232	*A. tumefaciens* AGL1	pICH86988::ViCE21_noSP::HA	C-term 6xHA	for *V. inaequalis* 120 ViCE 21 transient expression without signal peptide	This study
1233	*A. tumefaciens* AGL1	pICH89988::ViCE22_noSP::HA	C-term 6xHA	for *V. inaequalis* 120 ViCE 22 transient expression without signal peptide	This study

Table 2.10. Constructs used for *Venturia inaequalis* predicted candidate effectors (ViCE) transient expression fused with PR1α signal peptide.

KSC #	Host strain	Vector	Epitope tag	Description	Source/reference
1245	*A. tumefaciens* AGL1	pICH86966::35Spro::PR1α::ViCE1::HA	C-term 6xHA	for *V. inaequalis* 120 ViCE 1 transient expression with *Nb* PR1α signal peptide	This study
1246	*A. tumefaciens* AGL1	pICH86966::35Spro::PR1α::ViCE2::HA	C-term 6xHA	for *V. inaequalis* 120 ViCE 2 transient expression with *Nb* PR1α signal peptide	This study
1247	*A. tumefaciens* AGL1	pICH86966::35Spro::PR1α::ViCE6::HA	C-term 6xHA	for *V. inaequalis* 120 ViCE 6 transient expression with *Nb* PR1α signal peptide	This study
1248	*A. tumefaciens* AGL1	pICH86966::35Spro::PR1α::ViCE9::HA	C-term 6xHA	for *V. inaequalis* 120 ViCE 9 transient expression with *Nb* PR1α signal peptide	This study
1249	*A. tumefaciens* AGL1	pICH86966::35Spro::PR1α::ViCE10::HA	C-term 6xHA	for *V. inaequalis* 120 ViCE 10 transient expression with *Nb* PR1α signal peptide	This study
1250	*A. tumefaciens* AGL1	pICH86966::35Spro::PR1α::ViCE11::HA	C-term 6xHA	for *V. inaequalis* 120 ViCE 11 transient expression with *Nb* PR1α signal peptide	This study
1251	*A. tumefaciens* AGL1	pICH86966::35Spro::PR1α::ViCE12::HA	C-term 6xHA	for *V. inaequalis* 120 ViCE 12 transient expression with *Nb* PR1α signal peptide	This study
1252	*A. tumefaciens* AGL1	pICH86966::35Spro::PR1α::ViCE13::HA	C-term 6xHA	for *V. inaequalis* 120 ViCE 13 transient expression with *Nb* PR1α signal peptide	This study
1253	*A. tumefaciens* AGL1	pICH86966::35Spro::PR1α::ViCE14::HA	C-term 6xHA	for *V. inaequalis* 120 ViCE 14 transient expression with *Nb* PR1α signal peptide	This study
1254	*A. tumefaciens* AGL1	pICH86966::35Spro::PR1α::ViCE15::HA	C-term 6xHA	for *V. inaequalis* 120 ViCE 15 transient expression with *Nb* PR1α signal peptide	This study
1255	*A. tumefaciens* AGL1	pICH86966::35Spro::PR1α::ViCE16::HA	C-term 6xHA	for *V. inaequalis* 120 ViCE 16 transient expression with *Nb* PR1α signal peptide	This study

KSC #	Host strain	Vector	Epitope tag	Description	Source/reference
1256	*A. tumefaciens* AGL1	pICH86966::35Spro::PR1α::ViCE17::HA	C-term 6xHA	for *V. inaequalis* 120 ViCE 17 transient expression with *Nb* PR1α signal peptide	This study
1257	*A. tumefaciens* AGL1	pICH86966::35Spro::PR1α::ViCE18::HA	C-term 6xHA	for *V. inaequalis* 120 ViCE 18 transient expression with *Nb* PR1α signal peptide	This study
1258	*A. tumefaciens* AGL1	pICH86966::35Spro::PR1α::ViCE19::HA	C-term 6xHA	for *V. inaequalis* 120 ViCE 19 transient expression with *Nb* PR1α signal peptide	This study
1259	*A. tumefaciens* AGL1	pICH86966::35Spro::PR1α::ViCE20::HA	C-term 6xHA	for *V. inaequalis* 120 ViCE 20 transient expression with *Nb* PR1α signal peptide	This study
1260	*A. tumefaciens* AGL1	pICH86966::35Spro::PR1α::ViCE21::HA	C-term 6xHA	for *V. inaequalis* 120 ViCE 21 transient expression with *Nb* PR1α signal peptide	This study
1261	*A. tumefaciens* AGL1	pICH86966::35Spro::PR1α::ViCE22::HA	C-term 6xHA	for *V. inaequalis* 120 ViCE 22 transient expression with *Nb* PR1α signal peptide	This study

2.1.3 Plant material

Arabidopsis thaliana

Arabidopsis accessions used in this study were obtained from The Sainsbury Laboratory [Norwich, UK) or Plant and Food [Mt. Albert, NZ). Dalton's Premium Seed raising mix [Fruitfed, NZ] mixed with coarse grain vermiculite with ratio 20:1 was used for seed sowing. After sowing pots were placed in a cold room (4°C) for 3-4 days for germination. After two weeks of growing in a common pot, individual plants were transferred to trays with separate cells and were grown in short day conditions with 11 hours light at 22°C with non-regulated humidity, which was approximately 60%, for 4-5 weeks before use.

Arabidopsis thaliana genotypes used in this study are listed in table 2.11. *Arabidopsis thaliana* genotypes generated in this study are listed in table 2.12.

Table 2.11. *Arabidopsis thaliana* genotypes used in this study.

Genotype	Description	WT/GM
Col-0	-	WT
rps2-101	EMS mutagenesis derived line with knock out *RPS2* gene (Bent et.al, 1994)	GM
rin4/rps2	Double KO plants containing T-DNA insertion knock out of *RIN4* and *rps2-101c* mutation (Belkhadir et al., 2004)	GM
rps2/rpm1	Double KO plants containing T-DNA insertion knock out of *RIN4* and *rpm1-3* mutation (Grant et.al., 1995)	GM
rin4/rps2/rpm1	Triple KO plants containing T-DNA insertion knock out of RIN4, *rps2-101* and *rpm1-3* mutations (Belkhadir et al., 2004)	GM

Table 2.12. *Arabidopsis thaliana* genotypes generated during this study.

Genotype	Description	WT/GM
rin4/rps2/rpm1 + 35Spro::MdRIN4	*A. thaliana rin4/rps2/rpm1* plants transformed with EpiGreenB5-GG::35Spro::Flag::MdRIN4 (KSC 1115).	GM
rin4/rps2/rpm1 + 35Spro::MdRIN4_CLV3	*A. thaliana rin4/rps2/rpm1* plants were transformed with EpiGreenB5-GG::35Spro::Myc::MdRIN4 (KSC 1116).	GM
rin4/rps2/rpm1 + rps2pro::MR5	*A. thaliana rin4/rps2/rpm1* plants were transformed with EpiGreenB5-GG::rps2pro::MR5::Myc (KSC 554)	GM

Genotype	Description	WT/GM
rin4/rps2/rpm1 + 35Spro::MdRIN4 + rps2pro::MR5	*A. thaliana* plants resulted from a cross of *rin4/rps2/rpm1* + rps2pro::MR5 line with *rin4/rps2/rpm1* + 35Spro::MdRIN4 line.	GM
rin4/rps2/rpm1 + rps2pro::RPS2 + rin4pro::AtRIN4	*A. thaliana rin4/rps2/rpm1* plants were transformed with pAGM4723::BAR::rin4pro::Myc::AtRIN4 + rps2pro::RPS2::Flag (KSC 1871).	GM
rin4/rps2/rpm1 + rps2pro::RPS2 + rin4pro::AtRIN4$^{N158D+Y165F}$	*A. thaliana rin4/rps2/rpm1* plants were transformed with pAGM4723::BAR::rin4pro::Myc::AtRIN4 $^{N158D+Y165F}$ + rps2pro::RPS2::Flag (KSC 1872).	GM
rin4/rps2/rpm1 + rps2pro::RPS2 + rin4pro::MdRIN4	*A. thaliana rin4/rps2/rpm1* plants were transformed with pAGM4723::BAR::rin4pro::Myc::MdRIN4 + rps2pro::RPS2::Flag (KSC 1873).	GM
rin4/rps2/rpm1 + rps2pro::RPS2 + rin4pro::MdRIN4$^{D186N+F193Y}$	*A. thaliana rin4/rps2/rpm1* plants were transformed with pAGM4723::BAR::rin4pro::Myc::MdRIN4 $^{D186N+F193Y}$ + rps2pro::RPS2::Flag (KSC 1874).	GM

- All the transgenic *A. thaliana* lines listed in Table 2.12 were generated using floral dip transformation method.

Nicotiana sp

Nicotiana tabacum Wisconsin 38 (a.k.a. Havana 38) and *Nicotiana benthamiana* seeds were sown on Dalton's Premium Seed raising mix [Fruitfed, NZ] and subjected to cold treatment (4°C) for 3-4 days for germination. Plants then were grown for one week at 24°C with 14 hours light (long day) with non-regulated humidity, which was approximately 60%. After that plantlets were transferred to individual pots (diameter - 10 cm, height - 11 cm) and grown at the same conditions for 4-5 weeks before use.

Malus sp

Before placing seeds in a cold-room (4°C), they were treated with a solution of Thiram (fungicide agent) [Kiwicare, NZ], to ensure absence of any fungal infection. To do so, we diluted approximately 20 mgs of Thiram in Petri dishes full of water and then soaked the seeds in them for 15-20 minutes. After treatment seeds were moved to zip lock plastic bags 2/3 full of wet vermiculate [Ausperl, NZ].

After 1-1,5 months seeds germinated in a cold room (4°C). After germination, seeds were transferred into Dalton's Premium Seed raising mix

[Fruitfed, NZ] one seed per pot and were grown in short day conditions with 11 hours light at 22°C with non-regulated humidity, which was approximately 60%.

2.1.4 Bacterial & Plant Media

The recipes of the media used for growing bacteria and plants are listed in this subchapter. All the media formulations are given for 1 L content. All the media were autoclave sterilized and cooled down prior to adding antibiotics or other selective agents

L medium used to grow *E. coli* DH5α and *HB101* strains contained:

Tryptone [Sigma Aldrich, NZ] – 10 g,

Yeast Extract [Sigma Aldrich, NZ] – 5 g,

Sodium chloride [Merck, NZ] – 5 g,

D-glucose [Merck, NZ] – 1 g;

Bacteriological agar [Sigma Aldrich, NZ] – 10 g were added for solid media. Depending on the plasmid carried, the appropriate antibiotic was added.

King's B medium used to grow *Pseudomonas sp* strains, including *P. fluorescens* Pf0-1 (T3S), contained:

Peptone [Sigma Aldrich, NZ] – 20 g,

K_2HPO_4 [Merck, NZ] – 1.5 g,

Glycerol [Merck, NZ] – 10 mL;

Bacteriological agar [Sigma Aldrich, NZ] – 15 g were added for solid media.

Solid MS (Murashige Skoog) media with B5 vitamins was used for selecting transgenic plants after floral dip transformation of *A. thalianana*.

MS with B5 vitamins [Duchefa, NL] – 4.4 g,

Sucrose [Sigma Aldrich, NZ] – 10 g,

Bacteriological agar [Sigma Aldrich, NZ] – 8 g.

pH of the media was adjusted to 5.8 by adding KOH solution.

PPT [Sigma Aldrich, NZ] (phosphinotricin) at 10 µg/ml or Kanamycin at 50 µg/ml were added to the media according to the constructs used for plant transformation. Used bigger Petri dishes (150 mm x 15 mm) for raising T1 and T2 plants.

2.1.5 Antibiotics

Antibiotics used for bacteria and plant selection are listed in this subchapter. All the stock solutions were made with distilled water, except that methanol was used for Rifampicin and Tetracycline, and ethanol was used for Chloramphenicol. Antibiotics were added to media after autoclave sterilization.

The final concentrations of antibiotics used for bacterial cultures and plants were: Ampicillin - 100 μg/ml; Spectinomycin – 100 μg/ml; Kanamycin – 50 μg/ml; Gentamicin – 20 μg/ml; Tetracycline – 5 μg/ml; Chloramphenicol – 30 μg/ml; Rifampicin – 50 μg/ml.

2.2 Microbiology methods

2.2.1 Bacterial conjugation

Bacterial conjugation was used to introduce broad-host vectors into *P. fluorescens* cells. Recipient strain was *P. fluorescens Pf*0-1(T3S), the donor was *E. coli* DH5α carrying a broad host-range plasmid pBBR1 MCS-5 with the desired insert. *E. coli* HB101 with pRK2013 was used as helper.

All strains mentioned above were streaked on King's B or L-agar medium with appropriate antibiotics and grown overnight. Then they were inoculated to liquid L medium with antibiotics and were grown in a shaking incubator at 28°C for *Pf*-0 and 37°C for *E. coli*. Overnight cultures were mixed as: Recipient (0.6 mL) + Donor (0.2 mL) + Helper (0.2 mL) at OD_{600}= ~2 in a 1.5 mL microcentrifuge tube and centrifuged at 4000 g for 3 min. Resulting bacterial cell pellet was resuspended/washed with 1 mL of L medium and centrifuged again.

After resuspending the pellet in 0.2 mL of fresh liquid L medium, ten 20 μL drops of culture with cells were placed on a solid L medium plate without antibiotics, dried and incubated for 6-8 hours at 28°C.

These incubated cells were then scraped off from the plate and restreaked on King's B plates. These plates contained 30 mg/mL Chloramphenicol and 5 mg/mL Tetracycline (*Pf*-0 selection) and an additional antibiotic for the target plasmid selection (Gentamycin for pBBR1 derived constructs). Plates were incubated for 48 hours at 28°C and single colonies were used to set up glycerol stocks.

2.2.2 Competent cell preparation & transformation

Electrocompetent cells of different bacterial strains were prepared to use for electrotransformation with plasmids generated in this study and previously. *E.coli* DH5α and *A. tumefaciens* GV3101 and AGL1 were made electrocompetent by growing in L-media to optical density of 0.7 and then washed 4 times with cold 10% glycerol followed by snap freezing 40 µL aliquots in liquid nitrogen.

Aliquots were stored in a freezer at -80°C. Competent cells were transformed by electroporation in a MicroPulser Electroporator [BioRad, NZ] at settings recommended by manufacturer and immediately resuspended in 0.5 mL liquid L medium without antibiotics. Cultures then were incubated at appropriate temperatures for 1-1.5 hours prior plating on agar L-media with corresponding antibiotic.

*P. fluorescens Pf*0-1 were grown overnight in 3 mL of liquid L-media in a shaking incubator at 28°C. In the morning of the next day, cells were spun down in 1.5 mL microcentrifuge tubes at 5000 g for 3 minutes and washed with 1 mL of sterile 300 mM sucrose solution. This wash was repeated for three times and after last wash cells were resuspended in 50 µL of 300 mM sucrose solution.

1-5 µL of the desired plasmid were added into 50 µL aliquot and cells were electroporated by MicroPulser Electroporator [Bio-Rad, NZ] at 2.5 kV, 2.5 seconds pulse. Cells were immediately resuspended in 500-1000 µL of liquid L-medium and grown in a shaking incubator at 200 rpm and 28°C for 1.5-2 hours. Then 150 µL of cells was plated on the solid KB-media containing plates with appropriate antibiotic selection and grown for 2 days at 28°C.

2.2.3 Glycerol stocks

Glycerol stocks of bacterial strains were used for long-term storage. They were made from overnight cultures of bacteria grown in liquid L-medium with appropriate antibiotics. 800 µL of overnight cell culture was mixed well with 400 µL of sterile 60% glycerol and frozen at -80°C for long-term storage.

2.3 Plant Methods

2.3.1 Hypersensitive response assays in *Arabidopsis thaliana* and *Malus* sp.

Infiltration of plant leaves with *P. syringae* Pf0-1(T3S) strains carrying specific effectors or effector candidates were used to assess the plant response.

Strains were streaked from glycerol stocks onto King's B media plates with appropriate antibiotic and grown for two days at 28°C. Cells were harvested and resuspended in 10 mM $MgCl_2$ and then diluted to OD_{600} 0.2 for infiltration. Infiltrations were carried out on 4-5 weeks old plants with fully expanded leaves using a blunt 1 mL syringe with as little damage as possible. HR symptoms were assayed visually at ~20 hours post infiltration (HPI) and photographs were taken.

2.3.2 *Agrobacterium tumefaciens* infiltration for transient protein expression

Agroinfiltration was used for transient expression of proteins of interest in leaves of *N. benthamiana* plants. For that, *A. tumefaciens* AGL1 or GV3101 were streaked onto L medium plates with appropriate antibiotic selection from glycerol stocks and grown for two days at 28°C. Cells then were inoculated in liquid L medium with antibiotics and grown overnight.

Overnight cultures were centrifuged at 2500 g and resuspended in Agro infiltration buffer (10 mM $MgCl_2$, 10 mM MES) and diluted to OD_{600} 0.4 or 0.2, 0.05 (depending on the *Agrobacterium* strain) for blunt syringe infiltrations into *N. benthamiana* or *N. tabacum*. HR was assayed at 2-3 days post infiltration (DPI) for tobacco and 3-4 DPI for *N. benthamiana* and photographs were taken. If the macroscopic HR phenotype seemed to be uncertain, further ion leakage analysis was performed as mentioned in subchapter 2.3.3.

2.3.3 *N. benthamiana* ion leakage assay

Ion leakage assay was used for precise quantification of the PCD response caused by agroinfiltration in *N. benthamiana* leaves. Plants were agroinfiltrated with strains carrying the constructs with genes of interest as mentioned in (2.3.2) and 8 mm diameter leaf discs were collected just after and 48 or 72 hours post infiltration. They were shaken in tissue culture plates with 2 ml of sterile miliQ water for 2 hours at 150 rpm. Then water conductivity in each well was measured using a Horiba B-771 LAQUAtwin compact conductivity meter [Horiba, JP]. 2 leaf

disks were placed in each well and 8 biological replicates per sample were measured.

Average (arithmetic mean) values were then plotted on the graphs with standard error of mean presented (SEM). Two tailed T-tests were performed to define the significant difference between sample groups.

2.3.4 Arabidopsis stable transformation

Arabidopsis stable transgenic lines were generated by the floral dip method (Clough & Bent, 1998). Agrobacterium strains carrying desired constructs were streaked on L agar plates and grown at 28°C for two days. 1-2 mL of liquid L media were poured onto the plate and bacteria were rubbed off with a sterile plastic hockey stick.

The resulting inoculum was used to inoculate 250 mL of liquid L media. Agrobacterium strains were grown for approximately 36 hours at 200 rpm shaking and 28°C temperature. Then they were chilled on ice for 20 minutes and spun down at 4°C, 5000 g for 20 minutes and resuspended in an equal volume of 5% cold sucrose solution. The optical density at 600 nm was measured and adjusted to OD_{600} = 0.8-1 in 400 ml of sucrose solution. Finally 160 µl of Pulse (Silwet L-77) was added into the suspension and mixed carefully.

Flowering Arabidopsis plants were dipped in the bacterial suspension and agitated for 2 minutes. Plants were then covered with plastic bags for 1 day and then bags were removed and plants left for seed formation. Watering was performed 2 times after dipping on every 3rd day.

When plants were dry, mature seeds were collected and subjected to selection. For Kanamycin and small scale BASTA selection, seeds were sown on plates containing solid MS media with either PPT (phosphinothricin) [Sigma, KR] or Kanamycin added. Seedlings were grown for two weeks and green healthy surviving plants were transferred to soil for further genotyping and phenotype analysis.

For large scale BASTA selection 0.5 mL volume of seeds of each line were evenly sown on soil in the cell-pot trays and were sprayed with commercial BASTA solution (final concentration was according to BASTA solution manufacturer instructions) [Bayer, KR] at 10, 12, 15, 18 days after sowing. Surviving plants were transferred to individual pots for further genotyping and phenotype analysis.

2.3.5 Arabidopsis crossing

For crossing of two Arabidopsis line of interest, mature siliques and open flowers were removed from maternal plant. Unopened flower buds were opened and the anthers were carefully removed with fine forceps. Mature and opened flowers were collected from a paternal plant and tapped on the stigma of the maternal plant. This was repeated roughly for 30 maternal stigmas per crossing event. Resulting siliques were left to develop and produce seeds which were collected for further analysis.

2.4 Molecular Biology Methods

2.4.1 Enzymes used in this study

Restriction enzymes used to cut the DNA were purchased from New England Biolabs [NEB, Thermo Fischer, NZ] and used with 10X buffer supplied with the enzymes under conditions recommended by manufacturer.

Phusion DNA polymerase and buffer [Thermo Fischer, NZ] were used for PCR amplification for cloning and Agilent Quickchange kit [Agilent, NZ] for site directed mutagenesis. NEB T4 DNA ligase was used with supplied buffer under recommended conditions for Golden Gate assemblies and blunt/sticky end ligations. Primers were designed using Geneious R8 [Biomatters, AU] and synthesized at Solgent or Macrogen, KR; list of primers used in this study can be found in appendices, Tables 6.1 and 6.2.

2.4.2 Bacterial genomic DNA extraction methods

Macherey-Nagel NucleoSpin Tissue kit [MediRay, NZ] was used for bacterial genomic DNA extraction according to manufacturer's instructions. DNA concentration was quantified by Nanodrop 1000 Specrophotometer [Thermo Fischer, NZ] and agarose gel electrophoresis.

2.4.3 Chelex plant genomic DNA extraction

A quick method utilizing Chelex for genomic DNA extraction was used for plant genotyping. One leaf disc (0.37 cm^2) was sampled from plant cotyledons or fully expanded leaves and ground with plastic pestle in 150 µl 5% chelex in 1.5 mL microcentrifuge tube. The resulting mixture was boiled at 96°C for 5 minutes then vortexed for 15 seconds and spun down at maximum speed for 1 minute. 100 µl

were transferred to the fresh microcentrifuge tube and spun down at maximum speed for 1 minute again. Then 2 µl of the supernatant were used for PCR (Hwang et al., 2010).

2.4.4 Plant genomic DNA extraction methods

Genomic DNA used for genotyping and gene amplification from *A. thaliana* or *Malus sp* was purified from liquid nitrogen frozen tissue using the GeneJet Plant Genomic DNA Kit [Thermo Fischer, NZ] according to instructions. DNA concentration was quantified by Nanodrop and agarose gel electrophoresis.

2.4.5 Polymerase chain reaction

Polymerase chain reactions were performed using Phusion High-Fidelity Polymerase [NEB, Thermo Fischer, NZ] or PrimeSTAR GXL DNA Polymerase [Clontech, USA] high fidelity polymerase under conditions recommended by manufacturer, in an Eppendorf Mastercycler Nexus machine [MediRay, NZ].

The following PCR programme was used for a routine gene amplification:

Denature: 96°C for 5 min

Denature: 96°C for 30 sec

Anneal: 52-60°C (depending on primer T_a) for 30 sec

Elongation: 72°C for 30-300 sec (depending on the amplicon size) for 35 cycles,

Elongation: 72°C for 5 min

Hold: 20°C – indefinite.

2.4.6 Nested PCR

Nested PCR was used to amplify ViCE genes from *Venturia inaequalis* 120 cDNA (acquired from Jo Bowen, PFR, Mt. Albert, NZ), because conventional PCR didn't provide enough PCR product for consequent cloning. First, the presence of all ViCE was confirmed using conventional PCR from *Vi* 120 genomic DNA. PCR reactions were performed using Phusion High-Fidelity Polymerase [NEB, Thermo Fischer, NZ] under recommended conditions in an Eppendorf Mastercycler Nexus machine [MediRay, NZ] using the same primers.

PCR programme used for the initial run:

Denature: 96°C for 5 min

Denature: 96°C for 30 sec

Anneal: 52-60°C (depending on primer T_a) for 30 sec

Elongation: 72°C for 30-300 sec (depending on the amplicon size) for 30 cycles,

Elongation: 72°C for 5 min

Hold: 20°C – indefinite.

After the initial run 5 µL of resulting product solution was used for the second run of amplification. Fresh polymerase, buffer and dNTPs were added.

PCR programme used for the 2nd run:

Denature: 96°C for 30 sec

Anneal: 52-60°C (depending on primer T_a) for 30 sec

Elongation: 72°C for 30-300 sec (depending on the amplicon size) for 30 cycles,

Elongation: 72°C for 5 min

Hold: 20°C – indefinite.

PCR products were visualized and their quality was assessed using agarose gel electrophoresis.

2.4.7 Colony PCR

Screening for recombinant plasmids during cloning was performed via colony PCR. Single colonies were transferred into 50 µl of sterile water and resuspended by pipetting. 2 µl of the colony suspensions were used as a template for PCR. Prime Taq polymerase [GenetBio, KR] was used for colony PCR and additional boiling step at 96°C for 5 minutes was added in the beginning of the PCR programme mentioned in subchapter 2.4.5.

2.4.8 Agarose gel electrophoresis

DNA fragments and PCR product visualization was performed using agarose gel electrophoresis. Gels prepared contained 1-2.5% (w/v) Low EEO

Agarose [Sigma Aldrich, NZ] in TAE buffer, melted in a microwave. Gels were cooled and solidified with combs in racks and then transferred to gel tanks [BioRad, NZ] containing TAE buffer with 20 µL ethidium bromide added for nucleic acid visualization.

Samples were loaded into wells in the agarose gel after mixing with 10X gel loading buffer along with 1 kb or 1 kb+ DNA ladder [NEB, Thermo Fischer, NZ and Enzynomics, KR] and run under constant voltage of 120 V for 24-60 minutes. Nucleic acid was visualized on a BioRad GelDoc 312 nm UV transilluminator [BioRad, NZ] or Da-Vinci GelDoc machine [Da-Vinci, KR] and photographed.

2.4.9 Agarose gel purification of DNA

DNA fragments separated on agarose gels were excised using clean razor blades and then purified using AxyPrep DNA gel extraction kit [MediRay, NZ] according to recommended conditions. Nanodrop quantification and gel electrophoresis were used to assess the quantity of purified DNA.

2.4.10 Blunt-end *Sma*I/T4 cloning

10 µL of agarose gel purified PCR products were used for blunt end ligation to 1 µL of pICH41021 vector. Digestion with 0.5 µL of *Sma*I and ligation using 0.5 µL T4 DNA ligase were performed in one tube at the same time at room temperature (~25°C) for 2-4 hours or overnight. The resulting ligation mix was spun down on a self-made Sepharose 4B (a small hole was made in 0.5 mL microcentrifuge tube and 150 µL of 5% Sepharose 4B solution was centrifuged in this tube at 2000 g for 2 minutes) [Sigma Aldrich, NZ] coloumns at 2000 g for 2 minutes for desalting, and then transformation into *E. coli* DH5α competent cells for selection.

2.4.11 Golden gate cloning

Golden Gate cloning (Engler et al., 2008) is a versatile tool for rapid gene cloning especially when quick swapping of protein tags, promoters or vector systems is required. Golden Gate cloning is also very useful for quick generation of various protein chimeras. This method is based on the ability of some restriction enzymes to cut the DNA molecules not at, but near the recognition site. This allows to generate the variety of 4 bp overhangs for sticky end ligation. The main

limitations for using Golden Gate method are that not all vector systems are compatible with it and also that neither vector, nor any of the inserts can carry the restriction sites for the *Bsa*I enzyme used in assembly.

The basic modules for Golden Gate cloning are referred as level 0 modules. They carry promoters, tags, reporter genes, terminators and etc. All the vectors with simple assembly blocks of genes of interest generated by researchers are level 0. These level 0 modules can be assembled into the level 1 destination vector generating the expression unit (contains promoters, tags, terminators and etc.) in a correct order. Further assembly of level 1 expression units into the multigene construct is available. These multigene constructs based on level 2 destination vectors are referred as level 2 assemblies.

There are plenty of vectors and standard modules available to date for Golden Gate assemblies (Engler & Marillonnet, 2013, 2014). In addition, every lab generates their own modules and vectors for their specific aims.

Golden gate cloning and assemblies in this study were performed according to Engler et al. (2008); Engler and Marillonnet (2014). In brief, the schematic of Golden Gate cloning is shown in Figure 2.1. Level 0 modules are generated by blunt end ligation of PCR products amplifying the gene of interest. Then these level 0 gene modules are being assembled in a single pot reaction with *Bsa*I restriction enzyme and T4-ligase resulting into the expression unit being inserted into the destination level 1 vector (pICH86988 or pBBR1MCS-5B).

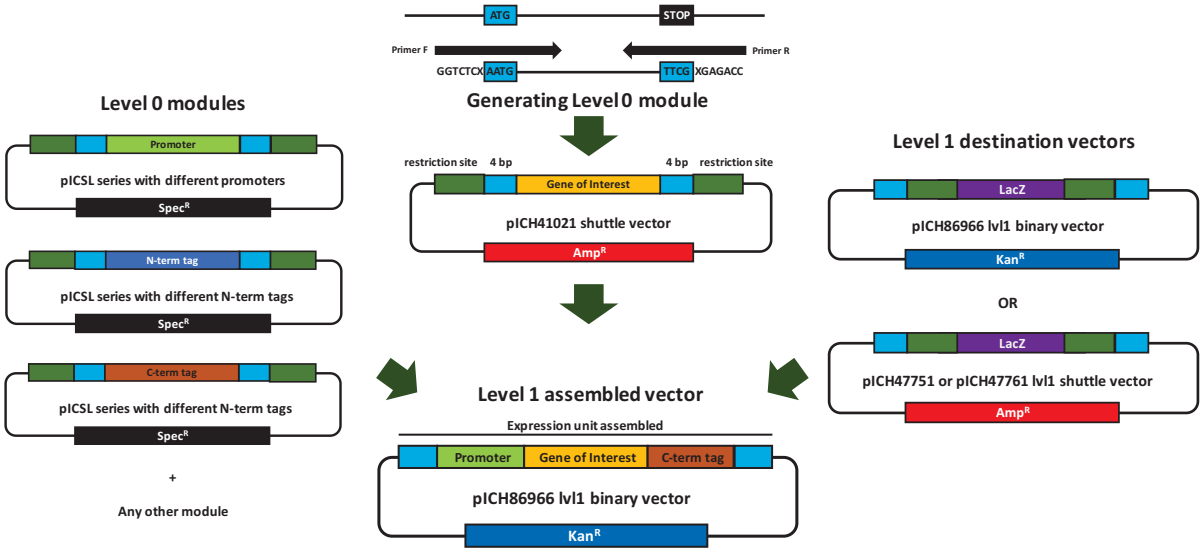

Figure 2.1. Schematic representation of Golden Gate cloning system.
Level 0 modules are generated by blunt-end ligation of amplified DNA fragments. Then these fragments can be assembled together with level 0 vectors containing promoters, tags, etc. into level 1 constructs containing the expression units.

Incubation of single pot assembly reaction mixture was conducted in a PCR machine using the following PCR programme:

***Bsa*I-digest: 37°C for 3 min**

Ligation: 16°C for 4 min

for 25 cycles

Denaturation: 50°C for 5 min

Denaturation: 80°C for 5 min

Commonly 10 µL of this reaction mix was Sepharose 4B [Sigma Aldrich, NZ] desalted (as described in subchapter 2.4.10) after the program run and then transformed into *E. coli* DH5α competent cells for selection.

In this study, some level 1 expression units were assembled into pICH47751 and pICH47761 shuttle vectors for further assembled into multigene level 2 constructs based on pAGM4723 backbone.

2.4.12 Plasmid DNA purification

Alkaline lysis method, AxyPrep Miniprep kit [MediRay, NZ] or Macherey Nagel NucleoSpin kit [MediRay, NZ] were used according to instructions to purify

plasmid DNA, which then was used for cloning and transformation. DNA concentration was quantified using Nanodrop and agarose gel electrophoresis.

2.4.13 Alkaline Lysis Miniprep

Bulk isolation of plasmids for restriction digest confirmation was carried out using manual alkaline lysis miniprep (Birnboim & Doly, 1979). 2 mL of overnight cultures were pelleted at 5000 g for 2 min and supernatant discarded.

The cell pellet was then resuspended in 250 µL of cold Solution I (50 mM glucose; 25 mM Tris-Cl, pH8.0; 10 mM EDTA, pH8.0) with RNAse added and 250 µL of Solution II (0.2N NaOH; 1% (w/v) SDS) was added. The tubes were gently inversed 4-5 times to mix samples and incubated at room temperature for 2 mins. 350 µL Solution III (3M potassium; 5M acetate solution, pH4.8) was then added and mixed by inversion 5-6 times, incubated again for 2 mins and then centrifuged at maximum speed for 10 min.

The supernatant was transferred to a new 1.5 mL microcentrifuge tube and 400 µL isopropanol added, mixed well and centrifuged at maximum speed for 2 mins to pellet plasmid DNA. The supernatant was then discarded, pellet washed with 70% ethanol and centrifuged at maximum speed for 1 min. Ethanol was removed and pellet air dried under the laminar flow hood at room temperature for 5-10 min. Finally, the pellet was resuspended in 50 µL dH2O for use in restriction digests. Concentration was measured using Nanodrop quantification and agarose gel electrophoresis.

2.4.14 Site-directed mutagenesis

Site directed mutagenesis for restriction enzyme site eliminations and amino acid changes were performed using the Agilent Quikchange Site-directed mutagenesis kit [Agilent, NZ] with consecutive *Dpn*I-dependent (3-5 hours at 37°C) methylated DNA degradation *in vitro* according to instructions. 10 µL of the resulting mix was transformed into electrocompetent *E. coli* DH5α cell and the colonies were screened for plasmids with the desired nucleotide change by sequencing or digestion with the restriction enzyme, the target site of which was mutagenized.

2.4.15 DNA sequencing

DNA sequencing was performed through Macrogen Inc, South Korea or SolGent, South Korea according to supplier instructions. 5 µL of DNA template (DNA concentration roughly 50-150 ng/µL) was sent with 5 µL of 5 µM sequencing primer using the EZ-seq barcoded label system (https://dna.macrogen.com/eng/support/seq/data/Macrogen_EZSeq.pdf) [Macrogen, KR].

2.4.16 RNA extraction

For total RNA extraction plant tissue was placed into 1.5 mL microcentrifuge tubes and snap frozen in liquid nitrogen. Samples were ground using a chilled pestle and mortar then frozen powder was transferred to 2 mL microcentrifuge tubes. Tubes were carefully opened in a fume hood and 1 ml of Tri reagent [Sigma Aldrich, NZ] was added. The mixture was vortexed for 30 seconds and incubated for 5 minutes at room temperature.

Then 100 µl of BCP (1-bromo-3-chloropropane) was added and tubes were mixed by inversion. The tubes were then incubated for 10 minutes at room temperature and spun down at 4°C, 12000 g for 10 minutes. The upper transparent layer was carefully transferred to a fresh 1.5 ml microcentrifuge tube and 0.25 ml of isopropanol and 0.25 ml of high salt precipitation solution (0.8M sodium citrate and 1.2M NaCl, 0.45 µM filtered) was added. Resulting solution was mixed by inversion and left for 5 minutes at room temperature.

The tubes were spun at 4°C, 12000 g for 15 minutes and supernatant was poured off. Resulting pellet was washed with 0.7 ml of 70% ethanol and then centrifuged at 4°C, 8000 g for 5 minutes. The pellet was air dried for 10-15 minutes at room temperature and resuspended in 50 µl of DEPC-treated water.

Next 5 µl of DNase and 5 µl of DNase 10X reaction buffer were added to each sample and incubated at room temperature for 15 minutes. After incubation 5 µl of DNase stop solution was added and incubated for 10 minutes at 70°C. To assess integrity of purified RNA 2 µl of the resulting solution was loaded on a 2% agarose gel for visualization. Further cDNA synthesis was performed only if discrete rRNA bands were visible on agarose gel. RNA concentration was measured using Nanodrop machine.

2.4.17 Reverse transcription PCR (RT-PCR)

RNA quantity was equalized in all compared samples by diluting RNA with DEPC-treated water up to 14 µl. Then 6 µl of RT mix (contained 2 µl of enzyme mix and 4 µl of reaction mix from Maxima First Strand cDNA Synthesis Kit [Thermo Fischer, NZ]) was added to bring up the total reaction volume to 20 µl. Samples were loaded into the thermocycler to run the following program: 25°C for 10 minutes, 55°C for 30 minutes, 85°C for 5 minutes. Resulting mix containing cDNA was diluted 5 times with sterile water and 2 µl was used for PCR reactions.

2.4.18 Semi-quantitative PCR

Equal amount of cDNA samples was subjected to PCR with gene-specific primers as described in subchapter 2.4.5. To visualize differential expression levels the cycle count for PCR reactions was 27 to 35. EF1α was used for the cDNA quantity control for Arabidopsis.

2.4.19 Total protein extraction

N. benthamiana 5-week old plant leaves were infiltrated with *A. tumefaciens* strains carrying binary vectors expressing the protein of interest. Plant tissue samples were collected at 2 dpi and snap frozen in liquid nitrogen.

Tissue then was ground in a liquid nitrogen chilled mortar using a pestle and transferred to an equal volume of protein extraction buffer (Complete Mini Protease Inhibitor Cocktail - 1/2 tablet [Roche, NZ], NP-40 – 30 µl [Sigma Aldrich, NZ], DTT – 75 µl [Sigma Aldrich, NZ], PVPP – 0.15 g [Sigma Aldrich, NZ], GTEN Buffer (10% glycerol [Sigma Aldrich, NZ], 25 mM Tris [Sigma Aldrich, NZ] pH7.5, 1 mM EDTA [Sigma Aldrich, NZ], 150 mM NaCl [Sigma Aldrich, NZ]) to 15mL), thawed on ice before vortexing. 2 mL of the sample was centrifuged at 5000 g at 4°C for 15 min, 5X SDS Loading buffer with 100 mM DTT added to 1X and then boiled at 96°C for 10 min. The sample was then vortexed before centrifugation at max speed. The proteins then were resolved using SDS-polyacrilamide gel electrophoresis.

2.4.20 SDS-PAGE & Western blot

SDS-polyacrylamide gel electrophoresis was performed to separate proteins by mass and consecutive blotting onto PVDF (Polyvinylidene difluoride) membrane [Sigma Aldrich, NZ] was used to visualize them.

6% - 15% SDS-polyacrylamide gels were used depending on the size of the proteins of interest. 15 – 30 µl of protein sample was loaded in each well in the gel and run at 120 V submerged in TG-SDS buffer (25 mM Tris-Cl/250 mM glycine/0.1% SDS [all supplied from Sigma Aldrich, NZ]) for 1 – 1.5 hours in a Mini-PROTEAN® Tetra vertical electrophoresis cell [Bio-Rad, NZ].

After the run, the gel with resolved protein samples was transferred into a transfer cassette [Bio-Rad, NZ] between Whatman filter paper sheets [Sigma Aldrich, NZ] and two sponges [Bio-Rad, NZ] together with activated PVDF membrane (submerged in methanol [Sigma Aldrich, NZ] for 1 minute). The cassette was then placed in a Mini-PROTEAN® Tetra vertical electrophoresis cell with 1 L of transfer buffer (25 mM Tris/250 mM glycine/20% methanol [all supplied from Sigma Aldrich, NZ]) and the protein samples were blotted for 2 – 2.5 hours at 70 V at 4°C.

The PVDF membrane was then blocked in 15 mL of 5% TBST skim milk (25 mM Tris/150 mM NaCl/1% Tween/5% skim milk powder) for 1 hour. Primary antibodies were added into 5% TBST skim milk to achieve the following dilutions: for anti-FLAG [Cat.# F3165, Sigma Aldrich, NZ] monoclonal antibodies – 1/5000, for anti Myc [Cat.# 2276, Cell signaling, KR] monoclonal antibodies – 1/2000. Primary antibodies were incubated with the PVDF membrane for 1 – 1.5 hours at constant shaking at 100 rpm and room temperature.

After that, the PVDF membrane was washed 3 times with TBST (25 mM Tris/150 mM NaCl/1% Tween) buffer for 10 minutes each wash. Then TBST buffer was discarded and 15 mL of 5% TBST skim milk was added with anti-mouse secondary horseradish peroxidase-conjugated polyclonal antibodies [Cat.# A9044, Sigma Aldrich, NZ] with dilution of 1/20000. The membrane was incubated with secondary antibodies for 1 hour with constant shaking at 100 rpm at room temperature.

Anti-HA monoclonal antibodies were horseradish peroxidase-conjugated (Cat.# SC7392, Santa Cruz, US), their working dilution was 1/2000 and incubation time 1.5 hours.

After incubation with antibodies, the PVDF membrane was washed 3 times with TBST buffer for 10 minutes each wash and visualization of proteins was achieved using different ratio of Pierce Pico and Femto reagents ranging from 1:9 to 1:1 (Pico : Femto) [Thermo Fischer, NZ].

The chemiluminescence was detected with the CCD sensor of a GE LAS-500 machine [GE, KR]. The membrane was consecutively stained with Ponceau S [Sigma Aldrich, NZ] to visualize protein loading.

2.4.21 CoIP

For immunoprecipitation proteins extracted with the protocol mentioned in subchapter 2.4.19 were mixed with 15 µl of Anti-FLAG beads from anti-FLAG M2 affinity gel [Cat.# A2220, Sigma Aldrich, NZ) and incubated on a rotary shaker at 4°C for 2 hours. After that beads were gently spun down and supernatant was discarded.

Beads were then washed 3 times with 1 mL of cold GTEN buffer and after the final wash supernatant was completely removed with a syringe needle.

Beads were incubated with 50 – 100 µl of GTEN buffer containing 3xFLAG peptide (Cat.# F4799, Sigma Aldrich, NZ) for 45 min at room temperature or at 4°C overnight at constant shaking at 100 rpm, to elute the proteins bound to beads. Further Western blot and visualization steps were performed as described in section 2.4.20.

Chapter 3: molecular basis of AvrRpt2 recognition by the NLR MR5 from the hybrid apple *Malus* x *robusta* 5

3.1 Introduction

3.1.1 AvrRpt2 homologs are important for successful plant infection

AvrRpt2 is an effector first described in *Pseudomonas syringae* pv. *tomato* strain JL1065 (Whalen et al., 1991) and has been intensively studied for the past 3 decades. AvrRpt2 is a cysteine protease, which cleaves itself as well as a variety of NOI-domain containing targets in the plant cell including RPM1 Interacting Protein 4 (RIN4). AvrRpt2 is delivered in an inactive form and a prolyl-peptidyl isomerase (PPlase) ROC1 stimulates AvrRpt2 activity to cleave itself, releasing the active form, which then can cleave its plant targets (Coaker et al., 2006).

Recent studies showed that AvrRpt2 is involved in PTI suppression via suppressing MPK4/MPK11 in the MAPK signaling pathway (Eschen-Lippold et al., 2016). In addition, AvrRpt2 was shown to promote AXR2 and AXR3 proteasome-dependent turnover. AXR2 and AXR3 are negative regulators of auxin responses and their degradation leads to auxin accumulation, which is associated with enhanced susceptibility to pathogen invasion (Cui et al., 2013).

On the other hand, AvrRpt2 cleaves the RIN4 protein in Arabidopsis, which leads to an RPS2-dependent ETI response. RIN4 is a major plant immunity regulator and it is guarded by two well-described NLR proteins, RPM1 and RPS2. Cysteine protease activity, which can be blocked by a mutation in a catalytically critical cysteine, is essential for both AvrRpt2 virulence and avirulence functions (Axtell et al., 2003; Axtell et al., 2001; Kim et al., 2005b; Lim & Kunkel, 2004).

AvrRpt2 homologs are found in different bacterial pathogens (Figure 3.1). One of them, the AvrRpt2 homolog from apple pathogen *Erwinia amylovora*, has 62% protein sequence identity to the *Pseudomonas syringae* variant (protein alignment can be found in appendices, Figure 6.1). *Erwinia amylovora* is a Gram-negative bacterium from the family *Enterobacteriaceae* and it is a causal agent of fire blight in apple and pear plants. This disease leads to significant loss of fruit yield in crop industry all over the world and no durably resistant industry apple cultivars are yet developed (Malnoy et al., 2012). AvrRpt2 is very widespread

among the vast majority of *E. amylovora* strains and it was shown to play a significant role in the development of fire blight symptoms (Zhao et al., 2006).

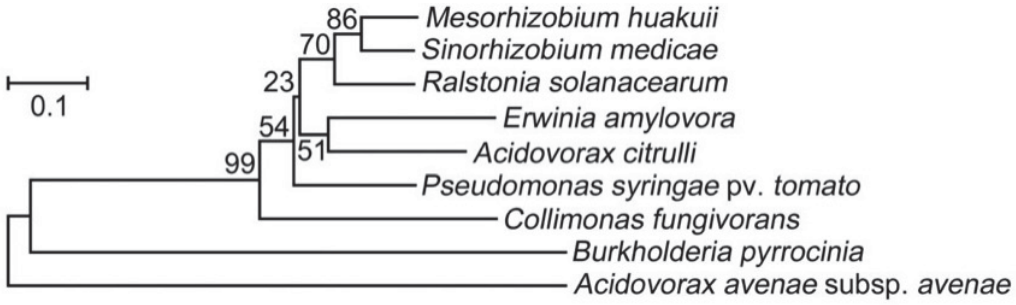

Figure 3.1: Phylogenetic analysis of AvrRpt2 homologs. The species are denoted on the end of branches. Phylogenetic tree is based on multiple sequence alignments performed with CLUSTALW. Bootstrap test values (%) are depicted next to the branches. Accession numbers of the sequences used to generate the phylogenetic tree are the following: *Pseudomonas syringae pv. tomato* JL1065 (CAA79815.2), *Mesorhizobium huakuii* 7653R (AID34449.1), *Erwinia amylovora* ATCC 49946 (CBJ45097.1), *Acidovorax avenae* subsp. *avenae* ATCC 19860 (ADX44172.1), *Burkholderia pyrrocinia* Lyc2 (KFL50402.1), *Collimonas fungivorans* (WP_041743564.1), *Acidovorax citrulli* tw6 (NZ_JXDJ01000021.1), *Sinorhizobium medicae* WSM1369 (NZ_AQUS01000051.1), *Ralstonia solanacearum* CMR15 (NC_017559.1
(REGION: 3241390-3241941)).

3.1.2 AvrRpt2 recognition in Arabidopsis

AvrRpt2 is recognized by a CC-type NLR called RPS2. This recognition is indirect and occurs via RIN4 cleavage. RIN4 is a plant immunity regulator. This protein carries two conserved NOI-domains, which contain the cleavage sites with the consensus sequence [LVI]PxFGxW (where x represents any amino acid) recognized and processed by AvrRpt2. It also carries a C-terminal palmitoylation sequence (GPI-anchor) important for RIN4 anchoring in the plasma membrane (Afzal et al., 2011; Kim et al., 2005a; Takemoto & Jones, 2005). Other domains of RIN4 are highly diversified among plant species and possess an intrinsically disordered structure (Afzal et al., 2013; Sun et al., 2014).

The RIN4 structure allows it to interact with both RPS2 and RPM1, and suppress their autoimmune activity (Figure 3.2A). The aforementioned GPI anchor is necessary for maintaining these interactions. *rin4* knockout Arabidopsis plants are not viable due to the collective autoimmunity of RPS2 and RPM1, but *rin4rps2* knockout plants can grow even though significantly stunted due to RPM1-mediated autoimmunity (Belkhadir et al., 2004; Day et al., 2005; Kim et al., 2005b). AvrRpt2-mediated cleavage of RIN4 leads to dissociation of cleavage products from the cell membrane, except the C-terminal cleavage product, which remains at the membrane. Interestingly only the cleavage at the C-terminal cleavage site activates RPS2 and it was shown that the C-terminal half of RIN4 is sufficient to keep RPS2 in a suppressed state (Day et al., 2005). The loss of structural integrity of RIN4 leads to the release of interaction with RPS2, resulting in ETI immune signaling activation (Figure 3.2B and C) (Day et al., 2005).

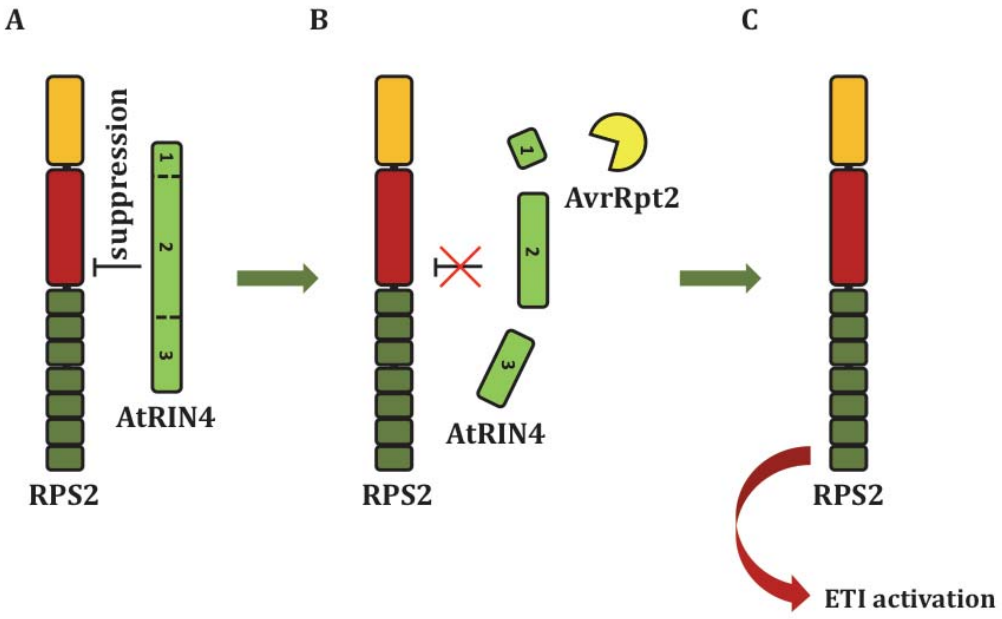

Figure 3.2: Model of RPS2 activation via RIN4 cleavage by AvrRpt2. A – interaction of AtRIN4 with RPS2 keeps it in suppressed state. **B –** AvrRpt2 cleaves AtRIN4 eliminating its suppressive activity. **C –** RPS2 activates ETI immune signaling in absence of AtRIN4-mediates suppression.

3.1.3 MR5 is a CC-type NLR conferring resistance to fire blight

Fire blight caused by *E. amylovora* is one of the most devastating diseases of apple and pear crops. The majority of contemporary industry apple and pear cultivars are susceptible to fire blight therefore antibiotic spraying in complex with horticultural methods (removal of early infected blossoms etc.) and application of natural antagonistic microbes allowed to minimize fire blight infection and spread (Burrill et al., 2003).

To improve the efficiency of fire blight control considerable effort is directed towards identifying possible sources of natural resistance in wild apple and pear relatives, which can be potentially transferred to industry cultivars. *Malus* x *robusta* is a hybrid of *Malus baccata* and *Malus prunifolia* (Gardner et al., 1980); the *Malus* x *robusta* 5 line was selected in the 1920s from an open-pollinated *Malus* x *robusta* population for its resistance to fire blight (Watkins & Spangelo, 1970). *Malus* x *robusta* 5 is widely used nowadays for rootstocks and apple research (Norelli et al., 2003).

The *Malus* x *robusta* 5 genotype was further studied and a major fire blight resistance QTL on linkage group 3 (LG3) was identified (Peil et al., 2007). Further research showed that the resistance phenotype depended on the presence of AvrRpt2 in invading *E. amylovora* strains, suggesting a typical gene for gene interaction (Flor, 1971; Vogt et al., 2013). A major CC-type NLR (called MR5) was mapped and identified in the *Malus* x *robusta* 5 resistance-associated locus on LG3.

The *MR5* gene was cloned and transformed into the susceptible apple cultivar “Gala” under the strong 35S CaMV (Cauliflower mosaic virus) promoter and, importantly, was shown to confer significant resistance against *E. amylovora* strains carrying AvrRpt2 (Broggini et al., 2014; Fahrentrapp et al., 2013). Further details of the molecular mechanism by which MR5 mediates AvrRpt2 recognition remained elusive and were the main focus of the current research.

3.2 Results

3.2.1 Transiently expressed AvrRpt2 homologs induce moderate cell death in *Nicotiana benthamiana* leaves

In order to validate if transient expression in *N. benthamiana* leaves can be used for studying AvrRpt2 and MR5, AvrRpt2 homologs were first expressed alone via Agroinfiltration in *N. benthamiana* leaves (method described in subchapter 2.3.2). In agreement with previous research reported by Vogt et al., 2013, using OD_{600}=0.2-0.4 of *Agrobacterium* strains carrying AvrRpt2 homologs triggered a moderate programmed cell death response, hereafter PCD (Figure 3.3, upper row).

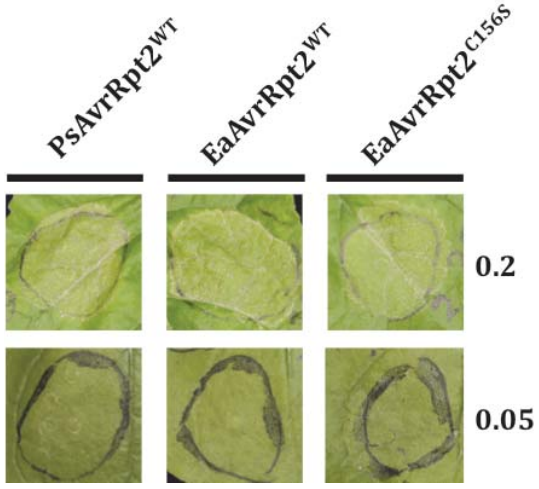

Figure 3.3: Agrobacterium mediated overexpression of *P. syringae* and *E. amylovora* AvrRpt2 variants in *N. benthamiana* leaves triggers mild programmed cell death (PCD) symptoms. Agrobacterium strains carrying AvrRpt2-coding constructs were infiltrated at OD_{600} = 0.2 or 0.05 and photographs taken at 3 dpi.

In order to reduce this PCD, lower OD_{600} of 0.05 for *Agrobacterium* carrying AvrRpt2 homologs was tested. In this case, PCD triggered by AvrRpt2 alone was not detectable by the naked eye (Figure 3.3, bottom row) but the amount of effector expressed was still enough to trigger a strong PCD response in the presence of AtRIN4 and RPS2 (Figure 3.4A).

3.2.2 AvrRpt2 activates MR5 by elimination of RIN4

RPS2 and MR5 confer recognition of AvrRpt2 in Arabidopsis and apple, respectively. In Arabidopsis, AtRIN4 is required for proper suppression of RPS2 prior to its AvrRpt2-mediated elimination. Previously, it was shown that agroinfiltration of RPS2 induces PCD in *N. benthamiana* (Day et al., 2005). RPS2-induced autoactivation of PCD is suppressed by co-expression of AtRIN4 and reactivated by addition of AvrRpt2 (Figure 3.4A). As shown previously, the wild-type but not the C122A variant of AvrRpt2 cleaves AtRIN4 and activates RPS2-mediated PCD in *N. benthamiana* (Day et al., 2005) (Figure 3.4A). This is because cysteine in position 122 is a crucial residue in a protease catalytic triad. In addition, EaAvrRpt2 can efficiently activate RPS2 but its catalytically inactive mutant with C88A mutation cannot (C88 of EaAvrRpt2 is homologous to C122 of PsAvrRpt2).

There are two RIN4 homologs, sharing 90% amino acid identity, in the apple genome: MdRIN4-1 (RefSeq accession: NM_001293994.1) and MdRIN4-2 (RefSeq accession: NP_001280834.1) (Vogt et al., 2013); a protein alignment is shown in appendices, Figure 6.2. In order to reconstitute the MR5 system in *N. benthamiana*, both RIN4 homologs were cloned and the agroinfiltration experiments shown in Figure 3.4B were conducted with both homologs. It was concluded that, there is no difference between the activities of the two RIN4 homologs in terms of their ability to activate MR5 (Figure 3.4B), so future work was carried out with MdRIN4-1 which is referred to as MdRIN4 in further descriptions.

To test the hypothesis that AvrRpt2-directed cleavage of MdRIN4 is required for activation of MR5, transient expression via agroinfiltration in *N. benthamiana* leaves was used. Surprisingly, in contrast to RPS2, agroinfiltration of MR5 did not induce PCD (Figure 3.4B) suggesting that MdRIN4-mediated suppression of MR5 activity is unnecessary. However, similarly to AtRIN4 and RPS2, MdRIN4 was required for AvrRpt2-triggered activation of MR5 (Figure 3.4B). This concludes that MdRIN4 is required for MR5-mediated recognition of AvrRpt2.

The PCD phenotypes observed were supported by protein accumulation studies (methods described in subchapters 2.4.19; 2.4.20). Both AtRIN4 and MdRIN4 were eliminated in the presence of PsAvrRpt2 and EaAvrRpt2 wild type proteins, while RIN4 homologs were not eliminated by catalytically inactive

versions of AvrRpt2 homologs. This further supports the requirement of MdRIN4 and its AvrRpt2-mediated cleavage for activation of MR5 (Figure 3.4C).

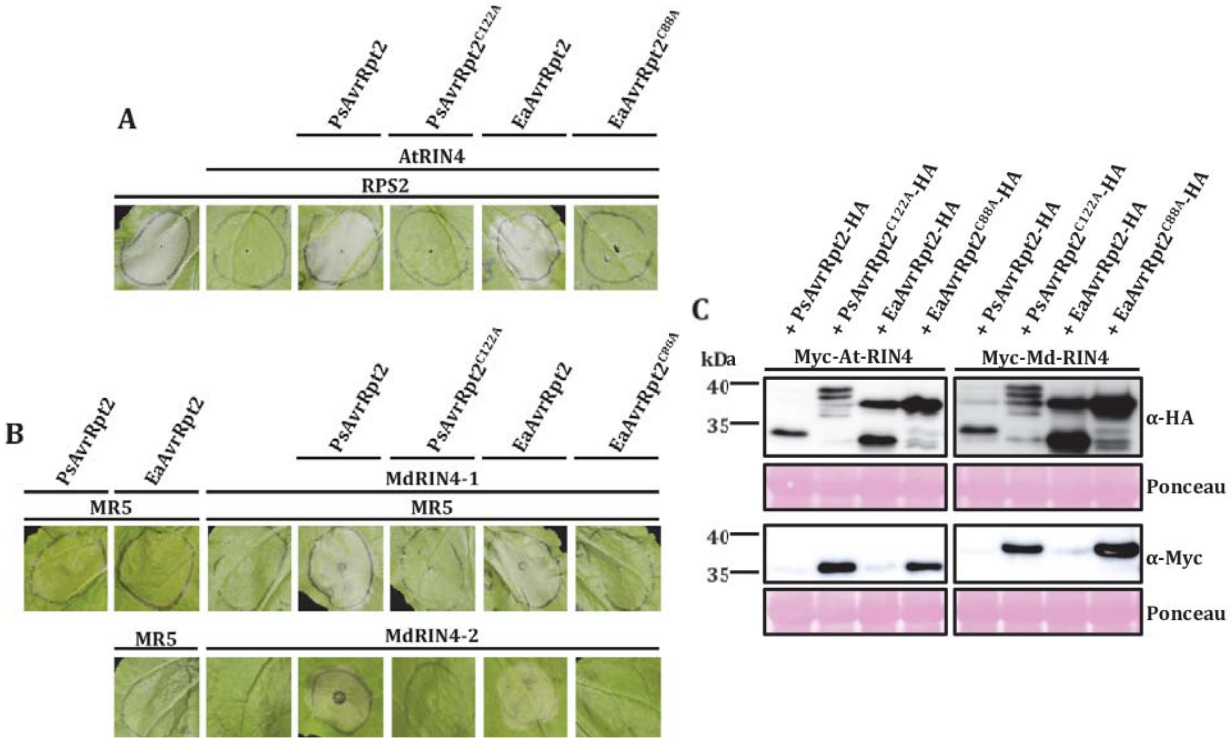

Figure 3.4: AvrRpt2-directed cleavage of MdRIN4 is recognized by both RPS2 and MR5. A - AtRIN4-dependent RPS2-mediated recognition of enzymatically active natural variants of AvrRpt2 in *Nicotiana benthamiana*. *N. benthamiana* was infiltrated with mixture of Agrobacterium strains carrying *35S:MR5:FLAG* (OD_{600}=0.4), *35S:RPS2:FLAG* (OD_{600}=0.1), *35S:Myc:RIN4-1* or *RIN4-2* (OD_{600}=0.4) or *35S:AvrRpt2:HA*(OD_{600}=0.05) variants. Programmed cell death was photographed at 3 dpi. **B** - MdRIN4-dependent MR5-mediated recognition of enzymatically active natural variants of AvrRpt2 in *N. benthamiana*. **C** - *In planta* processing of AvrRpt2 and RIN4 variants. *N. benthamiana* leaves were infiltrated with Agrobacterium strains carrying *35S:Myc:RIN4-1* (OD_{600}=0.4) and *35S:AvrRpt2:HA* (OD_{600}=0.2) variants and leaf samples were taken for protein extraction at 2 dpi. Total protein extracts were probed with anti-Myc or anti-HA antibody to visualize epitope-tagged proteins. Ponceau staining of rubisco protein band is provided to confirm equal protein loading.

3.2.3 EaAvrRpt2-mediated elimination of RIN4 homologs from apple closely-related species can activate MR5

To test the hypothesis that RIN4 homologs from close apple relatives can activate MR5 upon EaAvrRpt2-mediated cleavage, RIN4 homologs were cloned from *Pyrus pyrifolia* and *Pyrus ussuriensis* genomic DNA sourced from RDA, Naju, Korea (method described in subchapter 2.4.11) and co-expressed in *N. benthamiana* together with MR5 and AvrRpt2. Both RIN4 homologs from close apple relatives could activate MR5 in presence of functional EaAvrRpt2 (Figure 3.5). This supports the theory that RIN4 homologs from the species closely related to apple can activate MR5 upon EaAvrRpt2-mediated cleavage.

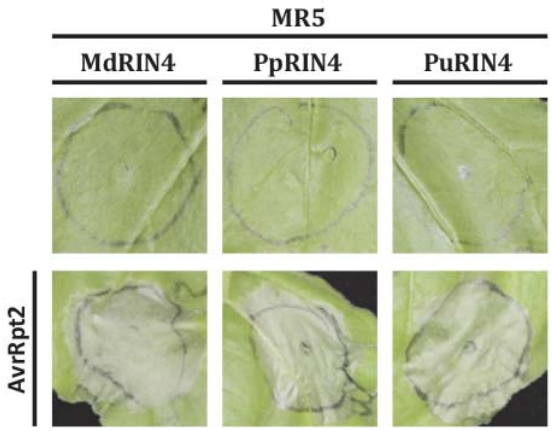

Figure 3.5: RIN4 homologs from *Pyrus* species can activate MR5 in presence of EaAvrRpt2. PpRIN4 is a RIN4 homolog from *Pyrus pyrifolia* and PuRIN4 is a RIN4 homolog from *Pyrus ussuriensis*. *N. benthamiana* leaves were agroinfiltrated as described in Figure 3.4A and photographs of PCD symptoms were taken at 3 dpi.

3.2.4 EaAvrRpt2^{C156S} does not lose catalytic activity and can be still recognized by MR5 and RPS2

It was previously published that a single amino acid polymorphism in position 156 from cysteine to serine in EaAvrRpt2 allows it to evade recognition by MR5 (Vogt et al., 2013). The same authors also reported a lack of RIN4 cleavage by EaAvrRpt2 carrying cysteine 156 (C-allele) and moderate cleavage by EaAvrRpt2 with serine 156 (S-allele). In contrast, Eschen-Lippold study (2016) showed that the EaAvrRpt2 C-allele homolog is able to induce RIN4 disappearance.

In order to validate the hypothesis that the S-allele of EaAvrRpt2 is able to evade MR5-mediated recognition and lacks RIN4 cleavage activity, the S-allele of EaAvrRpt2 was generated. As no *E. amylovora* strains in New Zealand carry the S-allele of AvrRpt2 and obtaining *E. amylovora* strains carrying the S-allele from overseas would be very difficult due to quarantine regulations, a site-directed mutagenesis approach was used to generate it (method described in subchapter 2.4.14).

Newly generated EaAvrRpt2 variants were expressed in the presence of MR5 and MdRIN4 or RPS2 and AtRIN4 combinations and no difference was observed in the ability to activate the R proteins (Figure 3.6A and B) or eliminate RIN4 homologs (Figure 3.6C and D). This result suggests no difference in protease activity and MR5-mediated recognition between the C-allele and S-allele of EaAvrRpt2.

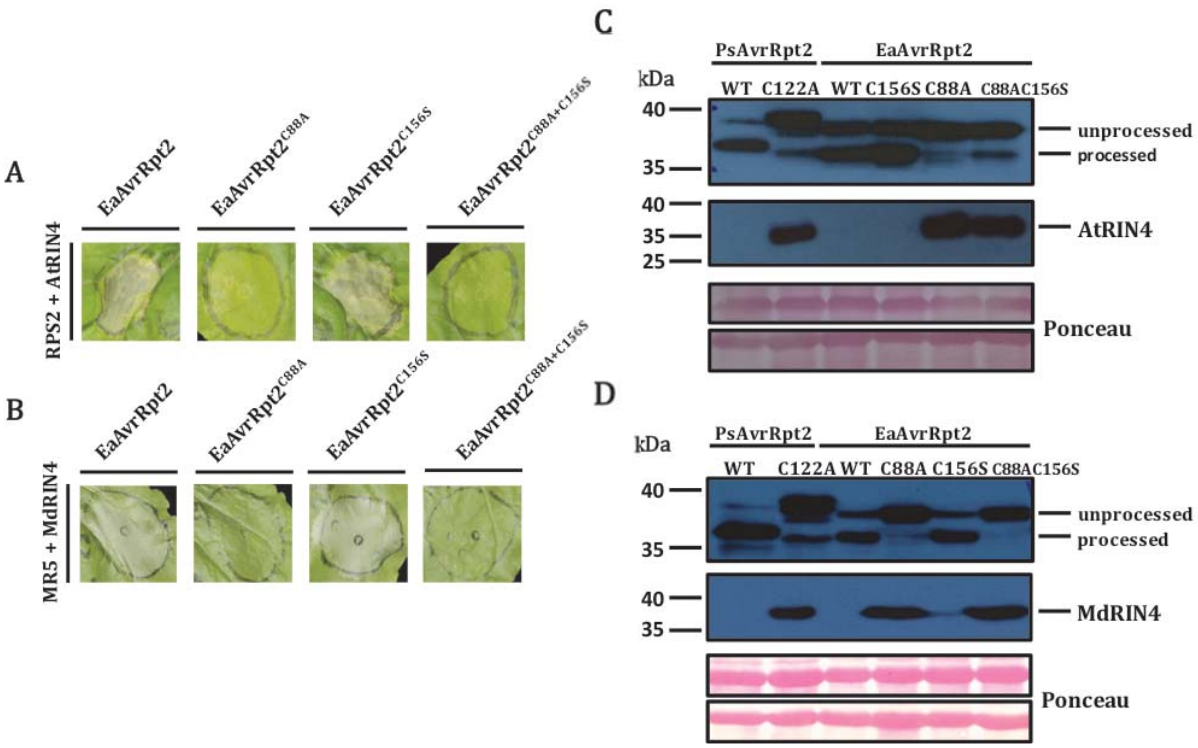

Figure 3.6: EaAvrRpt2^{C156S} can be recognized by RPS2 and MR5 systems.

A – EaAvrRpt2^{C156S} can be recognized by RPS2 + AtRIN4 system the same as EaAvrRpt2. **B** - EaAvrRpt2^{C156S} can be recognized in MR5 + MdRIN4 system the same as EaAvrRpt2. In panels A and B leaves of *N. benthamiana* were infiltrated as in Figure 3.4A and B. Programmed cell death was photographed at 3 dpi. **C** – AtRIN4 is eliminated in presence of both EaAvrRpt2^{WT} and EaAvrRpt2^{C156S} while this elimination is not observed in presence of catalytically inactive versions of EaAvrRpt2. **D** - MdRIN4 is eliminated in presence of both EaAvrRpt2^{WT} and EaAvrRpt2^{C156S} while this elimination is not observed in presence of catalytically inactive versions of EaAvrRpt2. In panels C and D leaves of *N. benthamiana* were infiltrated as in Figure 3.4C and leaf samples were taken for protein extraction at 2 dpi. Total protein extracts were probed with anti-Myc (for AtRIN4 and MdRIN4) or anti-HA antibody (AvrRpt2 variants) to visualize epitope-tagged proteins. Ponceau staining of rubisco protein band is provided to confirm equal protein loading.

3.2.5 Mutation analysis of MR5 critical domains

Mutations in functionally important regions of NLRs modulate their activities. Correctly switching between active and inactive states is a key activity of these proteins and is facilitated by the NB-ARC domain. This domain is responsible for ATP hydrolysis. Introducing mutations in the P-loop region of this domain often results in an inactive R protein variant (Dinesh-Kumar et al., 2000; Takken et al., 2006).

Furthermore, mutation of D to V in the highly conserved MHD motif within the NB-ARC domain often results in an autoactive version of the NLR (Takken et al., 2006). In order to test the hypothesis that these mutations have an effect on MR5, the residues corresponding to previously published important ones in NB-ARC domain were mutagenized. I aligned RPS2 and RPM1 protein sequences to MR5 and could identify p-loop motif and MHD-motif for mutagenesis. The newly generated MR5 mutant variants were co-expressed with MdRIN4 and AvrRpt2. As expected, $MR5^{K206A}$ with a mutated P-loop showed complete loss of AvrRpt2 recognition while $MR5^{D493V}$ with a mutated MHD motif retained activity even in absence of AvrRpt2 and MdRIN4. In addition, $MR5^{K206A+D493V}$ did not trigger any cell death suggesting that the NB-ARC domain functions in both AvrRpt2-mediated signaling and autoactivation (Figure 3.7A). These observations support the suggestion that MR5 is a classic example of a CC-NB-LRR R protein.

In the case of RPS2, its canonical MHD motif is instead an MHN motif, and based on this fact the analogous D493N mutation was introduced into MR5. The aim was to test if the $MR5^{D493N}$ variant would gain an autoactive phenotype like that of RPS2. Interestingly, this MR5 variant did not show any autoactivity and the native AvrRpt2 recognition was preserved (Figure 3.7A). This concludes that 493N is not sufficient to generate autoimmune MR5 variant analogous to RPS2.

Protein accumulation of MR5 mutant variants was assessed and it was found that autoactive PCD symptoms were not the result of $MR5^{D493V}$ overaccumulation in comparison to the wild type (Figure 3.7B).

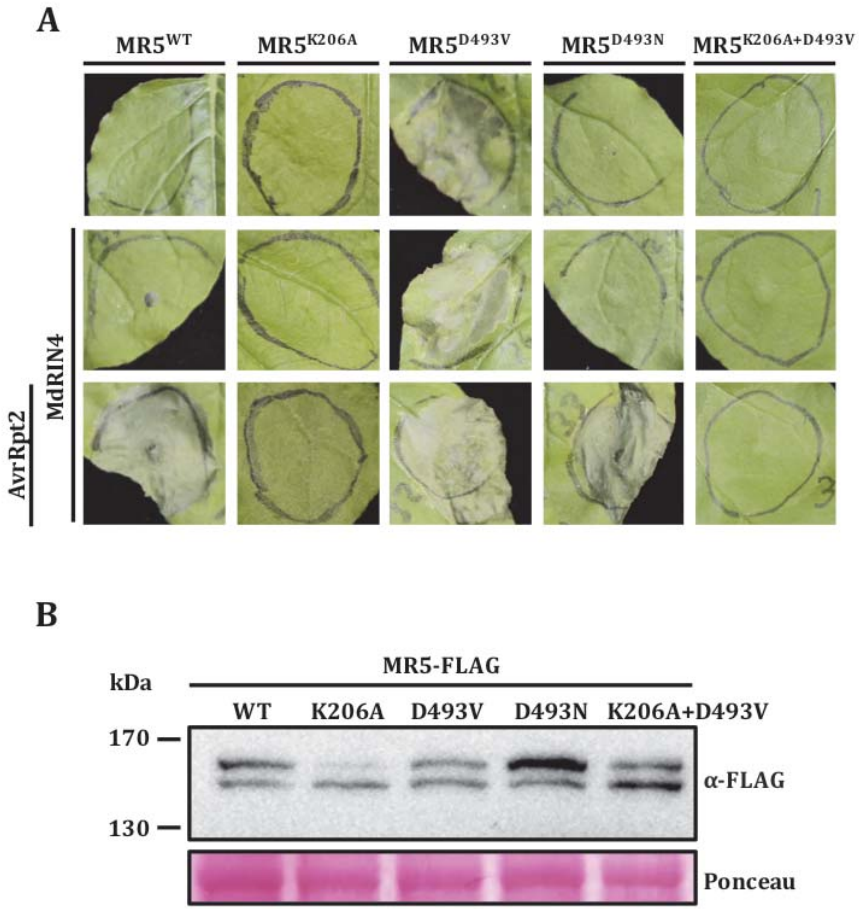

Figure 3.7: Expression of MR5 variants with mutations in critical domains. These mutations in MR5 alter the ability to cause PCD response. **A -** The MR5^{K206A} mutation in the P-loop region of MR5 NB domain abolishes MR5^{D493V}-mediated PCD. All MR5 variants and MdRIN4 were expressed via agroinfiltration with a mixture of strains carrying MR5 (OD_{600} = 0.4), EaAvrRpt2 (OD_{600} = 0.05) or MdRIN4 (OD600=0.4). PCD symptoms were photographed at 3 dpi. **B** - Expression of MR5 variants *in planta*. Agroinfiltration and immunoblot analysis were performed as described in Figure 3.4C except that anti-FLAG antibody was used.

3.2.6 RIN4 natural variants have differing abilities to suppress or activate NLRs

AtRIN4 is able to effectively suppress RPS2-mediated autoimmunity. To test whether MdRIN4 could do the same, agroinfiltration experiments to co-express AtRIN4 and MdRIN4 with RPS2 or MR5^{D493V} were carried out. Stronger macroscopic PCD symptoms were observed in the case of MdRIN4 co-expression with RPS2 in comparison to AtRIN4 and, consequently, significantly higher associated ion leakage (method described in 2.3.3) (Figure 3.8A and C). Similarly, AtRIN4 co-expression with autoactive MR5^{D493V} variant resulted in less macroscopic PCD symptoms and associated ion leakage in comparison to MdRIN4 co-expression.

This suggests that MdRIN4 has a significantly weaker ability to suppress signaling by both RPS2 and MR5. Notably, both AtRIN4 and MdRIN4 suppressed MR5^{D493V} significantly less than RPS2. Protein accumulation analysis showed comparable levels of RIN4 homologs accumulation *in planta*, supporting the hypothesis that the difference in suppression ability is not a result of varied protein stability for the different RIN4 homologs (Figure 3.8B).

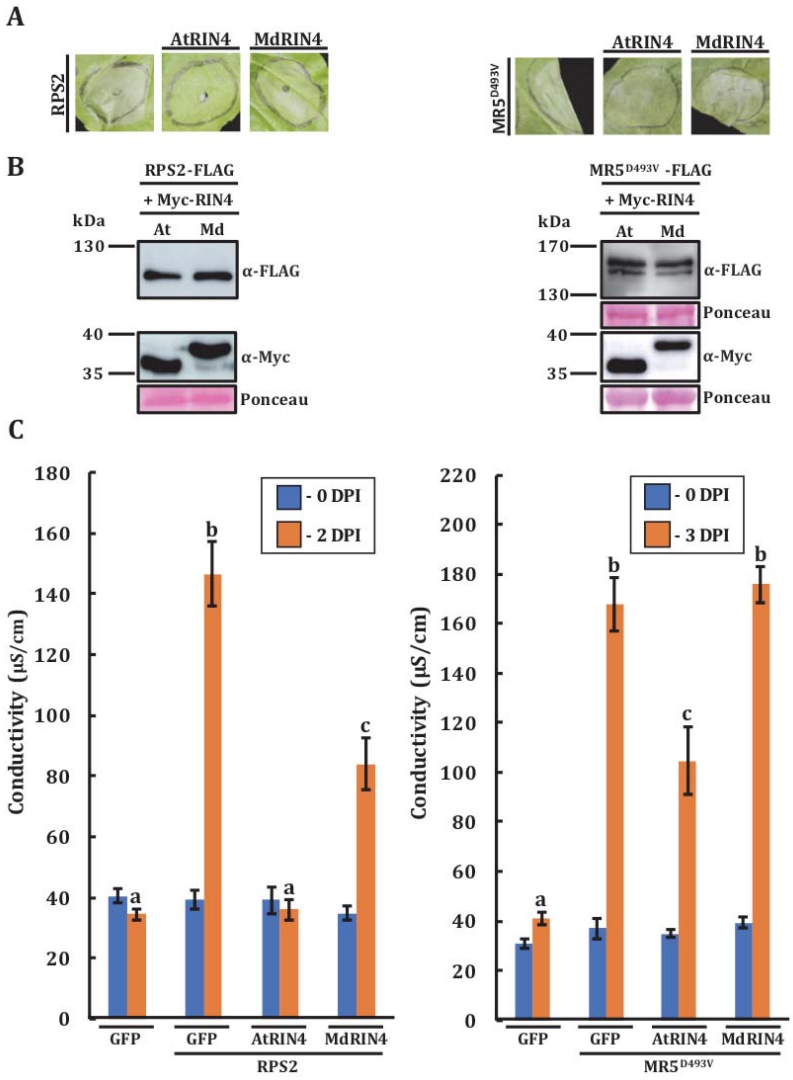

Figure 3.8: RIN4 natural variants have different abilities to suppress autoactive NLRs.

A - AtRIN4 but not MdRIN4 efficiently suppresses RPS2 or MR5^{D493V}-mediated PCD. The agroinfiltration assay was performed as described in Figure 3.4A and photographs were taken at 2 dpi or 3 dpi. **B -** RIN4 natural variants are accumulating to a similar level *in planta*. Agroinfiltration and immunoblot analysis were performed as described in Figure 3.4C. RPS2-FLAG was immunoprecipitated with anti-FLAG beads in order to remove non-specific bands. **C -** MdRIN4 shows significantly reduced suppression activity of autoactivity induced by RPS2 or MR5^{D493V} in comparison to AtRIN4. The agroinfiltration assay was performed as described in Figure 3.4A and leaf samples were taken at 0 and 2 dpi for ion leakage measurement. Each bar represents average of 8 electrolyte leakage measurements (n = 8). Error bars represent S.E.M. Statistical significance was assessed by a two tailed Student's T-test. Bars labeled with identical letters indicate that there is no significant statistical difference (*P* - value < 0.05). Final concentration (OD_{600}) of *Agrobacterium* strains were 0.1 for RPS2 and MR5^{D493V} and 0.4 for RIN4 variants and GFP.

The vast majority of RIN4 homologs have two highly conserved regions surrounding RIN4 cleavage sites (hereafter RCS1 and RCS2). AvrRpt2-mediated processing of RIN4 in these cleavage sites results in release of the cleavage products from the plasma membrane and overall RIN4 degradation. Interestingly, only cleavage of RIN4 at RCS2 is required for RPS2 activation (Day et al., 2005). The highly conserved regions around RCS1 and 2 show similarity to NOI-domains and their importance for RIN4 functioning was proposed (Afzal et al., 2011; Afzal et al., 2013), also the C-terminal NOI (C-NOI) was shown to interact with AvrB effector (Desveaux et al., 2007). These data taken together suggest the particular importance of RCS2 and the surrounding C-NOI for RIN4 functioning.

To study the requirements of the various RIN4 regions for NLR suppression and/or activation, a series of RIN4 chimeras representing region swaps between AtRIN4 and MdRIN4 were generated (Figure 3.9A). The A1-2M3 chimera carried cleavage products 1 and 2 (hereafter CLV1 and CLV2) from Arabidopsis fused with cleavage product 3 (hereafter CLV3) from apple. Conversely, the M1-2A3 chimera carried CLV1 and CLV2 from apple fused with CLV3 from Arabidopsis. Co-expression of these chimeras with RPM1, RPS2, MR5 and their corresponding effectors showed that MR5 can be activated upon AvrRpt2-mediated cleavage of A1-2M3 but not AtRIN4 or M1-2A3 (Figure 3.9B). This suggests a strict requirement for CLV3 of MdRIN4 for MR5 activation. In contrast, A1-2M3 showed a significantly higher ability to suppress RPS2-mediated autoimmunity in comparison to M1-2A3, suggesting that the AtRIN4 CLV1-2 region is involved in RPS2 suppression. On the other hand, A1-2M3 could not suppress autoactivity triggered by RPM1 while M1-2A3 could, indicating the importance of the AtRIN4 CLV3 region for correct RPM1 suppression and activation (Figure 3.9B).

Unlike in previously published research from other labs (Gao et al., 2011; Li et al., 2014), strong PCD symptoms when RPM1 was agroinfiltrated in *N. benthamiana* were observed. But in agreement with previously published data this PCD could be fully suppressed by AtRIN4. Co-expression of RPM1, AtRIN4 and AvrRpm1 resulted in PCD symptoms confirming the ability of AvrRpm1 to activate RPM1 via AtRIN4 in our conditions (Figure 3.9B). It seems that in our conditions RPM1 is highly active, possibly due to expression under the strong constitutive 35S

CaMV promoter. I aimed to check if MdRIN4 can also suppress RPM1 when co-expressed in *N. benthamiana* leaves and found that MdRIN4 has no ability to suppress RPM1 (Figure 3.9B). Due to that fact, further ability of MdRIN4 to be phosphorylated in the presence of AvrRpm1 and activate RPM1 could not be tested. Figure 3.9B can give an impression of different levels of PCD in between MdRIN4 + RPS2 and M1-2A3 + RPS2 panels, but based on multiple observations we could not rule out any significant and stable PCD difference between them.

All chimeric RIN4 protein variants accumulated to similar amounts and were eliminated in the presence of AvrRpt2 *in planta* (Figure 3.9C). This supports the hypothesis that the phenotypes observed are not a product of differential protein accumulation of RIN4 variants or their different ability to be cleaved by AvrRpt2.

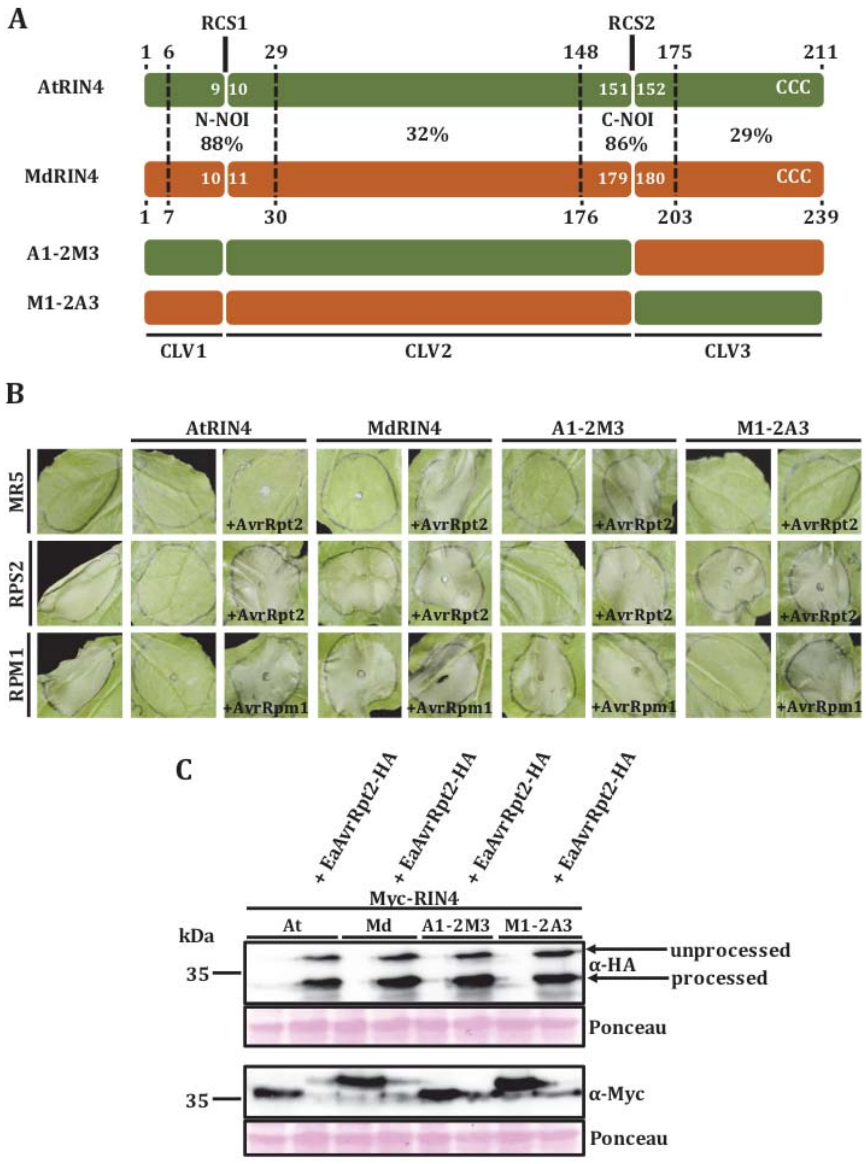

Figure 3.9: Different regions of RIN4 are required for suppression and activation of NLRs. A - Schematic representation of wild-type and chimeric AtRIN4 and MdRIN4 variants. Percentage shows the level of protein sequence identity between AtRIN4 and MdRIN4 within the indicated regions. Numbers indicate the amino acid positions in the corresponding wild-type RIN4 proteins. CCC indicates the putative palmitoylation sequence. NOI; NO_3-induced domain, RCS; RIN4 cleavage site, CLV; RIN4 cleaved product. **B** - Distinct properties of RIN4 natural variants are required for suppression of RPS2 or RPM1 autoactivity or activation of MR5. RIN4 variants were expressed in 5 week-old *N. benthamiana* leaves using agroinfiltration. Inoculum densities (OD_{600}) used were: MR5 – 0.4, RPS2 – 0.1, RPM1 – 0.1, RIN4 variants – 0.4, AvrRpt2 – 0.05 and AvrRpm1 – 0.1. PCD symptoms were photographed at 3 dpi. **C** - RIN4 chimeric proteins are processed by AvrRpt2. RIN4 chimeric proteins and AvrRpt2 variants were transiently expressed as mentioned in Figure 3.4C. Leaf samples were taken for protein extraction at 2 dpi. Total protein extracts were probed with anti-Myc or anti-HA antibody to visualize epitope-tagged proteins. Ponceau staining of rubisco protein band is provided to confirm equal protein loading.

3.2.7 The presence of MdRIN4 CLV3 is necessary and sufficient to elicit MR5-mediated cell death

AvrRpt2-mediated AtRIN4 cleavage can be abolished by specific mutations in RCS1 and RCS2 (Chisholm et al., 2005). To test the hypothesis that MdRIN4 is processed by AvrRpt2 in the same manner as AtRIN4, MdRIN4 variants with analogous mutations were generated (Table 2.7, constructs #696, #697, #801) and co-expressed with AvrRpt2. As expected, MdRIN4 was processed in the same manner as AtRIN4 and cleavage in RCS2 alone was required for MR5 activation (Figure 3.10A and B). This finding led us to speculate that the presence of CLV3 alone but not full length RIN4 is sufficient for MR5 activation.

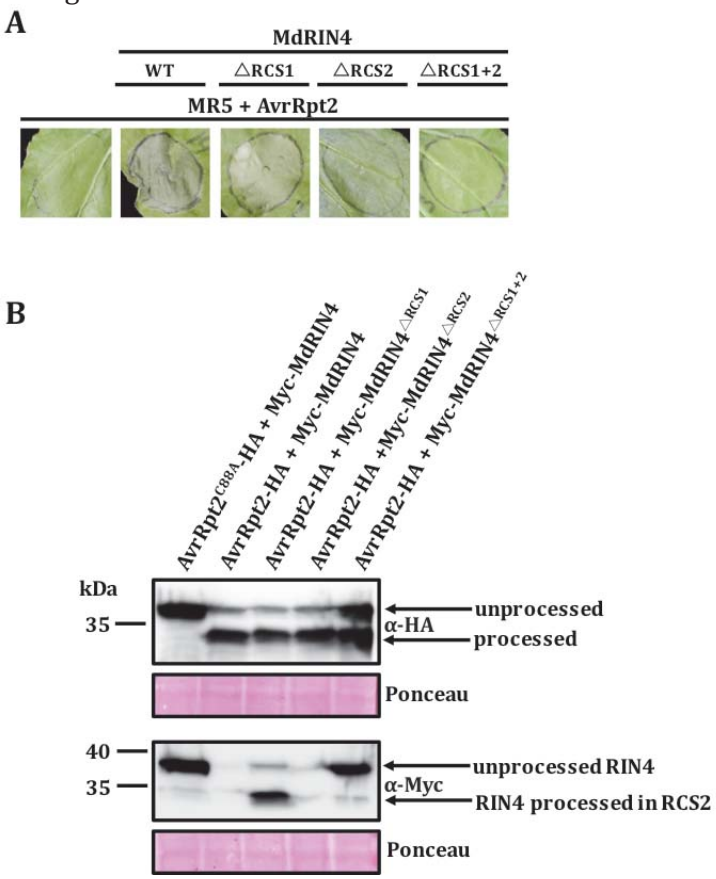

Figure 3.10: Cleavage at MdRIN4 RCS2 is required for MR5 activation.

A - AvrRpt2-directed cleavage at RCS2 but not RCS1 is required for activation of MR5-dependent PCD. The agroinfiltration assay was performed as described in Figure 3.4A and photographs were taken 3 dpi. **B -** Immunoblot analysis of MdRIN4 variants carrying RCS mutations. Mutations in RCS1 and RCS2 abolish the cleavage in corresponding sites. Agroinfiltration and immunoblot assays were performed as described in Figure 3.4C. Ponceau staining of rubisco protein band is provided to confirm equal protein loading.

To further validate the hypothesis the MdRIN4 CLV3 is sufficient to activate MR5, AtRIN4 and MdRIN4 truncated variants mimicking cleavage products were co-expressed with MR5 (Table 2.7, constructs #673, #676, #563, #565, #564, #808, #566). CLV1, 2, and 3 of AtRIN4 and CLV1 and 2 of MdRIN4 could not activate MR5 to induce PCD when co-expressed in *N. benthamiana* leaves. In agreement with our prediction, co-expression of only the MdRIN4 CLV3 was sufficient to activate MR5 without the presence of AvrRpt2. In addition, an MdRIN4 CLV3 mimic with mutated C-terminal GPI anchor sequence lost the ability to activate MR5 (Figure 3.11), suggesting the importance of MdRIN4 CLV3 plasma membrane localization for MR5 activation.

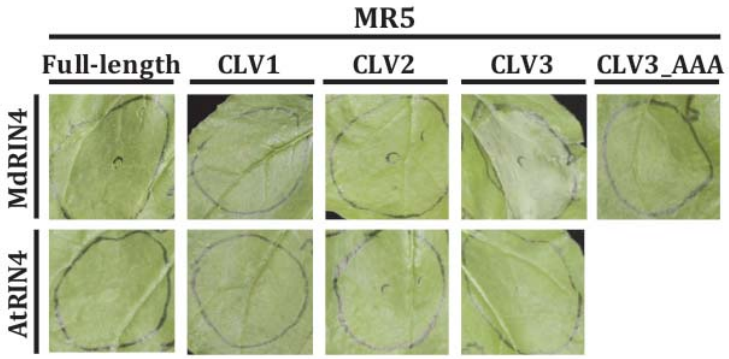

Figure 3.11: MdRIN4 CLV3 can activate MR5 even in absence of AvrRpt2. Full-length and truncated variants of AtRIN4 and MdRIN4 were transiently expressed by using agroinfiltration (OD_{600} = 0.4) in *N. benthamiana* leaves. Programmed cell death response was photographed at 3 dpi.

3.2.8 Only fully intact version of MR5 can be activated by MdRIN4 CLV3

CC domains of barley (*Hordeum vulgare*) Mla10, tobacco (*Nicotiana tabacum*) NRG1 and *Arabidopsis thaliana* ADR-1 proteins are sufficient to trigger PCD when expressed in *N. tabacum* leaves alone (Collier et al., 2011; Maekawa et al., 2011). On the other hand, in the case of the potato (*Solanum tuberosum*) Rx R protein, which confers resistance to Potato Virus X (PVX), the CC domain alone does not trigger PCD. In contrast, Rx CC-domain co-expressed with only Rx NB-ARC-LRR can recapitulate the PCD in response to the PVX coat protein (Rairdan et al., 2008).

Based on this data, a series of constructs coding for truncated versions of MR5 was generated to test the hypothesis that certain domains of MR5 can perform signaling when expressed alone or co-expressed with MdRIN4 CLV3.

As MdRIN4 CLV3 overexpression does not trigger any macroscopic response in *N. benthamiana* leaves, this assay is far more sensitive than co-expression of MR5 truncated variants with MdRIN4 and AvrRpt2, due to absence of weak AvrRpt2 background PCD response.

Constructs coding for the following truncated variants of MR5 were generated: CC-domain (1-161 aa) (Table 2.7, construct #168), CC-NB-domain (1-333 aa) (#470), CC-NB-ARC-domain (1-582 aa) (#471), CC-NB-ARC-LRR (1-873 aa) (#473), CC-NB-ARC-LRR (1-1151 aa) (#474) and NB-ARC-LRR (169-1388 aa) (#475), which were co-expressed with MdRIN4 CLV3. None of these truncated proteins could trigger any PCD symptoms (Figure 3.12). This result suggests that full length MR5 is required for proper immune signaling, but further experiments to validate protein accumulation of MR5 truncated variants are required.

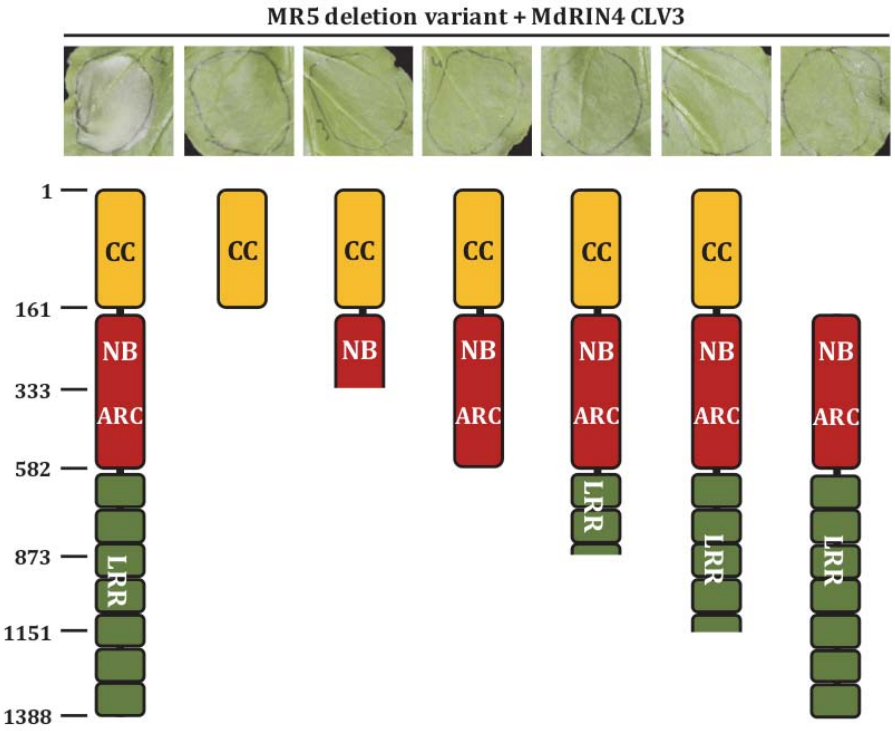

Figure 3.12: Only fully intact MR5 protein can initiate signaling when co-expressed with MdRIN4 CLV3. The schematic represents deletion variants of MR5 which were expressed with MdRIN4 CLV3 in *N. benthamiana* leaves via agroinfiltration. MR5 deletion variants and MdRIN4 CLV3 carrying agrobacterium were infiltrated at OD_{600} = 0.4. Photographs were taken at 3 dpi.

3.2.9 MR5 domain combinations cannot be activated by MdRIN4 CLV3

To test if any combination of MR5 domains can substitute for full length version, further co-expression of different truncated MR5 variants mixed together and with MdRIN4 CLV3 was carried out. No combination of co-expressed domains could result in any PCD symptoms (Figure 3.13). Further protein accumulation analysis should be performed for MR5 truncated variants in order to conclude that MR5 can only function as a full-length protein and no combination of domains co-expressed can substitute for it.

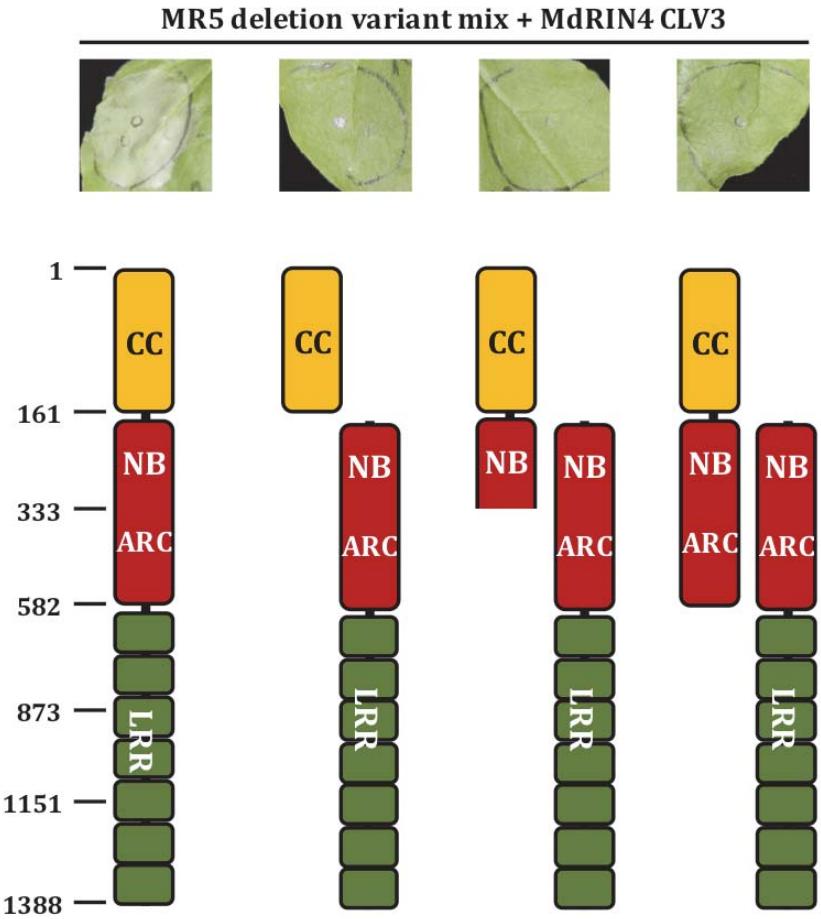

Figure 3.13: Co-expression of separate domains of MR5 cannot recapitulate PCD-triggering activity in the presence of MdRIN4 CLV3.

The schematic represents MR5 deletion variant combinations which were expressed with MdRIN4 CLV3 in *N. benthamiana* leaves via agroinfiltration. MR5 deletion variants and MdRIN4 CLV3 carrying Agrobacterium were infiltrated at OD_{600} = 0.4. Photographs were taken at 3 dpi.

3.2.10 Two amino acid residues in a highly conserved part of MdRIN4 CLV3 are critical for MR5 activation

In order to elucidate which parts of MdRIN4 CLV3 are required for activation of MR5, protein sequence identity between AtRIN4 and MdRIN4 CLV3 variants was checked. A highly-conserved region (showing 80% aa identity) in the N-terminal portion of CLV3, which carries part of the C-terminal NOI domain (C-NOI), and a highly diverse (showing 32% aa identity) C-terminal portion of CLV3 were defined (Figure 3.14A).

Constructs coding for chimeric CLV3 proteins with a swap point at the end of the C-NOI domain (amino acid residue positions 175 in AtRIN4 and 203 in MdRIN4) were generated (Table 2.7, constructs #1509, #1537) and assessed for their ability to activate MR5 (Figure 3.14B). To our surprise, the A-M-CLV3 chimera, carrying a C-terminal polymorphic portion of MdRIN4 CLV3 that was evolutionarily non-conserved, could not activate MR5 in our experiments. In contrast, the M-A-CLV3 chimera carrying a highly conserved N-terminal region of MdRIN4 CLV3 was able to activate MR5 (Figure 3.14B). Protein immunoblot analysis showed that AtRIN4 and MdRIN4 CLV3 variants accumulated to a similar level, demonstrating that the MR5 activation phenotype is not a product of allele-dependent CLV3 protein stability *in planta*. This is further supported by the fact that the A-M-CLV3 chimera could not activate MR5 even though its protein accumulation was significantly higher than that for M-A-CLV3 (Figure 3.14C).

Comparison of the N-terminal sequences of AtRIN4 and MdRIN4 CLV3 led to identify 4 polymorphic amino acid residues in this conserved N-terminal portion before the CLV3 chimera swap point (Figure 3.14A). To test their requirement for MR5 activation, these residues were individually mutated to the corresponding amino acid residues from the other homolog (Table 2.7, constructs #1855, #1856, #1569, #1570, #1628, #1571, #1629, #1572, #1649, #1650). It was found that introducing D153E and S160A mutations into A-M-CLV3 did not result in a gain of MR5 activation. Similarly, the reciprocal mutations E181D and A188S in M-A-CLV3 did not abolish MR5 activation, suggesting that these residues do not play a significant role in MR5 activation. In contrast, introducing N158D and Y165F mutations into A-M-CLV3 resulted in a gain of MR5 recognition, while reciprocal D186N and F193Y mutations in M-A-CLV3 led to complete loss of MR5 recognition (Figure 3.14D).

In order to test if the aforementioned mutations act in a same way in native CLV3 contest, each of the mutations was generated in the native CLV3 background and the similar tendencies could be observed (Table 2.7, constructs #1703, #1704, #1705, #1706, #1707, #1708), albeit slightly attenuated (Figure 3.14E). Furthermore, both chimeric A-M-CLV3 and native AtRIN4 CLV3 carrying double N158D and Y165F mutations resulted in a strong MR5 activation. Conversely, chimeric M-A-CLV3 and native MdRIN4 CLV3 carrying the reciprocal double mutations showed a complete loss of MR5 activation (Figure3.14E).

Protein immunoblot analysis showed that the N158D and Y165F mutations appear to slightly stabilize AtRIN4 CLV3 while the D186N+F193Y mutations in MdRIN4 CLV3 similarly led to significantly higher protein accumulation. Based on this, no association can be found between the level of protein accumulation and MR5 activation (Figure 3.14F), eliminating the hypothesis that the phenotypes observed are the product of differential protein accumulation of mutant variants.

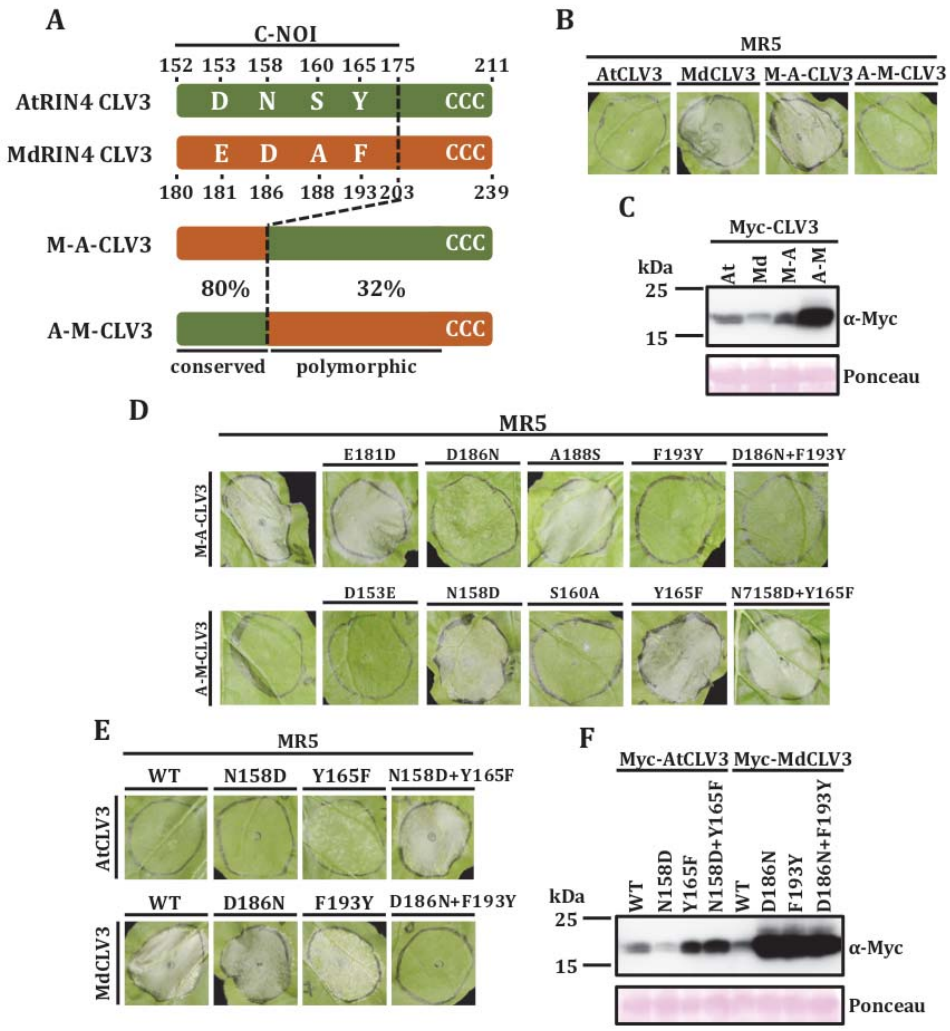

Figure 3.14: Two amino acid residues in the conserved C-NOI domain of CLV3 are critical for NLR compatibility

A - Schematic representation of wild-type and chimeric CLV3 variants. Four polymorphic amino acid residues in the C-terminal NOI (C-NOI) domain are indicated. Numbers indicate amino acid positions in AtRIN4 or MdRIN4, percentage shows aa identity. **B** - The highly conserved region of MdCLV3 is required for MR5 activation. Indicated wild-type or chimeric CLV3 variants were co-expressed with MR5 in *N. benthamiana* via agroinfiltration (OD_{600}=0.4) for all the strains. PCD symptoms were photographed at 3 dpi. **C** - Immunoblot analysis of chimeric CLV3 variants. CLV3 variants were expressed without MR5 via agroinfiltration and samples were taken at 2 dpi. Ponceau staining of rubisco protein band is provided to confirm equal protein loading. **D** – Mutation of polymorphic amino acid residues in conserved region of CLV3 to the ones from the other RIN4 variant in the CLV3 chimeric background causes gain or loss of MR5 activation. Agroinfiltration was carried out as mentioned in B. PCD symptoms were photographed at 3 dpi. **E** - Reciprocal mutation at N/D or D/F residues of AtCLV3 or MdCLV3 causes gain or loss of MR5 activation, respectively. The agroinfiltration assay was carried out in as described in B. **F** - Immunoblot analysis of wild-type or mutant CLV3 variants expressed in absence of MR5. Agroinfiltration and immunoblot analysis were performed as described in C.

3.2.11 MR5 is not able to recognize RIN4 phosphorylation by AvrRpm1 or AvrB

As one of the critically important amino acid residues for MR5 activation at position 193 in MdRIN4 turned out to be just next to a prospective phosphorylation site at position 194, it was curious to check if MR5 can be activated by AvrB or AvrRpm1-mediated phosphorylation of RIN4 homologs. AtRIN4 was reported to be phosphorylated in aa positions T21, S160 and T166. These phosphorylation events led to RPM1 activation. Interestingly these phosphorylation events can be imitated by substituting amino acid residues at those positions for D (Liu et al., 2011).

The amino acid residues T22, A188 and T194 in MdRIN4, which correspond to the phosphorylation sites in AtRIN4, were identified. They were mutated to D to imitate the fully phosphorylated state of MdRIN4. Resulting constructs (Table 2.7, constructs #287, #294) expressing RIN4 phosphorylation mimics (RIN4_ppp) were co-expressed with MR5 and RPM1 alongside with AtRIN4 or MdRIN4 co-expressed together with RPM1 or MR5 and AvrRpm1 or AvrB as controls. None of the phosphorylation mimics could activate MR5. Similarly, neither AvrRpm1, nor AvrB could activate MR5 via AtRIN4 or MdRIN4 (Figure 3.15), supporting the hypothesis that RIN4 phosphorylation cannot activate MR5.

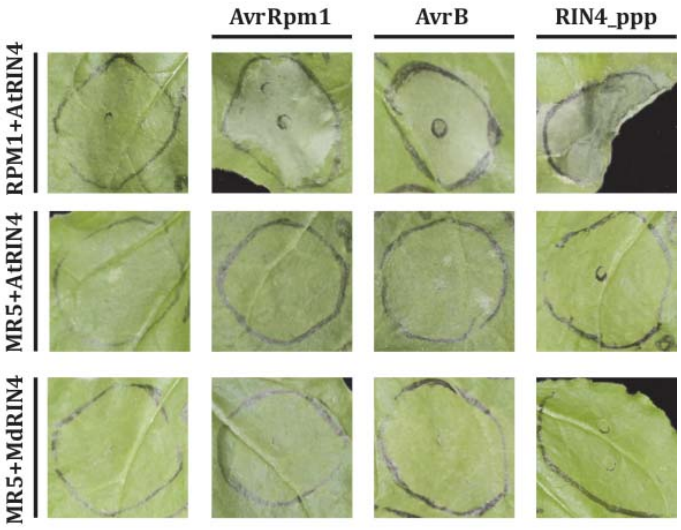

Figure 3.15: MR5 cannot activate PCD in presence of AvrRpm1 and AvrB or RIN4 phosphorylation mimic (RIN4_ppp). The RIN4_ppp column shows phosphorylation mimics of the corresponding RIN4 proteins denoted on the left of the figure. Agroinfiltration was carried out as mentioned in Figure 3.8B, and the OD_{600} of AvrB carrying strain was 0.02. Photographs were taken at 3 dpi.

3.2.12 Polymorphic residues alter the suppression and activation properties of full length RIN4

In the previous experiment (subchapter 3.2.10), the amino acid residues in RIN4 CLV3 important for MR5 activation were defined. To assess the importance of these residues for correct functioning of full length RIN4 homologs in NLR suppression/activation. The following RIN4 variants with the aforementioned mutations were generated: AtRIN4^{N158D} (Table 2.7, constructs #1661), AtRIN4^{Y165F} (#1662), AtRIN4$^{N158D+Y165F}$ (#1663), as well as MdRIN4^{D186N} (#1664), MdRIN4^{F193Y} (#1665) and MdRIN4$^{D186N+F193Y}$ (#1666).

These variants of AtRIN4 and MdRIN4 were co-expressed with RPS2, RPM1 or MR5 in the presence or absence of their corresponding effectors (Figure 3.16A and B). AtRIN4 suppressed RPM1- and RPS2-triggered autoimmunity, as expected. Introducing the N158D and Y165F mutations into full length AtRIN4 resulted in the loss of this suppression ability for both RPS2 and RPM1. In addition, introducing D186N and F193Y mutations into MdRIN4 resulted in gain of complete RPM1 and RPS2 suppression. To our surprise, introduction of D186N and F193Y mutations into MdRIN4 resulted in loss of full-scale PCD and significantly lower ion leakage phenotype upon AvrRpt2 co-expression (Figure 3.16A and D). Protein immunoblot analysis confirmed that all RIN4 variants accumulated to similar levels *in planta* (Figure 3.16C). These results show that the amino acid residues in positions critically important for MR5 activation are also important for the ability of full length RIN4 to suppress RPS2 and RPM1.

In agreement with previous results, it was observed that AtRIN4$^{N158D+Y165F}$ gained the ability to activate MR5 when co-expressed with AvrRpt2, while MdRIN4$^{D186N+F193Y}$ lost this ability (Figure 3.16B). Again, the phenotypes observed could not be explained by differential RIN4 variants' protein accumulation, as determined by protein immunoblot analysis (Figure 3.16C).

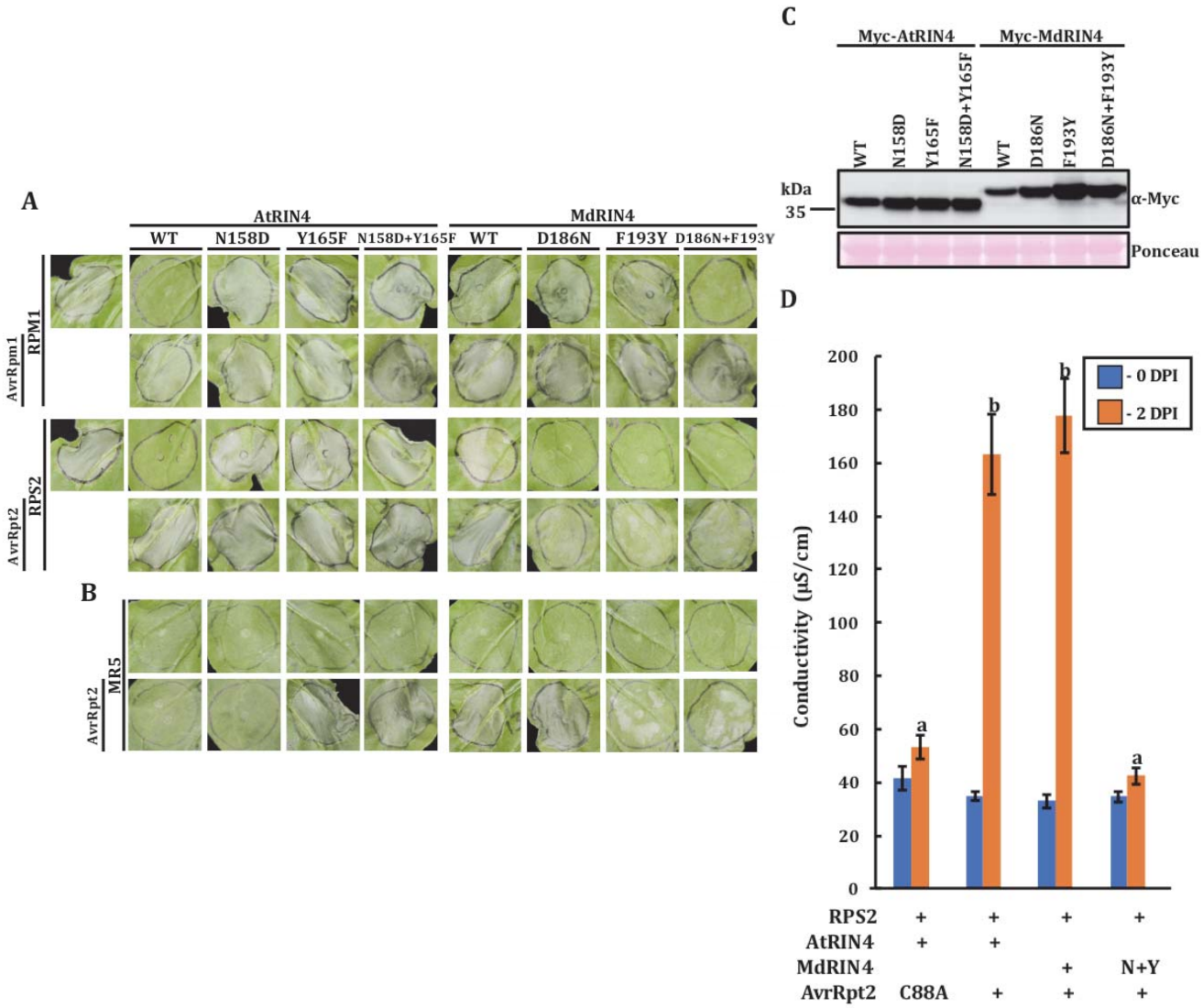

Figure 3.16: Two amino acid residues in the conserved C-NOI domain of CLV3 are critical for NLR compatibility with full length RIN4 variants.

A - Reciprocal mutation at N/D or D/F residues of AtCLV3 or MdCLV3 caused loss or gain of NLR autoactivity suppression by full length RIN4 variants, respectively. The agroinfiltration assay was carried out in as described in figure 3.8A. **B -** Reciprocal mutation at N/D or D/F residues of AtCLV3 or MdCLV3 causes gain or loss of MR5 activation upon AvrRpt2-mediated cleavage of full length RIN4 variants, respectively. The agroinfiltration assay was carried out in as described in 3.8B. **C** – full length RIN4 variants with N/D or D/F mutations residues of CLV3 are accumulated to similar level *in planta*. Agroinfiltration and immunoblots were performed as mentioned in Figure 3.8C. Ponceau staining of rubisco protein band is provided to confirm equal protein loading. **D** – MdRIN4$^{\mathbf{D186N+F193Y}}$ (N+Y) has reduced PCD symptoms upon expression with AvrRpt2 in comparison to MdRIN4. The agroinfiltration assay was performed as described in A and leaf samples were taken at 0 and 2 dpi for ion leakage measurement. Each bar represents average of 8 electrolyte leakage measurements (n = 8). Error bars represent S.E.M. Statistical significance was assessed by a two tailed Student's T-test. Bars labeled with identical letters indicate that there is no significant statistical difference (*P* - value < 0.05).

3.2.13 Polymorphic residues alter the suppression and activation properties of RIN4 CLV3

To further dissect the role of RIN4 CLV3 in suppression of RPS2 and RPM1-triggered autoactivity, CLV3 variants were co-expressed with either RPS2 or RPM1. AtRIN4 CLV3 was insufficient to suppress either RPS2 or RPM1. Additionally, N158D and Y165F mutations in AtRIN4 CLV3 did not significantly alter the PCD and ion leakage phenotypes triggered by either of these NLRs. On the other hand, MdRIN4 CLV3 showed a partial ability to suppress RPS2, but not RPM1, with introduction of D186N and F193Y mutations allowing a complete gain of suppression of PCD triggered by both NLRs (Figure 3.17A and B).

Interestingly, the PCD suppression phenotype does appear to correlate with protein accumulation in the case of MdRIN4 CLV3 (Figure 3.14F). Taken together these results imply that the mutations in critical positions can alter the RIN4 CLV3 ability to suppress RPM1 and RPS2 and this phenotype might be the product of protein stability in the case of MdRIN4 CLV3.

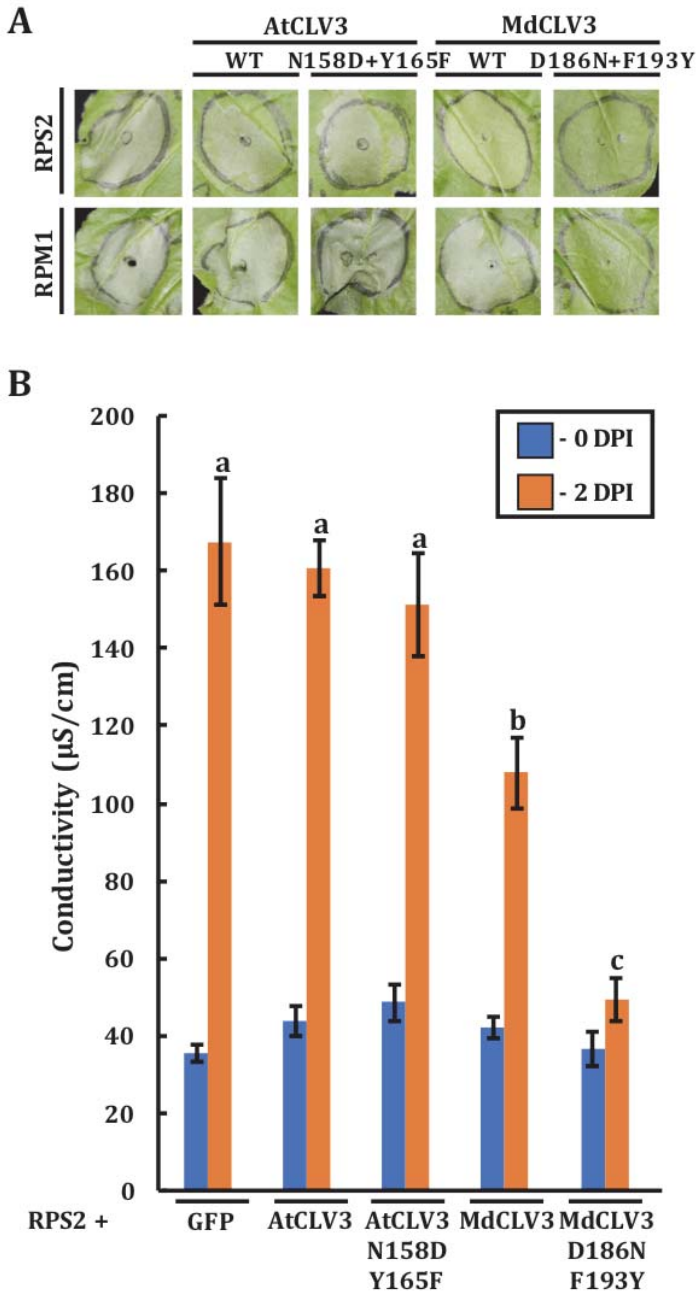

Figure 3.17: MdRIN4 CLV3 carrying D186N and F193Y mutations suppresses NLR autoactivity. A - MdCLV3$^{D186N+F193Y}$ but not AtCLV3 $^{N158D+Y165F}$ suppresses RPS2 or RPM1 autoactivity. RIN4 CLV3 variants were expressed in *N. benthamiana* leaves via agroinfiltration. Bacterial inoculum density (OD_{600}) for *Agrobacterium* strains carrying *NLR* gene or *RIN4 CLV3* were 0.05 or 0.4, respectively. **B** - Electrolyte leakage analysis of CLV3-mediated suppression of RPS2 autoactivity. Each bar represents mean average of 8 electrolyte leakage measurements. Statistical significance was assessed by two tailed T-test. Bars labeled with identical letters indicate that there is no significant statistical difference (P-value < 0.05).

3.2.14 Polymorphic residues alter interaction of MdRIN4 with RPS2 and MR5

Previous research by Brad Day et al. (2005) stated that interaction of RPS2 with AtRIN4 is essential for proper suppression of RPS2-triggered autoactivity. To test if the newly described mutations disrupting this suppression could also abolish the interaction between the NLRs and RIN4 variants, the *in planta* co-immunoprecipitation experiments were carried out. MdRIN4 did not precipitate with RPS2 or MR5, while MdRIN4$^{D186N+F193Y}$ was precipitated with both RPS2 and MR5 (Figure 3.18A and B). This aligns well with previously described PCD phenotypes and hints at the importance of an artificial MdRIN4–RPS2 interaction for sufficient PCD suppression.

As expected, AtRIN4 interaction with RPS2 could be detected (Day et al., 2005). Surprisingly, N158D and Y165F mutations in AtRIN4 did not disrupt its interaction with RPS2 despite causing a loss of RPS2 and RPM1 autoactivity suppression. This discrepancy between protein interaction and PCD phenotype suggests involvement of an additional layer of RIN4 regulation.

Interestingly, only a weak interaction between AtRIN4 and MR5 could be detected. Also, just as in the case of RPS2, N158D and Y165F mutations in AtRIN4 did not alter this interaction (Figure 3.18A and B).

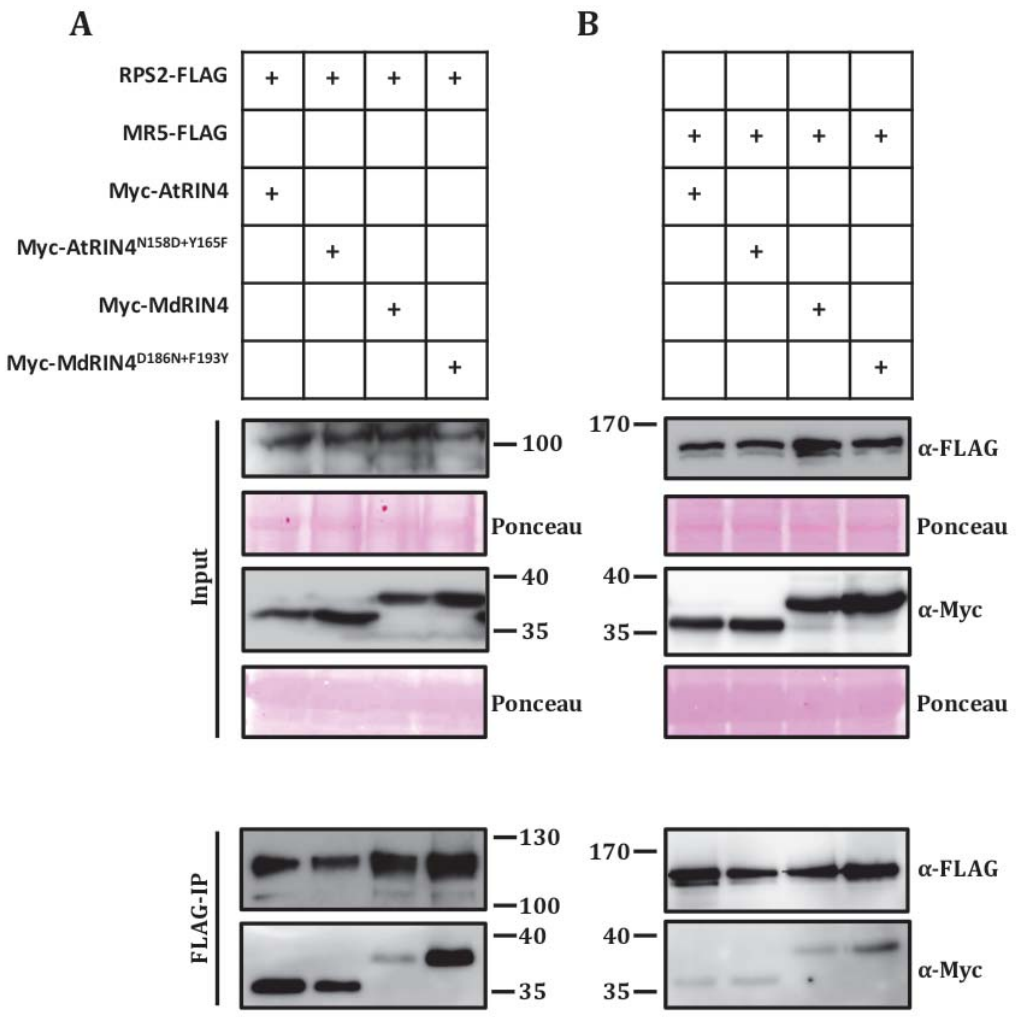

Figure 3.18: An MdRIN4 variant showing enhanced suppression of RPS2 autoactivity forms a stronger association with RPS2.

A - AtRIN4 and AtRIN4 $^{N158D+Y165F}$ show similar level of interaction with RPS2, while MdRIN4$^{D186N+F193Y}$ has a significantly stronger interaction with RPS2 in comparison to WT. **B** - Mutations in critical residues of RIN4 homologs do not significantly alter the interaction with MR5. Tagged proteins were expressed in *N. benthamiana* leaves via agroinfiltration and sampled at 2 dpi. Total protein extracts were incubated with FLAG-beads and immunocomplexes were probed with anti-Myc and anti-FLAG antibodies. Ponceau staining of rubisco protein band is provided to confirm equal protein loading.

3.3 Discussion

3.3.1 Cysteine to serine substitution in position 156 in *E. amylovora* AvrRpt2 does not alter its RIN4 cleavage ability but might interfere with its delivery

MR5 is a CC-NB-LRR protein derived from the fire blight-resistant hybrid apple, *Malus* x *robusta* 5. If transformed into susceptible apple cultivars, it confers resistance to *E. amylovora* strains carrying a homolog of type III secreted effector AvrRpt2. According to previous studies, this resistance can be broken by *E. amylovora* strains carrying an S156 variant (S-allele) of AvrRpt2 (Vogt et al., 2013).

Our results contradict these data as we could not see any difference between C-allele and S-allele of EaAvrRpt2 recognition by MR5 in our agroinfiltration experiments. Furthermore, both of these EaAvrRpt2 alleles were able to induce disappearance of both AtRIN4 and MdRIN4 homologs, which is in agreement with a recent study (Eschen-Lippold et al., 2016). Our data also showed that the catalytically inactive mutant EaAvrRpt2^{C88A} lost the ability to induce RIN4 disappearance, as well as the loss of PCD phenotype associated with that; this further supports the importance of cysteine protease activity of AvrRpt2 for its function.

The explanation for the fact that apple plants carrying MR5 cannot recognize EaAvrRpt^{C156S} might be improper translocation of the effector, which leads to absence of AvrRpt2 cleavage and, consequently, absence of MR5 response. The serine in position 156 may interfere with correct AvrRpt2 translocation and in case where EaAvrRpt2 does not need to be translocated from bacterial cells (when transiently expressed in *N. benthamiana*), it possesses full scale RIN4 cleavage activity and consequent MR5 activation.

3.3.2 MR5 uses activation rather than de-repression to trigger immune responses upon recognition of AvrRpt2

In this study, we were able to reconstitute AvrRpt2 recognition by MR5 in a transient expression system in *N. benthamiana*. Even though expression of AvrRpt2 homologs triggers mild PCD symptoms, the optical density of the Agrobacterium carrying AvrRpt2 constructs could be adjusted to OD_{600} – 0.05, which was detected by RPS2 or MR5 but could not trigger significant PCD symptoms alone. In addition, it seems that *N. benthamiana* native RIN4 homologs

are not able to activate MR5 in agreement with the critical amino acid pattern observed in them. Overexpression of these native RIN4 homologs together with MR5 and AvrRpt2 can be carried out in future to completely make sure that they do not play role in MR5 activation.

The MR5 recognition system is similar to, but distinct from, the well-described RPS2 system from Arabidopsis (Day et al., 2005; Mackey et al., 2003). However, while they both require RIN4 cleavage for triggering defense responses, MR5 does not show autoactivity. Consequently, MdRIN4 is not necessary for suppression of MR5 (Figure 3.19). This might explain why MdRIN4 only showed weak suppression ability on RPS2 and RPM1 (subchapter 3.2.6) and, furthermore, did not interact with either RPS2, or MR5, in contrast to AtRIN4 (subchapter 3.2.14).

Based on the observation that only MdRIN4 CLV3 can activate MR5 but not full length and also that MdRIN4 does not interact with MR5, we speculate that there is intramolecular suppression of CLV3 by the CLV1-2 region, which is released when AvrRpt2 cleaves MdRIN4. In addition, it is likely that there is an intermediate signaling component between RIN4 and MR5, because they do not interact directly, but MdRIN4 is still required for MR5 activation. However, this component still remains elusive.

We suspect that, in contrast to the RPS2 system where AtRIN4 degradation by AvrRpt2 leads to immunity derepression (Day et al., 2005), MR5 presumably requires MdRIN4 cleavage to release its CLV3 fragment from CLV1-2 mediated self-suppression, thereby leading to MR5 activation.

It also seems that only CLV3 from specific RIN4 homologs can activate MR5, as supported by observation of MR5 activation by MdRIN4 CLV3 homologs from *Pyrus pyrifolia* and *Pyrus ussuriensis*, but not by homologs from Arabidopsis.

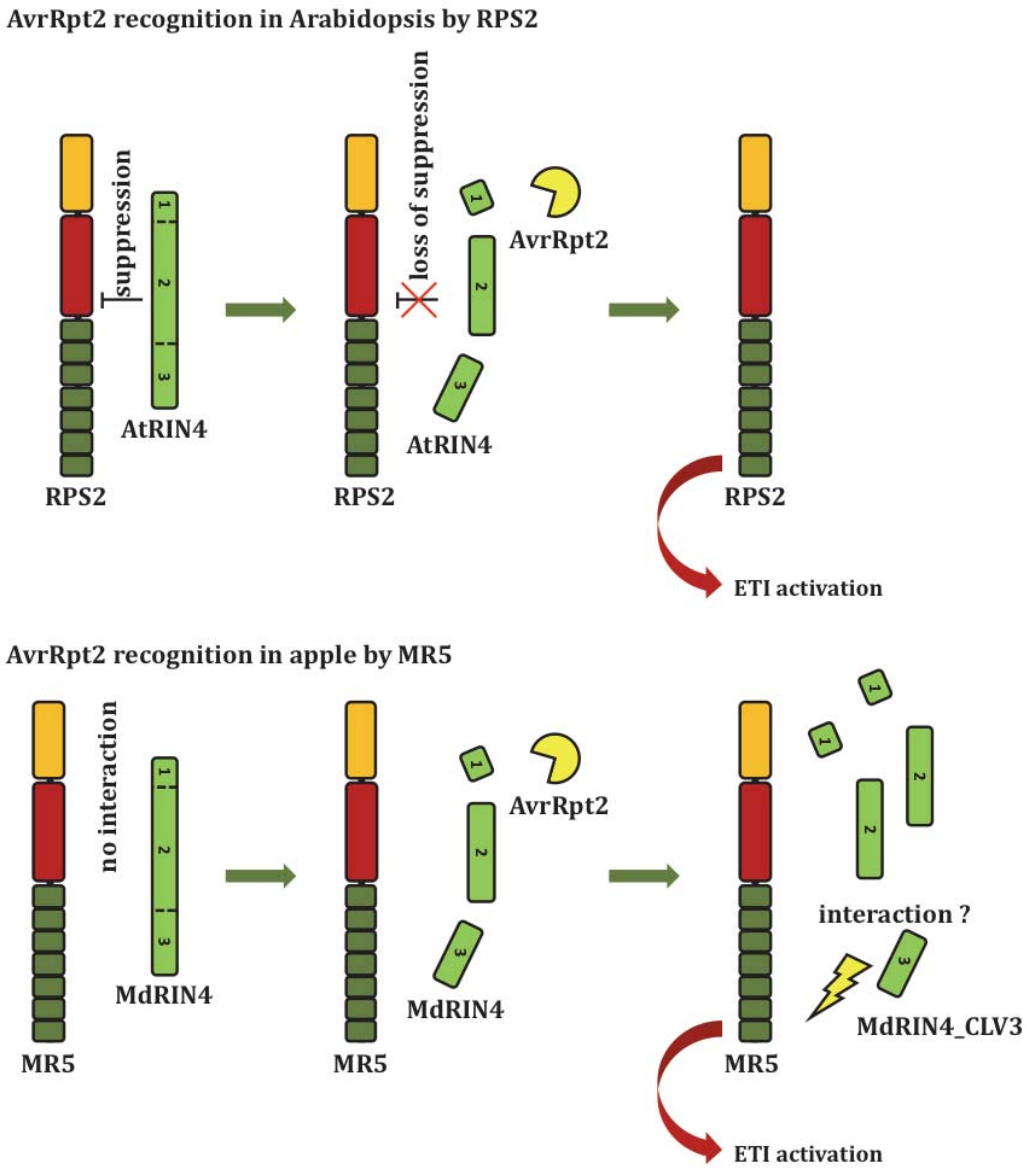

Figure 3.19: Comparison of well-studied RPS2-mediated AvrRpt2 recognition and proposed model of MR5-mediated AvrRpt2 recognition.

3.3.3 Two polymorphic residues in a conserved region of CLV3 dramatically alter RIN4 properties

Two amino acid residues within the CLV3 region that are crucial for MR5 activation were identified in this study. Notably, residues in the same positions of MdRIN4 that support MR5 activation appear to play an antagonistic role in AtRIN4 ability to suppress NLR-triggered autoactivity and subsequent effector-driven activation.

The aforementioned mutations did not have a significant influence on full length RIN4 protein stability but altered the interaction of MdRIN4 with RPS2 or MR5. However, these mutations do seem to alter the protein stability of RIN4 CLV3 variants. It is especially noticeable in MdRIN4 CLV3, as the MdRIN4$^{D186N+F193Y}$ CLV3 variant accumulated to significantly higher levels than MdRIN4 CLV3. This might explain why there were no proper RPS2-mediated PCD symptoms in response to MdRIN4$^{D181N+F193Y}$ cleavage by AvrRpt2. It seems that an excessive amount of MdRIN4$^{D181N+F193Y}$ CLV3 allows it to stay in the membrane, thereby suppressing quick and proper release of RPS2, which results in delayed development of PCD symptoms.

Interestingly, even though the mutations in polymorphic residues altered the protein accumulation level of CLV3 variants, this change of accumulation level did not correlate with the MR5 activation phenotypes observed.

It was also surprising that AtRIN4$^{N158D+Y165F}$ did not lose its ability to interact with RPS2, despite the fact that it lost the ability to suppress RPS2 autoactivity. This suggests another requirement for RPS2 autoactivity suppression by RIN4 in addition to direct interaction. It may be intramolecular interaction of RIN4 domains, which might be disrupted by the mutations in these residues. In contrast, the reciprocal mutations in MdRIN4 enable it to interact with RPS2 and MR5, and to suppress RPS2 autoactivity.

It is worth mentioning that RPM1, in contrast to RPS2, seems to only require the AtRIN4 CLV3 region intact for effective suppression of its autoimmunity. AtRIN4 CLV3 in the M1-2A3 chimera was sufficient to suppress RPM1 but not RPS2, leading to speculation that different regions of RIN4 are important to form an interface between RIN4 and corresponding NLRs. Very surprisingly, the AtRIN4$^{N158D+Y165F}$ variant, which is very similar to the A1-2M3 chimera, was unable

to suppress NLRs. This further supports the speculation that intermolecular interactions in RIN4 variants might be involved in their functionality.

In summary, the AvrRpt2 detection system in apple was dissected to discover a novel activation-based mechanism for MR5 in contrast to the well-characterized de-repression based RPS2-system in Arabidopsis. It was further shown that the each of the R proteins required their cognate RIN4 guardee for proper functionality. This specificity appears to be determined by two critical amino acid residues in the conserved C-NOI region of RIN4. Lessons from studying this system may be applicable across other R protein/guardee pairs, adding depth and providing better understanding of their function.

Chapter 4. Validating and characterization of prospective *Venturia inaequalis* effectors

4.1 Introduction

4.1.1 *Venturia inaequalis* is the causal agent of apple scab disease

Venturia inaequalis Cooke (Wint.) is a hemibiotrophic ascomycete fungus and causal agent of apple scab disease. In addition to members of the *Malus* genus, it can also infect several other rosaceous species, such as *Crataegus*, *Sorbus*, *Pyracantha* and *Eriobotrya* (MacHardy, 1996).

The fact that this disease is found in all regions where apples are grown commercially makes it one of the most important apple diseases to study. It has been reported to be the costliest apple disease to control (Carisse & Bernier, 2002). The New Zealand apple industry is suffering significant cost, especially because of the climate, which is moist and cool and is very favorable for apple scab pathogen proliferation (MacHardy, 1996; Manktelow et al., 1996).

4.1.2 The *Venturia inaequalis* and *Malus* pathosystem

Interactions of *V. inaequalis* and *Malus* sp. fall into the classical gene-for-gene pattern, following the theory proposed by Flor in the 1970s (Flor, 1971). This states that for every *Avr* gene in the pathogen, there is a corresponding *R* gene in the plant host. This means that, if a pathogen carries the *Avr* gene matching the *R* gene from the plant host, there will be a recognition leading to resistance. As recognition can occur directly or indirectly, be influenced by other *Avr* genes from the pathogen or additional resistance genes in a plant host, the complexity of this system increases and it becomes more difficult to predict the outcome of the recognition event.

To date three classes of resistance to *V. inaequalis* have been defined (Figure 4.1): hypersensitive response (HR) is defined as Class 1; stellate necrosis (SN) as Class 2; and chlorosis (Chl) with limited sporulation as Class 3 (Bowen et al., 2011; Shay & Hough, 1952).

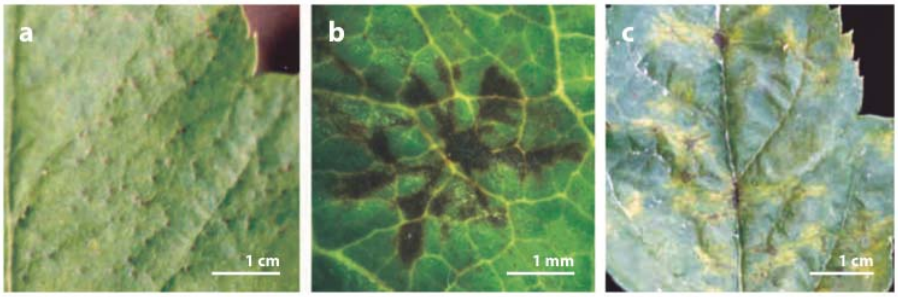

Figure 4.1: Scab resistance reactions on apple leaves.

(A) Pin point hypersensitive response conditioned by the *Rvi4* gene, (B) stellate necrosis reaction conditioned by the *Rvi2* gene. (C) Chlorosis reaction, associated with limited sporulation, conditioned by the *Rvi6* gene. Reproduced from J. Bowen at al., 2011.

Natural populations of *V. inaequalis* are often highly genetically diverse. This is because of the annual sexual phase followed by asexual multiplication during the growing season. This provides opportunities for adaptive selection of new strains able to evade the recognition conferred by plant host *R* genes (Gladieux et al., 2008; Tenzer & Gessler, 1997, 1999).

In natural habitats of the pathogen, this selection can be balanced out by a high diversity of scab *R* genes. On the other hand, in monoculture orchards used for today's horticulture, there is a narrow range of *R* genes present and this generates a higher risk of an outbreak with *V. inaequalis* overcoming this narrow *R* gene set (Bus et al., 2011).

Contemporary understanding of the *V. inaequalis* and *Malus* pathosystem can be presented as an interaction table between several well-described pathogen races and apple cultivars or accessions with differential resistance (Table 4.1). A *V. inaequalis* race is defined as a single spore isolate of the pathogen which cannot be recognized in a specific host. Furthermore, mutations of the pathogen *Avr* locus or genes responsible for *Avr* locus control lead to absence of recognition by the host, consequently leading to complete susceptibility. The race spectrum is defined by a combination of *R* genes it can overcome (Bus et al., 2011).

Historically, researchers have concentrated on pathogen avirulence rather than host resistance. Extensive genetic analysis revealed 19 *Avr* genes, which were called pathogenicity (*p*) genes (Boone, 1971). Most of these loci are inherited independently which provides a large potential for a pathogen to develop new

pathotypes during the sexual reproduction stage (Boone, 1971). Nevertheless, some loci can be linked, for example *p-8*, *p-9* and *p-12* (Williams & Shay, 1957), or even clustered together (Broggini et al., 2011). Further research led to defining races only based on the isolates that could overcome broad spectrum *R* genes with potential for resistance breeding (MacHardy, 1996).

The current nomenclature system for the *V. inaequalis* avirulence genes and races was proposed in a recent review (Bus et al., 2011). In this nomenclature, each *Avr-R* interaction ideally is represented by a differential host carrying only the specific *R* gene and an isolate of the pathogen having altered or lost the complementary allele, identified as *avr*, at the *Avr* locus.

Once the specific *Avr-R* interaction has been defined, isolates lacking multiple avirulences can then be identified by their formula based on the combination of the individual virulences. It includes complex loci as well as quantitative resistance loci (QRLs) for which differential host-pathogen interactions are demonstrated. Major *R* genes are called *Rvi* and corresponding *Avr* alleles are called *AvrRvi* (Bus et al., 2011).

Bus et al. (2011) outlined the minimum requirements to define a new *Arv-R* pair as follows:: "(i) the *R* gene has been shown to segregate in a simple manner and is present in a genetic background from which a suitable reference host can be selected.; (ii) the *R-Avr* interaction has (sufficiently) been shown to be novel either with the aid of a breaking race that has been screened against all other reference hosts to establish that the new *Avr* allele is different from existing alleles or preferably also by screening the *R* gene against all the established race reference isolates to demonstrate that none of them breaks the resistance. Novelty is also confirmed when a gene maps to a position where no known genes have been mapped previously, in the expectation that the genetics of the GfG relationships will be elucidated.; (iii) plant material of the differential host and, where one is known to exist, also the corresponding reference race of the pathogen are available, so that the system can be readily utilized to build on current knowledge." Quoted from Bus et al. (2011).

To date, there are 17 gene-for-gene relationships defined plus relationship (0) involving host (0) that does not carry any resistance genes to any known reference race of *V. inaequalis* (Table 4.1).

Malus						*Venturia inaequalis*		
Differential host			Resistance locus			Avirulence locus		
Number	Accession	Phenotype	Historical	LG[a]	New	New	Old	Race
h(0)	Royal Gala	susceptibility			–	–		(0)
h(1)	Golden Delicious	necrosis	*Vg*	12	*Rvi1*	*AvrRvi1*		(1)
h(2)	TSR34T15	stellate necrosis	*Vh2*	02	*Rvi2*	*AvrRvi2*	*p-9*	(2)
h(3)	Geneva[b]	stellate necrosis	*Vh3*	04	*Rvi3*	*AvrRvi3*[d]	*p-10*	(3)
h(4)	TSR33T239	hypersensitive response	*Vh4 = Vx = Vr1*	02	*Rvi4*	*AvrRvi4*[d]		(4)
h(5)	9-AR2T196	hypersensitive response	*Vm*	17	*Rvi5*	*AvrRvi5*		(5)
h(6)	Priscilla	chlorosis	*Vf*	01	*Rvi6*	*AvrRvi6*		(6)
h(7)	*Malus* x *floribunda* 821[b]	hypersensitive response	*Vfh*	08	*Rvi7*	*AvrRvi7*		(7)
h(8)	B45	stellate necrosis	*Vh8*	02	*Rvi8*	*AvrRvi8*		(8)
h(9)	K2	stellate necrosis	*Vdg*	02	*Rvi9*	*AvrRvi9*	*p-8*	(9)
h(10)	A723–6[b]	hypersensitive response	*Va*	01[c]	*Rvi10*	*AvrRvi10*[d]		(10)
h(11)	A722–7	stellate necrosis/chlorosis	*Vbj*	02	*Rvi11*	*AvrRvi11*[d]		(11)
h(12)	Hansen's baccata #2[b]	chlorosis	*Vb*	12	*Rvi12*	*AvrRvi12*[d]		(12)
h(13)	Durello di Forlì	stellate necrosis	*Vd*	10	*Rvi13*	*AvrRvi13*[d]		(13)
h(14)	Dülmener Rosenapfel[b]	chlorosis	*Vdr1*	06	*Rvi14*	*AvrRvi14*[d]		(14)
h(15)	GMAL2473	hypersensitive response	*Vr2*	02	*Rvi15*	*AvrRvi15*[d]		(15)
h(16)	MIS op 93.051 G07–098[b]	hypersensitive response	*Vmis*	03	*Rvi16*	*AvrRvi16*[d]		(16)
h(17)	Antonovka APF22[b]	chlorosis	*Va1*	01	*Rvi17*	*AvrRvi17*[d]		(17)

Table 4.1: Representation of gene-for-gene relationships between *Venturia inaequalis* and *Malus*.

The pathogen races are defined by the avirulence genes they are lacking, hence resulting in susceptibility on the complementary host.

[b] Temporary host until has been confirmed to be monogenic, or a monogenic progeny from this polygenic host has been selected.

[c] Provisional, based on the assumption that the resistance in sources PI 172623 and PI 172633 are identical.

[d]Gene-for-gene relationship not confirmed to date.

Reproduced from V. Bus et al., 2011.

Relationship (0) – Host (0) lacks any *R* genes and consequently is susceptible to all *V. inaequalis* isolates. Currently, Gala cultivar of apple or its derivatives are broadly used as universally susceptible host (0) in scab research. Gala is also a common cultivar grown worldwide. Despite Gala carries two QRLs (Soufflet-Freslon et al., 2008) linked to decreased growth of *V. inaequalis* in comparison to Golden Delicious (Parisi et al., 2004), it is still generally highly susceptible. The *V. inaequalis* strain described in (Williams & Shay, 1957) was

assigned as race (0), and it is avirulent to any host carrying *R* genes, therefore this race can only induce disease developments in host (0).

Relationship (1) – is the susceptible interaction between the Golden Delicious cultivar carrying *Rvi1*(*Vg*) gene and a pathogen isolate 101. Differential interactions of *V. inaequalis* isolates with this apple cultivar implied the presence of an *R* gene. The fact that there is only one *R* gene was supported by the research of the avirulent isolate 101 and further confirmed with isolate 1066 (Benaouf & Parisi, 2000). *Rvi1(Vg)* was mapped on the distal end of linkage group (LG) 12 of the Prima cultivar (Durel et al., 2000), which is the derivative of Golden Delicious. The *Rvi1* gene is responsible for necrotic resistance reaction, which may show weak sporulation of the pathogen (Chevalier & Parisi, 2000). The segregation of the *Avr* gene was shown in a cross between the virulent *V. inaequalis* isolate 104 (Laurens et al., 2004; Parisi et al., 2004) and avirulent isolate 147 (Hernandez, 1990).

Relationship (2) – host (2) is apple line TSR34T15, which is a derivative of Russian apple R12740-7A. *Rvi2* has been mapped to the lower end of LG2 in accession TSR34T15. Currently the 1770-3 isolate of *V. inaequalis* identified in the Purdue-Rutgers-Illinois (PRI) program is assigned as race (2). Isolate 1639 was shown to break the *Rvi2* mediated resistance (Bus et al., 2005b), but *AvrRvi2* in this isolate segregated in a 3:1 ratio instead of expected 1:1, and it is also linked to other *AvrRvi* genes, which indicates that this relationship may be more complex than a simple gene-for-gene one (Broggini et al., 2011).

Relationship (3) – host (3) is Geneva cultivar and *Rvi3* gene candidates were mapped to LG4 in progenies of Geneva crossed with Elstar and Braeburn. The corresponding *Avr* gene in the pathogen was identified as *AvrVh3.2* in an *Avr* gene cluster of isolate 1639 (Broggini et al., 2011). Until further dissection of the *Avr-R* pair gene clusters, Geneva is proposed to be host (3) and the U.S. isolate 1774-1 of *V. inaequalis* to be reference race (3).

Relationship (4) – host (4) was identified as Russian apple R12740-7A F2 derivative TSR33T239. The *Rvi4* gene in this derivative is associated with HR when challenged with race (4) of the pathogen. This *R* gene was mapped to LG2 of TSR33T239 (Bus et al., 2005b). A few isolates of *V. inaequalis* from the United States and France were assigned as race (4), nevertheless, none of these races were fully compatible with hosts carrying the *Rvi4* gene (Bus, 2006).

Relationship (5) - *M. micromalus* derivative 9-AR2T196 is referred to as host (5). It carries the HR-conditioning gene *Rvi5* which was segregating as a single gene in the F1 progeny of a *Malus micromalus* 245-38 and accession PRI 76-27 cross (Shay et al., 1953). The presence of this gene was also shown later in related progenies (Bus et al., 2000). A few race (5) isolates were acquired from hosts carrying *Rvi5*, including isolate 147, which was also incompatible with host plants carrying *Rvi1* (Hernandez, 1990). Three candidate effector proteins were identified in isolate MNH120 (Win et al., 2003), and one of them may be *AvrRvi5* effector.

Relationship (6) – host (6) was defined by presence of the *Rvi6 R* gene derived from *Malus* x *floribunda* 821. Sequencing of the *Rvi6* locus pointed out that it contains four paralogs (Vinatzer et al., 2001; Xu & Korban, 2002). In backcross progenies of *M.* x *floribunda* 821, resistance was shown to clearly segregate as a single gene (Hough et al., 1953), but differential interactions of a number of F2 descendants from *M.* x *floribunda* 821 crosses (Parisi & Lespinasse, 1998) implied the presence another gene (Benaouf & Parisi, 2000). Race (6) of *V. inaequalis* is defined by its ability to cause disease in the hosts carrying *Rvi6* only, but recently many of the commonly host (6) accessions used earlier (e.g., Prima and Florina) were found to also carry *Rvi1*. As Priscilla cultivar does not carry *Rvi1* (Benaouf & Parisi, 2000), it is the best host (6) representative to date.

Relationship (7) – extensive research of *M.* x *floribunda* 821 and isolate 1066 interaction led to the discovery of the *Rvi7* gene. It segregates independently from *Rvi6* (Benaouf & Parisi, 2000) and was mapped to LG8. For a long time, *M.* x *floribunda* 821 which carries *Rvi6* and *Rvi7* was used as host (7). A recent study proposes better host (7) which is LPG3-29 (derived from 'Golden Delicious' × *M. floribunda* 821 cross) carrying only *Rvi7* (Caffier et al., 2014). From the pathogen side, gene-for-gene interaction for *Rvi7* was most clearly shown via differential interactions of the set of incompatible isolates 104, 301, 302, and 1093, and the compatible isolate 1066 on certain representatives from the progeny from a Golden Delicious x *M.* x *floribunda* crosses (Benaouf & Parisi, 2000).

Relationship (8) – host (8) is assigned as *M. sieversii* accession GMAL3631-W193B from the Tarbagatai mountain range in Kazakhstan. It carries the *Rvi8* gene, which confers stellate necrosis very similar to the one triggered by *Rvi2.* Both genes were mapped to the lower end of LG2 (Bus, 2006; Bus et al., 2005a). *V.*

inaequalis isolate NZ188B.2 is the race 8 representative as it carries virulent variant of *AvrRvi8*. Interestingly, *Rvi2* and *Rvi8* genes are linked, but still clearly separate. This was proven with the research of isolate NZ188B.2 which cannot infect host (2) plants. Similarly, the pathogens *Avr* loci showed genetic interaction too (Broggini et al., 2011). The compatible interaction of race (8) isolate NZ188B.2 with a range of different *M. sieversii* hosts (Bus et al., 2005a) implies that *Rvi8* is a common *R* gene widespread in the Kazakh accessions.

Relationship (9) – crabapple Dolgo was assigned as host (9) and was shown to carry a major resistance gene *Rvi9*. *Rvi2* and *Rvi9* trigger same stellate necrosis reaction. Pathogens isolate 356-2, from South Dakota, is able to overcome both of these genes' conditioned resistance. These observations implied that there is only one gene-for-gene interaction. However, research of a 356-2 x 651 isolate cross progeny clearly demonstrated two separate interactions. The corresponding *Avr* loci from fungus, formerly were known as *p-9* and *p-8* and now assigned as *AvrRvi9*. Interestingly, *Rvi2* and *Rvi9* are mapped to be clustered together on LG2 and corresponding *AvrRvi2* and *AvrRvi9* loci are also linked in the pathogen. Moreover, *AvrRvi9*, like *AvrRvi2*, shows a 3:1 segregation ratio of avirulence, with two progeny of the EU-B04 x 1639 cross carrying only *AvrRvi9* (Broggini et al., 2011) and therefore making perfect candidates to be assigned as reference race (9).

Relationship (10) – the preferred host (10) is Antonovka PI 172623, as *Rvi10* gene was originally identified in this accession (Dayton & Williams, 1968). In addition, this gene was also found in PI 172633 (Lespinasse, 1989), PI 172612 (Williams & Kuc, 1969), Freedom (Zini, 2005), and as *Va2* in Antonovka APF22 (Dunemann & Egerer, 2010). Because all of these accessions are open-pollinated Antonovka derivatives, they all may carry *Rvi10*. The *Rvi10* has been mapped about 24 cM above the *Rvi6* region on LG1 (Hemmat et al., 2003).

Relationship (11) – the *Rvi11* gene was identified in *Malus baccata jackii* as an *R* locus near simple sequence repeat (SSR) marker CH05e03, below the middle of LG2 (Gygax et al., 2004). A722-7 from an *M. baccata jackii* cross with Starking is a preferred host (11), because the resistance of A722-7 was shown to be monogenetic, and *M. baccata jackii* has at least one additional narrow spectrum *R* gene (Bus et al., 2011). No race (11) *V. inaequalis* isolates were reported to date.

Relationship (12) – *Rvi12* was discovered as an independently segregating gene in Hansen's baccata #2 (Dayton & Williams, 1968). It was mapped to LG12 (Erdin et al., 2006) at a significant distance from *Rvi1*. In many cases *Rvi12* gene confers chlorosis, while some of the progenies show a necrotic reaction to *V. inaequalis* (Dayton & Williams, 1968; Erdin et al., 2006). As Hansen's baccata #2 carries more than one *R* gene, the search for appropriate host (12) is still in progress. No differential interactions with *Rvi12* have been reported to date.

Relationship (13) – an Italian cultivar Durello di Forli was assigned as host (13) and carries the major *R* gene *Rvi13* (De Wit et al., 2004). It was mapped to the proximal end of LG10 near SSR marker CH02b07 (De Wit et al., 2004). The resistance response conferred by this gene ranges from stellate necrosis in the case of single isolate infection by *V. inaequalis* EU-D42, to chlorosis when infected by a mixture of isolates (De Wit et al., 2004). It is not yet clear if the resistance is monogenic and isolates 1066 and EU-NL05, are able to overcome *Rvi13* mediated resistance (Laurens et al., 2004; Parisi et al., 2004).

Relationship (14) – the prospective host (14) is Dulmener Rosenapfel, which is a scab resistant cultivar derived from open-pollinated Gravenstein (Laurens et al., 2004). One of the resistance components is designated as *Rvi14*, which confers a chlorosis reaction. This gene is mapped to the upper end of LG6 near SSR marker HB09 (Soufflet-Freslon et al., 2008). The resistance can be broken by *V. inaequalis* isolates 301, EU-D42, and EU-B04. All of them are under investigation in order to define their ability to serve as reference isolates.

Relationship (15) – the *Rvi15* gene was initially assumed to be a third scab *R* gene from Russian apple (Gessler et al., 2006). Later it was confirmed that its source accession GMAL 2473 is not related to Russian apple (Patocchi et al., 2004). This gene was shown to condition a range of resistance reactions from no symptoms to chlorosis in a progeny of a cross with Idared (Patocchi et al., 2004). In contrast, this gene confers only necrotic reaction in a cross with Golden Delicious (Gessler et al., 2006). Further investigation led to determining the phenotype as HR (Galli et al., 2010a), similar to the one conditioned by *Rvi4*, to which it appears to be closely linked on LG2 (Patocchi et al., 2004). The locus contains three genes coding for TIR-NBS-LRR proteins (Galli et al., 2010b) and at least one of them should be the functional *Rvi15*. No *V. inaequalis* isolate virulent on *Rvi15*-harboring hosts has been identified to date.

Relationship (16) – the *Rvi16* gene was originally identified in the open-pollinated mildew immune selection (MIS) progeny 93.051 G07-098 (Bus et al., 2010). This gene conditions a range of resistance reactions from no visible symptoms in case of infection with isolate J222, to chlorosis in case of infection with a mixture of *V. inaequalis* isolates. The gene was mapped to the lower end of LG3, near SSR marker AU223657. The work to identify an appropriate monogenetic host (16) is still in progress (Bus et al., 2011).

Relationship (17) – from two novel resistance genes in Antonovka APF22 progeny, one seems to be the same as *Rvi10* and the other one was assigned to be *Rvi17* (Dunemann & Egerer, 2010). The *Rvi17* gene was shown to confer scab resistance in field trials; it maps to within 1 cM of *Rvi6* on LG1, but it is different from *Rvi6* since it is not overcome by race (6) (Dunemann & Egerer, 2010). A suitable differential host is being selected for the determination of differential interactions with *V. inaequalis* (Bus et al., 2011).

Mapped positions of the 17 known *R* gene loci are summarized in Figure 4.2.

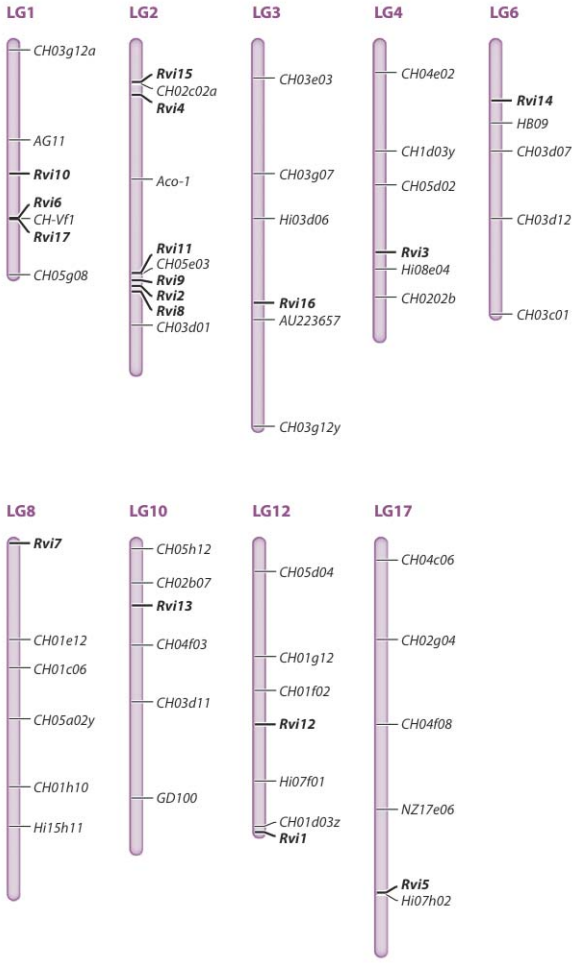

Figure 4.2: Global positions of the 17 *Rvi* scab resistance genes identified in the apple genome to date. The skeleton genetic map is based on the integrated consensus map by N'Diaye et al. Reproduced from V. Bus et al., 2011.

4.1.3 Relationship (8) of *V. inaequalis* NZ188B.2 and *M. sieversii* W193B

The major scab-resistance gene called *Rvi8* (old name - *Vh8*) derived from *M. sieversii* W193B was identified in the cross of Royal Gala x *M. sieversii* W193B segregating for resistance to mixed isolate *V. inaequalis* inoculation. Further dissection of this resistance led to discovery of strong linkage between *Rvi8* and *Rvi2* (old name - *Vh2*) genes from *Malus pumila* Russian apple R12740-7A (Bus et al., 2005a).

In the same research, the *V. inaequalis* race NZ188B.2 able to overcome *Rvi8* conditioned resistance was found. This race was avirulent on the differential hosts TSR34T15 (host 2), Geneva (host 3), TSR33T239 (host 4), 9-AR2T196 (host 5),

Prima (host 6) and *M. floribunda* 821 (host 7) and it was virulent on Royal Gala (host 0) and Golden Delicious (host 1) (Bus et al., 2005a). Interestingly, recent phenotyping study confirmed the results of Bus et al., yet the differential host (7) (new host (7) was used, which only carries the *Rvi7* locus) showed a compatible interaction (Caffier et al., 2014). *V. inaequalis* strain NZ110.1 was shown to be avirulent in *M. sieversii* W193B (host 8) and assumed to carry *avrRvi8* avirulent locus variant (Bus et al., 2005a). Further study of *V. inaequalis* EU-B04 x 1639 cross progenies on different *Malus* hosts allowed the mapping of the *AvrRvi8* locus to linkage group A4 (Broggini et al., 2011).

Similarly to *Rvi2*, *Rvi8* confers the stellate necrosis reaction when inoculated with avirulent *V. inaequalis* strains. This necrosis area is 20-30 cells across in palisade mesophyll and is overlaid with necrotic epidermal cells spanning 10-15 cells. Some of the plants carrying *Rvi8* or *Rvi2* show limited sporulation of the pathogen only in the necrotic zone, while others show limited sporulation with pathogen mycelium advancing beyond the necrotic zone (Bus et al., 2005a).

The *Rvi8* resistance gene was mapped to the same region with *Rvi2* of the lower end of LG2. Both *Rvi2* and *Rvi8* were close to and nearly the same distance from OPL19SCAR marker which may mean they comprise the same complex locus. Interestingly, over 90% of *M. sieversii* originating from seven different regions of Kazakhstan (Luby et al., 2001), carry the SCAR marker associated with *Rvi8* locus. This fact implies that *Rvi8* is the major scab resistance gene in natural *M. sieversii* accessions.

The *AvrRvi8* locus was mapped in *Venturia inaequalis* (*Vi*) (Broggini et al., 2011). Further studies in Dr. J. Bowen's lab (PFR, Mt. Albert, NZ) led to identification of the *AvrRvi8* gene candidates (J. Bowen. et al., unpublished). The top candidate matching the physical mapping position was the *ATG12431* gene, which was assigned the new name *AvrRv8-7*. In addition, there were 8 more paralogs identified based on similarity to *AvrRvi8-7*.

Furthermore, three more candidates were identified on the same scaffold with putatively secreted protein products but with no up-regulation of gene expression during growth *in planta*. These three candidates were *ATG7647*, *ATG12412* and *ATG12414* and they were single genes with no paralogues identified in the whole genome sequence. The first aim of chapter 4 was to clone and identify which of the aforementioned candidates is true *AvrRvi8* gene.

The full genome sequence and transcriptome analysis data relating to *V. inaequalis* 120 were acquired at PFR, Mt. Albert, NZ. This strain was used as it is avirulent on all known differential hosts and presumably carries the most complete effector set that is currently known to be recognized.

Further analysis in Dr. J. Bowen's group resulted in the identification of candidate *V. inaequalis* effectors (ViCE) (Deng et al., 2017). Genes were predicted and validated by RNAseq data, then the genes which were expressed by *V. inaequalis* at 2 and 7 dpi on susceptible apple plants were selected for further analysis. Another round of selection was carried out on the resulting set of candidates. This included search for ORFs coding for small (less than 450 aa), secreted (having a eukaryotic signal peptide), with no significant similarity with known genes non-related to pathogenesis (Deng et al., 2017). The list of the top 22 candidate sequences was generated and the second aim of the research in chapter 4 was to analyze and validate their sequences and physiological function.

4.2 Results

4.2.1 Cloning of AvrRvi8 effector candidate genes

In order to validate *AvrRvi8* candidate genes, they were amplified with gene specific primers using nested PCR approach (subchapter 2.4.6). The cDNA extracted from susceptible apple infected by *V. inaequalis* at 7 dpi was used for that and resulting fragments were ligated into pICH41021 (KSC# 746) vector for further sequencing.

AvrRvi8-1 and *8-2* paralogs were amplified with the same pair of primers as the ends of the predicted gene models were identical. Interestingly, instead of two, there were six different paralogs revealed by sequencing of the PCR products. Nucleotide alignments of bioinformatically predicted and PCR acquired DNA fragment sequences are listed in appendices, Figure 6.3.

AvrRvi8-3, *8-4* and *8-5*, homologs were identical or, in case of *AvrRvi8-4*, had one silent nucleotide mismatch, to the bioinformatically predicted sequence. *AvrRvi8-6* and *8-8* nucleotide sequences were 69% and 86% identical to the ones predicted *in silico* respectively (alignments can be found in appendices, Figure 6.4). Finally, *AvrRvi8-9* had 51% nucleotide identity to the predicted sequence and carried unexpected premature STOP-codons, resulting in significantly truncated candidate version (alignment can be found in appendices, Figure 6.5). A summary of *AvrRvi8* candidate gene validation is listed in Table 4.2.

Another three distinct paralogs were cloned and validated. For convenience, these candidates were named as *AvrRvi8-10* (original gene *ATG7647*), *8-11* (original gene *ATG12412*) and *8-12* (original gene *ATG12414*). Their analysis showed that *AvrRvi8-10* and *8-11* had incorrectly *in silico* annotated introns, and this was corrected by using the PCR product sequencing data acquired in this chapter. In addition, these different intron patterns led to early STOP-codons.

Table 4.2. Sequence analysis and validation of 12 *in silico* predicted *AvrRvi8* gene candidates.

AvrRvi8 homolog #	Nucleotide identity to *in silico* prediction	Nucleotide identity to *AvrRvi8-7* (originally mapped candidate)	Description of the differences between cloned fragments and *in silico* predicted ones
AvrRvi8-1	avg. 87.3%	avg. 91%	six different homologs, fairly high similarity
AvrRvi8-2			
AvrRvi8-3	100%	63.7%	n/a
AvrRvi8-4	99.9%	64.4%	one silent nt polymorphism
AvrRvi8-5	100%	71.4%	n/a
AvrRvi8-6	69.2%	64.4%	n/a
AvrRvi8-8	86%	99.7%	n/a
AvrRvi8-9	51%	51.3%	premature STOP-codon

4.2.2 Functional validation of *AvrRvi8* gene candidates *in planta*

A particle bombardment approach was chosen as an initial method to transiently express the candidate effector proteins in apple leaves. *AvrRvi8* candidates were sub-cloned into binary vectors and transformed into apple leaves by Simon Deroles, PFR, Palmerston North. Unfortunately, apple leaves were not suitable for transformation by this method. Positive control plasmids carrying the GFP coding gene under the strong 35S CaMV promoter did not register a sufficient level of construct expression *in planta*.

As an alternative, constructs carrying the HA-tagged *AvrRvi8* homologs were expressed in *Nicotiana benthamiana* and *Nicotiana tabacum* using an agroinfiltration method (subchapter 2.3.2). The aim was to test if there would be any non-host immunity response to AvrRvi8 candidates in *N. benthamiana* or *N. tabacum*. Because *AvrRvi8-7* candidate was identified in the originally mapped region for *AvrRvi8*, the binary vector carrying this gene was expressed *in planta*.

Furthermore, it is not known if the AvrRvi8 effector is delivered to the plant apoplast or into the host cell. Thus, native AvrRvi8 and a truncated variant lacking the predicted signal peptide were expressed in this experiment. Response to effector expression was assessed at 4 dpi and no macroscopic changes were detected in contrast to the positive control (Figure 4.3). Positive control was co-

expression of the well-characterized Cf-4 receptor from tomato with its corresponding effector Avr4 from fungal pathogen *C. fulvum,* which results in macroscopic response (Thomas et al., 1997).

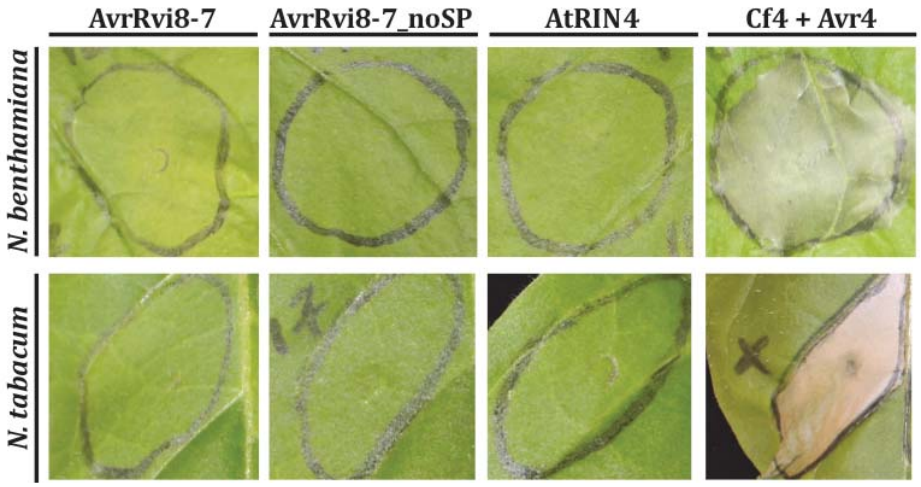

Figure 4.3: AvrRvi8-7 overexpression in *N. benthamiana* and *N. tabacum* does not trigger a macroscopic response.

Leaves of 4-5 week old plants were agroinfiltrated with *Agrobacterium* strains carrying the constructs of interest. OD_{600} was 0.5 for each strain and an *Agrobacterium* strain carrying GFP was used to equalise the OD in mixtures. Cf4 + Avr4 infiltration was a positive control. Photographs were taken at 4 dpi.

4.2.3 *Pseudomonas fluorescens* mediated delivery of AvrRvi8-7 into apple leaves

The *AvrRvi8-7* candidate gene was subcloned into the pBBR-series broad host vector downstream of the *AvrRps4* or *AvrRpm1* promoter fused with the gene part coding for first 1-136 aa (for AvrRps4) or 1-89 aa (for AvrRpm1) to use with the disarmed *P. fluorescens* Pf0-1 strain for effector delivery (constructs described in subchapter 2.1.2, Table 2.3).

As the resistance *Rvi8* locus was segregating in the apple seeds available, genotyping was carried out at PFR, Palmerston North, NZ by Deepa Bowatte. The leaves of susceptible (not carrying *Rvi8* locus) and resistant (carrying *Rvi8* locus) *Malus* plants were infiltrated with *P. fluorescens* carrying the broad host constructs mentioned earlier. No macroscopic response was detected at 7 dpi (Figure 4.4). The brightness difference observed between *Rvi8+* and *Rvi8*– rows (Figure 4.4) could be explained by different germination time between seedlings.

Unfortunately, due to time and material availability restrictions, only the *AvrRvi8-7* candidate was tested via *P. fluorescens* delivery.

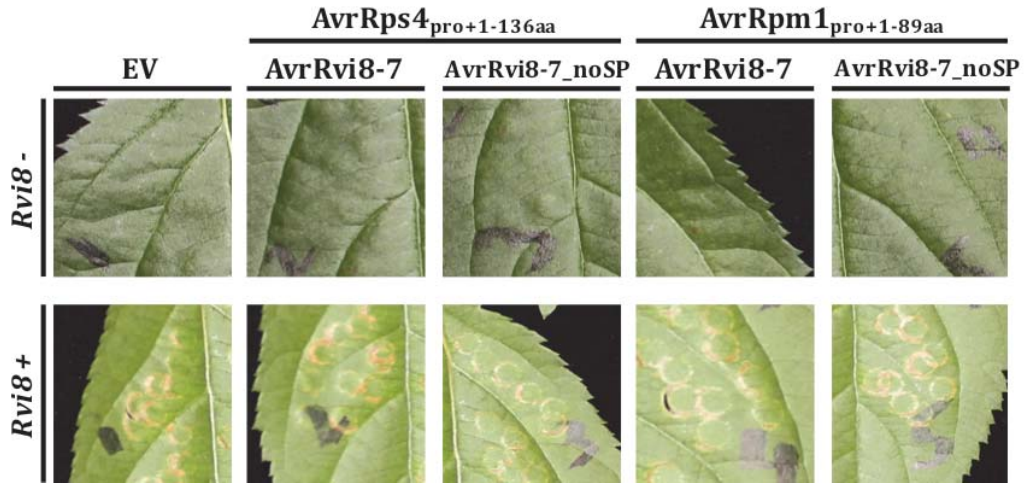

Figure 4.4: AvrRvi8-7 delivery via *P. fluorescens* T3SS does not trigger a macroscopic response in susceptible or resistant apple plants.
Leaves of susceptible (*Rvi8 -*) and resistant (*Rvi8 +*) apple plants were infiltrated with OD_{600} = 0.4 of *P. flourescens* carrying the AvrRvi8 effector candidate. AvrRvi8-7 WT and truncated version lacking the predicted signal peptide were fused with the first 136 aa of AvrRps4 or 89 aa of AvrRpm1 under control of the corresponding native promoters. Photographs were taken at 7 dpi.

4.2.4 Validating *Venturia inaequalis* 120 Candidate Effectors

To validate the short-listed *ViCE,* they were amplified with gene specific primers by using a nested PCR approach (chapter 2.4.6) from *V. inaequalis* cDNA obtained from infected plants at 7 dpi. 20 out of 22 *ViCE* genes could be amplified and were subjected to resequencing to validate them. 17 of these genes were identical to the *in silico* predicted ones and were used for further analysis (Table 4.3). *ViCE5, 7* and *8* were carrying mis-annotated introns and their nucleotide alignments to the predicted genes can be found in appendices, Figure 6.7.

Table 4.3. Sequence validation of *V. inaequalis* candidate effectors (*ViCE*).

ViCE #	Original ATG # (from J. Bowen's group)	Description
ViCE1	1013	sequence confirmed
ViCE2	1497	sequence confirmed
ViCE3	3050	no amplification
ViCE4	3086	no amplification
ViCE5	3803	intron mis-annotation, early STOP-codon
ViCE6	4475	sequence confirmed
ViCE7	4706	intron mis-annotation, early STOP-codon
ViCE8	4855	intron mis-annotation, missing STOP-codon
ViCE9	4972	sequence confirmed
ViCE10	5172	sequence confirmed
ViCE11	5886	sequence confirmed
ViCE12	6097	sequence confirmed
ViCE13	6945	sequence confirmed
ViCE14	7338	sequence confirmed
ViCE15	7585	sequence confirmed
ViCE16	9790	sequence confirmed
ViCE17	10344	sequence confirmed
ViCE18	10389	sequence confirmed
ViCE19	10672	sequence confirmed
ViCE20	10823	sequence confirmed
ViCE21	10983	sequence confirmed
ViCE22	11273	sequence confirmed

17 *ViCE* that showed identical sequences compared to the *in silico* predicted ones were subcloned into binary vectors under the strong 35S CaMV promoter and used for heterologous expression *in planta*. As the target localisation of the ViCEs is not known, the genes were cloned without the predicted native signal peptides or fused with the *N. benthamiana* (*Nb*) PR1α signal peptide to ensure transport to the apoplast.

Expression of the ViCE set in *N. benthamiana* leaves via agroinfiltration showed no macroscopic response at 3-4 dpi in comparison to RPS2 overexpression (the autoimmune R protein from *Arabidopsis thaliana* that was used as a control (Figure 4.5).

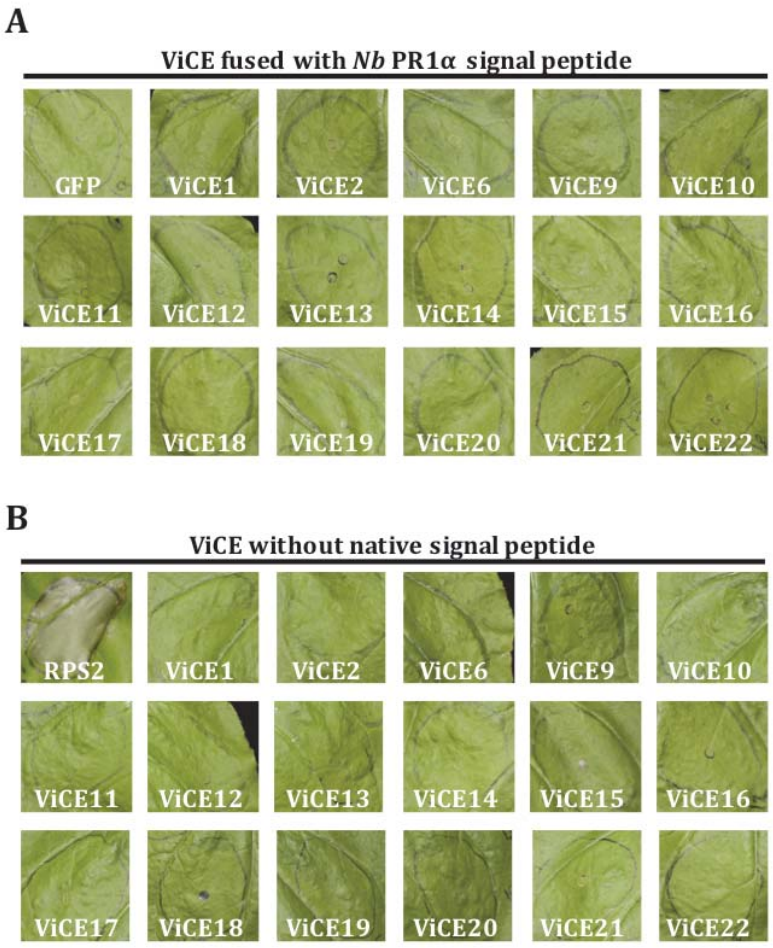

Figure 4.5: *V. inaequalis* candidate effectors do not trigger any macroscopic response when expressed in *N. benthamiana* leaves.
Candidate effectors were fused with *Nb* PR1α signal peptide (A) or lacked the native signal peptides (B). Candidate effectors were expressed via agroinfiltration with OD_{600} = 0.5 for each strain. Agroinfiltration with *Agrobacterium* carrying constructs with GFP (OD_{600}=0.5) or RPS2 (OD_{600}=0.1) were used as controls. Photographs were taken at 4 dpi.

As some effectors can suppress plant immune responses triggered by another known immunity response elicitor, constructs carrying *ViCE* with or without signal peptide were agroinfiltrated into *N. benthamiana*. Each ViCE was expressed with GFP (as a negative control) and with (i) HopAS1 effector from *P. syringae*; (ii) RPS2 (autoimmune *R* gene from *A. thaliana*); (iii) Cf4 and Avr4 (Cf4

is the receptor recognising the Avr4 effector from *C. fulvum*); and (iv) Pto and AvrPto (Pto is the receptor recognizing effector AvrPto from *P. syringae*).

Certain attenuation of macroscopic response was observed at 3 dpi for RPS2 co-expressed with SP::ViCE2, SP::ViCE11 and SP::ViCE12 (SP stands for *Nb* PR1α signal peptide). Similar attenuated phenotype was also observed for HopAS1 co-expression with SP::ViCE2, ViCE12 and ViCE14 (Figure 4.6). The phenotypes observed should be further confirmed by ion leakage analysis.

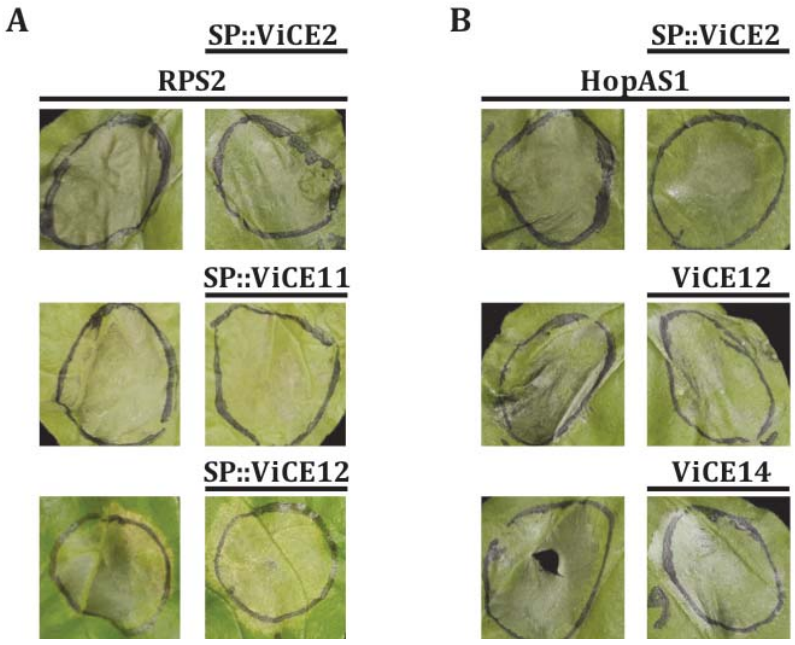

Figure 4.6: *V. inaequalis* candidate effectors are able to attenuate RPS2 (A) and HopAS1 (B) –mediated response when expressed in *N. benthamiana* leaves.

Candidate effectors were agroinfiltrated in the *N. benthamiana* leaves and cell death was photographed at 3 dpi.

4.3 Discussion

4.3.1 Sequence and functional validation of *V. inaequalis* AvrRvi8

Research of fungal and oomycete plant pathogens' effectors has been carried out for several decades but despite significant progress in this area, is still less developed than phytopathogenic bacterial effector research. This is due to the more complex organisation of the fungal and oomycete pathogen genomes and in some cases difficulties of fungal genetic manipulation and cultivation.

Most fungal and oomycete effectors have been discovered through a classical genetic map-based cloning approach. Some examples of these effectors include AvrPi-ta (Orbach et al., 2000), ACE1 (Bohnert et al., 2004), and Avr-CO39 (Farman & Leong, 1998) from *M. oryzae*; AvrLm1 (Gout et al., 2006), Avrlm4-7 (Parlange et al., 2009), AvrLm6 (Fudal et al., 2007) from *L. maculans*. *V. inaequalis AvrRvi8* loci was also roughly mapped by a classical genetic approach and candidate genes were predicted and ranked as *AvrRvi8* candidates by using bioinformatic analysis tools (Broggini et al., 2011; Bowen. et al., unpublished).

The aim of the research in this chapter was to validate and characterise the AvrRvi8 effector. This effector candidate paralogs were cloned and sequence validated in this study. Interestingly, only paralogs *AvrRvi8-3, 8-5, 8-7* and *8-12* were identical to the *in silico* prediction. The other homologs had mis-annotated introns (*AvrRvi8-10, 8-11*), insignificant mismatches (*AvrRvi8-4*), premature STOP-codon (*Avr8-9*) or significant sequence variations (*AvrRvi8-1, 8-2, 8-6, 8-8*).

The premature STOP-codon in *AvrRvi8-9* leads to severe ORF truncation and thus suggests that it is unlikely to be *AvrRvi8*. The other artefacts observed might be the result of the non-specific amplification during PCR or sequencing assembly and analysis problems. Sequencing assembly could be the likely reason as the draft genome used to mine for effector candidates for this study was generated from Illumina sequencing reads without Sanger sequencing validation. Further resequencing with the PacBio platform and bioinformatic re-analysis with the latest tools could provide better input data for effector validation.

Originally mapped, the strongest *AvrRvi8* candidate was studied in more detail. The aim was to validate this effector as being able to initiate a stellate necrosis response inresistant apple plants. The biolistic approach to express the effector candidate failed at the test-run stage. The transformation of detached apple leaves showed insufficient efficiency, possibly due to the thick cuticle layer

on the leaf surface, as well as the overall fragile structure of the leaf. An alternative could be Agrobacterium mediated expression in apple fruit (Spolaore et al., 2001) or using protoplasts for the transformation procedure.

Agroinfiltration of non-host *N. benthamiana* and *N. tabacum* showed no significant response. This might be because of low expression or protein instability *in planta*, which can be validated by immunoblotting of the effector candidate. In addition, there might be no non-host recognition in the plants tested and in this case, a wider selection of plants can be used for the heterologous expression studies.

Finally, the artificial effector candidate delivery was performed using the *P. fluorescens* T3SS. The results obtained indicated no response in susceptible or resistant apple plants. This might be due to inability of *P. fluorescens* to translocate the effectors into apple plant cells because of a host plant PTI response. This could be addressed by using the natural *Pseudomonas* sp. strains virulent in apple or *E. amylovora*.

Another explanation would be the absence of correct processing of eukaryotic effectors in bacterial delivery systems. To address this problem a eukaryotic delivery system should be used.

4.3.1 Sequence and functional validation of novel *in silico* predicted *V. inaequalis* effector candidates

The latest progress in effector research from filamentous plant pathogens is the result of significant improvement of whole genome sequencing techniques and consequent bioinformatic data analysis. For example the emerging availability of transcriptomic and genomic sequences led to the discovery and characterisation of Avr3a (Armstrong et al., 2005) and Avr4 (Van Poppel et al., 2008) effectors from *P. infestans* and AvrL567 from *M. lini* (Dodds et al., 2004). Nowadays significant research is concentrated on expressed sequence tags (EST) screening for bioinformatically predicted N-terminal secretion signals to mine for prospective effectors (Vleeshouwers et al., 2008; Zhu et al., 2012).

Venturia inaequalis whole genome data became available recently (Cooke et al., 2014; Deng et al., 2017). Bioinformatic analysis was also performed and prospective effector genes were predicted (Deng et al., 2017). The *in silico* predicted *V. inaequalis* effector candidates (ViCE) were cloned and validated

during this study. After cloning the majority were identical to the *in silico* sequence. Nevertheless, *ViCE5, 7* and *8* showed mis-annotated introns and *ViCE3* and *4* showed significantly different sequences. This can be due to non-specific PCR amplification or incorrect genome assembly.

Expression of the set of ViCE in non-host *N. benthamiana* did not lead to a macroscopic response. Interestingly, ViCE co-expression with known plant response elicitors showed reproducible immunity attenuation in several cases. ViCE12 could only attenuate RPS2 and HopAS1 –mediated response when fused with the PR1α signal peptide, that might imply that it is an apoplastic effector. The resistance genes cloned from apple varieties include *Vfa1* and *Vfa2* (the genes from the *Rvi6* locus) which were shown to grant resistance to *V. inaequalis* and seem to be TM-LRR receptors with an extracellular LRR domain (Belfanti et al., 2004; Vinatzer et al., 2001; Xu & Korban, 2002). Furthermore, another gene cloned is *Vr2* (*Rvi15*) which shows TIR-NBS-LRR structure and presumably detects a cytosolic effector (Schouten et al., 2014). These observations show that apple varieties carry several types of receptors able to recognise a variety of effectors translocated to the apoplast and plant cell cytosol.

In any case, *in planta* stability of the ViCE should be assessed before making any conclusion. Future work on ViCE validation could include measuring the attenuation of the immune response via checking ion leakage from infected leaves.

The constructs generated in this study can be used to knock out the candidate effector genes in *V. inaequalis* with consequent complementation to assess their contribution to virulence based on any changes in pathogenenicity. Another strategy would be introducing the candidate effectors into the *Venturia* sp. strains able to infect different *Rosaceae* species other than apple and analyse whether the effectors contribute to host range determination.

Chapter 5. General conclusions and Future directions

The main focus of this thesis was the in-depth research of effector triggered immunity against two of the most important apple pathogens – the bacterium *E. amylovora* and fungus *V. inaequalis*. Interestingly, ETI mechanisms are quite conserved and act similarly in response to effectors derived from the pathogens of different kingdoms.

The vast majority of the immune responses against those effectors are facilitated by NLRs. In addition to that, many NLRs are activated indirectly via surveillance of physiologically important plant signaling proteins or their decoys. That implies that it is not the pathogen derived effector itself that is recognized, but its activity in the plant cell. These effectors' activities (proteolytic cleavage, phosphorylation, acetylation, urydilylation and etc.) are well conserved in a variety of pathogens. This brings us to idea of engineering universal receptors for multiple effectors from a variety of kingdoms based just on their activity in the plant cell.

In recent pioneering research it was shown that an R protein which normally recognizes a bacterial effector, can be engineered to also recognize the activity of a plant virus component. In this particular case both the bacterial AvrPphB and viral NIa protease function by cleaving their target proteins based on the peptide sequence; this allowed the switching of Arabidopsis NLR RPS5 from one form to another via changing the cleavage site in its guarded decoy PBS1 (Kim et al., 2016). Based on this, it seems a promising strategy to develop universal receptors against the variety of effectors from different pathogens.

In order to be able to engineer such a receptor, in-depth knowledge of how plant immunity and pathogen effectors function needs to be revealed. Extensive research should be carried out to identify the effector targets in the plant cell as well as the effector activity on these targets. Ultimately, this knowledge will lead researchers to engineer a few receptors covering most of the pathogen resistance for important crop species, rather than trying to deploy the whole pool of known NLRs against known pathogen effectors.

5.1 General conclusions from a detailed study of MR5-RIN4 system

The recently discovered *MR5 R* gene from hybrid apple *Malus* x *robusta* 5 was shown to recognize the AvrRpt2 effector from *E. amylovora* (Broggini et al., 2014; Fahrentrapp et al., 2013; Vogt et al., 2013), suggesting a typical gene for gene interaction. No further details of how this recognition occurs were available prior to the research conducted in the current thesis. The extensively studied RPS2-RIN4 system (Afzal et al., 2011; Afzal et al., 2013; Belkhadir et al., 2004; Day et al., 2005; Mackey et al., 2003) from *A. thaliana*, that recognizes AvrRpt2 from *P. syringae,* was used to gain insights into MR5 function in apple.

RIN4 is necessary in *A. thaliana* for correct RPS2 functioning towards AvrRpt2 recognition. In particular, RIN4 is responsible for the suppression of RPS2 immunity signaling in the absence of AvrRpt2 effector and it was further shown that direct cleavage of RIN4 by AvrRpt2 leads to RPS2-mediated immunity (Day et al., 2005).

Interestingly RIN4 acts as a one of the links between PTI and ETI branches of plant immunity. In a resting state RIN4 is residually phosphorylated at S141 and T166. The PTI component comprising the FLS2-mediated recognition of flagella and EFR-mediated recognition of bacterial Ef-tu lead to accumulation of RIN4 with phosphorylated S141, which in turn leads to a further relay and amplification for downstream PTI-signaling. During the co-evolutionary arms race invading bacteria gained AvrB and AvrRpm1 effectors which effectively hijack the plant RIPK to increase phosphorylation of RIN4 at T166, shifting the RIN4 back into resting state to suppress PTI. In response to that, plants evolved the RPM1 NLR protein which monitors the RIN4 T166 state and in case of its over phosphorylation leads to ETI immune response (Chung et al., 2014).

In addition, plant ROC1 proline isomerization activity was shown to play an important role in maintaining correct RIN4 conformation, allowing for maintenance of the RPM1 and RPS2 suppressed resting state. Of particular interest is the fact that the same ROC1-mediated activity is required for AvrRpt2-self processing and activation in the plant cell, which leads to RIN4 elimination and RPS2-mediated immunity (Li et al., 2014). It is plausible to suggest that AvrRpt2 might have been evolved to both hijack the ROC1 activity important for RPM1 immunity and elimination of RIN4 to perturb the normal PTI response.

Both of the abovementioned points illustrate that RIN4 is an important target and a signaling hub around which the plant immunity components and bacterial effectors evolve in the 'arms race' between the pathogen and its host.

Based on the particular importance of RIN4 for AvrRpt2 recognition in Arabidopsis, MR5 was speculated to require RIN4 too, and this was clearly shown via transient expression experiments in *N. benthamiana*. Interestingly, MR5 overexpression, in contrast to RPS2, did not result in any autoimmunity, proposing a different model of activation by AvrRpt2. This well-established MR5 recognition system allowed me to test the importance of several MR5 canonical domains for its function and validated it as a typical member of the CC-NB-LRR family (subchapters 3.2.2 and 3.2.5).

Further dissection of the MR5 system led to the finding that only cleavage product 3 (CLV3) of essentially apple RIN4 homologs (or very close relatives) is required and sufficient for MR5 activation (subchapter 3.2.2 and 3.2.7). This is a novel NLR activation model which also relies on RIN4 as an effector target, yet different from well-studied RPM1 and RPS2 systems. Of particular interest is the fact that MR5 does not need RIN4 for maintaining the resting state and only activates the immune signaling in the presence of specific RIN4 cleavage product.

Finally, it was shown that RIN4 homologs from apple and *A. thaliana* have different abilities to suppress unrelated autoimmune R proteins (subchapter 3.2.6). These lines of evidence pointed to the strict requirement of certain RIN4 homologs to function with certain R proteins.

5.2 Evidence supporting co-evolution of guarded proteins with their cognate NLRs

The 'arms race' concept stating the co-evolution of pathogen invasion tools and plant immunity components is one of the most important concepts in contemporary plant pathology. It can be clearly illustrated by the examples of plant receptors directly binding their corresponding pathogen effectors. For instance, ATR1 effector from *Hyaloperonospora arabidopsidis* shows significant variation among the pathogen strains. Furthermore, the corresponding NLR, RPP1 from Arabidopsis recognizing this effector, shows high level of variation (Krasileva et al., 2010; Rehmany et al., 2005). This RPP1 variation defines the recognition spectrum of the specific *RPP1* allele: for example, *RPP1-NdA* (from the Niederzenz ecotype)

and *RPP1-WsB* (from the Wassilewskija ecotype), where *RPP1-NdA* recognizes a smaller subset of the *ATR1* alleles recognized by *RPP1-WsB*. It was further shown that that most diversified domain of RPP1 was LLR-domain and the direct interaction between NLR and its effector is crucial for immune signaling (Krasileva et al., 2010). Interestingly, the *Hpa* Cala2 *ATR1* allele was not recognized by naturally occurring *RPP1* alleles and artificial evolution of *RPP1* successfully led to generation of the novel allele capable of this recognition (Steinbrenner et al., 2015).

Another effector from the same pathogen is ATR13, and it was also shown to be highly polymorphic among the pool of pathogen strains and to be recognized by *RPP13* alleles which are under strong selection pressure (Bakker et al., 2006; Rose et al., 2004). It was further demonstrated that one version of the *RPP13* allele can only recognize the *ATR13* alleles from the same phylogenetic clade (Hall et al., 2009).

Rust flax effector AvrL567 shows a high level of amino acid polymorphism and is proposed to be under strong selective pressure (Dodds et al., 2006). Crystal structure studies revealed that most of the polymorphic residues are surface exposed and likely to participate in recognition by cognate R protein in the host plant (Wang et al., 2007). In agreement with the 'arms race' concept the *L* locus in flax is also shown to be under significant selective pressure harboring *L5* and *L6* alleles with specific recognition subsets of *AvrL567*, where *AvrL567-A* allele is recognized by *L5* and *L6*, but *AvrL567-D* allele only by *L6* (Dodds et al., 2006).

The NLRs which are activated indirectly are also products of evolution under the pathogen effector pressure. As mentioned in chapter 5.1, they seem to evolve alongside their guarded proteins, for example RIN4. RIN4 homologs are widespread in plants. They are highly diversified proteins and usually have one or two conserved regions surrounding RCS1 and RCS2. There is only one functional RIN4 homolog in Arabidopsis known to date, which plays a major role in regulating both PTI and ETI branches of plant immunity. However, there are several more NOI-domain containing proteins in Arabidopsis, but no function was defined for them (Takemoto & Jones, 2005). In contrast, soybean has 4 RIN4 homologs identified and, similarly to Arabidopsis, they are targeted by AvrB and AvrRpm1 effectors from *Pseudomonas syringae*. RIN4 homologs in soybean are guarded by

Rpg1b and Rpg1r NLR proteins, which specifically confer resistance to AvrB and AvrRpm1 respectively (Ashfield et al., 2014; Kessens et al., 2014).

Another example of RIN4 function is its involvement in hybrid incompatibility in lettuce. Two species, *Lactuca sativa* and *Lactuca saligna*, are known to generate progeny with hybrid incompatibility symptoms. Two loci have been shown to be involved and one of them is a RIN4 homolog. It was shown that the *L. saligna* variant of RIN4 homolog triggers necrosis in plants carrying the other incompatibility locus. Interestingly, there are three amino acid differences responsible for that phenotype and they all are located in the C-terminal half of *L. saligna* RIN4 (Jeuken et al., 2009).

The examples described above prompt the speculation that RIN4 is a flexible guardee, functioning together with different *R* genes in different plant species. In addition, the mentioned research in lettuce and soybean imply the importance of certain RIN4 amino acid residues for correct functioning with corresponding R proteins and tight links between them.

In the current research, it was found that two polymorphisms in a critical region of RIN4 can affect both suppression and activation abilities in relation to different NLRs (subchapters 3.2.10 and 3.2.12). In addition, swapping domains of different RIN4 in chimeric protein variants significantly perturbed their functionality. This observation further supports that RIN4 homologs of plant species are very tightly linked to the NLRs in the given plant and their properties.

Based on the aforementioned observations, it can be proposed that not only NLR proteins adapt to the genetic environment in their respective species, but also the guarded proteins like RIN4 may adapt to the *NLR* genes present in the plant species. One can suspect that MdRIN4 has a reduced ability to suppress NLR-triggered autoactivity due to the absence of evolutionary pressure from autoactivity in its NLR guard protein – MR5. In contrast, AtRIN4 has evolved a strong NLR suppressing ability in order to keep RPS2 and RPM1 autoactivity tightly regulated until pathogens, carrying a corresponding effector, release it.

It is plausible to speculate that a plant species with a RIN4 homolog carrying an MR5-activating pattern of polymorphisms would likely carry a non-autoimmune NLR(s). Conversely, a plant with a RIN4 homolog carrying an RPS2-suppressing pattern would be more likely to harbor autoimmune NLRs. This speculation is further supported by the fact that MR5 can be activated by AvrRpt2-

mediated RIN4 cleavage in closely related *Pyrus pyrifolia* and *Pyrus ussuriensis*. In agreement with our hypothesis, RIN4 homologs in these species have an MR5-activating pattern of critical polymorphisms.

5.3 Significance and future directions of the MR5-RIN4 system research

Research in the current thesis revealed the similar yet different mechanism of recognition of AvrRpt2 effector by R proteins (RPS2 and MR5) from distant plant species. These proteins are members of the same family of CNL proteins but they do not share significant homology, so they seem to have evolved independently. This adds up to the current knowledge of RPS2-RIN4 and RPS5-PBS1 systems, as a similar but yet mechanistically distinct independently evolved R protein/guardee system and expands general understanding of indirect recognition of effectors theory.

The most of current understanding of RIN4 functions is based on research performed in *A. thaliana*. However some research was carried out in soybean, showing the requirement of RIN4 for RPG1-dependant resistance (Ashfield et al., 2014; Kessens et al., 2014; Selote & Kachroo, 2010), as well as a role for RIN4 in suppression of unknown R protein suppression in hybrid lettuce plants (*L. sativa* x *L. saligna*) was proposed (Jeuken et al., 2009). The bioinformatic-based study by Afzal et al, 2013, validated RIN4 homologs in a diversity of plant species and proposed the importance of conserved NOI domains (Afzal et al., 2013).

Based on that one of the future directions for this research would be further comparative analysis of RIN4 homologs from a variety of plant species. It is planned to create a library of RIN4 homologs and test if they show suppression of the known autoimmune R proteins, as well as activation of known non-autoimmune R proteins in the presence of a variety of RIN4 targeting effectors. The results obtained from this prospective screening for suppression/activation of R proteins can be coupled with RIN4 proteins sequence data, as well as structure predictions, to elucidate the functions of RIN4 protein regions and finally decipher the precise function of this protein in plant physiology and defense.

Another future direction branching from the current research could be engineering of MR5 as a universal receptor for different effectors from distant pathogens. It was shown in the RPS5-PBS1 system that switching effector recognition is possible. MR5 seems like a promising candidate for similar work as

it is non-autoimmune, even when overexpressed at high levels and its activation mechanisms by RIN4 CLV3 were dissected in the current thesis. Future experiments can include swapping the native cleavage site in RIN4 for other proteolytic effectors cleavage sites and testing if the recognition by MR5 extends for these new proteolytic effectors.

5.4 General conclusions from *V. inaequalis* prospective effector genes research

The key knowledge required for mounting ETI for plant protection is elucidating the *R* genes responsible for resistance from the side of the plants and elucidating the effectors, which trigger the resistance response. Further functional studies of the effectors are required for advanced resistance engineering. The aim of the *V. inaequalis* effector research carried out in the current thesis was to mine for prospective *V. inaequalis* effector genes, as none of them were cloned to date.

Certain difficulties with genetic manipulation with *V. inaequalis* led to using the artificial bacterial-based systems to deliver the prospective fungal and oomycete effectors into host plant. This approach is a promising strategy for fungal and oomycete effector research as shown by Sohn et al., 2007. In this study, authors could achieve sufficient delivery of ATR1 and ATR13 effectors of *Hpa* via T3SS of *Pseudomonas syringae* DC3000 and further virulence increase of this bacterium on Arabidopsis was shown (Sohn et al., 2007).

In another study it was shown that effectors identified in *Puccinia graminis* f. sp. *tritici* can be also efficiently delivered via artificial T3SS of *Pseudomonas fluorescens,* leading to immune response in wheat cultivars carrying the corresponding *R* loci (Upadhyaya et al., 2013).

Unfortunately, not all the eukaryotic effectors are predicted to be efficiently delivered by bacterial systems, this can be due to absence of intron processing and appropriate protein modifications in bacterial cell. To address that, researchers need to develop the reliable eukaryotic based effector delivery systems. The first report to show such effector delivery is possible by transformed *U. maydis* into maize was published recently (Presti et al., 2017). This and further research in the field would help to identify the appropriate system for *V. inaequalis* prospective effector delivery in the future research.

The whole genome sequencing and RNAseq data of *V. inaequalis* became available recently (Deng et al., 2017). The preliminary draft genome was used earlier to identify the prospective effector gene candidates at J. Bowen research group, PFR, Mt. Albert, NZ. These data were used in the current thesis for sequence validation and functional analysis of previously mapped *AvrRvi8* gene candidates, as well as novel bioinformatically predicted *V. inaequalis* candidate effector (ViCE) genes.

12 independent candidates of *AvrRvi8* gene, found across the whole genome sequence were sequence validated based on PCR amplification of *V. inaequalis* cDNA (subchapter 4.2.1). Two approaches to validate the recognition of *AvrRvi8* top candidate in the resistant apple plants (carrying *Rvi8* loci) were used. Transient expression of the candidate genes via particle bombardment transformation (Biolistics) of the detached leaves did not provide sufficient levels of protein expression (subchapter 4.2.2). As an alternative, the bacterial T3SS based delivery of the AvrRvi8 effector candidates using *P. fluorescens* was carried out. The AvrRvi8-7 candidate did not trigger any macroscopic response when delivered by *P. fluorescens* (subchapter 4.2.3). In addition, the ability of the AvrRvi8-7 to trigger a non-host response, when overexpressed in the *N. benthamiana* and *N. tabacum* leaves was assessed and showed no macroscopic response (subchapter 4.2.2).

The 22 strongest *ViCE* genes were chosen for sequence and functional analysis. Sequence analysis of *ViCE* amplified from *V. inaequalis* cDNA showed that 17 of them are identical to their prediction *in silico* (subchapter 4.2.4). They were further overexpressed in *N. benthamiana* leaves and the development of a macroscopic response was assessed (subchapter 4.2.4). As none of them elicited any visible response, their ability to suppress ETI signaling induced by well-characterized R proteins and effectors was assessed (subchapter 4.2.4). Certain ETI attenuation was observed for ViCE2, ViCE11, ViCE12 and ViCE14 when expressed with either RPS2 or HopAS1 (subchapter 4.2.4).

5.5 Significance and future directions of the *V. inaequalis* prospective effector genes research

As a result of the current research, a library of prospective *AvrRvi8* gene candidate constructs was created. In addition, a construct library of *ViCE* genes was created. These can be very useful materials for further *V. inaequalis* effector

research. These constructs can be used for generating the *V. inaequalis* effector knock-out lines and for further testing on various apple cultivars.

Future experiments for *AvrRvi8* elucidation include the protein expression validation of the AvrRvi8 candidates, when expressed in non-host *N. benthamiana* and *N. tabacum*. In addition, the inability of AvrRvi8-7 to elicit any response when delivered via *P. fluorescens* T3SS can be explained by the PTI response against the mentioned bacterium. This can be addressed by using the *P. syringae* or *E. amylovora* strains, naturally virulent towards apple and pears, to deliver the AvrRvi8 candidates. Then development of PCD, plant defense related gene expression and bacterial growth restriction can be assessed to make the conclusion about AvrRvi8 recognition.

Protein expression of ViCE candidates in non-host *N. benthamiana* and *N. tabacum* should be confirmed via immunoblotting. Then the ETI attenuation results obtained in the current study should be revalidated several more times to ensure reproducibility and, in addition, more precise ion leakage measurement methods can be applied to quantify the PCD symptoms attenuation. The construct libraries generated in the current research can be used to create effector knock-out lines of *V. inaequalis* for further validation of their function. In addition, *ViCE* genes can be sub-cloned into broad-host delivery vectors for consequent delivery via bacterial T3SS of the *P. syringae* strains naturally virulent on apple and pears.

In conclusion, this thesis sought to research the molecular mechanisms leading to avirulence to two different pathogens, *E. amylovora* and *V. inaequalis.* Ultimately aiming to identify R genes amenable to engineering, the scope of this project encompassed an R protein from apple recognizing a well-known bacterial effector as well as mining for avirulence to fungal effectors in both the host plant, apple, and non-host *Nicotiana* spp. The rationale for this search is that immunity triggered by a pathogen is often effective against a cross-kingdom spectrum of other invasive organisms. The molecular mechanisms required for R-Avr pairs from a large number of agriculturally important crops and their pathogens may be applicable in future work resulting from the discoveries in this thesis.

While the MR5-AvrRpt2 system has been elucidated more in depth, considerable work on AvrRvi8 candidates as well as avirulent ViCEs remains to be undertaken. Identification of AvrRvi8 will significantly advance progress towards

discovery of Rvi8 and its mechanism of action, opening avenues towards engineering a more robust immune response than currently available. Simultaneously, discovery of avirulence ViCEs in non-host plants allows manipulation of the R genes present there to confer novel resistance introduction to apple plants. The findings herein coupled with the potential for future development will move growers, breeders and researchers closer towards developing durable resistance in a crop species important to New Zealand.

References

Aarts, N., Metz, M., Holub, E., Staskawicz, B. J., Daniels, M. J., & Parker, J. E. (1998). Different requirements for *EDS1* and *NDR1* by disease resistance genes define at least two *R* gene-mediated signaling pathways in *Arabidopsis*. *Proceedings of the National Academy of Sciences of the United States of America, 95*(17), 10306-10311.

Abramovitch, R. B., Janjusevic, R., Stebbins, C. E., & Martin, G. B. (2006). Type III effector AvrPtoB requires intrinsic E3 ubiquitin ligase activity to suppress plant cell death and immunity. *Proceedings of the National Academy of Sciences of the United States of America, 103*(8), 2851-2856.

Ade, J., DeYoung, B. J., Golstein, C., & Innes, R. W. (2007). Indirect activation of a plant nucleotide binding site-leucine-rich repeat protein by a bacterial protease. *Proceedings of the National Academy of Sciences of the United States of America, 104*(7), 2531-2536.

Afzal, A. J., da Cunha, L., & Mackey, D. (2011). Separable fragments and membrane tethering of *Arabidopsis* RIN4 regulate its suppression of PAMP-triggered immunity. *The Plant Cell, 23*(10), 3798-3811.

Afzal, A. J., Kim, J. H., & Mackey, D. (2013). The role of NOI-domain containing proteins in plant immune signaling. *BMC Genomics, 14*, 327.

Albert, I., Bohm, H., Albert, M., Feiler, C. E., Imkampe, J., Wallmeroth, N., Brancato, C., Raaymakers, T. M., Oome, S., Zhang, H., Krol, E., Grefen, C., Gust, A. A., Chai, J., Hedrich, R., Van den Ackerveken, G., & Nurnberger, T. (2015). An RLP23-SOBIR1-BAK1 complex mediates NLP-triggered immunity. *Nature Plants, 1*, 15140.

Alfano, J. R., & Collmer, A. (2004). Type III secretion system effector proteins: double agents in bacterial disease and plant defense. *Annual Review of Phytopathology, 42*, 385-414.

Anderson, P. A., Lawrence, G. J., Morrish, B. C., Ayliffe, M. A., Finnegan, E. J., & Ellis, J. G. (1997). Inactivation of the flax rust resistance gene *M* associated with loss of a repeated unit within the leucine-rich repeat coding region. *The Plant Cell, 9*(4), 641-651.

Armstrong, M. R., Whisson, S. C., Pritchard, L., Bos, J. I., Venter, E., Avrova, A. O., Rehmany, A. P., Bohme, U., Brooks, K., Cherevach, I., Hamlin, N., White, B., Fraser, A., Lord, A., Quail, M. A., Churcher, C., Hall, N., Berriman, M., Huang, S., Kamoun, S., Beynon, J. L., & Birch, P. R. (2005). An ancestral oomycete locus contains late blight avirulence gene *Avr3a*, encoding a protein that is recognized in the host cytoplasm. *Proceedings of the National Academy of Sciences of the United States of America, 102*(21), 7766-7771.

Ashfield, T., Redditt, T., Russell, A., Kessens, R., Rodibaugh, N., Galloway, L., Kang, Q., Podicheti, R., & Innes, R. W. (2014). Evolutionary relationship of disease resistance genes in soybean and Arabidopsis specific for the *Pseudomonas syringae* effectors AvrB and AvrRpm1. *Plant Physiology, 166*(1), 235-251.

Axtell, M. J., Chisholm, S. T., Dahlbeck, D., & Staskawicz, B. J. (2003). Genetic and molecular evidence that the *Pseudomonas syringae* type III effector protein AvrRpt2 is a cysteine protease. *Molecular Microbiology, 49*(6), 1537-1546.

Axtell, M. J., McNellis, T. W., Mudgett, M. B., Hsu, C. S., & Staskawicz, B. J. (2001). Mutational analysis of the *Arabidopsis RPS2* disease resistance gene and the corresponding pseudomonas syringae *AvrRpt2* avirulence gene. *Molecular Plant-Microbe Interactions Journal, 14*(2), 181-188.

Axtell, M. J., & Staskawicz, B. J. (2003). Initiation of RPS2-specified disease resistance in Arabidopsis is coupled to the AvrRpt2-directed elimination of RIN4. *Cell, 112*(3), 369-377.

Ayliffe, M. A., Frost, D. V., Finnegan, E. J., Lawrence, G. J., Anderson, P. A., & Ellis, J. G. (1999). Analysis of alternative transcripts of the flax *L6* rust resistance gene. *Plant Journal, 17*(3), 287-292.

Bakker, E. G., Toomajian, C., Kreitman, M., & Bergelson, J. (2006). A genome-wide survey of *R* gene polymorphisms in *Arabidopsis*. *Plant Cell, 18*(8), 1803-1818.

Bakshi, M., & Oelmuller, R. (2014). WRKY transcription factors: Jack of many trades in plants. *Plant Signaling & Behavior, 9*(2), e27700.

Bauer, R., Oberwinkler, F., & Vánky, K. (1997). Ultrastructural markers and systematics in smut fungi and allied taxa. *Canadian Journal of Botany, 75*(8), 1273-1314.

Belfanti, E., Silfverberg-Dilworth, E., Tartarini, S., Patocchi, A., Barbieri, M., Zhu, J., Vinatzer, B. A., Gianfranceschi, L., Gessler, C., & Sansavini, S. (2004). The *HcrVf2* gene from a wild apple confers scab resistance to a transgenic cultivated variety. *Proceedings of the National Academy of Sciences of the United States of America, 101*(3), 886-890.

Belkhadir, Y., Nimchuk, Z., Hubert, D. A., Mackey, D., & Dangl, J. L. (2004). Arabidopsis RIN4 negatively regulates disease resistance mediated by RPS2 and RPM1 downstream or independent of the NDR1 signal modulator and is not required for the virulence functions of bacterial type III effectors AvrRpt2 or AvrRpm1. *The Plant Cell, 16*(10), 2822-2835.

Benaouf, G., & Parisi, L. (2000). Genetics of Host-Pathogen Relationships Between *Venturia inaequalis* Races 6 and 7 and *Malus* Species. *Phytopathology, 90*(3), 236-242.

Bendahmane, A., Farnham, G., Moffett, P., & Baulcombe, D. C. (2002). Constitutive gain-of-function mutants in a nucleotide binding site-leucine rich repeat protein encoded at the *Rx* locus of potato. *Plant Journal, 32*(2), 195-204.

Bent, A. F., Kunkel, B. N., Innes, R. W., & Staskawicz, B. J. (1993). Use of *Arabidopsis thaliana* and *Pseudomonas syringae* in the study of plant disease resistance and tolerance. *Journal of Nematology, 25*(4), 519-525.

Bigeard, J., Colcombet, J., & Hirt, H. (2015). Signaling mechanisms in pattern-triggered immunity (PTI). *Molecular Plant, 8*(4), 521-539.

Birnboim, H. C., & Doly, J. (1979). A rapid alkaline extraction procedure for screening recombinant plasmid DNA. *Nucleic Acids Research, 7*(6), 1513-1523.

Boch, J., & Bonas, U. (2010). *Xanthomonas* AvrBs3 family-type III effectors: discovery and function. *Annual Review of Phytopathology, 48*, 419-436.

Boch, J., Bonas, U., & Lahaye, T. (2014). TAL effectors-pathogen strategies and plant resistance engineering. *New Phytologist, 204*(4), 823-832.

Boch, J., Scholze, H., Schornack, S., Landgraf, A., Hahn, S., Kay, S., Lahaye, T., Nickstadt, A., & Bonas, U. (2009). Breaking the code of DNA binding specificity of TAL-type III effectors. *Science, 326*(5959), 1509-1512.

Bohnert, H. U., Fudal, I., Dioh, W., Tharreau, D., Notteghem, J. L., & Lebrun, M. H. (2004). A putative polyketide synthase/peptide synthetase from *Magnaporthe grisea* signals pathogen attack to resistant rice. *The Plant Cell, 16*(9), 2499-2513.

Boone, D. M. (1971). Genetics of *Venturia Inaequalis*. *Annual Review of Phytopathology, 9*(1), 297-318.

Botella, M. A., Parker, J. E., Frost, L. N., Bittner-Eddy, P. D., Beynon, J. L., Daniels, M. J., Holub, E. B., & Jones, J. D. (1998). Three genes of the *Arabidopsis* RPP1 complex resistance locus recognize distinct *Peronospora parasitica* avirulence determinants. *The Plant Cell, 10*(11), 1847-1860.

Boudsocq, M., Willmann, M. R., McCormack, M., Lee, H., Shan, L., He, P., Bush, J., Cheng, S. H., & Sheen, J. (2010). Differential innate immune signalling via Ca(2+) sensor protein kinases. *Nature, 464*(7287), 418-422.

Boukema, I. W. (1981). Races of *Cladosporium fulvum* Cke. (*Fulvia fulva*) and genes for resistance in the tomato (*Lycopersicon* Mill.). *Genetics and breeding of tomato: proceedings of the meeting of the Eucarpia Tomato Working Group, Avignon-France, May 18-21, 1981*.

Boutte, Y., Vernhettes, S., & Satiat-Jeunemaitre, B. (2007). Involvement of the cytoskeleton in the secretory pathway and plasma membrane organisation of higher plant cells. *Cell Biology International, 31*(7), 649-654.

Bowen, J. K., Mesarich, C. H., Bus, V. G., Beresford, R. M., Plummer, K. M., & Templeton, M. D. (2011). *Venturia inaequalis*: the causal agent of apple scab. *Molecular Plant Pathology, 12*(2), 105-122.

Boyer, H. W., & Roulland-Dussoix, D. (1969). A complementation analysis of the restriction and modification of DNA in *Escherichia coli*. *Journal of Molecular Biology, 41*(3), 459-472.

Broggini, G. A., Bus, V. G., Parravicini, G., Kumar, S., Groenwold, R., & Gessler, C. (2011). Genetic mapping of 14 avirulence genes in an EU-B04 x 1639 progeny of *Venturia inaequalis*. *Fungal Genetics and Biology, 48*(2), 166-176.

Broggini, G. A., Duffy, B., Holliger, E., Schärer, H. J., Gessler, C., & Patocchi, A. (2005). Detection of the fire blight biocontrol agent *Bacillus subtilis* BD170 (Biopro®) in a Swiss apple orchard. *European Journal of Plant Pathology, 111*(2), 93-100.

Broggini, G. A., Wohner, T., Fahrentrapp, J., Kost, T. D., Flachowsky, H., Peil, A., Hanke, M. V., Richter, K., Patocchi, A., & Gessler, C. (2014). Engineering fire blight resistance into the apple cultivar 'Gala' using the *FB_MR5* CC-NBS-LRR resistance gene of *Malus* x *robusta* 5. *Plant Biotechnology Journal, 12*(6), 728-733.

Brueggeman, R., Druka, A., Nirmala, J., Cavileer, T., Drader, T., Rostoks, N., Mirlohi, A., Bennypaul, H., Gill, U., Kudrna, D., Whitelaw, C., Kilian, A., Han, F., Sun, Y., Gill, K., Steffenson, B., & Kleinhofs, A. (2008). The stem rust resistance gene *RPG5* encodes a protein with nucleotide-binding-site, leucine-rich, and protein kinase domains. *Proceedings of the National Academy of Sciences of the United States of America, 105*(39), 14970-14975.

Bryan, G. T., Wu, K. S., Farrall, L., Jia, Y., Hershey, H. P., McAdams, S. A., Faulk, K. N., Donaldson, G. K., Tarchini, R., & Valent, B. (2000). A single amino acid difference distinguishes resistant and susceptible alleles of the rice blast resistance gene *Pi-ta*. *The Plant Cell, 12*(11), 2033-2046.

Buell, C. R., Joardar, V., Lindeberg, M., Selengut, J., Paulsen, I. T., Gwinn, M. L., Dodson, R. J., Deboy, R. T., Durkin, A. S., Kolonay, J. F., Madupu, R., Daugherty, S., Brinkac, L., Beanan, M. J., Haft, D. H., Nelson, W. C., Davidsen, T., Zafar, N., Zhou, L., Liu, J., Yuan, Q., Khouri, H., Fedorova, N., Tran, B., Russell, D., Berry, K., Utterback, T., Van Aken, S. E., Feldblyum, T. V., D'Ascenzo, M., Deng, W. L., Ramos, A. R., Alfano, J. R., Cartinhour, S., Chatterjee, A. K., Delaney, T. P., Lazarowitz, S. G., Martin, G. B., Schneider, D. J., Tang, X., Bender, C. L., White, O., Fraser, C. M., & Collmer, A. (2003). The complete genome sequence of the Arabidopsis and tomato pathogen *Pseudomonas syringae* pv. *tomato* DC3000. *Proceedings of the National Academy of Sciences of the United States of America, 100*(18), 10181-10186.

Burdon, J. J., & Thrall, P. H. (2003). The fitness costs to plants of resistance to pathogens. *Genome Biology, 4*(9), 227.

Burrill, T. J., Arthur, J. C., & Waite, M. B. (2003). *Fire blight: the foundation of phytobacteriology*: APS Press.

Bus, V. G. (2006). *Differential host-pathogen interactions of Venturia inaequalis and Malus.* (Doctoral thesis), University of Auckland, New Zealand.

Bus, V. G., Bassett, H. C., Bowatte, D., Chagné, D., Ranatunga, C. A., Ulluwishewa, D., Wiedow, C., & Gardiner, S. E. (2010). Genome mapping of an apple scab, a powdery mildew and a woolly apple aphid resistance gene from open-pollinated Mildew Immune Selection. *Tree Genetics & Genomes, 6*(3), 477-487.

Bus, V. G., Laurens, F. N., van de Weg, W. E., Rusholme, R. L., Rikkerink, E. H., Gardiner, S. E., Bassett, H. C., Kodde, L. P., & Plummer, K. M. (2005a). The *Vh8* locus of a new gene-for-gene interaction between *Venturia inaequalis* and the wild apple *Malus sieversii* is closely linked to the *Vh2* locus in *Malus pumila* R12740-7A. *New Phytologist, 166*(3), 1035-1049.

Bus, V. G., Ranatunga, C., Gardiner, S. E., Bssett, H., & Rikkerink, E. H. (2000). Marker assisted selection for pest and disease resistance in the New Zealand apple breeding programme. *Acta Horticulturae, 538*(95), 541-547.

Bus, V. G., Rikkerink, E. H., Caffier, V., Durel, C. E., & Plummer, K. M. (2011). Revision of the nomenclature of the differential host-pathogen interactions of *Venturia inaequalis* and *Malus*. *Annual Review of Phytopathology, 49*, 391-413.

Bus, V. G., Rikkerink, E. H., Van de Weg, E., Rusholme, R. L., & Gardiner, S. E. (2005b). The *Vh2* and *Vh4* scab resistance genes in two differential hosts derived from Russian apple R12740-7A map to the same linkage group of apple. *Molecular Breeding, 15*(103), 16.

Buscaill, P., & Rivas, S. (2014). Transcriptional control of plant defence responses. *Current Opinion in Plant Biology, 20*, 35-46.

Buttner, D. (2012). Protein export according to schedule: architecture, assembly, and regulation of type III secretion systems from plant- and animal-pathogenic bacteria. *Microbiology and Molecular Biology Reviews, 76*(2), 262-310.

Caffier, V., Patocchi, A., Expert, P., Bellanger, M. N., Durel, C. E., Hilber-Bodmer, M., Broggini, G. A., Groenwold, R., & Bus, V. G. (2014). Virulence Characterization of *Venturia inaequalis* reference isolates on the differential set of *Malus* hosts. *Plant Disease, 99*(3), 370-375.

Carisse, O., & Bernier, J. (2002). *Microsphaeropsis ochracea sp*. nov. associated with dead apple leaves. *Mycologia, 94*(2), 297-301.

Chang, J. H., Tai, Y. S., Bernal, A. J., Lavelle, D. T., Staskawicz, B. J., & Michelmore, R. W. (2002). Functional analyses of the *Pto* resistance gene family in tomato and the identification of a minor resistance determinant in a susceptible haplotype. *Molecular Plant-Microbe Interactions Journal, 15*(3), 281-291.

Chen, Z., Agnew, J. L., Cohen, J. D., He, P., Shan, L., Sheen, J., & Kunkel, B. N. (2007). *Pseudomonas syringae* type III effector AvrRpt2 alters *Arabidopsis thaliana* auxin physiology. *Proceedings of the National Academy of Sciences of the United States of America, 104*(50), 20131-20136.

Cheng, W., Munkvold, K. R., Gao, H., Mathieu, J., Schwizer, S., Wang, S., Yan, Y. B., Wang, J., Martin, G. B., & Chai, J. (2011). Structural analysis of *Pseudomonas syringae* AvrPtoB bound to host BAK1 reveals two similar kinase-interacting domains in a type III effector. *Cell Host Microbe, 10*(6), 616-626.

Cheong, M. S., Kirik, A., Kim, J. G., Frame, K., Kirik, V., & Mudgett, M. B. (2014). AvrBsT acetylates Arabidopsis ACIP1, a protein that associates with microtubules and is required for immunity. *PLOS Pathogens, 10*(2), e1003952.

Chevalier, M., Bernard, C., Tellier, M., Audrain, C., & Durel, C. E. (2004). *Host and non-host interaction of Venturia inaequalis and Venturia pirina on Pyrus communis and Malus x domestica*.

Chevalier, M., & Parisi, L. (2000). Expression of Golden Delicious resistance to race 7 of *Venturia inaequalis*. *IOBC-WPRS Bulletin, 23*(12), 239–244.

Chinchilla, D., Bauer, Z., Regenass, M., Boller, T., & Felix, G. (2006). The Arabidopsis receptor kinase FLS2 binds flg22 and determines the specificity of flagellin perception. *The Plant Cell, 18*(2), 465-476.

Chinchilla, D., Zipfel, C., Robatzek, S., Kemmerling, B., Nurnberger, T., Jones, J. D., Felix, G., & Boller, T. (2007). A flagellin-induced complex of the receptor FLS2 and BAK1 initiates plant defence. *Nature, 448*(7152), 497-500.

Chisholm, S. T., Coaker, G., Day, B., & Staskawicz, B. J. (2006). Host-microbe interactions: shaping the evolution of the plant immune response. *Cell, 124*(4), 803-814.

Chisholm, S. T., Dahlbeck, D., Krishnamurthy, N., Day, B., Sjolander, K., & Staskawicz, B. J. (2005). Molecular characterization of proteolytic cleavage sites of the *Pseudomonas syringae* effector AvrRpt2. *Proceedings of the National Academy of Sciences of the United States of America, 102*(6), 2087-2092.

Chosed, R., Tomchick, D. R., Brautigam, C. A., Mukherjee, S., Negi, V. S., Machius, M., & Orth, K. (2007). Structural analysis of *Xanthomonas* XopD provides insights into substrate specificity of ubiquitin-like protein proteases. *The Journal of Biological Chemistry, 282*(9), 6773-6782.

Christie, P. J., Atmakuri, K., Krishnamoorthy, V., Jakubowski, S., & Cascales, E. (2005). Biogenesis, architecture, and function of bacterial type IV secretion systems. *Annual Review of Microbiology, 59*, 451-485.

Chung, E. H., da Cunha, L., Wu, A. J., Gao, Z., Cherkis, K., Afzal, A. J., Mackey, D., & Dangl, J. L. (2011). Specific threonine phosphorylation of a host target by two unrelated type III effectors activates a host innate immune receptor in plants. *Cell Host Microbe, 9*(2), 125-136.

Chung, E. H., El-Kasmi, F., He, Y., Loehr, A., & Dangl, J. L. (2014). A plant phosphoswitch platform repeatedly targeted by type III effector proteins regulates the output of both tiers of plant immune receptors. *Cell Host Microbe, 16*(4), 484-494. doi:10.1016/j.chom.2014.09.004

Clough, S. J., & Bent, A. F. (1998). Floral dip: a simplified method for *Agrobacterium*-mediated transformation of *Arabidopsis thaliana*. *Plant Journal, 16*(6), 735-743.

Coaker, G., Zhu, G., Ding, Z., Van Doren, S. R., & Staskawicz, B. (2006). Eukaryotic cyclophilin as a molecular switch for effector activation. *Molecular Microbiology, 61*(6), 1485-1496.

Collier, S. M., Hamel, L. P., & Moffett, P. (2011). Cell death mediated by the N-terminal domains of a unique and highly conserved class of NB-LRR protein. *Molecular Plant-Microbe Interactions Journal, 24*(8), 918-931.

Collier, S. M., & Moffett, P. (2009). NB-LRRs work a "bait and switch" on pathogens. *Trends in Plant Science, 14*(10), 521-529.

Cook, D. E., Mesarich, C. H., & Thomma, B. P. (2015). Understanding plant immunity as a surveillance system to detect invasion. *Annual Review of Phytopathology, 53*, 541-563.

Cooke, I. R., Jones, D., Bowen, J. K., Deng, C., Faou, P., Hall, N. E., Jayachandran, V., Liem, M., Taranto, A. P., Plummer, K. M., & Mathivanan, S. (2014). Proteogenomic analysis of the *Venturia pirina* (pear scab fungus) secretome reveals potential effectors. *Journal of Proteome Research, 13*(8), 3635-3644.

Cornelis, G. R., & Van Gijsegem, F. (2000). Assembly and function of type III secretory systems. *Annual Review of Microbiology, 54*, 735-774.

Couto, D., & Zipfel, C. (2016). Regulation of pattern recognition receptor signalling in plants. *Nature Reviews Immunology, 16*(9), 537-552.

Cui, F., Wu, S., Sun, W., Coaker, G., Kunkel, B., He, P., & Shan, L. (2013). The *Pseudomonas syringae* type III effector AvrRpt2 promotes pathogen virulence via stimulating *Arabidopsis* auxin/indole acetic acid protein turnover. *Plant Physiology, 162*(2), 1018-1029.

Dangl, J. L., Ritter, C., Gibbon, M. J., Mur, L. A., Wood, J. R., Goss, S., Mansfield, J., Taylor, J. D., & Vivian, A. (1992). Functional homologs of the Arabidopsis RPM1 disease resistance gene in bean and pea. *The Plant Cell, 4*(11), 1359-1369.

Day, B., Dahlbeck, D., Huang, J., Chisholm, S. T., Li, D., & Staskawicz, B. J. (2005). Molecular basis for the RIN4 negative regulation of RPS2 disease resistance. *The Plant Cell, 17*(4), 1292-1305.

Day, B., Dahlbeck, D., & Staskawicz, B. J. (2006). NDR1 interaction with RIN4 mediates the differential activation of multiple disease resistance pathways in Arabidopsis. *The Plant Cell, 18*(10), 2782-2791.

Day, B., Henty, J. L., Porter, K. J., & Staiger, C. J. (2011). The pathogen-actin connection: a platform for defense signaling in plants. *Annual Review of Phytopathology, 49*, 483-506.

Day, P. R., Boone, D. M., & Keitt, G. W. (1956). *Venturia inaequalis* (Cke.) Wint. XI. the chromosome number. *American Journal of Botany, 43*(10), 835-838.

Dayton, D. F., & Williams, E. B. (1968). Independent genes in *Malus* for resistance to *Venturia inaequalis*. *Proceedings of the American Society for Horticultural Science, 92*, 89-94.

de Jonge, R., van Esse, H. P., Kombrink, A., Shinya, T., Desaki, Y., Bours, R., van der Krol, S., Shibuya, N., Joosten, M. H., & Thomma, B. P. (2010). Conserved fungal LysM effector Ecp6 prevents chitin-triggered immunity in plants. *Science, 329*(5994), 953-955.

de Souza, T. A., Soprano, A. S., de Lira, N. P., Quaresma, A. J., Pauletti, B. A., Paes Leme, A. F., & Benedetti, C. E. (2012). The TAL effector PthA4 interacts with nuclear factors involved in RNA-dependent processes including a HMG protein that selectively binds poly(U) RNA. *PLoS One, 7*(2), e32305.

De Wit, I., Cook, N. C., & Keulemans, J. (2004). Characterization of tree architecture in two-year-old apple seedling populations of different progenies with a common columnar gene parent. *Acta Horticulturae, 663*, 363-368.

Deng, C. H., Plummer, K. M., Jones, D. A. B., Mesarich, C. H., Shiller, J., Taranto, A. P., Robinson, A. J., Kastner, P., Hall, N. E., Templeton, M. D., & Bowen, J. K. (2017). Comparative analysis of the predicted secretomes of *Rosaceae* scab pathogens *Venturia inaequalis* and *V. pirina* reveals expanded effector families and putative determinants of host range. *BMC Genomics, 18*(1), 339.

Deng, D., Yan, C., Pan, X., Mahfouz, M., Wang, J., Zhu, J. K., Shi, Y., & Yan, N. (2012). Structural basis for sequence-specific recognition of DNA by TAL effectors. *Science, 335*(6069), 720-723.

Deslandes, L., Olivier, J., Peeters, N., Feng, D. X., Khounlotham, M., Boucher, C., Somssich, I., Genin, S., & Marco, Y. (2003). Physical interaction between RRS1-R, a protein conferring resistance to bacterial wilt, and PopP2, a type

III effector targeted to the plant nucleus. *Proceedings of the National Academy of Sciences of the United States of America, 100*(13), 8024-8029.

Desveaux, D., Singer, A. U., Wu, A. J., McNulty, B. C., Musselwhite, L., Nimchuk, Z., Sondek, J., & Dangl, J. L. (2007). Type III effector activation via nucleotide binding, phosphorylation, and host target interaction. *PLOS Pathogens, 3*(3), e48.

DeYoung, B. J., & Innes, R. W. (2006). Plant NBS-LRR proteins in pathogen sensing and host defense. *Nature Immunology, 7*(12), 1243-1249.

DeYoung, B. J., Qi, D., Kim, S. H., Burke, T. P., & Innes, R. W. (2012). Activation of a plant nucleotide binding-leucine rich repeat disease resistance protein by a modified self protein. *Cellular Microbiology, 14*(7), 1071-1084.

Di, X., Gomila, J., Ma, L., Van den Burg, H. A., & Takken, F. L. (2016). Uptake of the *Fusarium* effector Avr2 by tomato is not a cell autonomous event. *Frontiers in Plant Science, 7*, 1915.

Diepold, A., & Wagner, S. (2014). Assembly of the bacterial type III secretion machinery. *FEMS Microbiology Reviews, 38*(4), 802-822.

Dinesh-Kumar, S. P., & Baker, B. J. (2000). Alternatively spliced N resistance gene transcripts: their possible role in tobacco mosaic virus resistance. *Proceedings of the National Academy of Sciences of the United States of America, 97*(4), 1908-1913.

Dinesh-Kumar, S. P., Tham, W. H., & Baker, B. J. (2000). Structure-function analysis of the tobacco mosaic virus resistance gene N. *Proceedings of the National Academy of Sciences of the United States of America, 97*(26), 14789-14794.

Dixon, M. S., Hatzixanthis, K., Jones, D. A., Harrison, K., & Jones, J. D. (1998). The tomato *Cf-5* disease resistance gene and six homologs show pronounced allelic variation in leucine-rich repeat copy number. *The Plant Cell, 10*(11), 1915-1925.

Dixon, M. S., Jones, D. A., Keddie, J. S., Thomas, C. M., Harrison, K., & Jones, J. D. (1996). The tomato *Cf-2* disease resistance locus comprises two functional genes encoding leucine-rich repeat proteins. *Cell, 84*(3), 451-459.

Djamei, A., Schipper, K., Rabe, F., Ghosh, A., Vincon, V., Kahnt, J., Osorio, S., Tohge, T., Fernie, A. R., Feussner, I., Feussner, K., Meinicke, P., Stierhof, Y. D., Schwarz, H., Macek, B., Mann, M., & Kahmann, R. (2011). Metabolic priming by a secreted fungal effector. *Nature, 478*(7369), 395-398.

Dodds, P. N., Lawrence, G. J., Catanzariti, A. M., Ayliffe, M. A., & Ellis, J. G. (2004). The *Melampsora lini AvrL567* avirulence genes are expressed in haustoria and their products are recognized inside plant cells. *The Plant Cell, 16*(3), 755-768.

Dodds, P. N., Lawrence, G. J., Catanzariti, A. M., Teh, T., Wang, C. I., Ayliffe, M. A., Kobe, B., & Ellis, J. G. (2006). Direct protein interaction underlies gene-for-gene specificity and coevolution of the flax resistance genes and flax rust avirulence genes. *Proceedings of the National Academy of Sciences of the United States of America, 103*(23), 8888-8893.

Dodds, P. N., & Rathjen, J. P. (2010). Plant immunity: towards an integrated view of plant-pathogen interactions. *Nature Reviews Genetics, 11*(8), 539-548.

Domingues, M. N., Campos, B. M., de Oliveira, M. L., de Mello, U. Q., & Benedetti, C. E. (2012). TAL effectors target the C-terminal domain of RNA polymerase II (CTD) by inhibiting the prolyl-isomerase activity of a CTD-associated cyclophilin. *PLoS One, 7*(7), e41553.

Dominguez-Ferreras, A., Kiss-Papp, M., Jehle, A. K., Felix, G., & Chinchilla, D. (2015). An overdose of the Arabidopsis coreceptor *BRASSINOSTEROID INSENSITIVE1-ASSOCIATED RECEPTOR KINASE1* or its ectodomain causes autoimmunity in a *SUPPRESSOR OF BIR1-1*-dependent Manner. *Plant Physiology, 168*(3), 1106-1121.

Dong, X., Mindrinos, M., Davis, K. R., & Ausubel, F. M. (1991). Induction of Arabidopsis defense genes by virulent and avirulent *Pseudomonas syringae* strains and by a cloned avirulence gene. *The Plant Cell, 3*(1), 61-72.

Dou, D., & Zhou, J. M. (2012). Phytopathogen effectors subverting host immunity: different foes, similar battleground. *Cell Host Microbe, 12*(4), 484-495.

Dowen, R. H., Engel, J. L., Shao, F., Ecker, J. R., & Dixon, J. E. (2009). A family of bacterial cysteine protease type III effectors utilizes acylation-dependent and -independent strategies to localize to plasma membranes. *The Journal of Biological Chemistry, 284*(23), 15867-15879.

Duffy, B., Schärer, H. J., Bünter, M., Klay, A., & Holliger, E. (2005). Regulatory measures against *Erwinia amylovora* in Switzerland. *EPPO Bulletin, 35*(2), 239-244.

Dunemann, F., & Egerer, J. (2010). A major resistance gene from Russian apple 'Antonovka' conferring field immunity against apple scab is closely linked to the *Vf* locus. *Tree Genetics & Genomes, 6*, 627-633.

Durel, C. E., Denance, C., & Brisset, M. N. (2009). Two distinct major QTL for resistance to fire blight co-localize on linkage group 12 in apple genotypes 'Evereste' and *Malus floribunda* clone 821. *Genome, 52*(2), 139-147.

Durel, C. E., van de Weg, E., Venisse, J. S., & Parisi, L. (2000). Localisation of a major gene for scab resistance on the European genetic map of the Prima x Fiesta cross. *IOBC-WPRS Bulletin, 23*(12), 245–248.

Ellis, J. G. (2016). Integrated decoys and effector traps: how to catch a plant pathogen. *BMC Biology, 14*, 13.

Ellis, J. G., Lawrence, G. J., Luck, J. E., & Dodds, P. N. (1999). Identification of regions in alleles of the flax rust resistance gene *L* that determine differences in gene-for-gene specificity. *The Plant Cell, 11*(3), 495-506.

Engler, C., Kandzia, R., & Marillonnet, S. (2008). A one pot, one step, precision cloning method with high throughput capability. *PLoS One, 3*(11), e3647.

Engler, C., & Marillonnet, S. (2013). Combinatorial DNA assembly using Golden Gate cloning. *Methods in Molecular Biology, 1073*, 141-156.

Engler, C., & Marillonnet, S. (2014). Golden Gate cloning. *Methods in Molecular Biology, 1116*, 119-131.

Erdin, N., Tartarini, S., Broggini, G. A., Gennari, F., Sansavini, S., Gessler, C., & Patocchi, A. (2006). Mapping of the apple scab-resistance gene *Vb*. *Genome, 49*(10), 1238-1245.

Eschen-Lippold, L., Jiang, X., Elmore, J. M., Mackey, D., Shan, L., Coaker, G., Scheel, D., & Lee, J. (2016). Bacterial AvrRpt2-Like cysteine proteases block activation of the Arabidopsis mitogen-activated protein kinases, MPK4 and MPK11. *Plant Physiology, 171*(3), 2223-2238.

Fabro, G., Steinbrenner, J., Coates, M., Ishaque, N., Baxter, L., Studholme, D. J., Korner, E., Allen, R. L., Piquerez, S. J., Rougon-Cardoso, A., Greenshields, D., Lei, R., Badel, J. L., Caillaud, M. C., Sohn, K. H., Van den Ackerveken, G., Parker, J. E., Beynon, J., & Jones, J. D. (2011). Multiple candidate effectors from the oomycete pathogen *Hyaloperonospora arabidopsidis* suppress host plant immunity. *PLOS Pathogens, 7*(11), e1002348.

Fahrentrapp, J., Broggini, G. A., Kellerhals, M., Peil, A., Richter, K., Zini, E., & Gessler, C. (2013). candidate gene for fire blight resistance in *Malus* × *robusta* 5 is coding for a CC–NBS–LRR. *v. 9*.

Farman, M. L., & Leong, S. A. (1998). Chromosome walking to the *AVR1-CO39* avirulence gene of *Magnaporthe grisea*: discrepancy between the physical and genetic maps. *Genetics, 150*(3), 1049-1058.

Felix, G., & Boller, T. (2003). Molecular sensing of bacteria in plants. The highly conserved RNA-binding motif RNP-1 of bacterial cold shock proteins is recognized as an elicitor signal in tobacco. *The Journal of Biological Chemistry, 278*(8), 6201-6208.

Felix, G., Duran, J. D., Volko, S., & Boller, T. (1999). Plants have a sensitive perception system for the most conserved domain of bacterial flagellin. *Plant Journal, 18*(3), 265-276.

Feng, F., & Zhou, J. M. (2012). Plant-bacterial pathogen interactions mediated by type III effectors. *Current Opinion in Plant Biology, 15*(4), 469-476.

Ferreira, A. O., Myers, C. R., Gordon, J. S., Martin, G. B., Vencato, M., Collmer, A., Wehling, M. D., Alfano, J. R., Moreno-Hagelsieb, G., Lamboy, W. F., DeClerck, G., Schneider, D. J., & Cartinhour, S. W. (2006). Whole-genome expression profiling defines the HrpL regulon of *Pseudomonas syringae* pv. *tomato* DC3000, allows *de novo* reconstruction of the Hrp cis clement, and identifies novel coregulated genes. *Molecular Plant-Microbe Interactions Journal, 19*(11), 1167-1179.

Feys, B. J., Moisan, L. J., Newman, M. A., & Parker, J. E. (2001). Direct interaction between the Arabidopsis disease resistance signaling proteins, EDS1 and PAD4. *The EMBO Journal, 20*(19), 5400-5411.

Feys, B. J., Wiermer, M., Bhat, R. A., Moisan, L. J., Medina-Escobar, N., Neu, C., Cabral, A., & Parker, J. E. (2005). Arabidopsis *SENESCENCE-ASSOCIATED GENE101* stabilizes and signals within an *ENHANCED DISEASE SUSCEPTIBILITY1* complex in plant innate immunity. *The Plant Cell, 17*(9), 2601-2613.

Flor, H. (1942). Inheritance of pathogenicity in *Melampsora lini*. *Phytopathology, 32*, 653-669.

Flor, H. (1955). Host-parasite interaction in flax rust-its genetics and other implications. *Phytopathology, 45*(12), 680-685.

Flor, H. (1971). Current status of the gene-for-gene concept. *Annual Review of Phytopathology, 9*(1), 275-296.

Fronzes, R., Christie, P. J., & Waksman, G. (2009). The structural biology of type IV secretion systems. *Nature Reviews Microbiology, 7*(10), 703-714.

Fudal, I., Ross, S., Gout, L., Blaise, F., Kuhn, M. L., Eckert, M. R., Cattolico, L., Bernard-Samain, S., Balesdent, M. H., & Rouxel, T. (2007). Heterochromatin-like regions as ecological niches for avirulence genes in the *Leptosphaeria maculans* genome: map-based cloning of *AvrLm6*. *Molecular Plant-Microbe Interactions Journal, 20*(4), 459-470.

Gadoury, D. M., & MacHardy, W. E. (1985). Negative geotropism in *Venturia inaequalis*. *Phytopathology, 75*, 856–859.

Galan, J. E., & Wolf-Watz, H. (2006). Protein delivery into eukaryotic cells by type III secretion machines. *Nature, 444*(7119), 567-573.

Galli, P., Broggini, G. A., Gessler, C., & Patocchi, A. (2010a). Phenotypic characterization of the *Rvi15* (*Vr2*) apple scab resistance. *Journal of Plant Pathology, 92*, 219-226.

Galli, P., Patocchi, A., Broggini, G. A., & Gessler, C. (2010b). The *Rvi15* (*Vr2*) apple scab resistance locus contains three TIR-NBS-LRR genes. *Molecular Plant-Microbe Interactions Journal, 23*(5), 608-617.

Gao, Z., Chung, E. H., Eitas, T. K., & Dangl, J. L. (2011). Plant intracellular innate immune receptor *RESISTANCE TO PSEUDOMONAS SYRINGAE PV. MACULICOLA 1 (RPM1)* is activated at, and functions on, the plasma membrane. *Proceedings of the National Academy of Sciences of the United States of America, 108*(18), 7619-7624.

Gardiner, S. E., Norelli, J. L., de Silva, N., Fazio, G., Peil, A., Malnoy, M., Horner, M., Bowatte, D., Carlisle, C., Wiedow, C., Wan, Y., Bassett, C. L., Baldo, A. M., Celton, J. M., Richter, K., Aldwinckle, H. S., & Bus, V. G. (2012). Putative resistance gene markers associated with quantitative trait loci for fire blight resistance in *Malus* '*Robusta* 5' accessions. *BMC Genetics, 13*, 25.

Gardner, R. G., Cummins, J. N., & Aldwinckle, H. S. (1980). Fire blight [*Erwinia amylovora*] resistance in the Geneva apple rootstock breeding program. *Journal of the American Society for Horticultural Science, 105*(6), 907-912..

Gessler, C., Patocchi, A., Sansavini, S., Tartarini, S., & Gianfranceschi, L. (2006). *Venturia inaequalis* resistance in apple. *Critical Reviews in Plant Sciences, 25*(6), 473-503.

Gimenez-Ibanez, S., Boter, M., Fernandez-Barbero, G., Chini, A., Rathjen, J. P., & Solano, R. (2014). The bacterial effector HopX1 targets JAZ transcriptional repressors to activate jasmonate signaling and promote infection in *Arabidopsis*. *PLOS Biology, 12*(2), e1001792.

Gimenez-Ibanez, S., Hann, D. R., Ntoukakis, V., Petutschnig, E., Lipka, V., & Rathjen, J. P. (2009). AvrPtoB targets the LysM receptor kinase CERK1 to promote bacterial virulence on plants. *Current Biology, 19*(5), 423-429.

Gimenez-Ibanez, S., & Solano, R. (2013). Nuclear jasmonate and salicylate signaling and crosstalk in defense against pathogens. *Frontiers in Plant Science, 4*, 72.

Giraldo, M. C., Dagdas, Y. F., Gupta, Y. K., Mentlak, T. A., Yi, M., Martinez-Rocha, A. L., Saitoh, H., Terauchi, R., Talbot, N. J., & Valent, B. (2013). Two distinct

secretion systems facilitate tissue invasion by the rice blast fungus *Magnaporthe oryzae*. *Nature Communications, 4*, 1996.

Gladieux, P., Zhang, X., Afoufa-Bastien, D., Valdebenito, S. R., Sbaghi, M., & Le Cam, B. (2008). On the origin and spread of the scab disease of apple: out of Central Asia. *PLoS One, 3*(1), e1455.

Glazebrook, J. (2005). Contrasting mechanisms of defense against biotrophic and necrotrophic pathogens. *Annual Review of Phytopathology, 43*, 205-227.

Gohre, V., Spallek, T., Haweker, H., Mersmann, S., Mentzel, T., Boller, T., de Torres, M., Mansfield, J. W., & Robatzek, S. (2008). Plant pattern-recognition receptor FLS2 is directed for degradation by the bacterial ubiquitin ligase AvrPtoB. *Current Biology, 18*(23), 1824-1832.

Gomez-Gomez, L., & Boller, T. (2000). FLS2: an LRR receptor-like kinase involved in the perception of the bacterial elicitor flagellin in *Arabidopsis*. *Molecular Cell, 5*(6), 1003-1011.

Gout, L., Fudal, I., Kuhn, M. L., Blaise, F., Eckert, M., Cattolico, L., Balesdent, M. H., & Rouxel, T. (2006). Lost in the middle of nowhere: the *AvrLm1* avirulence gene of the *Dothideomycete Leptosphaeria maculans*. *Molecular Microbiology, 60*(1), 67-80.

Granado, J., Felix, G., & Boller, T. (1995). Perception of fungal sterols in plants (subnanomolar concentrations of ergosterol elicit extracellular alkalinization in tomato cells). *Plant Physiology, 107*(2), 485-490.

Griffith, C. S., Sutton, T. B., & Peterson, P. D. (2003). *Fire blight: the foundation of phytobacteriology*. St. Paul: American Phytopathological Society (APS Press).

Gu, B., Kale, S. D., Wang, Q., Wang, D., Pan, Q., Cao, H., Meng, Y., Kang, Z., Tyler, B. M., & Shan, W. (2011). Rust secreted protein Ps87 is conserved in diverse fungal pathogens and contains a RXLR-like motif sufficient for translocation into plant cells. *PLoS One, 6*(11), e27217.

Gust, A. A. (2015). Peptidoglycan perception in plants. *PLOS Pathogens, 11*(12), e1005275.

Guy, E., Lautier, M., Chabannes, M., Roux, B., Lauber, E., Arlat, M., & Noel, L. D. (2013). XopAC-triggered immunity against *Xanthomonas* depends on *Arabidopsis* receptor-like cytoplasmic kinase genes *PBL2* and *RIPK*. *PLoS One, 8*(8), e73469.

Gygax, M., Gianfranceschi, L., Liebhard, R., Kellerhals, M., Gessler, C., & Patocchi, A. (2004). Molecular markers linked to the apple scab resistance gene *Vbj* derived from *Malus baccata jackii*. *Theoretical and Applied Genetics, 109*(8), 1702-1709.

Hall, S. A., Allen, R. L., Baumber, R. E., Baxter, L. A., Fisher, K., Bittner-Eddy, P. D., Rose, L. E., Holub, E. B., & Beynon, J. L. (2009). Maintenance of genetic variation in plants and pathogens involves complex networks of gene-for-gene interactions. *Mol Plant Pathol, 10*(4), 449-457. doi:10.1111/j.1364-3703.2009.00544.x

Hanson, P. I., & Whiteheart, S. W. (2005). AAA+ proteins: have engine, will work. *Nature Reviews Molecular Cell Biology, 6*(7), 519-529.

Harshman, J. M., Evans, K. M., Allen, H., Potts, R., Flamenco, J., Aldwinckle, H. S., Wisniewski, M. E., & Norelli, J. L. (2017). Fire blight resistance in wild accessions of *Malus sieversii*. *Plant Disease, 101*(10), 1738-1745.

He, P., Shan, L., Lin, N. C., Martin, G. B., Kemmerling, B., Nurnberger, T., & Sheen, J. (2006). Specific bacterial suppressors of MAMP signaling upstream of MAPKKK in *Arabidopsis* innate immunity. *Cell, 125*(3), 563-575.

He, S. Y., Nomura, K., & Whittam, T. S. (2004). Type III protein secretion mechanism in mammalian and plant pathogens. *Biochimica et Biophysica Acta, 1694*(1-3), 181-206.

Heath, M. C. (1976). Ultrastructural and functional similarity of the haustorial neckband of rust fungi and the Casparian strip of vascular plants. *Canadian Journal of Botany, 54*(21), 2484-2489.

Heese, A., Hann, D. R., Gimenez-Ibanez, S., Jones, A. M., He, K., Li, J., Schroeder, J. I., Peck, S. C., & Rathjen, J. P. (2007). The receptor-like kinase SERK3/BAK1 is a central regulator of innate immunity in plants. *Proceedings of the National Academy of Sciences of the United States of America, 104*(29), 12217-12222.

Hellens, R. P., Edwards, E. A., Leyland, N. R., Bean, S., & Mullineaux, P. M. (2000). pGreen: a versatile and flexible binary Ti vector for *Agrobacterium*-mediated plant transformation. *Plant Molecular Biology, 42*(6), 819-832.

Hematy, K., Cherk, C., & Somerville, S. (2009). Host-pathogen warfare at the plant cell wall. *Current Opinion in Plant Biology, 12*(4), 406-413.

Hemmat, M., Brown, S. K., Aldwinckle, H. S., Mehlenbacher, S. A., & Weeden, N. F. (2003). Identification and mapping of markers for resistance to apple scab from 'Antonovka' and 'Hansen baccata #2'. *Acta Horticulturae, 622*, 153-161.

Henty-Ridilla, J. L., Shimono, M., Li, J., Chang, J. H., Day, B., & Staiger, C. J. (2013). The plant actin cytoskeleton responds to signals from microbe-associated molecular patterns. *PLOS Pathogens, 9*(4), e1003290.

Hernandez, C. D. (1990). *La tavelure du pommier Venturia inaequalis (Cke.) Wint.: e´tude du pouvoir pathoge`ne des races 1 et 5 et essai de lutte raisonne´e.* (Doctoral thesis), Univ. Nantes, France.

Hirano, S. S., & Upper, C. D. (2000). Bacteria in the leaf ecosystem with emphasis on *Pseudomonas syringae* - a pathogen, ice nucleus, and epiphyte. *Microbiology and Molecular Biology Reviews, 64*(3), 624-653.

Holland, P., & Rahman, A. (1999). Review of trends in agricultural pesticide use in New Zealand. *MAF Policy technical paper, 99/11*.

Hotson, A., Chosed, R., Shu, H., Orth, K., & Mudgett, M. B. (2003). *Xanthomonas* type III effector XopD targets SUMO-conjugated proteins in planta. *Molecular Microbiology, 50*(2), 377-389.

Hough, L. F., Shay, J. R., & Dayton, D. F. (1953). Apple scab resistance from *Malus floribunda* Sieb. . *Proceedings of the American Society for Horticultural Science, 62*(341-347).

Hueck, C. J. (1998). Type III protein secretion systems in bacterial pathogens of animals and plants. *Microbiology and Molecular Biology Reviews, 62*(2), 379-433.

Hwang, B. K., Son, S. H., Lee, J. S., Min, S. R., Ko, S. M., Liu, J. R., Choi, D. S., & Jeong, W. J. (2010). Rapid and simple method for DNA extraction from plant and algal species suitable for PCR amplification using a chelating resin Chelex 100. *Plant Biotechnology Reports, 4*(1), 49-52. doi:10.1007/s11816-009-0117-4

Innes, R. W., Bisgrove, S. R., Smith, N. M., Bent, A. F., Staskawicz, B. J., & Liu, Y. C. (1993). Identification of a disease resistance locus in *Arabidopsis* that is functionally homologous to the *RPG1* locus of soybean. *Plant Journal, 4*(5), 813-820.

Jacobson, E. S. (2000). Pathogenic roles for fungal melanins. *Clinical Microbiology Reviews, 13*(4), 708-717.

Janjusevic, R., Abramovitch, R. B., Martin, G. B., & Stebbins, C. E. (2006). A bacterial inhibitor of host programmed cell death defenses is an E3 ubiquitin ligase. *Science, 311*(5758), 222-226.

Jeuken, M. J., Zhang, N. W., McHale, L. K., Pelgrom, K., den Boer, E., Lindhout, P., Michelmore, R. W., Visser, R. G., & Niks, R. E. (2009). RIN4 causes hybrid necrosis and race-specific resistance in an interspecific lettuce hybrid. *The Plant Cell, 21*(10), 3368-3378.

Jha, G., Rajeshwari, R., & Sonti, R. V. (2005). Bacterial type two secretion system secreted proteins: double-edged swords for plant pathogens. *Molecular Plant-Microbe Interactions Journal, 18*(9), 891-898.

Jha, G., Rajeshwari, R., & Sonti, R. V. (2007). Functional interplay between two *Xanthomonas oryzae* pv. *oryzae* secretion systems in modulating virulence on rice. *Molecular Plant-Microbe Interactions Journal, 20*(1), 31-40.

Jha, G., Thakur, K., & Thakur, P. (2009). The *Venturia* apple pathosystem: pathogenicity mechanisms and plant defense responses. *Journal of Biomedicine and Biotechnology, 2009*, 680160.

Jia, Y., McAdams, S. A., Bryan, G. T., Hershey, H. P., & Valent, B. (2000). Direct interaction of resistance gene and avirulence gene products confers rice blast resistance. *The EMBO Journal, 19*(15), 4004-4014.

Jiang, R. H., Tripathy, S., Govers, F., & Tyler, B. M. (2008). RXLR effector reservoir in two *Phytophthora* species is dominated by a single rapidly evolving superfamily with more than 700 members. *Proceedings of the National Academy of Sciences of the United States of America, 105*(12), 4874-4879.

Jiang, S., Yao, J., Ma, K. W., Zhou, H., Song, J., He, S. Y., & Ma, W. (2013). Bacterial effector activates jasmonate signaling by directly targeting JAZ transcriptional repressors. *PLOS Pathogens, 9*(10), e1003715.

Jin, Q., Thilmony, R., Zwiesler-Vollick, J., & He, S. Y. (2003). Type III protein secretion in *Pseudomonas syringae*. *Microbes and Infection, 5*(4), 301-310.

Jirage, D., Tootle, T. L., Reuber, T. L., Frost, L. N., Feys, B. J., Parker, J. E., Ausubel, F. M., & Glazebrook, J. (1999). *Arabidopsis thaliana* PAD4 encodes a lipase-like gene that is important for salicylic acid signaling. *Proceedings of the National Academy of Sciences of the United States of America, 96*(23), 13583-13588.

Johansson, O. N., Nilsson, A. K., Gustavsson, M. B., Backhaus, T., Andersson, M. X., & Ellerstrom, M. (2015). A quick and robust method for quantification of the hypersensitive response in plants. *PeerJ, 3*, e1469.

Johnson, K. B., & Stockwell, V. O. (1998). Management of fire blight: a case study in microbial ecology. *Annual Review of Phytopathology, 36*, 227-248.

Jones, D. A., Thomas, C. M., Hammond-Kosack, K. E., Balint-Kurti, P. J., & Jones, J. D. (1994). Isolation of the tomato *Cf-9* gene for resistance to *Cladosporium fulvum* by transposon tagging. *Science, 266*(5186), 789-793.

Jones, J. D., & Dangl, J. L. (2006). The plant immune system. *Nature, 444*(7117), 323-329.

Joshi, S. G., Schaart, J. G., Groenwold, R., Jacobsen, E., Schouten, H. J., & Krens, F. A. (2011). Functional analysis and expression profiling of *HcrVf1* and *HcrVf2* for development of scab resistant cisgenic and intragenic apples. *Plant Molecular Biology, 75*(6), 579-591.

Julien, J. B. (1958). Cytological studies of *Venturia inaequalis*. *Canadian Journal of Botany, 36*(5), 607-613. doi:10.1139/b58-056

Kaku, H., Nishizawa, Y., Ishii-Minami, N., Akimoto-Tomiyama, C., Dohmae, N., Takio, K., Minami, E., & Shibuya, N. (2006). Plant cells recognize chitin fragments for defense signaling through a plasma membrane receptor. *Proceedings of the National Academy of Sciences of the United States of America, 103*(29), 11086-11091.

Kale, S. D., Gu, B., Capelluto, D. G., Dou, D., Feldman, E., Rumore, A., Arredondo, F. D., Hanlon, R., Fudal, I., Rouxel, T., Lawrence, C. B., Shan, W., & Tyler, B. M. (2010). External lipid PI3P mediates entry of eukaryotic pathogen effectors into plant and animal host cells. *Cell, 142*(2), 284-295.

Kamoun, S. (2006). A catalogue of the effector secretome of plant pathogenic oomycetes. *Annual Review of Phytopathology, 44*(1), 41-60.

Kang, Y., Jelenska, J., Cecchini, N. M., Li, Y., Lee, M. W., Kovar, D. R., & Greenberg, J. T. (2014). HopW1 from *Pseudomonas syringae* disrupts the actin cytoskeleton to promote virulence in *Arabidopsis*. *PLOS Pathogens, 10*(6), e1004232.

Katagiri, F., Thilmony, R., & He, S. Y. (2002). The *Arabidopsis thaliana* - *Pseudomonas syringae* interaction. *Arabidopsis Book, 1*, e0039.

Katsir, L., Schilmiller, A. L., Staswick, P. E., He, S. Y., & Howe, G. A. (2008). COI1 is a critical component of a receptor for jasmonate and the bacterial virulence factor coronatine. *Proceedings of the National Academy of Sciences of the United States of America, 105*(19), 7100-7105.

Kazan, K. (2006). Negative regulation of defence and stress genes by EAR-motif-containing repressors. *Trends in Plant Science, 11*(3), 109-112.

Kazan, K., & Lyons, R. (2014). Intervention of phytohormone pathways by pathogen effectors. *The Plant Cell, 26*(6), 2285-2309.

Kessens, R., Ashfield, T., Kim, S. H., & Innes, R. W. (2014). Determining the GmRIN4 requirements of the soybean disease resistance proteins RPG1-b and RPG1-r using a nicotiana glutinosa-based agroinfiltration system. *PLoS One, 9*(9), e108159.

Khang, C. H., Berruyer, R., Giraldo, M. C., Kankanala, P., Park, S. Y., Czymmek, K., Kang, S., & Valent, B. (2010). Translocation of *Magnaporthe oryzae* effectors into rice cells and their subsequent cell-to-cell movement. *The Plant Cell, 22*(4), 1388.

Kim, H. S., Desveaux, D., Singer, A. U., Patel, P., Sondek, J., & Dangl, J. L. (2005a). The *Pseudomonas syringae* effector AvrRpt2 cleaves its C-terminally acylated target, RIN4, from *Arabidopsis* membranes to block RPM1 activation. *Proceedings of the National Academy of Sciences of the United States of America, 102*(18), 6496-6501.

Kim, J. G., Stork, W., & Mudgett, M. B. (2013). *Xanthomonas* type III effector XopD desumoylates tomato transcription factor SlERF4 to suppress ethylene responses and promote pathogen growth. *Cell Host Microbe, 13*(2), 143-154.

Kim, M. G., da Cunha, L., McFall, A. J., Belkhadir, Y., DebRoy, S., Dangl, J. L., & Mackey, D. (2005b). Two *Pseudomonas syringae* type III effectors inhibit RIN4-regulated basal defense in *Arabidopsis*. *Cell, 121*(5), 749-759.

Kim, S. H., Qi, D., Ashfield, T., Helm, M., & Innes, R. W. (2016). Using decoys to expand the recognition specificity of a plant disease resistance protein. *Science, 351*(6274), 684-687.

Kim, Y. J., Lin, N. C., & Martin, G. B. (2002). Two distinct *Pseudomonas* effector proteins interact with the Pto kinase and activate plant immunity. *Cell, 109*(5), 589-598.

Kobe, B., & Deisenhofer, J. (1994). The leucine-rich repeat: a versatile binding motif. *Trends in Biochemical Sciences, 19*(10), 415-421.

Kollar, A. (1998). Characterization of an endopolygalacturonase produced by the apple scab fungus, *Venturia inaequalis*. *Mycological Research, 102*(3), 313-319.

Koller, W., & Parker, D. M. (1989). Purification and characterization of cutinase from *Venturia inaequalis*. *Phytopathology, 79*, 278-283.

Koller, W., Parker, D. M., & Becker, C. M. (1991). Role of cutinase in the penetration of apple leaves by *Venturia inaequalis*. *Phytopathology, 81*, 1375-1379.

Koronakis, V., Hughes, C., & Koronakis, E. (1991). Energetically distinct early and late stages of HlyB/HlyD-dependent secretion across both *Escherichia coli* membranes. *The EMBO Journal, 10*(11), 3263-3272.

Krasileva, K. V., Dahlbeck, D., & Staskawicz, B. J. (2010). Activation of an *Arabidopsis* resistance protein is specified by the in planta association of its leucine-rich repeat domain with the cognate oomycete effector. *The Plant Cell, 22*(7), 2444-2458.

Kubori, T., Matsushima, Y., Nakamura, D., Uralil, J., Lara-Tejero, M., Sukhan, A., Galan, J. E., & Aizawa, S. I. (1998). Supramolecular structure of the *Salmonella typhimurium* type III protein secretion system. *Science, 280*(5363), 602-605.

Kubori, T., Sukhan, A., Aizawa, S. I., & Galan, J. E. (2000). Molecular characterization and assembly of the needle complex of the *Salmonella typhimurium* type III

protein secretion system. *Proceedings of the National Academy of Sciences of the United States of America, 97*(18), 10225-10230.

Kucheryava, N., Bowen, J. K., Sutherland, P. W., Conolly, J. J., Mesarich, C. H., Rikkerink, E. H., Kemen, E., Plummer, K. M., Hahn, M., & Templeton, M. D. (2008). Two novel *Venturia inaequalis* genes induced upon morphogenetic differentiation during infection and in vitro growth on cellophane. *Fungal Genetics and Biology, 45*(10), 1329-1339.

Kunze, G., Zipfel, C., Robatzek, S., Niehaus, K., Boller, T., & Felix, G. (2004). The N terminus of bacterial elongation factor Tu elicits innate immunity in *Arabidopsis* plants. *The Plant Cell, 16*(12), 3496-3507.

Laurens, F. N., Chevalier, M., Dolega, E., Gennari, F., Goerre, M., Fischer, C., Kellerhals, M., Lateur, M., Lefrancq, B., Parisi, L., Schouten, H. J., & Tartarini, S. (2004). Local European cultivars as sources of durable scab resistance in apple. *Acta Horticulturae, 663*, 115-121.

Lawrence, G. J., Finnegan, E. J., Ayliffe, M. A., & Ellis, J. G. (1995). The *L6* gene for flax rust resistance is related to the *Arabidopsis* bacterial resistance gene *RPS2* and the tobacco viral resistance gene *N*. *The Plant Cell, 7*(8), 1195-1206.

Le Roux, C., Huet, G., Jauneau, A., Camborde, L., Tremousaygue, D., Kraut, A., Zhou, B., Levaillant, M., Adachi, H., Yoshioka, H., Raffaele, S., Berthome, R., Coute, Y., Parker, J. E., & Deslandes, L. (2015). A receptor pair with an integrated decoy converts pathogen disabling of transcription factors to immunity. *Cell, 161*(5), 1074-1088.

Lee, A. H., Hurley, B., Felsensteiner, C., Yea, C., Ckurshumova, W., Bartetzko, V., Wang, P. W., Quach, V., Lewis, J. D., Liu, Y. C., Bornke, F., Angers, S., Wilde, A., Guttman, D. S., & Desveaux, D. (2012). A bacterial acetyltransferase destroys plant microtubule networks and blocks secretion. *PLOS Pathogens, 8*(2), e1002523.

Lee, S. W., Han, S. W., Bartley, L. E., & Ronald, P. C. (2006). From the Academy: Colloquium review. Unique characteristics of *Xanthomonas oryzae* pv. *oryzae* AvrXa21 and implications for plant innate immunity. *Proceedings of the National Academy of Sciences of the United States of America, 103*(49), 18395-18400.

Lee, W. S., Rudd, J. J., Hammond-Kosack, K. E., & Kanyuka, K. (2014). *Mycosphaerella graminicola* LysM effector-mediated stealth pathogenesis subverts recognition through both CERK1 and CEBiP homologues in wheat. *Molecular Plant-Microbe Interactions Journal, 27*(3), 236-243.

Leipe, D. D., Koonin, E. V., & Aravind, L. (2004). STAND, a class of P-loop NTPases including animal and plant regulators of programmed cell death: multiple, complex domain architectures, unusual phyletic patterns, and evolution by horizontal gene transfer. *Journal of Molecular Biology, 343*(1), 1-28.

Lespinasse, Y. (1989). Breeding pome fruits with stable resistance to diseases. Genes, resistance mechanisms, present work and prospects. *IOBC-WPRS Bulletin, 12*(6), 100-115.

Lewis, J. D., Lee, A. H., Hassan, J. A., Wan, J., Hurley, B., Jhingree, J. R., Wang, P. W., Lo, T., Youn, J. Y., Guttman, D. S., & Desveaux, D. (2013). The Arabidopsis ZED1

pseudokinase is required for ZAR1-mediated immunity induced by the *Pseudomonas syringae* type III effector HopZ1a. *Proceedings of the National Academy of Sciences of the United States of America, 110*(46), 18722-18727.

Li, M., Ma, X., Chiang, Y. H., Yadeta, K. A., Ding, P., Dong, L., Zhao, Y., Li, X., Yu, Y., Zhang, L., Shen, Q. H., Xia, B., Coaker, G., Liu, D., & Zhou, J. M. (2014). Proline isomerization of the immune receptor-interacting protein RIN4 by a cyclophilin inhibits effector-triggered immunity in *Arabidopsis*. *Cell Host Microbe, 16*(4), 473-483.

Liebrand, T. W., van den Berg, G. C., Zhang, Z., Smit, P., Cordewener, J. H., America, A. H., Sklenar, J., Jones, A. M., Tameling, W. I., Robatzek, S., Thomma, B. P., & Joosten, M. H. (2013). Receptor-like kinase SOBIR1/EVR interacts with receptor-like proteins in plant immunity against fungal infection. *Proceedings of the National Academy of Sciences of the United States of America, 110*(24), 10010-10015.

Liebrand, T. W., Van den Burg, H. A., & Joosten, M. H. (2014). Two for all: receptor-associated kinases SOBIR1 and BAK1. *Trends in Plant Science, 19*(2), 123-132.

Lim, M. T., & Kunkel, B. N. (2004). Mutations in the *Pseudomonas syringae* AvrRpt2 gene that dissociate its virulence and avirulence activities lead to decreased efficiency in AvrRpt2-induced disappearance of RIN4. *Molecular Plant-Microbe Interactions Journal, 17*(3), 313-321.

Liu, J., Elmore, J. M., & Coaker, G. (2009a). Investigating the functions of the RIN4 protein complex during plant innate immune responses. *Plant Signaling & Behavior, 4*(12), 1107-1110.

Liu, J., Elmore, J. M., Fuglsang, A. T., Palmgren, M. G., Staskawicz, B. J., & Coaker, G. (2009b). RIN4 functions with plasma membrane H+-ATPases to regulate stomatal apertures during pathogen attack. *PLOS Biology, 7*(6), e1000139.

Liu, J., Elmore, J. M., Lin, Z. J., & Coaker, G. (2011). A receptor-like cytoplasmic kinase phosphorylates the host target RIN4, leading to the activation of a plant innate immune receptor. *Cell Host Microbe, 9*(2), 137-146.

Liu, Y., Huang, X., Li, M., He, P., & Zhang, Y. (2016). Loss-of-function of *Arabidopsis* receptor-like kinase BIR1 activates cell death and defense responses mediated by BAK1 and SOBIR1. *New Phytologist, 212*(3), 637-645.

Llorca, C. M., Potschin, M., & Zentgraf, U. (2014). bZIPs and WRKYs: two large transcription factor families executing two different functional strategies. *Frontiers in Plant Science, 5*, 169.

Lo Presti, L., & Kahmann, R. (2017). How filamentous plant pathogen effectors are translocated to host cells. *Current Opinion in Plant Biology, 38*, 19-24.

Lohou, D., Lonjon, F., Genin, S., & Vailleau, F. (2013). Type III chaperones & Co in bacterial plant pathogens: a set of specialized bodyguards mediating effector delivery. *Frontiers in Plant Science, 4*, 435.

Lu, D., Wu, S., Gao, X., Zhang, Y., Shan, L., & He, P. (2010). A receptor-like cytoplasmic kinase, BIK1, associates with a flagellin receptor complex to initiate plant innate immunity. *Proceedings of the National Academy of Sciences of the United States of America, 107*(1), 496-501.

Luby, J., Forsline, P., Aldwinckle, H. S., Bus, V. G., & Geibel., M. (2001). Silkroad apples—collection, evaluation, and utilization of *Malus sieversii* from Central Asia. *HortScience, 36*(2), 225-231.

Lukasik, E., & Takken, F. L. (2009). STANDing strong, resistance proteins instigators of plant defence. *Current Opinion in Plant Biology, 12*(4), 427-436.

MacHardy, W. E. (1996). *Apple scab : biology, epidemiology, and management*. St. Paul: APS Press.

MacHardy, W. E., Gadoury, D. M., & Gessler, C. (2001). Parasitic and biological fitness of *Venturia inaequalis*: relationship to disease management strategies. *Plant Disease, 85*(10), 1036-1051.

Macho, A. P., Schwessinger, B., Ntoukakis, V., Brutus, A., Segonzac, C., Roy, S., Kadota, Y., Oh, M. H., Sklenar, J., Derbyshire, P., Lozano-Duran, R., Malinovsky, F. G., Monaghan, J., Menke, F. L., Huber, S. C., He, S. Y., & Zipfel, C. (2014). A bacterial tyrosine phosphatase inhibits plant pattern recognition receptor activation. *Science, 343*(6178), 1509-1512.

Mackey, D., Belkhadir, Y., Alonso, J. M., Ecker, J. R., & Dangl, J. L. (2003). Arabidopsis RIN4 is a target of the type III virulence effector AvrRpt2 and modulates RPS2-mediated resistance. *Cell, 112*(3), 379-389.

Mackey, D., Holt, B. F., Wiig, A., & Dangl, J. L. (2002). RIN4 interacts with *Pseudomonas syringae* type III effector molecules and is required for RPM1-mediated resistance in *Arabidopsis*. *Cell, 108*(6), 743-754.

Maekawa, T., Cheng, W., Spiridon, L. N., Toller, A., Lukasik, E., Saijo, Y., Liu, P., Shen, Q. H., Micluta, M. A., Somssich, I. E., Takken, F. L. W., Petrescu, A. J., Chai, J., & Schulze-Lefert, P. (2011). Coiled-coil domain-dependent homodimerization of intracellular barley immune receptors defines a minimal functional module for triggering cell death. *Cell Host Microbe, 9*(3), 187-199.

Mak, A. N., Bradley, P., Cernadas, R. A., Bogdanove, A. J., & Stoddard, B. L. (2012). The crystal structure of TAL effector PthXo1 bound to its DNA target. *Science, 335*(6069), 716-719.

Malnoy, M., Martens, S., Norelli, J. L., Barny, M. A., Sundin, G. W., Smits, T. H., & Duffy, B. (2012). Fire blight: applied genomic insights of the pathogen and host. *Annual Review of Phytopathology, 50*, 475-494.

Manktelow, D. W., Beresford, R. M., Batchelor, T. A., & Walker, J. T. S. (1996). Use of patterns and economics of fungicides for disease control in New Zealand apples. *Acta Horticulturae, 0567-7572*.

Marshall, R., Kombrink, A., Motteram, J., Loza-Reyes, E., Lucas, J., Hammond-Kosack, K. E., Thomma, B. P., & Rudd, J. J. (2011). Analysis of two in planta expressed LysM effector homologs from the fungus *Mycosphaerella graminicola* reveals novel functional properties and varying contributions to virulence on wheat. *Plant Physiology, 156*(2), 756-769.

Martin, G. B., Brommonschenkel, S. H., Chunwongse, J., Frary, A., Ganal, M. W., Spivey, R., Wu, T., Earle, E. D., & Tanksley, S. D. (1993). Map-based cloning of a protein kinase gene conferring disease resistance in tomato. *Science, 262*(5138), 1432-1436.

Martin, J. T. (1964). Role of cuticle in the defense against plant disease. *Annual Review of Phytopathology, 2*(1), 81-100.

Mattick, J. S. (2002). Type IV pili and twitching motility. *Annual Review of Microbiology, 56*, 289-314.

McManus, P. S., Stockwell, V. O., Sundin, G. W., & Jones, A. L. (2002). Antibiotic use in plant agriculture. *Annual Review of Phytopathology, 40*, 443-465.

Mentlak, T. A., Kombrink, A., Shinya, T., Ryder, L. S., Otomo, I., Saitoh, H., Terauchi, R., Nishizawa, Y., Shibuya, N., Thomma, B. P., & Talbot, N. J. (2012). Effector-mediated suppression of chitin-triggered immunity by magnaporthe oryzae is necessary for rice blast disease. *The Plant Cell, 24*(1), 322-335.

Mesarich, C. H., Griffiths, S. A., van der Burgt, A., Okmen, B., Beenen, H. G., Etalo, D. W., Joosten, M. H., & de Wit, P. J. (2014). Transcriptome sequencing uncovers the *Avr5* avirulence gene of the tomato leaf mold pathogen *Cladosporium fulvum*. *Molecular Plant-Microbe Interactions Journal, 27*(8), 846-857.

Meyers, B. C., Kozik, A., Griego, A., Kuang, H., & Michelmore, R. W. (2003). Genome-wide analysis of NBS-LRR-encoding genes in *Arabidopsis*. *The Plant Cell, 15*(4), 809-834.

Michael Weaver, L., Swiderski, M. R., Li, Y., & Jones, J. D. (2006). The Arabidopsis thaliana TIR-NB-LRR R-protein, RPP1A; protein localization and constitutive activation of defence by truncated alleles in tobacco and *Arabidopsis*. *Plant Journal, 47*(6), 829-840.

Michelmore, R. W., & Meyers, B. C. (1998). Clusters of resistance genes in plants evolve by divergent selection and a birth-and-death process. *Genome Research, 8*(11), 1113-1130.

Mindrinos, M., Katagiri, F., Yu, G. L., & Ausubel, F. M. (1994). The *A. thaliana* disease resistance gene *RPS2* encodes a protein containing a nucleotide-binding site and leucine-rich repeats. *Cell, 78*(6), 1089-1099.

Momol, M. T., Norelli, J. L., Piccioni, D. E., Momol, E. A., Gustafson, H. L., Cummins, J. N., & Aldwinckle, H. S. (1998). Internal movement of *Erwinia amylovora* through symptomless apple scion tissues into the rootstock. *Plant Disease, 82*(6), 646-650.

Moscou, M. J., & Bogdanove, A. J. (2009). A simple cipher governs DNA recognition by TAL effectors. *Science, 326*(5959), 1501.

Mukhtar, M. S., Carvunis, A. R., Dreze, M., Epple, P., Steinbrenner, J., Moore, J., Tasan, M., Galli, M., Hao, T., Nishimura, M. T., Pevzner, S. J., Donovan, S. E., Ghamsari, L., Santhanam, B., Romero, V., Poulin, M. M., Gebreab, F., Gutierrez, B. J., Tam, S., Monachello, D., Boxem, M., Harbort, C. J., McDonald, N., Gai, L., Chen, H., He, Y., Vandenhaute, J., Roth, F. P., Hill, D. E., Ecker, J. R., Vidal, M., Beynon, J., Braun, P., & Dangl, J. L. (2011). Independently evolved virulence effectors converge onto hubs in a plant immune system network. *Science, 333*(6042), 596-601.

Nemri, A., Saunders, D. G., Anderson, C., Upadhyaya, N. M., Win, J., Lawrence, G. J., Jones, D. A., Kamoun, S., Ellis, J. G., & Dodds, P. N. (2014). The genome

sequence and effector complement of the flax rust pathogen *Melampsora lini*. *Frontiers in Plant Science, 5*, 98.

Newman, M. A., Dow, J. M., Molinaro, A., & Parrilli, M. (2007). Priming, induction and modulation of plant defence responses by bacterial lipopolysaccharides. *Journal of Endotoxin Research, 13*(2), 69-84.

Nicholson, R. L., Kuc, J., & Williams, E. B. (1972). Histochemical demonstration of transitory esterase activity in *Venturia inaequalis*. *Phytopathology, 62*, 1242-1247.

Nishimura, T., Mochizuki, S., Ishii-Minami, N., Fujisawa, Y., Kawahara, Y., Yoshida, Y., Okada, K., Ando, S., Matsumura, H., Terauchi, R., Minami, E., & Nishizawa, Y. (2016). *Magnaporthe oryzae* glycine-rich secretion protein, Rbf1 critically participates in pathogenicity through the focal formation of the biotrophic interfacial complex. *PLOS Pathogens, 12*(10), e1005921.

Norelli, J. L., Jones, A. L., & Aldwinckle, H. S. (2003). Fire blight management in the twenty-first century: using new technologies that enhance host resistance in apple. *Plant Disease, 87*(7), 756-765.

Ntoukakis, V., Balmuth, A. L., Mucyn, T. S., Gutierrez, J. R., Jones, A. M., & Rathjen, J. P. (2013). The tomato Prf complex is a molecular trap for bacterial effectors based on Pto transphosphorylation. *PLOS Pathogens, 9*(1), e1003123.

Ogura, T., & Wilkinson, A. J. (2001). AAA+ superfamily ATPases: common structure-diverse function. *Genes to Cells, 6*(7), 575-597.

Omori, K., & Idei, A. (2003). Gram-negative bacterial ATP-binding cassette protein exporter family and diverse secretory proteins. *Journal of Bioscience and Bioengineering, 95*(1), 1-12.

Orbach, M. J., Farrall, L., Sweigard, J. A., Chumley, F. G., & Valent, B. (2000). A telomeric avirulence gene determines efficacy for the rice blast resistance gene *Pi-ta*. *The Plant Cell, 12*(11), 2019-2032.

Paiva, P., Gomes, F., Napoleão, T., Sá, R., Correia, M., & Coelho, L. (2010). Antimicrobial activity of secondary metabolites and lectins from plants. *Current Research, Technology and Education Topics in Applied Microbiology and Microbial Biotechnology, 1*, 396-406.

Parisi, L., Fouillet, V., Schouten, H. J., Groenwold, R., Laurens, F., Didelot, F., Evans, K., Fischer, C., Gennari, F., Kemp, H., Lateur, M., Patocchi, A., Thissen, J., & Tsipouridis, C. (2004). *Variability of the pathogenicity of Venturia inaequalis in Europe*.

Parisi, L., & Lespinasse, Y. (1998). *Pathogenicity of a strain of Venturia inaequalis race 6 on apple clones (Malus spp.)*.

Parker, J. E., Coleman, M. J., Szabo, V., Frost, L. N., Schmidt, R., Van der Biezen, E. A., Moores, T., Dean, C., Daniels, M. J., & Jones, J. D. (1997). The *Arabidopsis* downy mildew resistance gene *RPP5* shares similarity to the toll and interleukin-1 receptors with *N* and *L6*. *The Plant Cell, 9*(6), 879-894.

Parker, J. E., Holub, E. B., Frost, L. N., Falk, A., Gunn, N. D., & Daniels, M. J. (1996). Characterization of *eds1*, a mutation in *Arabidopsis* suppressing resistance to *Peronospora parasitica* specified by several different *RPP* genes. *The Plant Cell, 8*(11), 2033-2046.

Parlange, F., Daverdin, G., Fudal, I., Kuhn, M. L., Balesdent, M. H., Blaise, F., Grezes-Besset, B., & Rouxel, T. (2009). *Leptosphaeria maculans* avirulence gene *AvrLm4-7* confers a dual recognition specificity by the *Rlm4* and *Rlm7* resistance genes of oilseed rape, and circumvents *Rlm4*-mediated recognition through a single amino acid change. *Molecular Microbiology, 71*(4), 851-863.

Patocchi, A., Bigler, B., Koller, B., Kellerhals, M., & Gessler, C. (2004). *Vr2*: a new apple scab resistance gene. *Theoretical and Applied Genetics, 109*(5), 1087-1092.

Peil, A., Garcia-Libreros, T., Richter, K., Trognitz, F. C., Trognitz, B., Hanke, M. V., & Flachowsky, H. (2007). Strong evidence for a fire blight resistance gene of *Malus robusta* located on linkage group 3. *Plant Breeding, 126*(5), 470-475.

Petre, B., & Kamoun, S. (2014). How do filamentous pathogens deliver effector proteins into plant cells? *PLOS Biology, 12*(2), e1001801.

Pitzschke, A., Schikora, A., & Hirt, H. (2009). MAPK cascade signalling networks in plant defence. *Current Opinion in Plant Biology, 12*(4), 421-426.

Plett, J. M., Kemppainen, M., Kale, S. D., Kohler, A., Legué, V., Brun, A., Tyler, B. M., Pardo, A. G., & Martin, F. (2011). A secreted effector protein of *Laccaria bicolor* is required for symbiosis development. *Current Biology, 21*(14), 1197-1203.

Postel, S., Kufner, I., Beuter, C., Mazzotta, S., Schwedt, A., Borlotti, A., Halter, T., Kemmerling, B., & Nurnberger, T. (2010). The multifunctional leucine-rich repeat receptor kinase BAK1 is implicated in *Arabidopsis* development and immunity. *European Journal of Cell Biology, 89*(2-3), 169-174.

Presti, L. L., Zechmann, B., Kumlehn, J., Liang, L., Lanver, D., Tanaka, S., Bock, R., & Kahmann, R. (2017). An assay for entry of secreted fungal effectors into plant cells. *New Phytologist, 213*(2).

Pruitt, R. N., Schwessinger, B., Joe, A., Thomas, N., Liu, F., Albert, M., Robinson, M. R., Chan, L. J., Luu, D. D., Chen, H., Bahar, O., Daudi, A., de Vleesschauwer, D., Caddell, D., Zhang, W., Zhao, X., Li, X., Heazlewood, J. L., Ruan, D., Majumder, D., Chern, M., Kalbacher, H., Midha, S., Patil, P. B., Sonti, R. V., Petzold, C. J., Liu, C. C., Brodbelt, J. S., Felix, G., & Ronald, P. C. (2015). The rice immune receptor XA21 recognizes a tyrosine-sulfated protein from a Gram-negative bacterium. *Science Advances, 1*(6), e1500245.

Puri, N., Jenner, C., Bennett, M., Stewart, R., Mansfield, J., Lyons, N., & Taylor, J. (1997). Expression of *avrPphB*, an avirulence gene from *Pseudomonas syringae* pv. *phaseolicola*, and the delivery of signals causing the hypersensitive reaction in bean. *Molecular Plant-Microbe Interactions Journal, 10*(2), 247-256.

Pusey, P. L., & Curry, E. A. (2004). Temperature and *Pomaceous* flower age related to colonization by *Erwinia amylovora* and antagonists. *Phytopathology, 94*(8), 901-911.

Pusey, P. L., Stockwell, V. O., Reardon, C. L., Smits, T. H., & Duffy, B. (2011). Antibiosis activity of *Pantoea agglomerans* biocontrol strain E325 against

Erwinia amylovora on apple flower stigmas. *Phytopathology, 101*(10), 1234-1241.

Qi, D., & Innes, R. W. (2013). Recent advances in plant NLR structure, function, localization, and signaling. *Frontiers in Immunology, 4*, 348.

Qianli, A., Ehlers, K., Kogel, K., Van Bel Aart, J. E., & Hückelhoven, R. (2006). Multivesicular compartments proliferate in susceptible and resistant MLA12-barley leaves in response to infection by the biotrophic powdery mildew fungus. *New Phytologist, 172*(3), 563-576.

Rafiqi, M., Gan, P. H., Ravensdale, M., Lawrence, G. J., Ellis, J. G., Jones, D. A., Hardham, A. R., & Dodds, P. N. (2010). Internalization of flax rust avirulence proteins into flax and tobacco cells can occur in the absence of the pathogen. *The Plant Cell, 22*(6), 2017-2032.

Rairdan, G. J., Collier, S. M., Sacco, M. A., Baldwin, T. T., Boettrich, T., & Moffett, P. (2008). The coiled-coil and nucleotide binding domains of the potato Rx disease resistance protein function in pathogen recognition and signaling. *The Plant Cell, 20*(3), 739-751.

Ranf, S., Gisch, N., Schaffer, M., Illig, T., Westphal, L., Knirel, Y. A., Sanchez-Carballo, P. M., Zahringer, U., Huckelhoven, R., Lee, J., & Scheel, D. (2015). A lectin S-domain receptor kinase mediates lipopolysaccharide sensing in *Arabidopsis thaliana*. *Nature Immunology, 16*(4), 426-433.

Rehmany, A. P., Gordon, A., Rose, L. E., Allen, R. L., Armstrong, M. R., Whisson, S. C., Kamoun, S., Tyler, B. M., Birch, P. R., & Beynon, J. L. (2005). Differential recognition of highly divergent downy mildew avirulence gene alleles by *RPP1* resistance genes from two *Arabidopsis* lines. *The Plant Cell, 17*(6), 1839-1850.

Rezzonico, F., Smits, T. H., Montesinos, E., Frey, J. E., & Duffy, B. (2009). Genotypic comparison of *Pantoea agglomerans* plant and clinical strains. *BMC Microbiology, 9*, 204.

Ridout, C. J., Skamnioti, P., Porritt, O., Sacristan, S., Jones, J. D., & Brown, J. K. (2006). Multiple avirulence paralogues in cereal powdery mildew fungi may contribute to parasite fitness and defeat of plant resistance. *The Plant Cell, 18*(9), 2402.

Riedl, S. J., Li, W., Chao, Y., Schwarzenbacher, R., & Shi, Y. (2005). Structure of the apoptotic protease-activating factor 1 bound to ADP. *Nature, 434*(7035), 926-933.

Rietz, S., Stamm, A., Malonek, S., Wagner, S., Becker, D., Medina-Escobar, N., Vlot, A. C., Feys, B. J., Niefind, K., & Parker, J. E. (2011). Different roles of Enhanced Disease Susceptibility1 (EDS1) bound to and dissociated from Phytoalexin Deficient 4 (PAD4) in *Arabidopsis* immunity. *New Phytologist, 191*(1), 107-119.

Robert-Seilaniantz, A., Grant, M., & Jones, J. D. (2011). Hormone crosstalk in plant disease and defense: more than just jasmonate-salicylate antagonism. *Annual Review of Phytopathology, 49*, 317-343.

Ron, M., & Avni, A. (2004). The receptor for the fungal elicitor ethylene-inducing xylanase is a member of a resistance-like gene family in tomato. *The Plant Cell, 16*(6), 1604-1615.

Ronald, P. C., Salmeron, J. M., Carland, F. M., & Staskawicz, B. J. (1992). The cloned avirulence gene *AvrPto* induces disease resistance in tomato cultivars containing the *Pto* resistance gene. *Journal of Bacteriology, 174*(5), 1604-1611.

Rose, L. E., Bittner-Eddy, P. D., Langley, C. H., Holub, E. B., Michelmore, R. W., & Beynon, J. L. (2004). The maintenance of extreme amino acid diversity at the disease resistance gene, RPP13, in *Arabidopsis thaliana*. *Genetics, 166*(3), 1517-1527.

Ross, A. F. (1961). Systemic acquired resistance induced by localized virus infections in plants. *Virology, 14*, 340-358.

Rouxel, T., & Balesdent, M. H. (2010). Avirulence genes. Encyclopedia of life sciences. *John Wiley & Sons Ltd., Chichester*.

Rushton, P. J., Somssich, I. E., Ringler, P., & Shen, Q. J. (2010). WRKY transcription factors. *Trends in Plant Science, 15*(5), 247-258.

Russell, A. R., Ashfield, T., & Innes, R. W. (2015). *Pseudomonas syringae* effector AvrPphB suppresses AvrB-Induced activation of RPM1 but not AvrRpm1-Induced activation. *Molecular Plant-Microbe Interactions Journal, 28*(6), 727-735.

Rutter, B. D., & Innes, R. W. (2017). Extracellular vesicles isolated from the leaf apoplast carry stress-response proteins. *Plant Physiology, 173*(1), 728.

Ryan, C. A., & Farmer, E. E. (1991). Oligosaccharide signals in plants: a current assessment. *Annual Review of Plant Physiology and Plant Molecular Biology, 42*(1), 651-674.

Samudrala, R., Heffron, F., & McDermott, J. E. (2009). Accurate prediction of secreted substrates and identification of a conserved putative secretion signal for type III secretion systems. *PLOS Pathogens, 5*(4), e1000375.

Sanchez-Vallet, A., Mesters, J. R., & Thomma, B. P. (2015). The battle for chitin recognition in plant-microbe interactions. *FEMS Microbiology Reviews, 39*(2), 171-183.

Sarris, P. F., Cevik, V., Dagdas, G., Jones, J. D., & Krasileva, K. V. (2016). Comparative analysis of plant immune receptor architectures uncovers host proteins likely targeted by pathogens. *BMC Biology, 14*, 8.

Sarris, P. F., Duxbury, Z., Huh, S. U., Ma, Y., Segonzac, C., Sklenar, J., Derbyshire, P., Cevik, V., Rallapalli, G., Saucet, S. B., Wirthmueller, L., Menke, F. L. H., Sohn, K. H., & Jones, J. D. (2015). A plant immune receptor detects pathogen effectors that target WRKY transcription factors. *Cell, 161*(5), 1089-1100.

Saunders, D. G., Win, J., Cano, L. M., Szabo, L. J., Kamoun, S., & Raffaele, S. (2012). Using hierarchical clustering of secreted protein families to classify and rank candidate effectors of rust fungi. *PLoS One, 7*(1), e29847.

Sawinski, K., Mersmann, S., Robatzek, S., & Bohmer, M. (2013). Guarding the green: pathways to stomatal immunity. *Molecular Plant-Microbe Interactions Journal, 26*(6), 626-632.

Schouten, H. J., Brinkhuis, J., Van der Burgh, A., Schaart, J. G., Groenwold, R., Broggini, G. A., & Gessler, C. (2014). Cloning and functional characterization of the *Rvi15* (*Vr2*) gene for apple scab resistance. *Tree Genetics & Genomes, 10*(2), 251-260.

Selin, C., de Kievit, T. R., Belmonte, M. F., & Fernando, W. G. (2016). Elucidating the role of effectors in plant-fungal interactions: progress and challenges. *Frontiers in Microbiology, 7*, 600.

Selote, D., & Kachroo, A. (2010). RPG1-B-derived resistance to AvrB-expressing *Pseudomonas syringae* requires RIN4-like proteins in soybean. *Plant Physiology, 153*(3), 1199-1211.

Shan, L., He, P., Li, J., Heese, A., Peck, S. C., Nurnberger, T., Martin, G. B., & Sheen, J. (2008). Bacterial effectors target the common signaling partner BAK1 to disrupt multiple MAMP receptor-signaling complexes and impede plant immunity. *Cell Host Microbe, 4*(1), 17-27.

Shao, F., Golstein, C., Ade, J., Stoutemyer, M., Dixon, J. E., & Innes, R. W. (2003). Cleavage of *Arabidopsis* PBS1 by a bacterial type III effector. *Science, 301*(5637), 1230-1233.

Shao, F., Merritt, P. M., Bao, Z., Innes, R. W., & Dixon, J. E. (2002). A *Yersinia* effector and a *Pseudomonas* avirulence protein define a family of cysteine proteases functioning in bacterial pathogenesis. *Cell, 109*(5), 575-588.

Shay, J. R., Dayton, D. F., & Hough, L. F. (1953). Apple scab resistance from a number of *Malus* species. *Proceedings of the American Society for Horticultural Science, 62*(348-356).

Shay, J. R., & Hough, L. F. (1952). Evaluation of apple scab resistance in selections of *Malus*. *American Journal of Botany, 39*(4), 288-297.

Shirasu, K. (2009). The HSP90-SGT1 chaperone complex for NLR immune sensors. *Annual Review of Plant Biology, 60*, 139-164.

Smereka, K. J., Machardy, W. E., & Kausch, A. P. (1987). Cellular differentiation in *Venturia inaequalis* ascospores during germination and penetration of apple leaves. *Canadian Journal of Botany, 65*(12), 2549-2561.

Smith, J. M., & Heese, A. (2014). Rapid bioassay to measure early reactive oxygen species production in *Arabidopsis* leave tissue in response to living *Pseudomonas syringae*. *Plant Methods, 10*(1), 6.

Sohn, K. H., Lei, R., Nemri, A., & Jones, J. D. (2007). The downy mildew effector proteins ATR1 and ATR13 promote disease susceptibility in *Arabidopsis thaliana*. *The Plant Cell, 19*(12), 4077-4090.

Soprano, A. S., Abe, V. Y., Smetana, J. H., & Benedetti, C. E. (2013). *Citrus* MAF1, a repressor of RNA polymerase III, binds the *Xanthomonas* citri canker elicitor PthA4 and suppresses citrus canker development. *Plant Physiology, 163*(1), 232-242.

Soufflet-Freslon, V., Gianfranceschi, L., Patocchi, A., & Durel, C. E. (2008). Inheritance studies of apple scab resistance and identification of *Rvi14*, a new major gene that acts together with other broad-spectrum QTL. *Genome, 51*(8), 657-667.

Spoel, S. H., & Dong, X. (2012). How do plants achieve immunity? Defence without specialized immune cells. *Nature Reviews Immunology, 12*(2), 89-100.

Spolaore, S., Trainotti, L., & Casadoro, G. (2001). A simple protocol for transient gene expression in ripe fleshy fruit mediated by *Agrobacterium*. *Journal of Experimental Botany, 52*(357), 845-850.

Starheim, K. K., Gevaert, K., & Arnesen, T. (2012). Protein N-terminal acetyltransferases: when the start matters. *Trends in Biochemical Sciences, 37*(4), 152-161.

Staskawicz, B. J., Dahlbeck, D., & Keen, N. T. (1984). Cloned avirulence gene of *Pseudomonas syringae* pv. *glycinea* determines race-specific incompatibility on *Glycine max Proceedings of the National Academy of Sciences of the United States of America, 81*(19), 6024-6028.

Steinbrenner, A. D., Goritschnig, S., & Staskawicz, B. J. (2015). Recognition and activation domains contribute to allele-specific responses of an *Arabidopsis* NLR receptor to an oomycete effector protein. *PLOS Pathogens, 11*(2), e1004665.

Stensvand, A., Eikemo, H., Seem, R. C., & Gadoury, D. M. (2009). Ascospore release by *Venturia inaequalis* during periods of extended daylight and low temperature at Nordic latitudes. *European Journal of Plant Pathology, 125*(1), 173-178.

Stergiopoulos, I., & de Wit, P. J. (2009). Fungal effector proteins. *Annual Review of Phytopathology, 47*, 233-263.

Sun, X., Greenwood, D. R., Templeton, M. D., Libich, D. S., McGhie, T. K., Xue, B., Yoon, M., Cui, W., Kirk, C. A., Jones, W. T., Uversky, V. N., & Rikkerink, E. H. (2014). The intrinsically disordered structural platform of the plant defence hub protein RPM1-interacting protein 4 provides insights into its mode of action in the host-pathogen interface and evolution of the nitrate-induced domain protein family. *The FEBS Journal, 281*(17), 3955-3979.

Sutton, T. B., Aldwinckle, H. S., Agnello, A. M., & Walgenbach, J. F. (2016). Introduction. In F. W. James, S. A. Herb, B. S. Turner, & M. A. Arthur (Eds.), *Compendium of Apple and Pear Diseases and Pests, Second Edition* (pp. 1-7): The American Phytopathological Society.

Swiderski, M. R., Birker, D., & Jones, J. D. (2009). The TIR domain of TIR-NB-LRR resistance proteins is a signaling domain involved in cell death induction. *Molecular Plant-Microbe Interactions Journal, 22*(2), 157-165.

Swiderski, M. R., & Innes, R. W. (2001). The *Arabidopsis* PBS1 resistance gene encodes a member of a novel protein kinase subfamily. *Plant Journal, 26*(1), 101-112.

Takemoto, D., & Jones, D. A. (2005). Membrane release and destabilization of *Arabidopsis* RIN4 following cleavage by *Pseudomonas syringae* AvrRpt2. *Molecular Plant-Microbe Interactions Journal, 18*(12), 1258-1268.

Takken, F. L., Albrecht, M., & Tameling, W. I. (2006). Resistance proteins: molecular switches of plant defence. *Current Opinion in Plant Biology, 9*(4), 383-390.

Takken, F. L., Thomas, C. M., Joosten, M. H., Golstein, C., Westerink, N., Hille, J., Nijkamp, H. J., De Wit, P. J., & Jones, J. D. (1999). A second gene at the tomato

Cf-4 locus confers resistance to *Cladosporium fulvum* through recognition of a novel avirulence determinant. *Plant Journal, 20*(3), 279-288.

Tameling, W. I., Elzinga, S. D., Darmin, P. S., Vossen, J. H., Takken, F. L., Haring, M. A., & Cornelissen, B. J. (2002). The tomato *R* gene products I-2 and MI-1 are functional ATP binding proteins with ATPase activity. *The Plant Cell, 14*(11), 2929-2939.

Tameling, W. I., Vossen, J. H., Albrecht, M., Lengauer, T., Berden, J. A., Haring, M. A., Cornelissen, B. J., & Takken, F. L. (2006). Mutations in the NB-ARC domain of I-2 that impair ATP hydrolysis cause autoactivation. *Plant Physiology, 140*(4), 1233-1245.

Tang, X., Xiao, Y., & Zhou, J. M. (2006). Regulation of the type III secretion system in phytopathogenic bacteria. *Molecular Plant-Microbe Interactions Journal, 19*(11), 1159-1166.

Tao, Y., Yuan, F., Leister, R. T., Ausubel, F. M., & Katagiri, F. (2000). Mutational analysis of the *Arabidopsis* nucleotide binding site-leucine-rich repeat resistance gene *RPS2*. *The Plant Cell, 12*(12), 2541-2554.

Taylor, R. G., Walker, D. C., & McInnes, R. R. (1993). *E. coli* host strains significantly affect the quality of small scale plasmid DNA preparations used for sequencing. *Nucleic Acids Research, 21*(7), 1677-1678.

Tenzer, I., & Gessler, C. (1997). Subdivision and genetic structure of four populations of *Venturia inaequalis* in Switzerland. *European Journal of Plant Pathology, 103*(6), 565-571.

Tenzer, I., & Gessler, C. (1999). Genetic diversity of *Venturia inaequalis* across Europe. *European Journal of Plant Pathology, 105*(6), 545-552.

Thomas, C. M., Jones, D. A., Parniske, M., Harrison, K., Balint-Kurti, P. J., Hatzixanthis, K., & Jones, J. D. (1997). Characterization of the tomato *Cf-4* gene for resistance to *Cladosporium fulvum* identifies sequences that determine recognitional specificity in *Cf-4* and *Cf-9*. *The Plant Cell, 9*(12), 2209-2224.

Thomma, B. P., Nurnberger, T., & Joosten, M. H. (2011). Of PAMPs and effectors: the blurred PTI-ETI dichotomy. *The Plant Cell, 23*(1), 4-15.

Thomson, S. V. (1986). The role of the stigma in fire blight infections. *Phytopathology, 76*, 476-482.

Tyler, B. M., Kale, S. D., Wang, Q., Tao, K., Clark, H. R., Drews, K., Antignani, V., Rumore, A., Hayes, T., Plett, J. M., Fudal, I., Gu, B., Chen, Q., Affeldt, K. J., Berthier, E., Fischer, G. J., Dou, D., Shan, W., Keller, N. P., Martin, F., Rouxel, T., & Lawrence, C. B. (2013). Microbe-independent entry of oomycete RxLR effectors and fungal RxLR-like effectors into plant and animal cells is specific and reproducible. *Molecular Plant-Microbe Interactions Journal, 26*(6), 611-616.

Tyler, B. M., Tripathy, S., Zhang, X., Dehal, P., Jiang, R. H., Aerts, A., Arredondo, F. D., Baxter, L., Bensasson, D., Beynon, J. L., Chapman, J., Damasceno, C. M., Dorrance, A. E., Dou, D., Dickerman, A. W., Dubchak, I. L., Garbelotto, M., Gijzen, M., Gordon, S. G., Govers, F., Grunwald, N. J., Huang, W., Ivors, K. L., Jones, R. W., Kamoun, S., Krampis, K., Lamour, K. H., Lee, M. K., McDonald, W. H., Medina, M., Meijer, H. J., Nordberg, E. K., Maclean, D. J., Ospina-Giraldo,

M. D., Morris, P. F., Phuntumart, V., Putnam, N. H., Rash, S., Rose, J. K., Sakihama, Y., Salamov, A. A., Savidor, A., Scheuring, C. F., Smith, B. M., Sobral, B. W., Terry, A., Torto-Alalibo, T. A., Win, J., Xu, Z., Zhang, H., Grigoriev, I. V., Rokhsar, D. S., & Boore, J. L. (2006). *Phytophthora* genome sequences uncover evolutionary origins and mechanisms of pathogenesis. *Science, 313*(5791), 1261-1266.

Upadhyaya, N. M., Mago, R., Staskawicz, B. J., Ayliffe, M. A., Ellis, J. G., & Dodds, P. N. (2013). A bacterial type III secretion assay for delivery of fungal fffector proteins into wheat. *Molecular Plant-Microbe Interactions Journal, 27*(3), 255-264.

Valsangiacomo, C., & Gessler, C. (1992). Purification and characterization of an exo-polygalacturonase produced by *Venturia inaequalis*, the causal agent of apple scab. *Physiological and Molecular Plant Pathology, 40*(1), 63-77.

Van Gijsegem, F., Gough, C., Zischek, C., Niqueux, E., Arlat, M., Genin, S., Barberis, P., German, S., Castello, P., & Boucher, C. (1995). The *hrp* gene locus of *Pseudomonas solanacearum*, which controls the production of a type III secretion system, encodes eight proteins related to components of the bacterial flagellar biogenesis complex. *Molecular Microbiology, 15*(6), 1095-1114.

Van Ooijen, G., Mayr, G., Kasiem, M. M., Albrecht, M., Cornelissen, B. J., & Takken, F. L. (2008). Structure-function analysis of the NB-ARC domain of plant disease resistance proteins. *Journal of Experimental Botany, 59*(6), 1383-1397.

Van Poppel, P. M., Guo, J., van de Vondervoort, P. J., Jung, M. W., Birch, P. R., Whisson, S. C., & Govers, F. (2008). The *Phytophthora infestans* avirulence gene *Avr4* encodes an RXLR-dEER effector. *Molecular Plant-Microbe Interactions Journal, 21*(11), 1460-1470.

Vanneste, J. L. (2000). *Fire blight : the disease and its causative agent, Erwinia amylovora*. Wallingford, Oxon, UK ; New York, NY, USA: CABI Pub.

Ve, T., Williams, S. J., Catanzariti, A. M., Rafiqi, M., Rahman, M., Ellis, J. G., Hardham, A. R., Jones, D. A., Anderson, P. A., Dodds, P. N., & Kobe, B. (2013). Structures of the flax-rust effector AvrM reveal insights into the molecular basis of plant-cell entry and effector-triggered immunity. *Proceedings of the National Academy of Sciences of the United States of America, 110*(43), 17594-17599.

Vergunst, A. C., Schrammeijer, B., den Dulk-Ras, A., de Vlaam, C. M., Regensburg-Tuink, T. J., & Hooykaas, P. J. (2000). VirB/D4-dependent protein translocation from *Agrobacterium* into plant cells. *Science, 290*(5493), 979-982.

Vinatzer, B. A., Patocchi, A., Gianfranceschi, L., Tartarini, S., Zhang, H. B., Gessler, C., & Sansavini, S. (2001). Apple contains receptor-like genes homologous to the *Cladosporium fulvum* resistance gene family of tomato with a cluster of genes cosegregating with *Vf* apple scab resistance. *Molecular Plant-Microbe Interactions Journal, 14*(4), 508-515.

Vleeshouwers, V. G., Rietman, H., Krenek, P., Champouret, N., Young, C., Oh, S. K., Wang, M., Bouwmeester, K., Vosman, B., Visser, R. G., Jacobsen, E., Govers, F., Kamoun, S., & Van der Vossen, E. A. (2008). Effector genomics accelerates discovery and functional profiling of potato disease resistance and *Phytophthora infestans* avirulence genes. *PLoS One, 3*(8), e2875.

Vogt, I., Wohner, T., Richter, K., Flachowsky, H., Sundin, G. W., Wensing, A., Savory, E. A., Geider, K., Day, B., Hanke, M. V., & Peil, A. (2013). Gene-for-gene relationship in the host-pathogen system *Malus* x *robusta* 5 - *Erwinia amylovora*. *New Phytologist, 197*(4), 1262-1275.

Wang, C. I., Gunčar, G., Forwood, J. K., Teh, T., Catanzariti, A. M., Lawrence, G. J., Loughlin, F. E., Mackay, J. P., Schirra, H. J., Anderson, P. A., Ellis, J. G., Dodds, P. N., & Kobe, B. (2007). Crystal structures of flax rust avirulence proteins *AvrL567-A* and *-D* reveal details of the structural basis for flax disease resistance specificity. *The Plant Cell, 19*(9), 2898.

Wang, D., Qi, M., Calla, B., Korban, S. S., Clough, S. J., Cock, P. J., Sundin, G. W., Toth, I., & Zhao, Y. (2012). Genome-wide identification of genes regulated by the Rcs phosphorelay system in *Erwinia amylovora*. *Molecular Plant-Microbe Interactions Journal, 25*(1), 6-17.

Wang, G., Roux, B., Feng, F., Guy, E., Li, L., Li, N., Zhang, X., Lautier, M., Jardinaud, M. F., Chabannes, M., Arlat, M., Chen, S., He, C., Noel, L. D., & Zhou, J. M. (2015). The decoy substrate of a pathogen effector and a pseudokinase specify pathogen-induced modified-self recognition and immunity in plants. *Cell Host Microbe, 18*(3), 285-295.

Wang, L., Albert, M., Einig, E., Furst, U., Krust, D., & Felix, G. (2016). The pattern-recognition receptor CORE of *Solanaceae* detects bacterial cold-shock protein. *Nature Plants, 2*, 16185.

Warren, R. F., Henk, A., Mowery, P., Holub, E., & Innes, R. W. (1998). A mutation within the leucine-rich repeat domain of the *Arabidopsis* disease resistance gene *RPS5* partially suppresses multiple bacterial and downy mildew resistance genes. *The Plant Cell, 10*(9), 1439-1452.

Watkins, R., & Spangelo, L. P. (1970). Components of genetic variance for plant survival and vigor of apple trees. *Theoretical and Applied Genetics, 40*(5), 195-203.

Wawra, S., Trusch, F., Matena, A., Apostolakis, K., Linne, U., Zhukov, I., Stanek, J., Kozminski, W., Davidson, I., Secombes, C. J., Bayer, P., & Van West, P. (2017). The RxLR motif of the host targeting effector AVR3a of *Phytophthora infestans* is cleaved before secretion. *The Plant Cell, 29*(6), 1184-1195.

Wessling, R., Epple, P., Altmann, S., He, Y., Yang, L., Henz, S. R., McDonald, N., Wiley, K., Bader, K. C., Glasser, C., Mukhtar, M. S., Haigis, S., Ghamsari, L., Stephens, A. E., Ecker, J. R., Vidal, M., Jones, J. D., Mayer, K. F., Ver Loren van Themaat, E., Weigel, D., Schulze-Lefert, P., Dangl, J. L., Panstruga, R., & Braun, P. (2014). Convergent targeting of a common host protein-network by pathogen effectors from three kingdoms of life. *Cell Host Microbe, 16*(3), 364-375.

Westerink, N., Brandwagt, B. F., de Wit, P. J., & Joosten, M. H. (2004). *Cladosporium fulvum* circumvents the second functional resistance gene homologue at the *Cf-4* locus (*Hcr9-4E*) by secretion of a stable avr4E isoform. *Molecular Microbiology, 54*(2), 533-545.

Whalen, M. C., Innes, R. W., Bent, A. F., & Staskawicz, B. J. (1991). Identification of *Pseudomonas syringae* pathogens of *Arabidopsis* and a bacterial locus determining avirulence on both *Arabidopsis* and soybean. *The Plant Cell, 3*(1), 49-59.

Williams, E. B., & Kuc, J. (1969). Resistance in *Malus* to *Venturia inaequalis*. *Annual Review of Phytopathology, 7*(1), 223-246.

Williams, E. B., & Shay, J. R. (1957). The relationship of genes for pathogenicity and certain other characters in *Venturia inaequalis* (*Cke*.) *Wint*. *Genetics, 42*(6), 704-711.

Williams, S. J., Sohn, K. H., Wan, L., Bernoux, M., Sarris, P. F., Segonzac, C., Ve, T., Ma, Y., Saucet, S. B., Ericsson, D. J., Casey, L. W., Lonhienne, T., Winzor, D. J., Zhang, X., Coerdt, A., Parker, J. E., Dodds, P. N., Kobe, B., & Jones, J. D. (2014). Structural basis for assembly and function of a heterodimeric plant immune receptor. *Science, 344*(6181), 299-303.

Willmann, R., Lajunen, H. M., Erbs, G., Newman, M. A., Kolb, D., Tsuda, K., Katagiri, F., Fliegmann, J., Bono, J. J., Cullimore, J. V., Jehle, A. K., Gotz, F., Kulik, A., Molinaro, A., Lipka, V., Gust, A. A., & Nurnberger, T. (2011). *Arabidopsis* lysin-motif proteins LYM1 LYM3 CERK1 mediate bacterial peptidoglycan sensing and immunity to bacterial infection. *Proceedings of the National Academy of Sciences of the United States of America, 108*(49), 19824-19829.

Win, J., Chaparro-Garcia, A., Belhaj, K., Saunders, D. G., Yoshida, K., Dong, S., Schornack, S., Zipfel, C., Robatzek, S., Hogenhout, S. A., & Kamoun, S. (2012). Effector biology of plant-associated organisms: concepts and perspectives. *Cold Spring Harb Symp Quant Biol, 77*, 235-247.

Win, J., Greenwood, D. R., & Plummer, K. M. (2003). Characterisation of a protein from *Venturia inaequalis* that induces necrosis in *Malus* carrying the *Vm* resistance gene. *Physiological and Molecular Plant Pathology, 62*(193-202).

Xiang, T., Zong, N., Zhang, J., Chen, J., Chen, M., & Zhou, J. M. (2011). BAK1 is not a target of the *Pseudomonas syringae* effector AvrPto. *Molecular Plant-Microbe Interactions Journal, 24*(1), 100-107.

Xiang, T., Zong, N., Zou, Y., Wu, Y., Zhang, J., Xing, W., Li, Y., Tang, X., Zhu, L., Chai, J., & Zhou, J. M. (2008). *Pseudomonas syringae* effector AvrPto blocks innate immunity by targeting receptor kinases. *Current Biology, 18*(1), 74-80.

Xiao, F., Giavalisco, P., & Martin, G. B. (2007). *Pseudomonas syringae* type III effector AvrPtoB is phosphorylated in plant cells on serine 258, promoting its virulence activity. *The Journal of Biological Chemistry, 282*(42), 30737-30744.

Xiao, Y., Heu, S., Yi, J., Lu, Y., & Hutcheson, S. W. (1994). Identification of a putative alternate sigma factor and characterization of a multicomponent regulatory cascade controlling the expression of *Pseudomonas syringae* pv. *syringae* Pss61 *hrp* and *hrmA* genes. *Journal of Bacteriology, 176*(4), 1025-1036.

Xu, M., & Korban, S. S. (2002). A cluster of four receptor-like genes resides in the *Vf* locus that confers resistance to apple scab disease. *Genetics, 162*(4), 1995.

Xu, X., Roberts, T., Barbara, D., Harvey, N. G., Gao, L., & Sargent, D. J. (2009). A genetic linkage map of *Venturia inaequalis*, the causal agent of apple scab. *BMC Research Notes, 2*, 163.

Yaeno, T., & Shirasu, K. (2013). The RXLR motif of oomycete effectors is not a sufficient element for binding to phosphatidylinositol monophosphates. *Plant Signaling & Behavior, 8*(4), e23865.

Yamada, K., Yamaguchi, K., Shirakawa, T., Nakagami, H., Mine, A., Ishikawa, K., Fujiwara, M., Narusaka, M., Narusaka, Y., Ichimura, K., Kobayashi, Y., Matsui, H., Nomura, Y., Nomoto, M., Tada, Y., Fukao, Y., Fukamizo, T., Tsuda, K., Shirasu, K., Shibuya, N., & Kawasaki, T. (2016). The *Arabidopsis* CERK1-associated kinase PBL27 connects chitin perception to MAPK activation. *The EMBO Journal, 35*(22), 2468-2483.

Yamaguchi, Y., Huffaker, A., Bryan, A. C., Tax, F. E., & Ryan, C. A. (2010). PEPR2 is a second receptor for the Pep1 and Pep2 peptides and contributes to defense responses in *Arabidopsis*. *The Plant Cell, 22*(2), 508-522.

Yamaguchi, Y., Pearce, G., & Ryan, C. A. (2006). The cell surface leucine-rich repeat receptor for AtPep1, an endogenous peptide elicitor in *Arabidopsis*, is functional in transgenic tobacco cells. *Proceedings of the National Academy of Sciences of the United States of America, 103*(26), 10104-10109.

Yan, N., Chai, J., Lee, E. S., Gu, L., Liu, Q., He, J., Wu, J. W., Kokel, D., Li, H., Hao, Q., Xue, D., & Shi, Y. (2005). Structure of the CED-4-CED-9 complex provides insights into programmed cell death in *Caenorhabditis elegans*. *Nature, 437*(7060), 831-837.

Yu, X., Tang, J., Wang, Q., Ye, W., Tao, K., Duan, S., Lu, C., Yang, X., Dong, S., Zheng, X., & Wang, Y. (2012). The RxLR effector Avh241 from *Phytophthora sojae* requires plasma membrane localization to induce plant cell death. *New Phytologist, 196*(1), 247-260.

Zhang, J., Li, W., Xiang, T., Liu, Z., Laluk, K., Ding, X., Zou, Y., Gao, M., Zhang, X., Chen, S., Mengiste, T., Zhang, Y., & Zhou, J. M. (2010). Receptor-like cytoplasmic kinases integrate signaling from multiple plant immune receptors and are targeted by a *Pseudomonas syringae* effector. *Cell Host Microbe, 7*(4), 290-301.

Zhang, J., Yin, Z., & White, F. (2015). TAL effectors and the executor *R* genes. *Frontiers in Plant Science, 6*, 641.

Zhang, S., & Klessig, D. F. (2001). MAPK cascades in plant defense signaling. *Trends in Plant Science, 6*(11), 520-527.

Zhang, W., Fraiture, M., Kolb, D., Loffelhardt, B., Desaki, Y., Boutrot, F. F., Tor, M., Zipfel, C., Gust, A. A., & Brunner, F. (2013). *Arabidopsis* receptor-like protein 30 and receptor-like kinase suppressor of BIR1-1/EVERSHED mediate innate immunity to necrotrophic fungi. *The Plant Cell, 25*(10), 4227-4241.

Zhang, X., Bernoux, M., Bentham, A. R., Newman, T. E., Ve, T., Casey, L. W., Raaymakers, T. M., Hu, J., Croll, T. I., Schreiber, K. J., Staskawicz, B. J., Anderson, P. A., Sohn, K. H., Williams, S. J., Dodds, P. N., & Kobe, B. (2017).

Multiple functional self-association interfaces in plant TIR domains. *Proceedings of the National Academy of Sciences of the United States of America, 114*(10), E2046-E2052.

Zhao, Y., He, S. Y., & Sundin, G. W. (2006). The *Erwinia amylovora avrRpt2* gene contributes to virulence on pear and AvrRpt2 is recognized by *Arabidopsis* RPS2 when expressed in *Pseudomonas syringae*. *Molecular Plant-Microbe Interactions Journal, 19*(6), 644-654.

Zhou, J., Wu, S., Chen, X., Liu, C., Sheen, J., Shan, L., & He, P. (2014). The *Pseudomonas syringae* effector HopF2 suppresses *Arabidopsis* immunity by targeting BAK1. *Plant Journal, 77*(2), 235-245.

Zhu, S., Li, Y., Vossen, J. H., Visser, R. G., & Jacobsen, E. (2012). Functional stacking of three resistance genes against *Phytophthora infestans* in potato. *Transgenic Research, 21*(1), 89-99.

Zini, E. (2005). *Construzione di una mappa diassociazione della popolazione di melo 'Golden Delicious ' x 'Freedom'e caratterizzazione del gene di resistenza Va a ticchiolatura.* (Doctoral Thesis), University of Bologna, Italy.

Zipfel, C. (2008). Pattern-recognition receptors in plant innate immunity. *Current Opinion in Immunology, 20*(1), 10-16.

Zipfel, C. (2014). Plant pattern-recognition receptors. *Trends in Immunology, 35*(7), 345-351.

Zipfel, C., Kunze, G., Chinchilla, D., Caniard, A., Jones, J. D., Boller, T., & Felix, G. (2006). Perception of the bacterial PAMP EF-Tu by the receptor EFR restricts *Agrobacterium*-mediated transformation. *Cell, 125*(4), 749-760.

Zipfel, C., & Robatzek, S. (2010). Pathogen-associated molecular pattern-triggered immunity: veni, vidi...? *Plant Physiology, 154*(2), 551-554.

Zipfel, C., Robatzek, S., Navarro, L., Oakeley, E. J., Jones, J. D., Felix, G., & Boller, T. (2004). Bacterial disease resistance in *Arabidopsis* through flagellin perception. *Nature, 428*(6984), 764-767.

Appendices

Table 6.1: Primers used in this study for Golden Gate module generation:

#	Primer name	Primer sequence
1	PsAvrRpt2_F	GGTCTCGAATGATGAAAATTGCTCCAGTTGCC
2	PsAvrRpt2_F	GGTCTCACGAAGCGGTAGAGCATTGCGTGT
3	EaAvrRpt2_F	GGTCTCGAATGAAAGTCAGTCATCTCACATCC
4	EaAvrRpt2_R	GGTCTCACGAAATTTTCACTGTATAACATGGCGTGT
5	RPS2_pt1_F	GGTCTCGAATGGATTTCATCTCATCTCTTATCGT
6	RPS2_pt1_R	GGTCTCACAACAACAAGAAACGTTTCTGTCT
7	RPS2_pt2_F	GGTCTCGGTTGCTAGATGATGTCTGGGAAG
8	RPS2_pt2_R	GGTCTCATTTCCAAGTATTCCAAGTCAGCG
9	RPS2_pt3_F	GGTCTCGGAAAACCTAACCACACTCGGTATC
10	RPS2_pt3_R	GGTCTCACGAAATTTGGAACAAAGCGCGGTAA
11	MR5_pt1_F	GGTCTCGAATGGGGGGAGAGGCTTTTCTT
12	MR5_pt1_R	GGTCTCAGACTCCACAGTTTGTTGTTCAAT
13	MR5_pt2_F	GGTCTCGAGTCTATCAAATGAGCACGACA
14	MR5_pt2_R	GGTCTCACTTGAATGGGACCATTCTAGCAC
15	MR5_pt3_F	GGTCTCGCAAGCGACACAAGAGAAACAGAA
16	MR5_pt3_R	GGTCTCATGTATTCTTCTGAGATTTTGGGGAA
17	MR5_pt1_F	GGTCTCGTACAGATAAGAGATTGCAGAAGTTTGA
18	MR5_pt1_F	GGTCTCACGAAAATCATCTTCCAATCTATATCTATGTA
19	RPM1_pt1_F	GGTCTCGAATGGCTTCGGCTACTGTTGATTT
20	RPM1_pt1_R	GGTCTCACTCTTTCTTTTCATCCGATAGTTCACA
21	RPM1_pt2_F	GGTCTCGAGAGGCTCATTAGGATGTGGATG
22	RPM1_pt2_R	GGTCTCACGAAAGATGAGAGGCTCACATAGAAAGAG
23	AtRIN4_F	GGTCTCGAATGGCACGTTCGAATGTACCA
24	AtRIN4_R	GGTCTCAAAGCTCATTTTCCTCCAAAGCCAAAGCA
25	MdRIN4_F	GGTCTCGAATGGCACAACGTTCACATGTAC
26	MdRIN4_R	GGTCTCACGAATCATTTTCTGCCCCATGGAAAG
27	MdRIN4_CLV1-2_R for Chimeric RIN4	GGTCTCAAAATTTGGGAACAGCAGCACCTTTC
28	AtRIN4_CLV3_F for Chimeric RIN4	GGTCTCGATTTGGTGACTGGGACGAGAACAAC
29	AtRIN4_CLV1-2_R for Chimeric RIN4	GGTCTCAGAATTTAGGCACCACTGTGAC
30	MdRIN4_CLV3_F for Chimeric RIN4	GGTCTCGATTCGGCGAGTGGGATGAGAAC
31	GFP_F	GGTCTCGAATGGTGAGCAAGGGCGAGGAG
32	AtRIN4_CLV1_R	GGTCTCACGAATCATCCAAATTTTGGTACATTCGAACG
33	MdRIN4_CLV1_R	GGTCTCACGAATCAGCCAAACTTTGGTACATGTGAAC
34	AtRIN4_CLV2_F	GGTCTCGAATGAACTGGGAAGCTGAGGAGAAT
35	AtRIN4_CLV2_R	GGTCTCACGAATCAACCGAATTTAGGCACCACTGT
36	MdRIN4_CLV2_F	GGTCTCGAATGAACTGGGAAGACCAAGAAAGTGT
37	MdRIN4_CLV2_R	GGTCTCACGAATCAGCCAAATTTGGGAACAGCAGC

#	Primer name	Primer sequence
38	AtRIN4_CLV3_F	GGTCTCGAATGGACTGGGACGAGAACAACCC
39	AtRIN4_CLV3_R	GGTCTCACGAATCATTTTCCTCCAAAGCCAAAGC
40	MdRIN4_CLV3_F	GGTCTCGAATGGAGTGGGATGAGAACGACCCG
41	MdRIN4_CLV3_R	GGTCTCACGAATCATTTTCTGCCCCATGGAAAG
42	AtRIN4_CLV3_pt1_R for Chimeric CLV3	GGTCTCAGCCTTCTCTTCACGGACTTTATTGAAGA
43	MdRIN4_CLV3_pt2_F for Chimeric CLV3	GGTCTCAAGGCGGGAAAAGCACCAGG
44	MdRIN4_CLV3_pt1_R for Chimeric CLV3	GGTCTCACTTCTCTCCTCCCGCACTTTGTTG
45	AtRIN4_CLV3_pt2_F for Chimeric CLV3	GGTCTCAGAAGTTCTGGAGCAAATGTGAGT
46	PbRIN4_F	GGTCTCAAATGGCACAACGTTCACATGTACCAAAGTTT
47	PbRIN4_R	GGTCTCAAAGCTCATTTTCTGCCCCACGGAA
48	MR5_CC_R	GGTCTCACGAACTAGGTGATATGTTTCGGCGTG
49	MR5_CC-NB(333aa)_R	GGTCTCACGAAACTTTCCATAGGCTCCAAATTGT
50	MR5_CC-NB-ARC(582aa)_R	GGTCTCACGAATCGTGGAAGAATAAACCCCTCG
51	MR5_noLRR(873aa)_R	GGTCTCACGAATAAGAGTGTTTTCAGGCAAGGGA
52	MR5_noLRR(1151aa)_R	GGTCTCACGAAGTCAAGTTCTCTAAGTGCCCTG
53	MR5_noCC(161-1388aa)_R	GGTCTCGAATGGTGATTGGAAGGGATGAGGACA
54	Nb_PR1_F	GGTCTCGCCATGGGATTTGTTCTCTTTTCACAATT
55	Nb_PR1_R	GGTCTCACATTTGGGCACGGCAAGAGTGGGATATTA
56	AvrRvi8-1F	GGTCTCGAATGCATCTCTCTACTCTTTTCAG
57	AvrRvi8-1R	GGTCTCACGAAAGTGCATTGCCCTTTGCAGG
58	AvrRvi8-3F	GGTCTCGAATGCATCTCTCTTCTCTTTTCAGC
59	AvrRvi8-3R	GGTCTCACGAAAACACATGTCTGTCTGCACTC
60	AvrRvi8-4R	GGTCTCACGAATGTACATTTCGGTCTGCACTC
61	AvrRvi8-5F	GGTCTCGAATGCATTTCTCTACTCTTTTTAGTAAC
62	AvrRvi8-5R	GGTCTCACGAAAGTGCATGTCGGTCTGCACTC
63	AvrRvi8-6R	GGTCTCACGAAAGTACATATCGGTCTGCACTC
64	AvrRvi8-7F	GGTCTCGAATGAGCTCCGTGGCCTTGCTTCC
65	AvrRvi8-7R	GGTCTCACGAAAAGTGCATTTCCCTCTGCAGG
66	AvrRvi8-8R	GGTCTCAGGAAAGTGCATTGCCCTCTGCA
67	AvrRvi8-9R	GGTCTCACGAATATCCGCGGCTGCGTTGG
68	AvrRvi8-10_F	GGTCTCGAATGTTTTTCAGCGCTCGATTCT
69	AvrRvi8-10_R	GGTCTCACGAATTTGGACACATCTATAGACACCG
70	AvrRvi8-11_F	GGTCTCGAATGTCTTTCTTTATTCACACTCTTTTGG
71	AvrRvi8-11_R	GGTCTCACGAACAAACCCTTGACACAATAATCATACC
72	AvrRvi8-12_F	GGTCTCGAATGAGATCCATGCTAGCCGC
73	AvrRvi8-12_R	GGTCTCACGAAAGAATACACAAAAGAGTTCAACGC
74	ViCE1_noSP_F	GGTCTCGAATGATCCCAGCACCGGCACCAG
75	ViCE1_R	GGTCTCACGAATTTGATGCCCAGCATGCCCG
76	ViCE2_noSP_F	GGTCTCGAATGCAAGTACCAAAGGGATCTGGGGC
77	ViCE2_R	GGTCTCACGAAAGCTGGAGGAGCAGCTCCA

#	Primer name	Primer sequence
78	ViCE3_noSP_F	GGTCTCGAATGATCCCAATCGATTCCACCACCTC
79	ViCE3_R	GGTCTCACGAACGCCCTCCTCAACATCTCAAC
80	ViCE4_noSP_F	GGTCTCGAATGGCGTAGACTGCCCAATCAAGC
81	ViCE4_R	GGTCTCACGAAAACGTGTCTCGCGTTTTGCC
82	ViCE5_noSP_F	GGTCTCGAATGCACTTACCATTCTCGGATTCTTCGT
83	ViCE5_R	GGTCTCACGAAAAAAGATCCAAACAATCCTTTGTTCTGC
84	ViCE6_noSP_F	GGTCTCGAATGATCAAATACCCTCCACTTGGACAC
85	ViCE6_R	GGTCTCACGAAACAAAGGACGTCGCATTGGACTC
86	ViCE7_noSP_F	GGTCTCGAATGGCCCCAGTTATGAGGCGCG
87	ViCE7_R	GGTCTCACGAACACTATAACGCCATCAAGCTTCGG
88	ViCE8_noSP_F	GGTCTCGAATGGCACCAATACCACAATTCGGCG
89	ViCE8_R	GGTCTCACGAAGAGCTTCCCTCCAAGTCCAAGG
90	ViCE9_noSP_F	GGTCTCGAATGGACTGGACCTACAAGAAAGCCGG
91	ViCE9_R	GGTCTCACGAAGCAGTGCACCTTCCAAGCC
92	ViCE10_noSP_F	GGTCTCGAATGATGCCAACAGCCATCGCT
93	ViCE10_R	GGTCTCACGAAATAGCCGCGGTTATTACCCTTGC
94	ViCE11_noSP_F	GGTCTCGAATGGCTCCTCAGGCCGGCGG
95	ViCE11_R	GGTCTCACGAATTTTGCTCCTTTTCCCAACTTCAT
96	ViCE12_noSP_F	GGTCTCGAATGGCTGTCCAAGAGCGCGCT
97	ViCE12_R	GGTCTCACGAATAAAGCGAGCATAGCCAAGAGTCCGGCAACACC
98	ViCE13_noSP_F	GGTCTCGAATGACACCAATAACCCTCGAAGAAAGG
99	ViCE13_R	GGTCTCACGAATTGAGGCACATCCCACTGATATTG
100	ViCE14_noSP_F	GGTCTCGAATGAACGGCGGCATCATCAACAG
101	ViCE14_R	GGTCTCACGAACAACGCGAGAGCAGCAAGACCCAA
102	ViCE15_noSP_F	GGTCTCGAATGCAAGAGGTGGACGTGGGATGTAT
103	ViCE15_R	GGTCTCACGAAATTGTAGTGGTAAGCAACACCGAA
104	ViCE16_noSP_F	GGTCTCGAATGCTCCCAACAGAGCAAGCTGGAC
105	ViCE16_R	GGTCTCACGAAGTTCTTCATGTCCATGCCTGGCA
106	ViCE17_noSP_F	GGTCTCGAATGGCTGCTCTTCAATCGCGCCAG
107	ViCE17_R	GGTCTCACGAATGCGATCCTCACGCATAGATACGAA
108	ViCE18_noSP_F	GGTCTCGAATGCAGCAAGTCTTCTTTCCTTCTCTCA
109	ViCE18_R	GGTCTCACGAACTGAATAGTGTAGGTGATACCATTTTG
110	ViCE19_noSP_F	GGTCTCGAATGGGCAAATACCACATTCAGACACGC
111	ViCE19_R	GGTCTCACGAAGCTTGACGCAACTGGGCATG
112	ViCE20_noSP_F	GGTCTCGAATGCACAGCTGCGGCGGCGGTAAA
113	ViCE20_R	GGTCTCACGAAACAGCAAATGTACATCACTTTCTCA
114	ViCE21_noSP_F	GGTCTCGAATGATCGCCCTGCCTTCTGCC
115	ViC21_R	GGTCTCACGAACTGTTTGCAAATAGTGCAAACCTCAGTGTATCC CAG
116	ViCE22_noSP_F	GGTCTCGAATGAACATTGTCTGCCAACCCGTG
117	ViCE22_R	GGTCTCACGAACCCACACCAGCAATCAAACTTCA

Table 6.2: Primers used in this study for site-directed mutagenesis:

#	Primer name	Primer sequence
118	EaAvrRpt2_C88A_F	CAACAGAATGAGCGAATGGGCGCCTGGTATGCCTGCACCAG
119	EaAvrRpt2_C88A_F	CTGGTGCAGGCATACCAGGCGCCCATTCGCTCATTCTGTTG
120	PsAvrRpt2_C122A_F	CGTATCCCAAGGTAATGAGCGAATGGGAGCTTGGTATGCCTGC
121	PsAvrRpt2_C122A_R	GCAGGCATACCAAGCTCCCATTCGCTCATTACCTTGGGATACG
122	MR5_K206A_F	GTATGGCTGGAGTCGGAGCGACAACACTTGCTGGAC
123	MR5_K206A_R	GTCCAGCAAGTGTTGTCGCTCCGACTCCAGCCATAC
124	MR5_D493V_F	TTTCAAAATATGTGATGCATGTCCTTATTGGTGATTTAGCACG
125	MR5_D493V_R	CGTGCTAAATCACCAATAAGGACATGCATCACATATTTTGAAA
126	MR5_D493N_F	CAAAATATGTGATGCATAACCTTATTGGTGATTTAGC
127	MR5_D493N_R	GCTAAATCACCAATAAGGTTATGCATCACATATTTTG
128	MdRIN4_F10A_F RCS1_mut	GTTCACATGTACCAAAGGCTGGCAATTGGGAAGACC
129	MdRIN4_F10A_R RCS1_mut	GGTCTTCCCAATTGCCAGCCTTTGGTACATGTGAAC
130	MdRIN4_F179A_F RCS2_mut	GGTGCTGCTGTTCCCAAAGCTGGCGAGTGGGATGAG
131	MdRIN4_F179A_R RCS2_mut	CTCATCCCACTCGCCAGCTTTGGGAACAGCAGCACC
132	MdRIN4_CCC_to_ACA_F GPI anchor mut	CAATGACAGTGCCAAGGCTTGCGCCTTTCCATGGGGC
133	MdRIN4_CCC_to_ACA_R GPI anchor mut	GCCCCATGGAAAGGCGCAAGCCTTGGCACTGTCATTG
134	MdRIN4_ACA_to_AAA_F GPI anchor mut	CAATGACAGTGCCAAGGCTGCCGCCTTTCCATGGGGC
135	MdRIN4_ACA_to_AAA_R GPI anchor mut	GCCCCATGGAAAGGCGGCAGCCTTGGCACTGTCATTG
136	AtRIN4_D153E_F	GGTCTCGAATGGAGTGGGACGAGAACAACCCGTC
137	AtRIN4_D153E_R	GACGGGTTGTTCTCGTCCCACTCCATTCGAGACC
138	AtRIN4_N158D_F	GGTGACTGGGACGAGAACGACCCGTCATCAGCTGA
139	AtRIN4_N158D_R	TCAGCTGATGACGGGTCGTTCTCGTCCCAGTCACC
140	AtRIN4_S160A_F	GGGACGAGAACAACCCGGCATCAGCTGACGGATAC
141	AtRIN4_S160A_R	GTATCCGTCAGCTGATGCCGGGTTGTTCTCGTCCC
142	AtRIN4_Y165F_F	CATCAGCTGACGGATTCACGCATATCTTCAATAA
143	AtRIN4_Y165F_R	TTATTGAAGATATGCGTGAATCCGTCAGCTGATG
144	MdtRIN4_E181D_F	GGTCTCGAATGGATTGGGATGAGAACGACCCGGC
145	MdRIN4_E181D_R	GCCGGGTCGTTCTCATCCCAATCCATTCGAGACC
146	MdRIN4_D186N_F	GGCGAGTGGGATGAGAACAACCCGGCATCAGCTG
147	MdRIN4_D186N_R	TCAGCTGATGCCGGGTTGTTCTCATCCCACTCGC
148	MdRIN4_A188S_F	GGGATGAGAACGACCCGTCATCAGCTGATGGTT
149	MdRIN4_A188S_R	AACCATCAGCTGATGACGGGTCGTTCTCATCCC
150	MdRIN4_F193Y_F	CATCAGCTGATGGTTACACTCATATATTCAACAA
151	MdRIN4_F193Y_R	TTGTTGAATATATGAGTGTAACCATCAGCTGATG
152	EaAvrRpt2_C156S_F	CAATGAACTCGGCAATCTCTTGTCTCGCCATGGACCCATTATG
153	EaAvrRpt2_C156S_R	CATAATGGGTCCATGGCGAGACAAGAGATTGCCGAGTTCATTG
154	ViCE7_mutBsaI_1_F	CTTCGAAAAGCGCGACGAAACCACCCCTGAGGCCGAC
155	ViCE7_mutBsaI_1_R	GTCGGCCTCAGGGGTGGTTTCGTCGCGCTTTTCGAAG

#	Primer name	Primer sequence
156	ViCE7_mutBsaI_2_F	GAGGTTGACCCCACCGCTGAAACCGGCTCGGCTATCAAC
157	ViCE7_mutBsaI_2_R	GTTGATAGCCGAGCCGGTTTCAGCGGTGGGGTCAACCTC
158	ViCE13_mutBsaI_1_F	GTTTCACAGGCATACAGCGGACTCACTACGGCATTCAAATG
159	ViCE13_mutBsaI_1_R	CATTTGAATGCCGTAGTGAGTCCGCTGTATGCCTGTGAAAC
160	ViCE13_mutBsaI_2_F	CGAACAAGCTGTGGGAGACAACCAACCGATTCTCG
161	ViCE13_mutBsaI_2_R	CGAGAATCGGTTGGTTGTCTCCCACAGCTTGTTCG
162	ViCE21_mutBsaI_F	CCAACATCATCTTCACTGGACTCCCACCTTACCACCC
163	ViCE21_mutBsaI_R	GGGTGGTAAGGTGGGAGTCCAGTGAAGATGATGTTGG

Figure 6.1: Protein alignment of AvrRpt2 effector from *Pseudomonas syringae* JL1506 and *Erwinia amylovora* Fb12-027.

Protein sequence of *Pseudomonas syringae* JL1506 (PsAvrRpt2) was retrieved with accession number CAA79815.2, and *Erwinia amylovora* Fb12-027 (EaAvrRpt2) was cloned and sequenced in this study and was 100% identical to AvrRpt2 from strain ATCC 49946 with accession number CBJ45097.1. Protein alignment was performed in Geneious R11 by BioMatters, using native aligner with Blosum62 cost matrix. Blue squares denote the critical aa residues of protease catalytic triad.

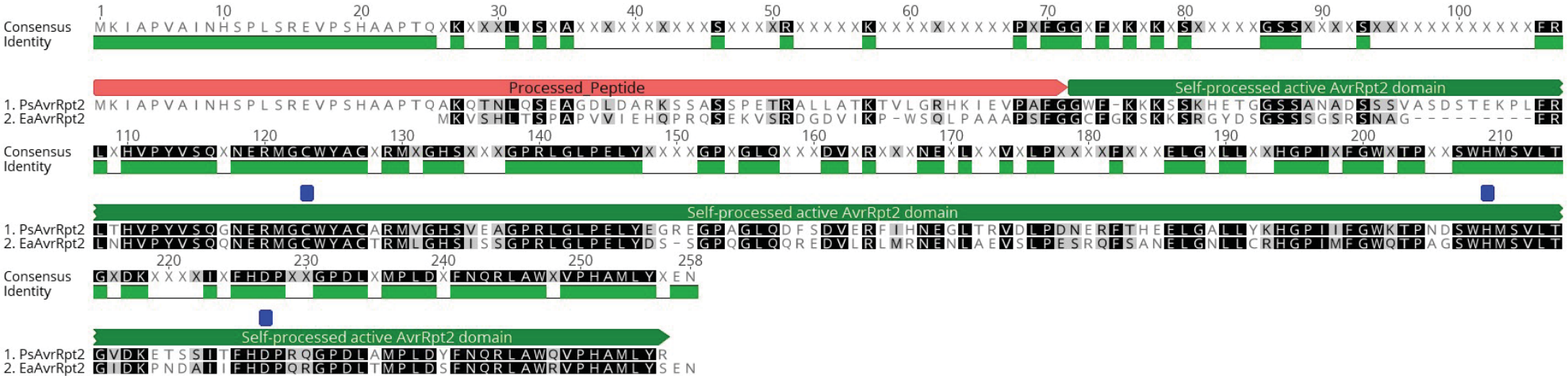

Figure 6.2: Protein alignment of *Malus domestica* RIN4-1 and RIN4-2 homologs.

Malus domestica RIN4-1 (MdRIN4-1) with RefSeq accession – NM_001293994.1 and MdRIN4-2 with RefSeq accession – NP_001280834.1 were used in this study. Protein alignment was performed in Geneious R11 by BioMatters, using native aligner with Blosum62 cost matrix. NOI-domains denoted in green, cleavage products denoted in blue, and membrane anchoring site denoted in yellow.

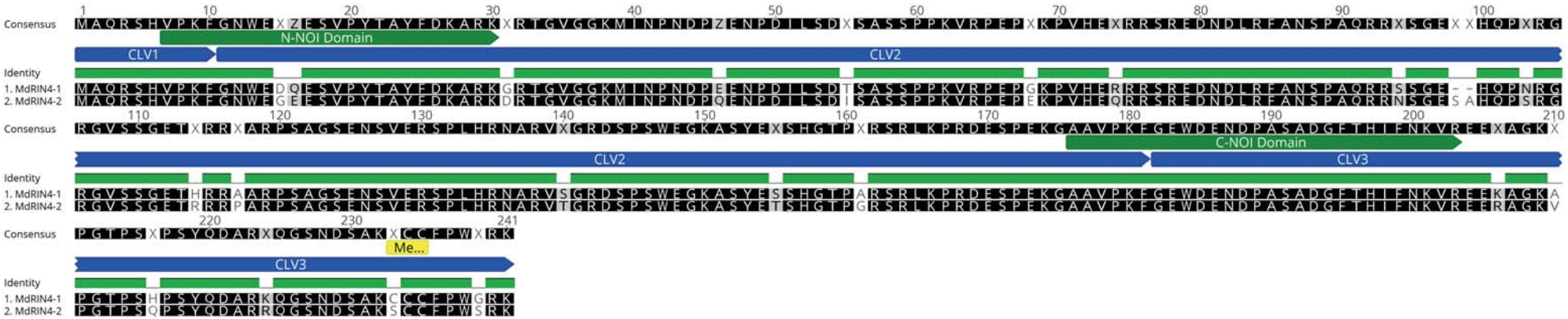

Figure 6.3: Nucleotide alignment of *Venturia inaequalis AvrRvi8-1* and *AvrRvi8-2* candidates predicted *in silico* with the sequencing results of amplification products from cDNA.

AvrRvi8-1 and *AvrRvi8-2* are the *in silico* predicted genes, and 1 – 6 are the sequences of amplified products from *V. inaequalis* cDNA. Nucleotide alignment was performed in Geneious R11 by BioMatters, using native aligner and default settings.

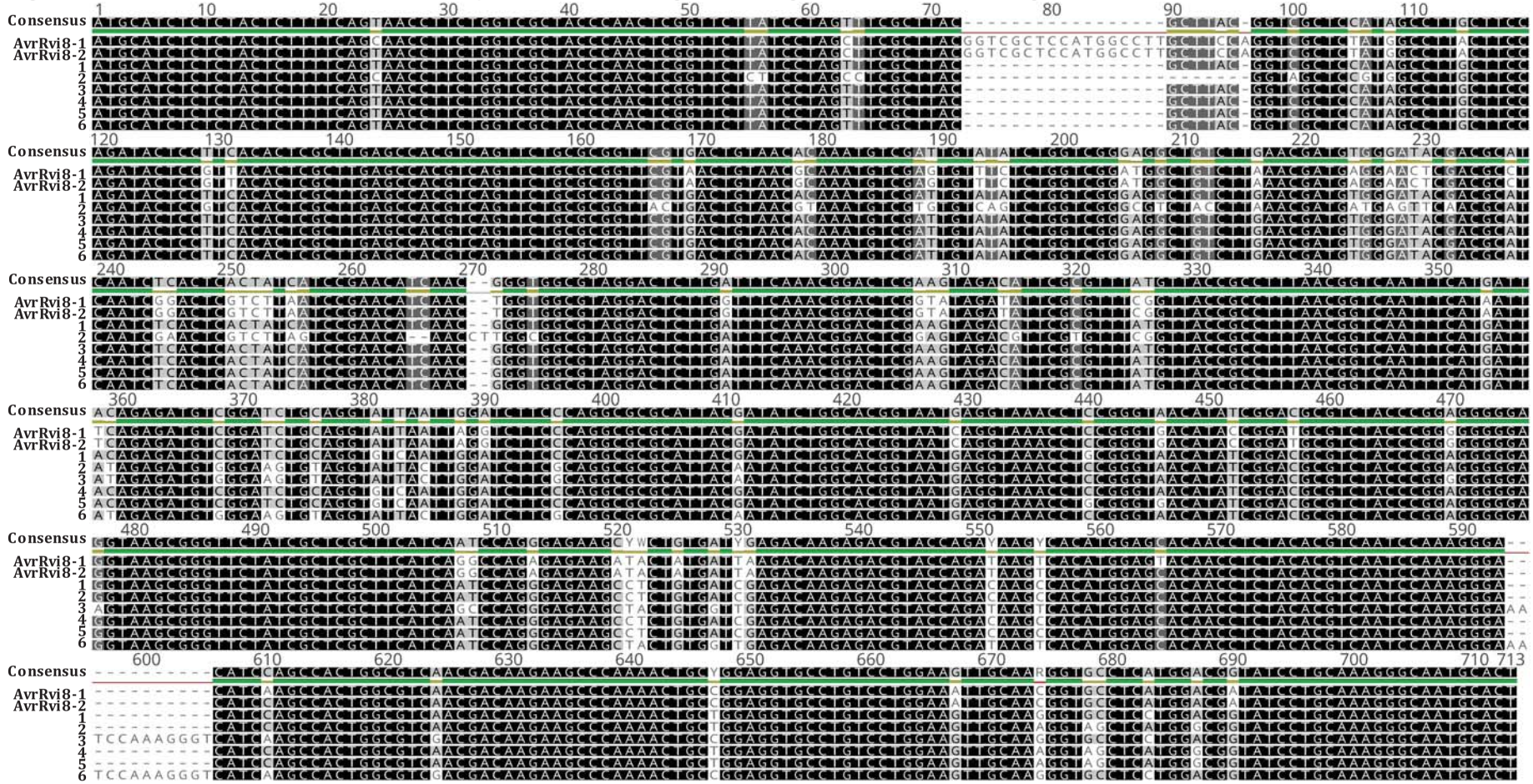

Figure 6.4: Nucleotide alignment of *Venturia inaequalis AvrRvi8-6* and *AvrRvi8-8* candidates predicted *in silico* with the sequencing results of amplification products from cDNA.

AvrRvi8-6 and *AvrRvi8-8* are the *in silico* predicted genes and the sequences of amplified products from *V. inaequalis* cDNA were aligned. Nucleotide alignment was performed in Geneious R11 by BioMatters, using native aligner and default settings.

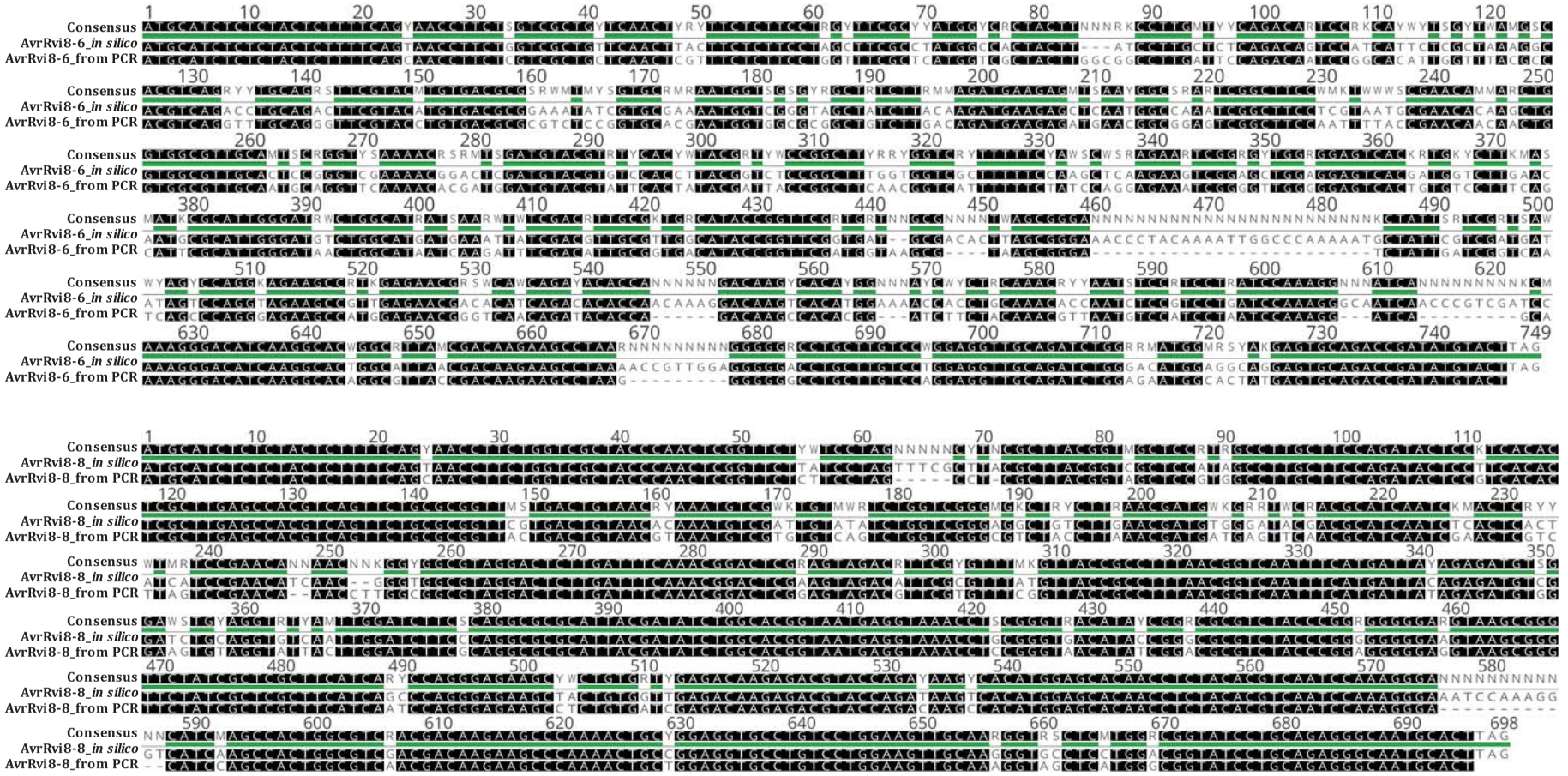

Figure 6.5: Nucleotide alignment of *Venturia inaequalis AvrRvi8*-candidate predicted *in silico* with the sequencing results of amplification products from cDNA.

AvrRvi8-9 is the *in silico* predicted gene and the sequence of amplified product from *V. inaequalis* cDNA were aligned, unexpected STOP-codon *AvrRvi8-9* in PCR product sequence outlined by a red square. Nucleotide alignment was performed in Geneious R11 by BioMatters, using native aligner and default settings.

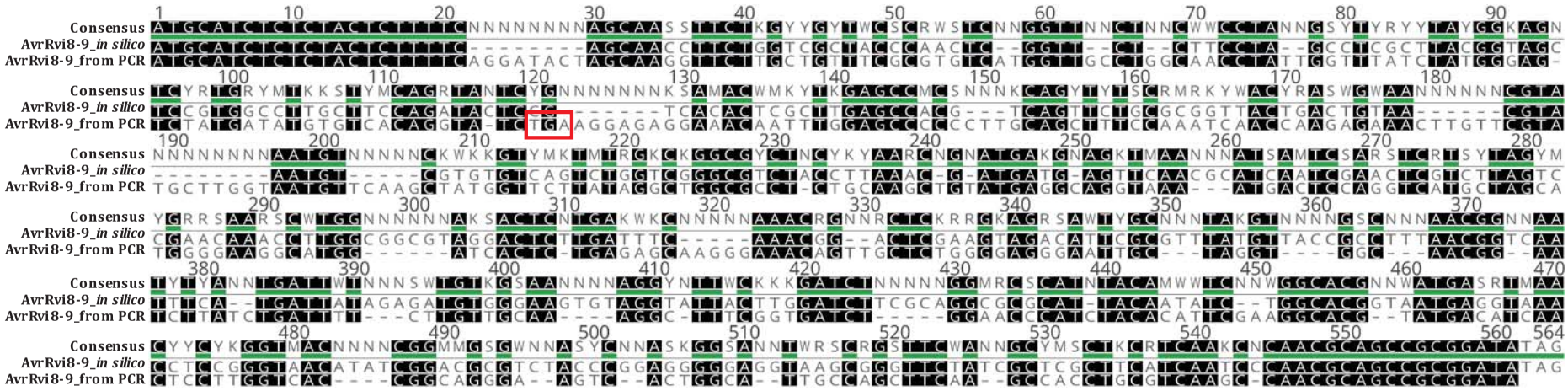

Figure 6.6: Schematic representation of intron mis-annotations and early STOP-codons in nucleotide alignments of *Venturia inaequalis AvrRvi8-10* and *AvrRvi8-11* candidates predicted *in silico* with the sequencing results of amplification products from cDNA.

AvrRvi8-10 and *AvrRvi8-11 in silico* predicted genes and their genomic DNA loci sequences were aligned with the sequences of amplified products from *V. inaequalis* cDNA. Nucleotide alignment was performed in Geneious R11 by BioMatters, using native aligner and default settings.

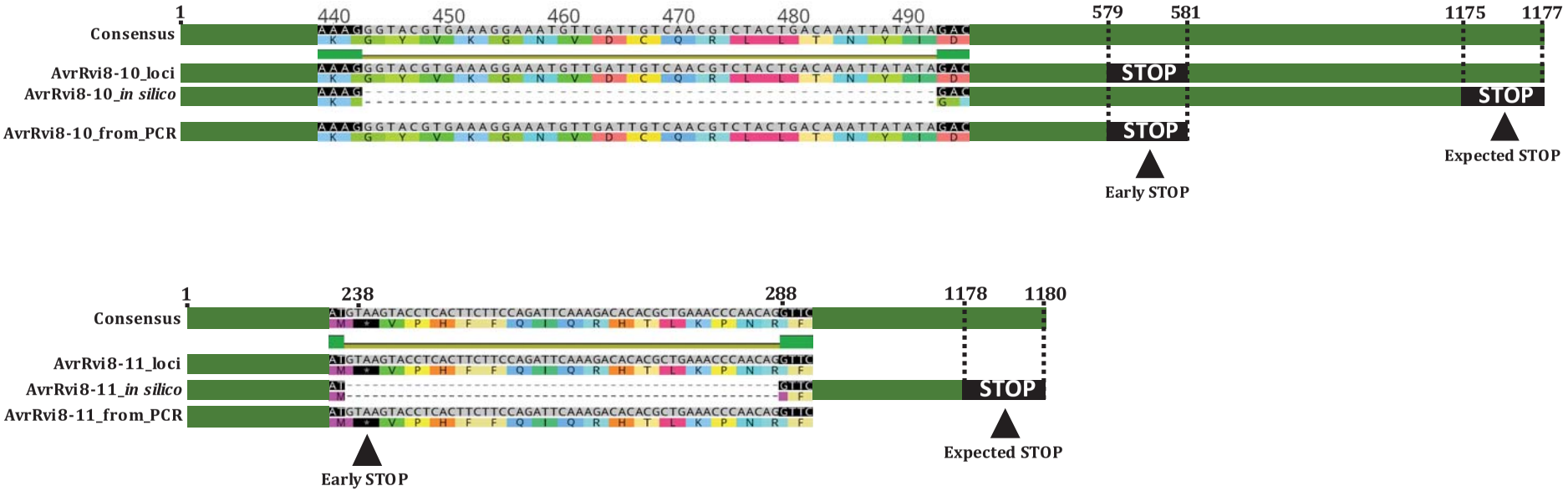

Figure 6.7: Schematic representation of intron mis-annotations STOP-codon variations in nucleotide alignments of *Venturia inaequalis ViCE5, 7 and 8* genes predicted *in silico* with the sequencing results of amplification products from cDNA.

ViCE5, 7 and 8 in silico predicted genes and their genomic DNA loci sequences were aligned with the sequences of amplified products from *V. inaequalis* cDNA. Nucleotide alignment was performed in Geneious R11 by BioMatters, using native aligner and default settings.

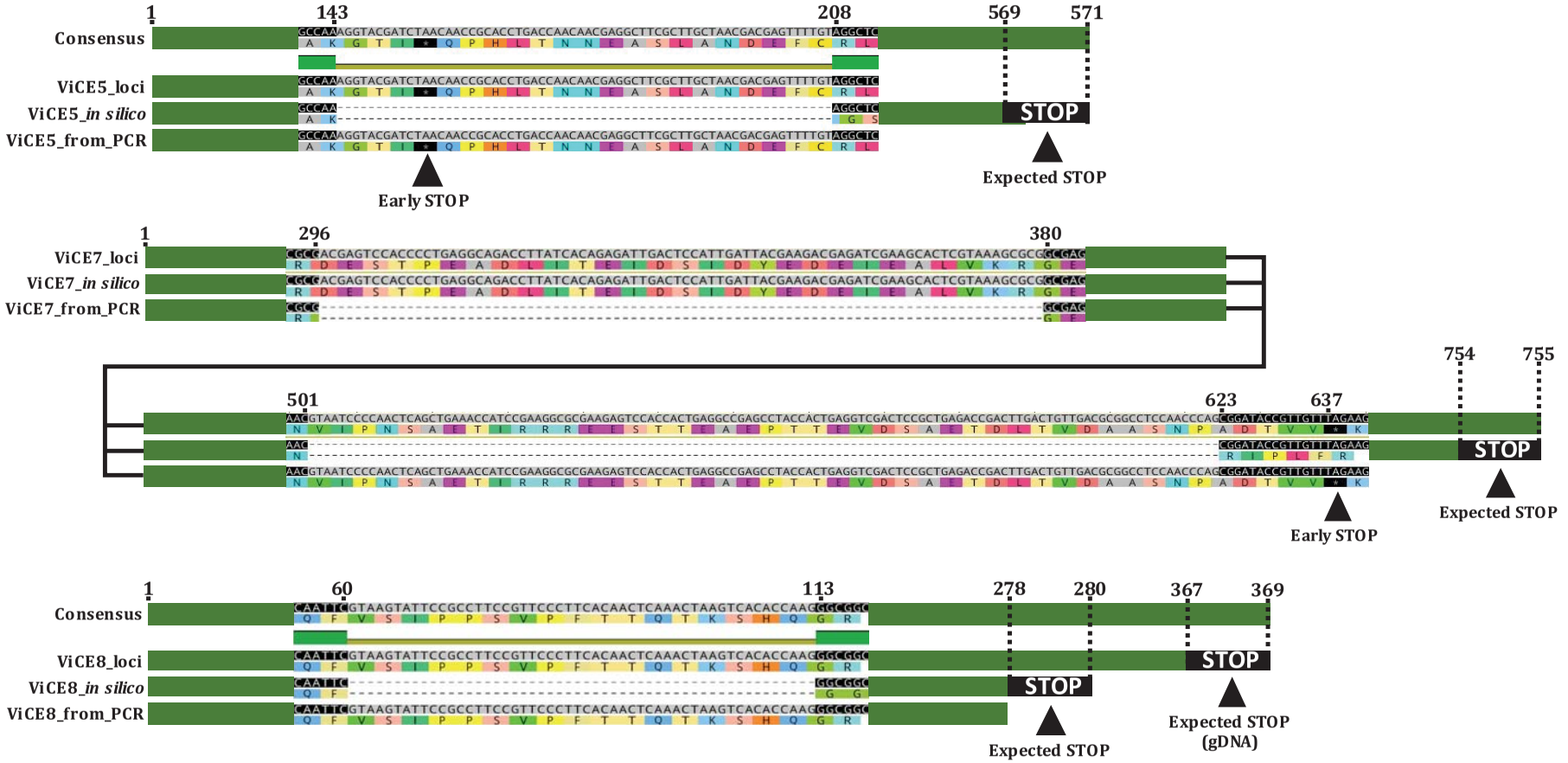

Figure 6.8: Plasmid map of pICH41021 (standard vector for blunt-end cloning of newly generated Golden Gate modules). Map created in Geneious R11 by BioMatters.

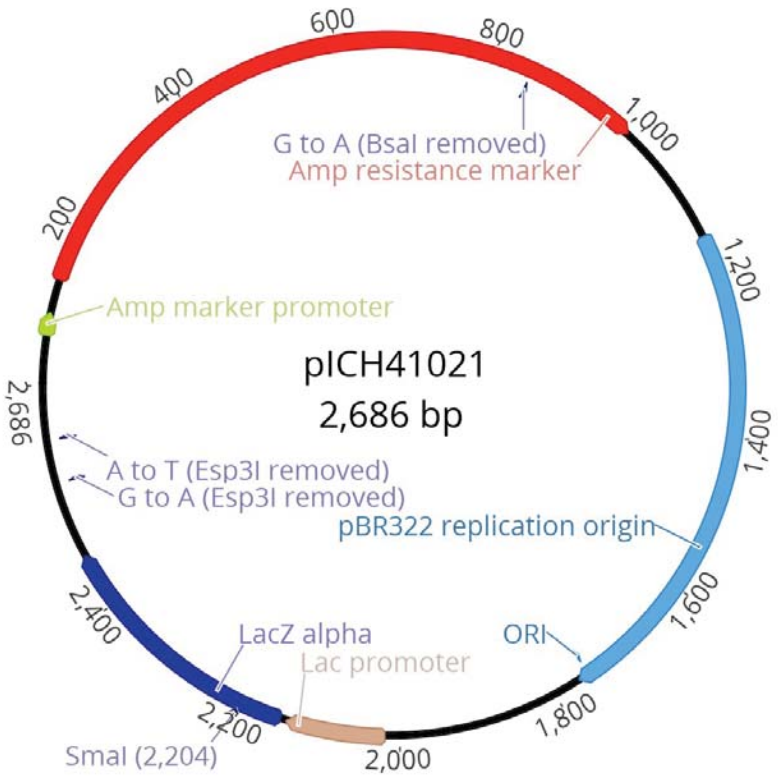

Figure 6.9: Plasmid map of pICH86966 (standard vector for *Agrobacterium* mediated transient protein expression *in planta*). Map created in Geneious R11 by BioMatters.

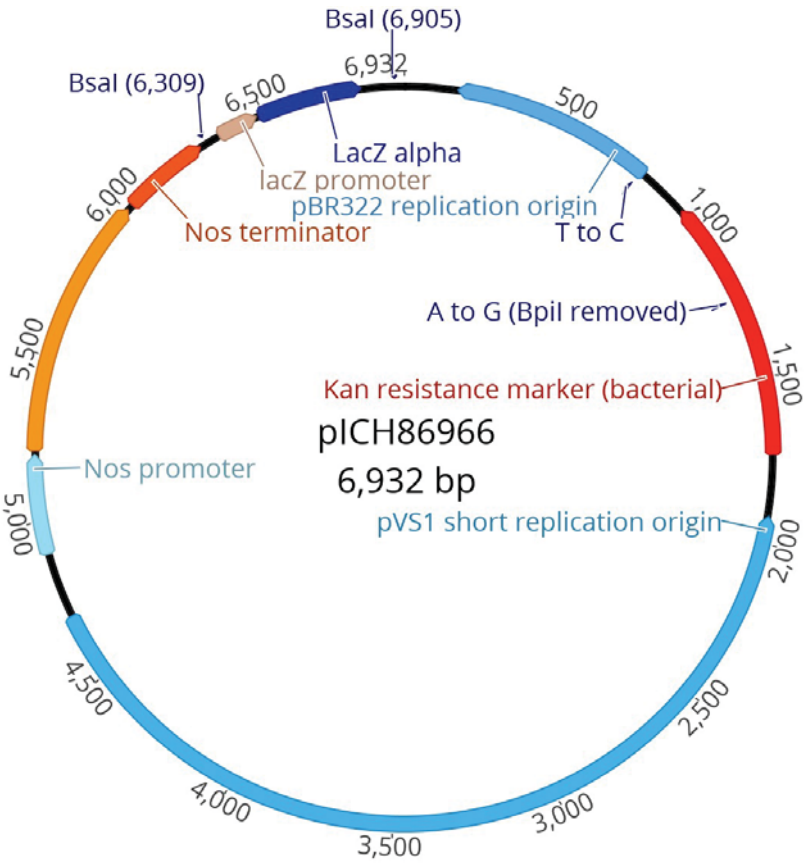

Figure 6.10: Plasmid map of pICH86988 (standard vector for *Agrobacterium* mediated transient protein expression *in planta*, contains 35S CaMV promoter). Map created in Geneious R11 by BioMatters.

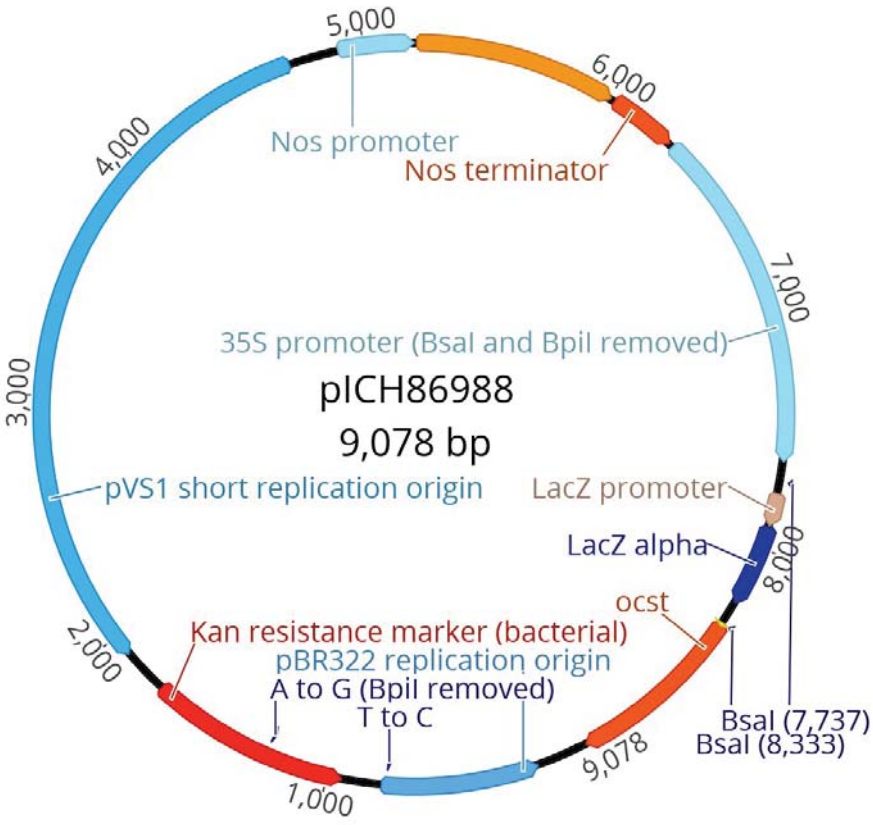

Figure 6.11: Plasmid map of EpiGreenB5::Spec::GG (standard vector for *Arabidopsis thaliana* stable transformation). Map created in Geneious R11 by BioMatters.

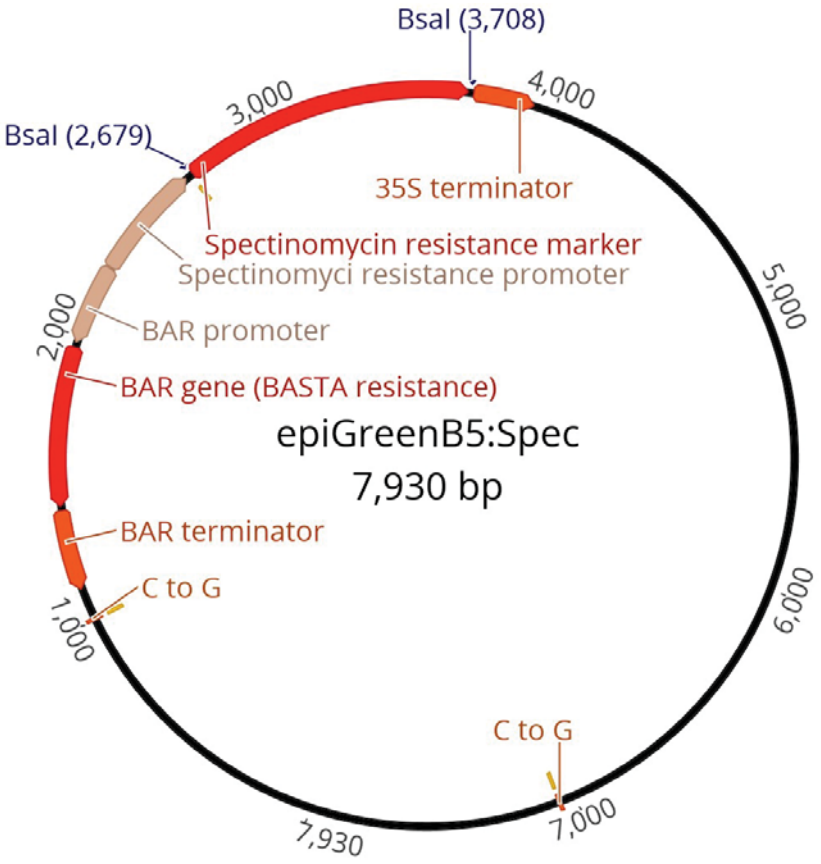

Figure 6.12: Plasmid map of pAGM4723 (standard vector for stable and transient transformation of plants with two genes). Map created in Geneious R11 by BioMatters.

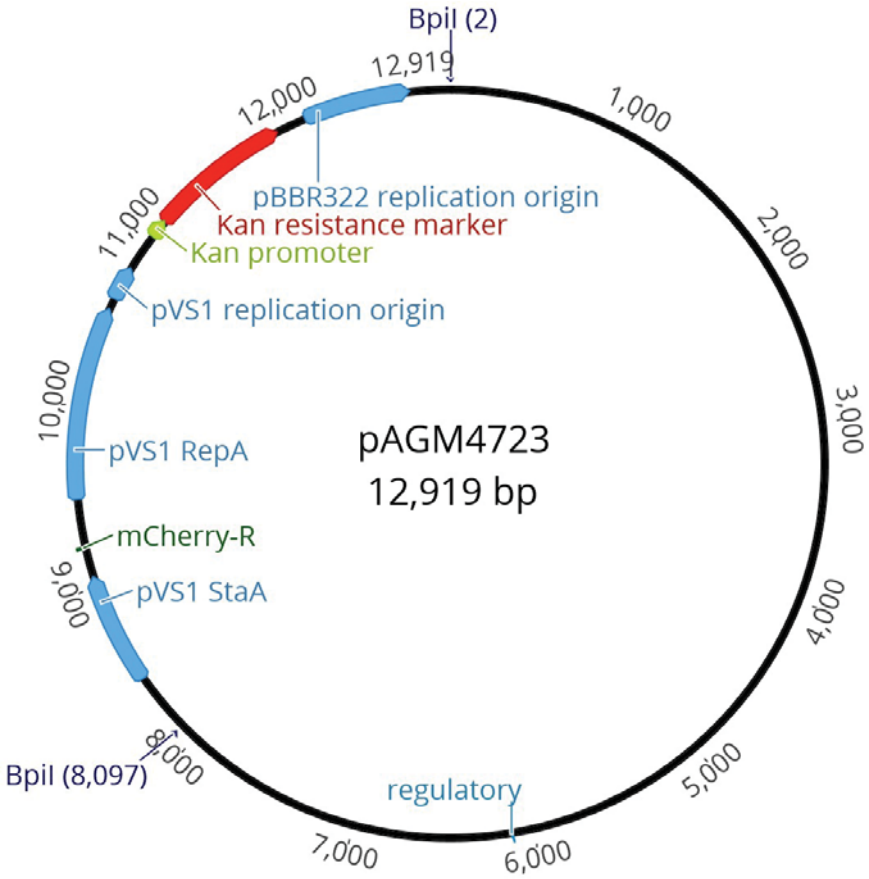

Figure 6.13: Plasmid map of pBBR1MCS-5 with AvrRps4 promoter and fragment coding for AvrRps4 secretion signal (standard vector *P. fluorescens Pf*-0 mediated effector delivery). Map created in Geneious R11 by BioMatters.

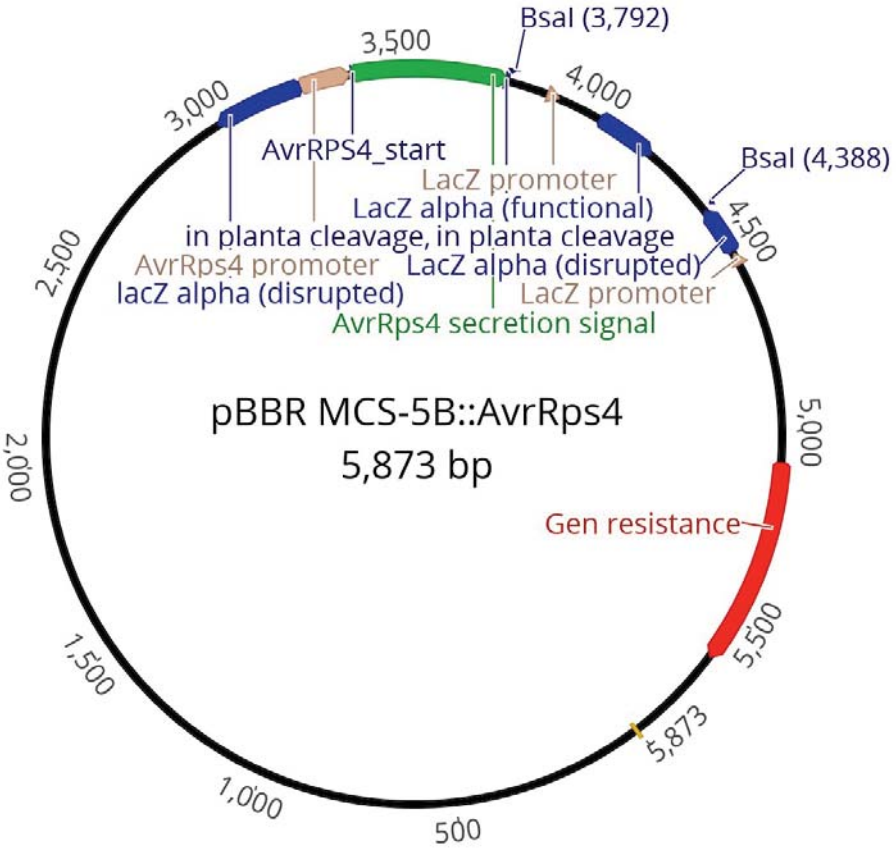

Figure 6.14: Plasmid map of pBBR1MCS-5 with AvrRpm1 promoter and fragment coding for AvrRpm1 secretion signal (standard vector *P. fluorescens Pf*-0 mediated effector delivery). Map created in Geneious R11 by BioMatters.